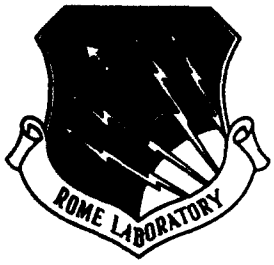

RL-TR-91-42
Final Technical Report
May 1991

INVESTIGATION OF A MULTIFREQUENCY RECONFIGURABLE PHASED ARRAY ANTENNA

Hazeltine Corporation

John F. Pedersen and Allan Gayer

APPROVED FOR PUBLIC RELEASE; DISTRIBUTION UNLIMITED.

Rome Laboratory
Air Force Systems Command
Griffiss Air Force Base, NY 13441-5700

This report has been reviewed by the Rome Laboratory Public Affairs Office (PA) and is releasable to the National Technical Information Service (NTIS). At NTIS it will be releasable to the general public, including foreign nations.

RL-TR-91-42 has been reviewed and is approved for publication.

APPROVED: Zachary O. White

ZACHARY O. WHITE
Project Engineer

APPROVED: John K. Schindler

JOHN K. SCHINDLER
Director of Electromagnetics

FOR THE COMMANDER: James W. Hyde III

JAMES W. HYDE III
Directorate of Plans & Programs

If your address has changed or if you wish to be removed from the Rome Laboratory mailing list, or if the addressee is no longer employed by your organization, please notify RL(EEAA) Hanscom AFB MA 01731-5000. This will assist us in maintaining a current mailing list.

Do not return copies of this report unless contractual obligations or notices on a specific document require that it be returned.

REPORT DOCUMENTATION PAGE

Form Approved
OMB No. 0704-0188

1. AGENCY USE ONLY (Leave Blank)	2. REPORT DATE	3. REPORT TYPE AND DATES COVERED
	May 1991	Final Oct 88 - Sep 90

4. TITLE AND SUBTITLE
INVESTIGATION OF A MULTIFREQUENCY RECONFIGURABLE PHASED ARRAY ANTENNA

5. FUNDING NUMBERS
C - F19628-87-C-0096
PE - 62702F
PR - 4600
TA - 14
WU - 1M

6. AUTHOR(S)
John F. Pedersen, Allan Gayer

7. PERFORMING ORGANIZATION NAME(S) AND ADDRESS(ES)
Hazeltine Corporation
Cuba Hill Road
Greenlawn NY 11740

8. PERFORMING ORGANIZATION REPORT NUMBER

9. SPONSORING/MONITORING AGENCY NAME(S) AND ADDRESS(ES)
Rome Laboratory (EEAA)
Hanscom AFB MA 01731-5000

10. SPONSORING/MONITORING AGENCY REPORT NUMBER
RL-TR-91-42

11. SUPPLEMENTARY NOTES
Rome Laboratory Project Engineer: Zachary White/EEAA/(617) 478-2055

12a. DISTRIBUTION/AVAILABILITY STATEMENT
Approved for public release; distribution unlimited.

12b. DISTRIBUTION CODE

13. ABSTRACT (Maximum 200 words)

The Government has a future requirement to operate several systems simultaneously from a common aperture. A technique has been studied to accomplish this objective by using a control circuit behind each element of the array. The control circuit consists of an arrangement of filters, an attenuator, and a phase shifter. The filters are used to partition the reconfigurable aperture into several simultaneously operating antennas. The attenuator provides independent illumination control while the phase shifters are used to scan individual antenna beams.

A laboratory model of a reconfigurable array was designed, fabricated, and tested. The results show that the proposed control circuit provides the desired aspects of reconfigurability.

14. SUBJECT TERMS
Reconfigurable Antenna, Simultaneous Operating Antenna, Self-Healing

15. NUMBER OF PAGES
166

16. PRICE CODE

17. SECURITY CLASSIFICATION OF REPORT	18. SECURITY CLASSIFICATION OF THIS PAGE	19. SECURITY CLASSIFICATION OF ABSTRACT	20. LIMITATION OF ABSTRACT
UNCLASSIFIED	UNCLASSIFIED	UNCLASSIFIED	U/A

CONTENTS

ILLUSTRATIONS

ILLUSTRATIONS (Continued)

TABLES

ABBREVIATIONS AND ACRONYMS

The abbreviations and acronyms used in this document are listed below. This list does not include abbreviations and acronyms that are in accordance with MIL-STD-12D.

ELINT	Electronics Intelligence
ESM	Electronic Support Measures
EW	Electronic Warfare
GTRI	Georgia Technical Research Institute
MMIC	Microwave Monolithic Integrated Circuit

SECTION I

INTRODUCTION

This final report describes the results of a 30-month program to study, design, and fabricate a laboratory model of a multifrequency, reconfigurable array antenna. The work is sponsored by RADC/Hanscom Field, under contract F19628-87-C-0096. The report covers the period from 25 October 1988 to 04 September 1990.

The purpose of the array antenna is to serve radar, electronic support measures/electronics intelligence (ESM/ELINT), electronic warfare (EW), and communications functions. Implicit in the multisystem function of the array is the need to operate many of these systems simultaneously. Additionally, the array should be capable of controlling fundamental radiation characteristics, such as beamwidth, beam shape, sidelobe levels, and radiated power, in order to realize the different antenna characteristics required by the various systems. It is also intended to have a "self-healing" capability to retain a degree of usefulness in the event of battle damage or component failures.

In order to meet the above objectives, the approach studied is an active array. The array aperture consists of a large number of radiating elements that are spaced approximately a half-wavelength at the upper end of the operational frequency band. The frequency response and excitation of each element in the aperture can be independently controlled. This enables the antenna to reconfigure around damaged areas or to vary the array illumination. The aperture can be fully utilized at the lowest frequency or can be shared among functions operating at higher frequencies. Figure 1-1 illustrates these concepts.

The capability of the array to provide multiple simultaneous configurations, and to rapidly alter the set of configurations, is due to an active element control circuit. One of many possible control circuits is shown in figure 1-2. The combination of the variable attenuator and phase shifter permits the array illumination to be modified and the antenna beam to be scanned in any direction.

The tunable filter specifies the portion of the aperture used by a particular system. Several MMIC circuits are envisioned to incorporate the above components.

The power divider operates over the specified frequency bandwidth, simultaneously receiving and/or transmitting the signals from the systems sharing the aperture - the signals are separated at the power divider input by a multiplexer.

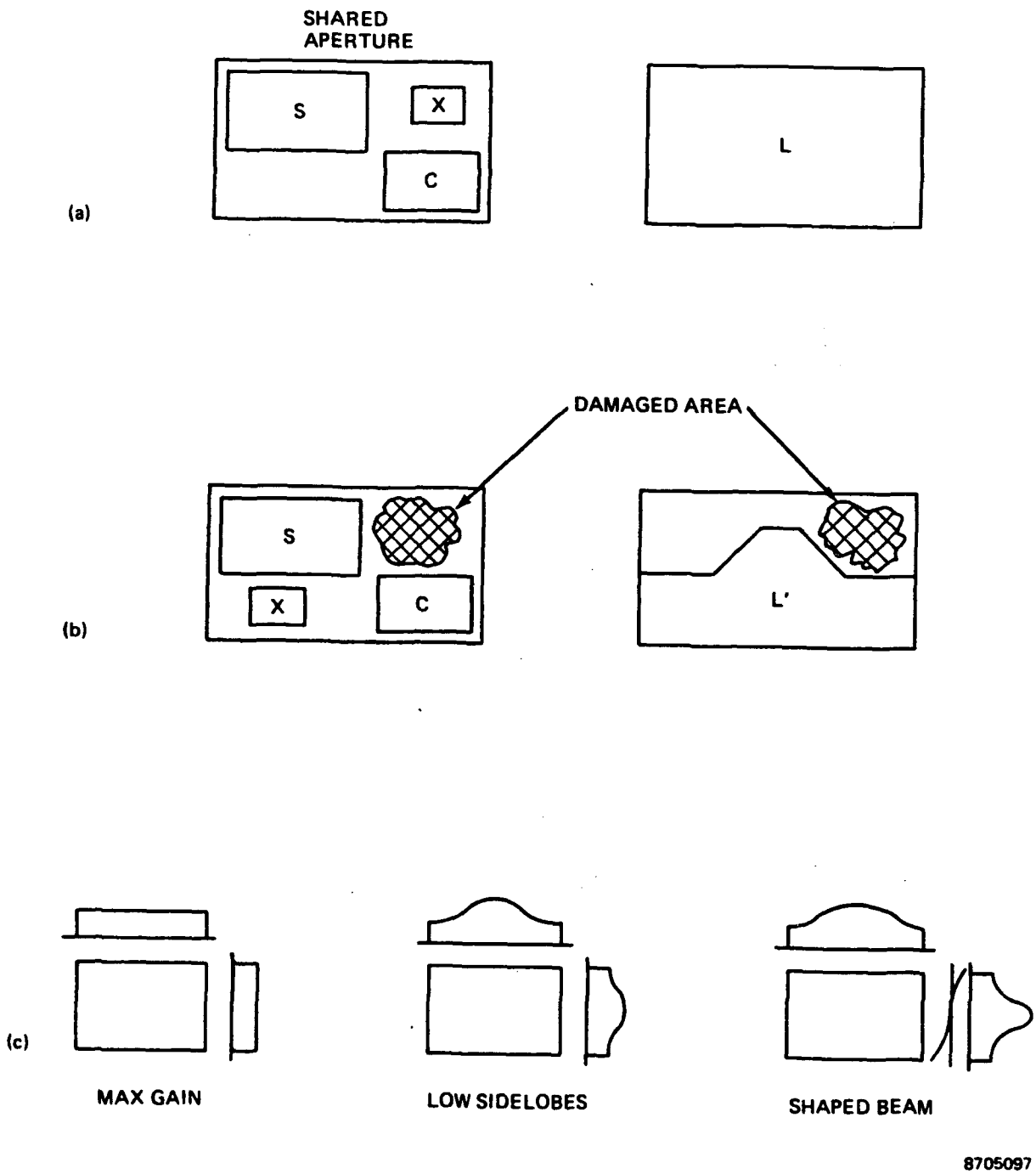

Figure 1-1. Reconfigurable Array Showing Multifrequency, "Self-Healing" Capabilities, and Control of Radiation Characteristics

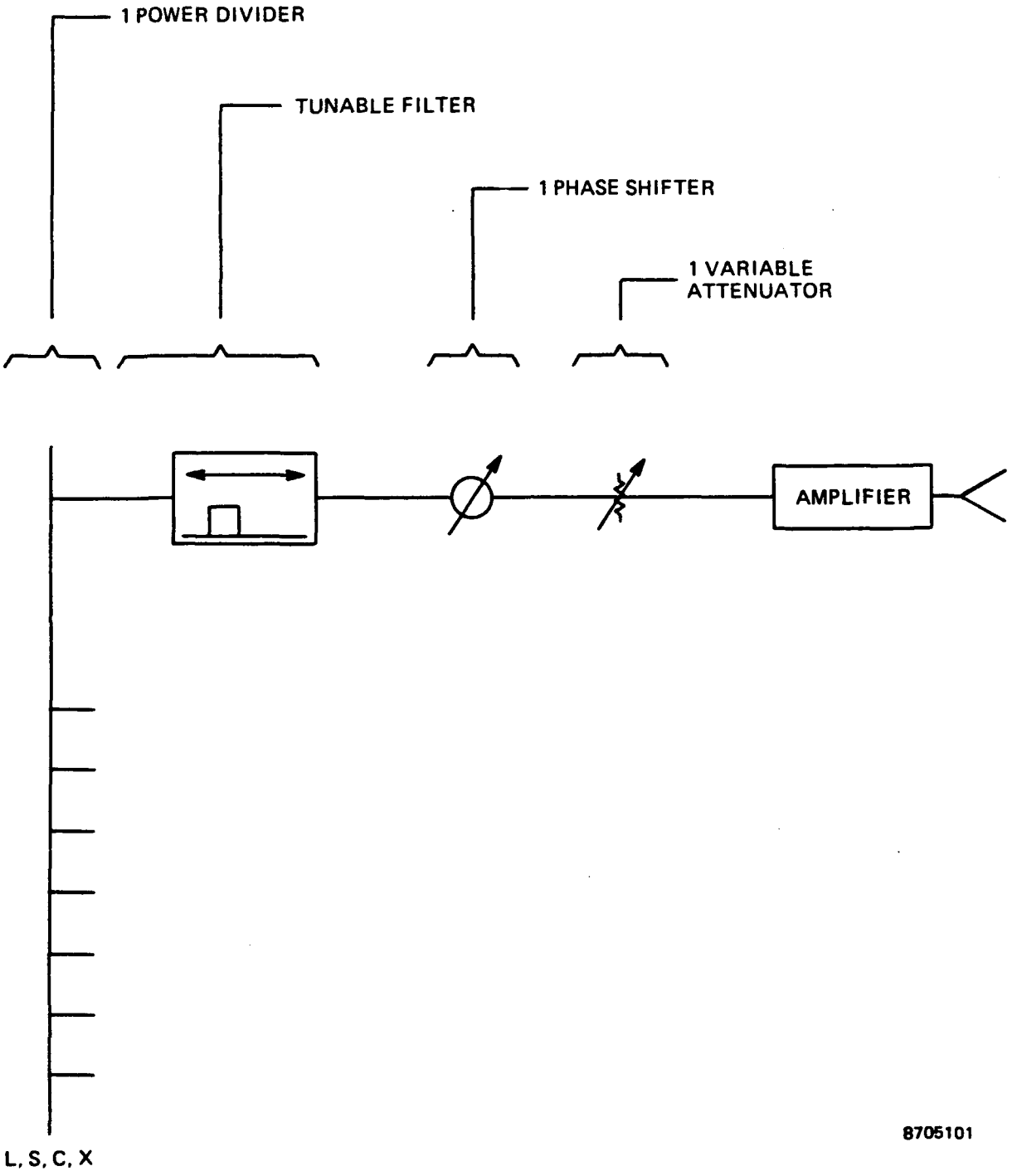

Figure 1-2. Active Element Control Circuit for Reconfigurable Antenna

A decade bandwidth power divider has been designed and tested under this program. This design is used in the laboratory model of the array discussed in this report. Also included in the laboratory model of the array are two other key features of the active element control circuit; these are aperture filtering and a MMIC variable attenuator. A photograph of the array is shown in figure 1-3.

The mathematical analysis has been completed and a computer code written for calculating the reflection and transmission coefficients of a radiating element in an infinite array. This program computes the fields scattered by a periodic structure or computes the induced fields on the structure excited by a current source. The structures, which can be modeled, are composed of metallic surface elements arranged in an array, in air, which is periodic in two dimensions and may have depth in the third dimension. The metal surfaces may have a non-zero surface impedance. Certain classes of feed structures, such as microstrip, can also be included in the element model. Consequently, the code can be used to evaluate the element/feed performance over wide frequency and scan ranges. This work was subcontracted to Georgia Technical Research Institute (GTRI).

This report is comprised of five sections. Section II describes the reconfigurable array concept in greater detail. The laboratory model of the array is described in Section III while the measured results illustrating array reconfigurability are presented in Section IV. Section V summarizes the program's accomplishments. An interim report describing a breadboard power divider and tunable filter, as well as a discussion of the radiating element analysis performed by GTRI, can be obtained from the Government's technical monitor.

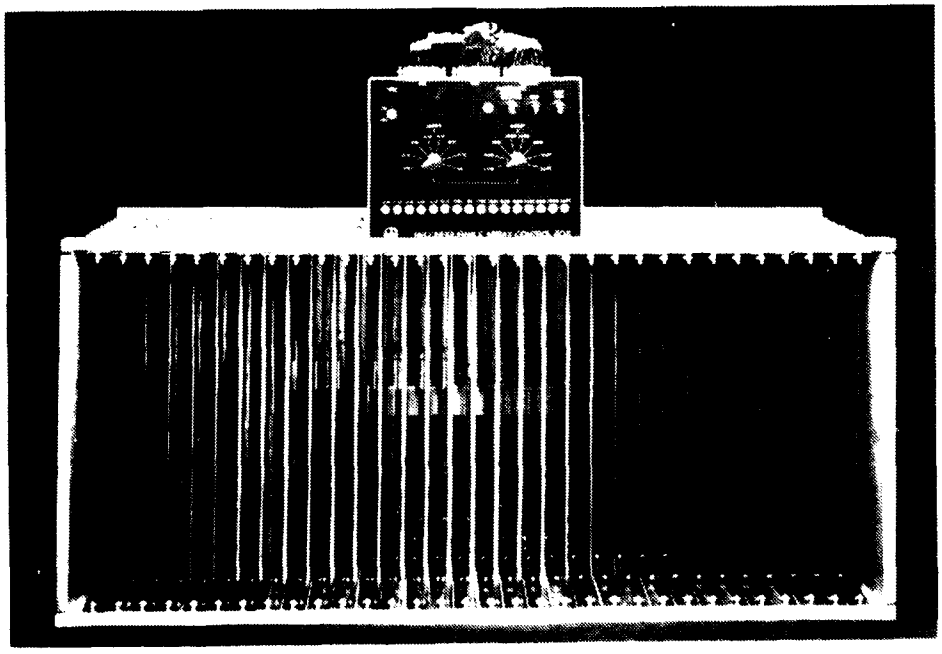

900422

Figure 1-3. Photograph of Demonstration Reconfigurable Array

SECTION II

RECONFIGURABLE ARRAY APPROACH

2.1 OVERVIEW

Airborne radar, EW, ESM/ELINT, and communication systems differ significantly in their antenna requirements. Not only do the various systems differ in the primary functions, but the many variations within any one system will affect antenna requirements. For example, an airborne radar system may be configured functionally as a tracking system, search and track, altimeter, navigation, ground mapping, target acquisition, terrain following, etc. Each of these radar systems has aperture requirements unique to its function as modified by the location on the airborne platform. Additionally, radar, EW, and communication systems require both emission and reception of energy, whereas ESM and ELINT systems require only the reception of energy.

Clearly, the antenna beamwidth, beam shape, as well as scan volume, radiated power, and frequency bandwidth will need reconfiguration to accommodate the various systems.

A tactical aircraft can operate with a radar operating at C- and X-band. However, the need to provide ESM/EW functions at S-band and identification functions at L-band drives the requirement for full-frequency coverage from L- to X-band. A surveillance aircraft would require radar operation at L- and S-band. Similar arguments for ESM/EW apply. Thus, we may conclude that it is desirable for all applications to have an array that covers L- through X-band; although two arrays operating over consecutive 3:1 bandwidths may be a more practical alternative when consideration is given to locating the array(s) on the aircraft.

The approach studied under this program can be utilized for either the narrow or wide bandwidth arrays. The capability for changing the array excitation amplitude and phase distribution across a particular aperture requires a control circuit.

2.2 CONTROL CIRCUIT ALTERNATIVES

Several control circuit configurations are feasible; each configuration contains an arrangement of filters, attenuators, and phase shifters. Because practical implementation of these components introduces substantial loss, a wideband amplifier used behind each radiating element overcomes the loss. This amplifier typically comprises a power amplifier for transmit and a low-noise amplifier for receive, plus transmit/receive switches.

One approach for the control circuit employs a separate power divider, phase shifter, and variable attenuator for each frequency band. Assuming four frequency bands (i.e., L, S, C, and X), there would be four power dividers feeding the entire array, and four phase shifters and variable attenuators for each radiating element of the array. This circuit is shown in figure 2-1. It gives a degree of control that is probably greater than necessary and requires a very large number of components packed into a small space. This approach is not recommended.

Another approach for the control circuit avoids the need for four power dividers by using four bandpass filters (or one equivalent multiplexer) per radiating element. This circuit is shown in figure 2-2. A single multiplexer at the input (not shown) would probably also be used. Four octave-band phase shifters are shown per element. These could be replaced by one decade-band phase shifter behind the amplifier, assuming that simultaneous multiband operation of each radiating element is not needed. There are still four variable attenuators needed per element in order to provide the necessary reconfigurability. A variation of this type of control circuit is used in the laboratory model of the array tested under this program and discussed later in this report.

An approach employing only one variable attenuator per element uses one electronically tunable bandpass filter per element. This circuit is shown in figure 2-3. One phase shifter per element is used in this approach, which assumes that simultaneous multiband operation of each radiating element is unnecessary. The practical tuning range of a filter limits the usefulness of this approach to the narrower bandwidth arrays.

A study on the tuning range of a lumped-element bandpass filter, using varactor diodes as the variable element, is discussed in the interim report under this program. The design is suitable for HIC-type construction; it uses 4-nH inductors formed from two turns of 1.4-mil-diameter wire. The varactor diodes have C_{j0} of 0.4 and 2.9 pF, with a capacitance range of 5:1 at maximum bias. Briefly summarizing, the filter could be tuned from 4.5 to 9.9 GHz using the pair of varactor diodes. The bandwidth of the filter varied between 25% and 11% at the frequency limits. The computed results are shown in figure 2-4. A recent publication [1] shows a similar tuning range for a varactor-tuned notch filter. Thus, a 2:1 tuning range is probably the limit for this type of control circuit. The relatively narrow tuning range of an electronically-tuned filter can be overcome by replacing it with a bank of fixed-tuned bandpass filters that are switch selectable. This alternative is shown in figure 2-5.

---

[1] Toyoda, S., "Notch Filters with Variable Center Frequency and Attenuation," IEEE MTT-S, Vol. II, pp 595-598, June 1989.

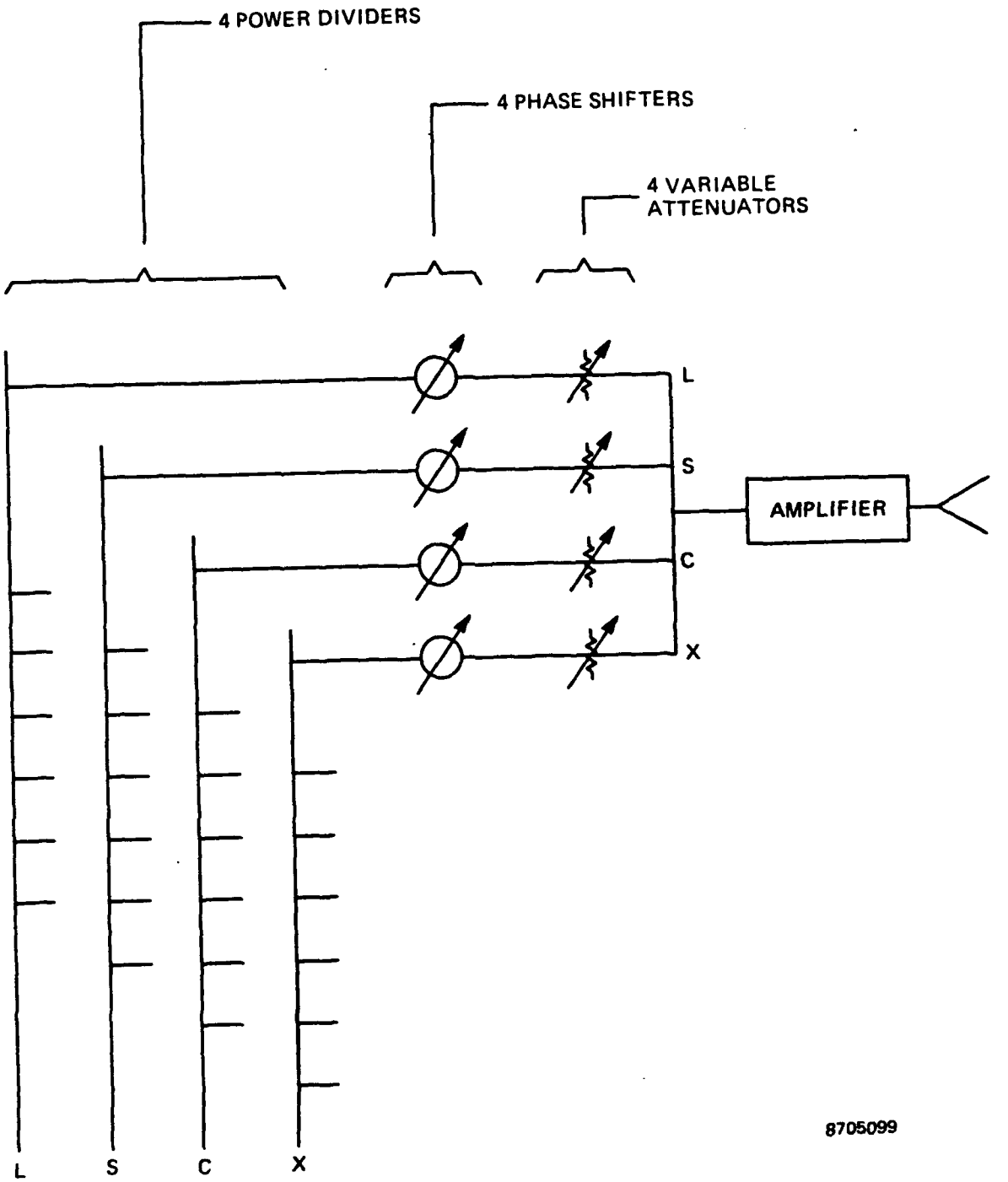

Figure 2-1. Multiple Divider Control Circuit Requires Complex Packaging of Components

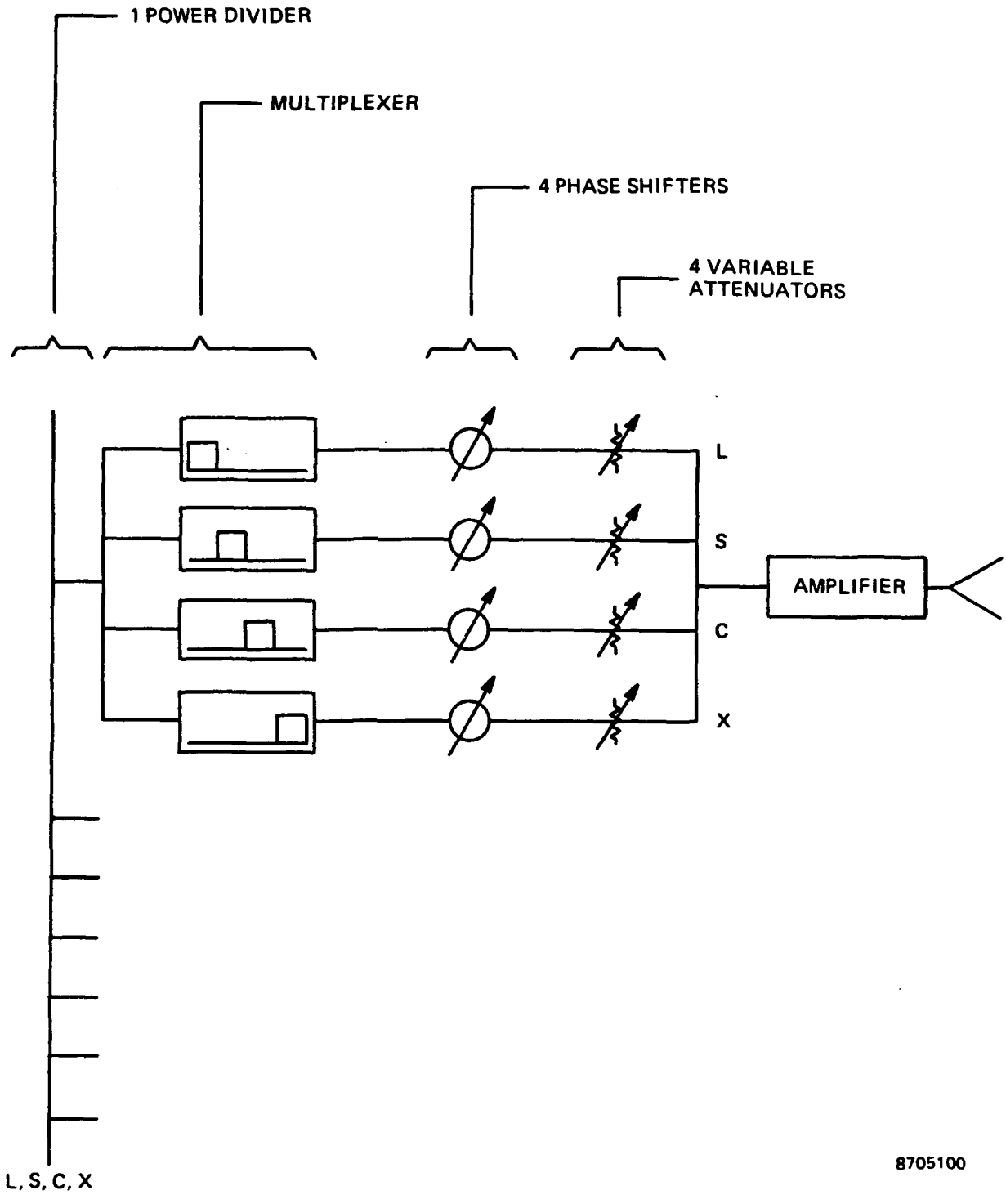

Figure 2-2. Multiplexer Control Circuit is Applicable for Widest Bandwidth Arrays

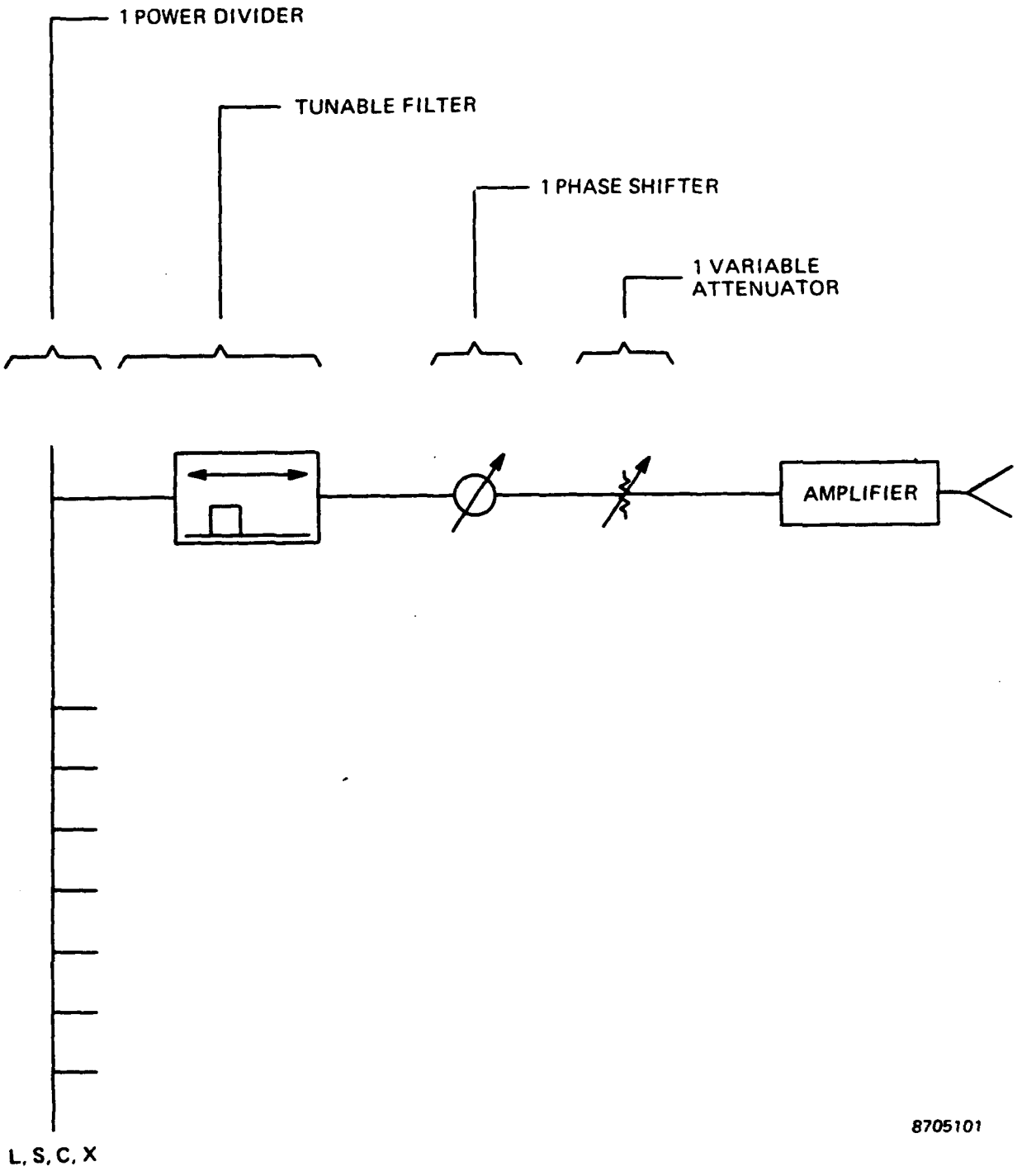

Figure 2-3. Tunable Filter Control Circuit is Useful for Narrower Bandwidth Arrays

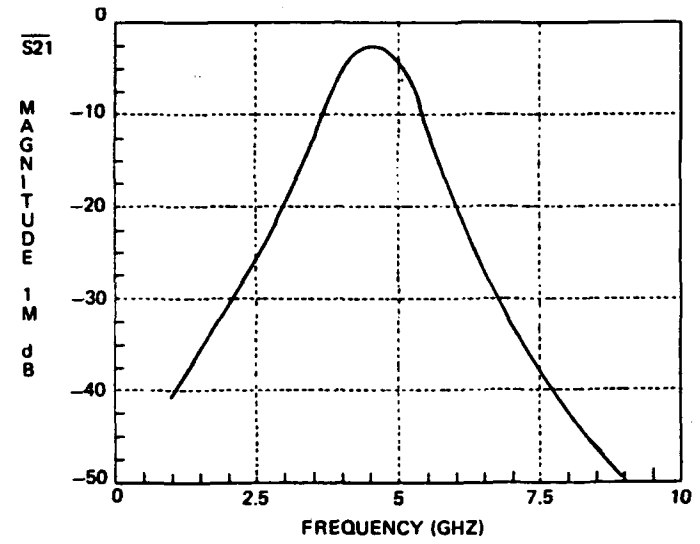

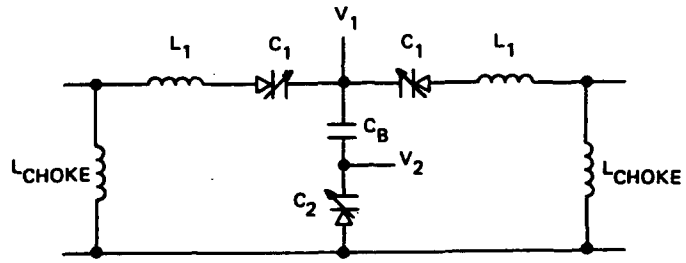

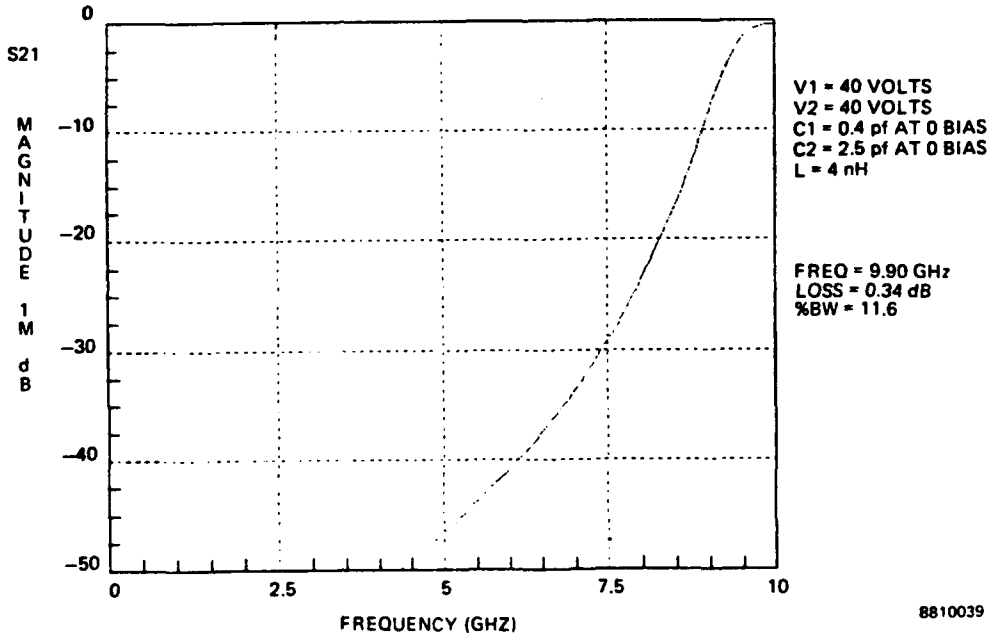

Figure 2-4. Computed Tuned-Frequency Responses of a Lumped-Element Two-Section Bandpass Filter

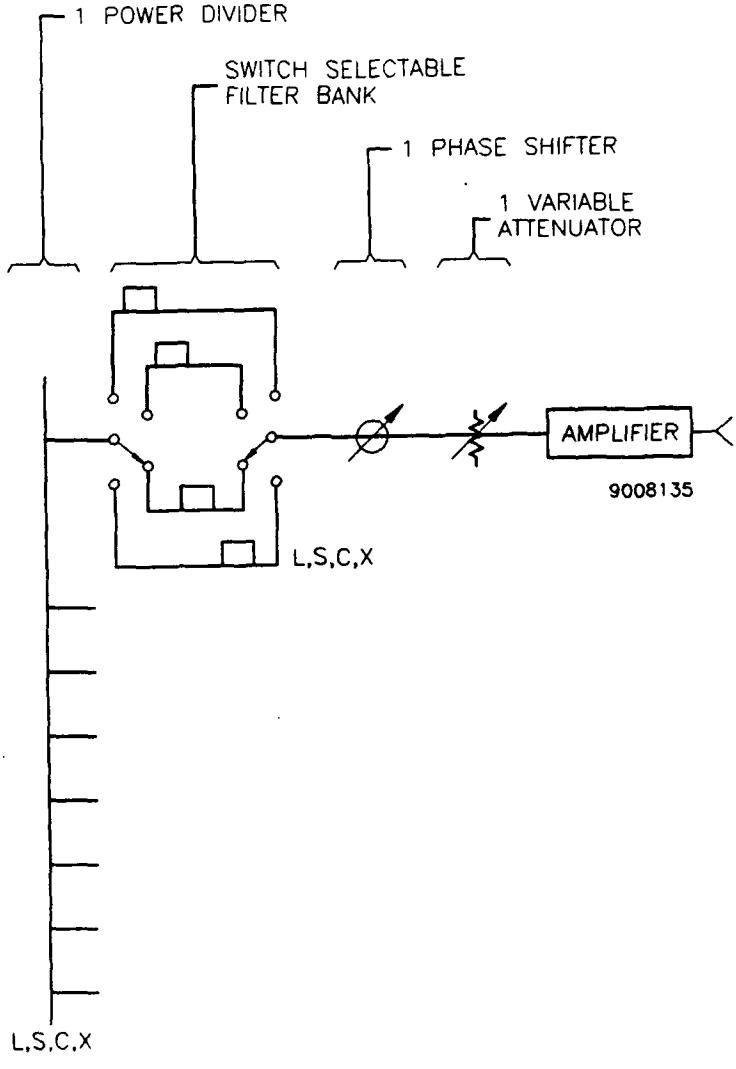

Figure 2-5. Switch Selectable Fixed-Tuned Bandpass Filter Control Circuit is Useful for Widest Bandwidth Arrays

There are various combinations of the several control circuits that can be considered. Figure 2-6 depicts an example in which there are two branches (rather than four or one) per element. One branch uses a fixed L-band (1- to 2-GHz bandpass) filter and a 1- to 2-GHz phase shifter, plus a variable attenuator. The other branch uses an electronically tunable bandpass filter. This approach allows simultaneous operation of each radiating element at 1 to 2 GHz (L-band) and over the tuning range of the filter. The end result can be an antenna that operates simultaneously at all frequencies, as indicated in figure 2-7. This capability is desirable in reception because the incoming signals at various frequencies may arrive simultaneously, are weak, and are not likely to create modulation products in the RF amplifier.

Additional filtering (not shown in figures 2-2 to 2-6) will likely be needed prior to the low-noise amplifier, in order to prevent amplifier saturation caused by a neighboring transmitting aperture operating in another frequency band. The practical aspect of operating a transmitting antenna in close proximity to a receiving aperture may ultimately limit the degree of reconfigurability possible.

The recommended configuration for decade-bandwidth operation utilizes a combination control circuit with a fixed-tuned L-band filter in one branch and a bank of switch selectable bandpass filters in the second branch. This approach allows simultaneous operation at L-, S-, C-, and X-bands, as shown in figure 2-8.

It is noted that if a part of the array is damaged or fails, the remaining undamaged part of the array may still be large enough to contain all of the X-, C-, and S-band apertures simultaneously. A smaller undamaged part could also be used for these frequencies, with some sacrifice of simultaneous operation. At L-band, a reshaping of the active aperture would allow operation with some sacrifice of gain and beamwidth, as illustrated in figure 1-1(b).

Laboratory Array Objectives

The laboratory model of the array designed, fabricated, and tested under this contract uses a form of the multiplexer control circuit. The principal objective of the laboratory array is to investigate interactions between filtered apertures. Another objective is to measure pattern degradation caused by using filters in each channel of the array.

A computed example of array interaction is shown in figure 2-9. Ideally, the filter provides infinite rejection of frequencies outside the signal passband. Areas of the aperture that do not contribute to the useful signal are completely blacked out by the ideal filter. A practical filter provides a large but finite rejection of signals outside the passband. This implies that power incident on the blacked-out sections of the array will introduce an unwanted signal at the input of the antenna.

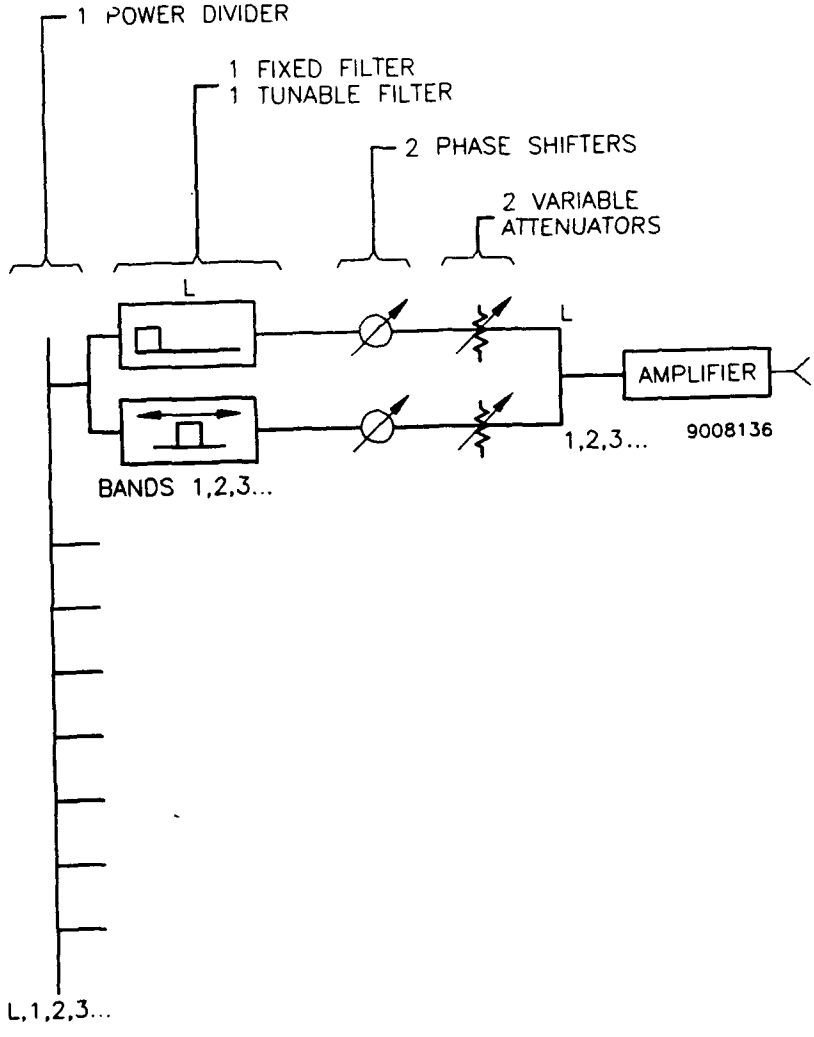

Figure 2-6. Combination Control Circuit Permits All Bands to be Received Simultaneously

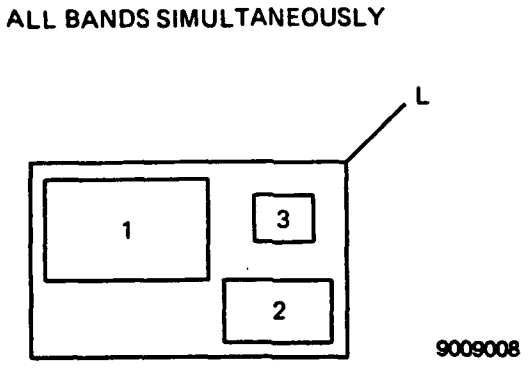

Figure 2-7. All Bands are Received with a Combination Control Circuit

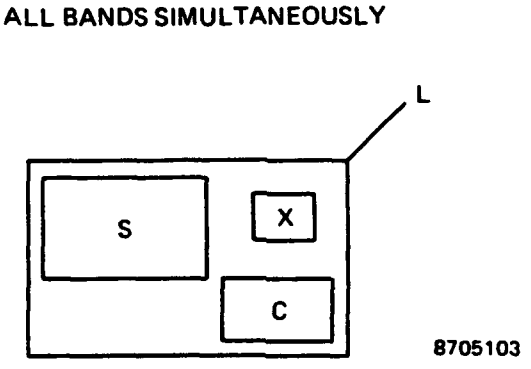

Figure 2-8. Decade-Bandwidth Reconfigurable Array Uses a Combination Control Circuit

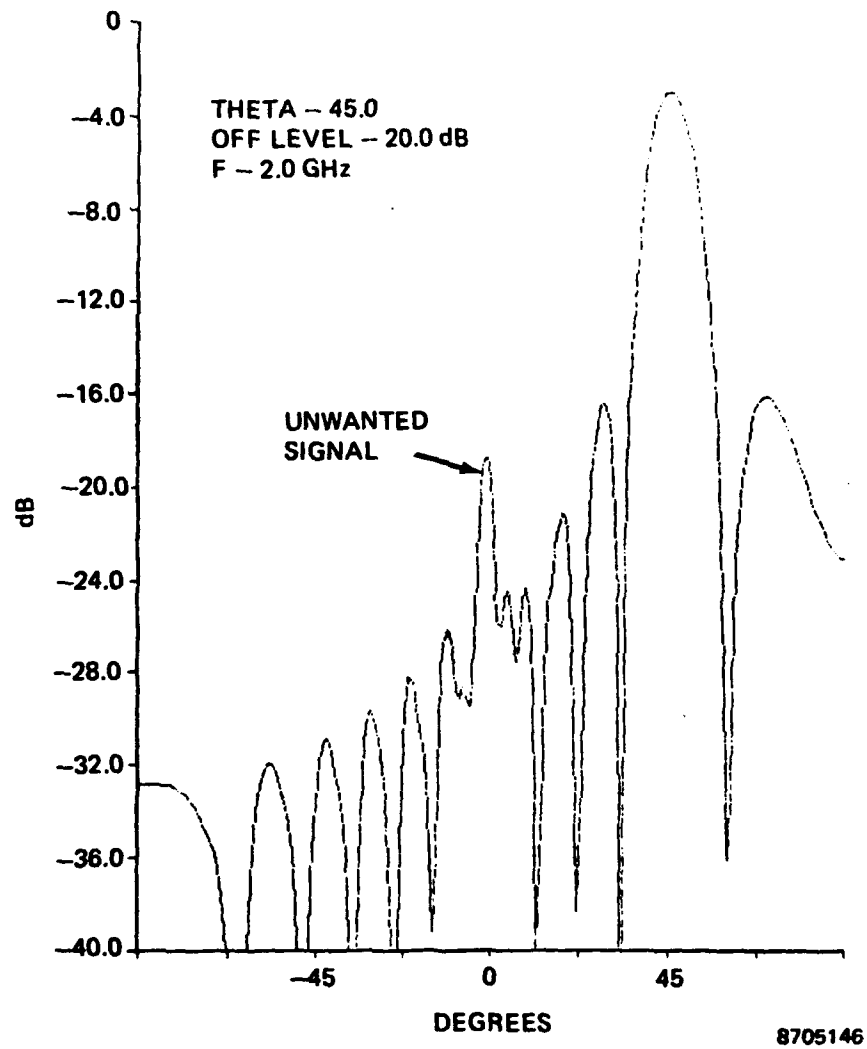

Figure 2-9. Effect of 20 dB of Filter Rejection on a 3-Foot by 3-Foot Array Located within a 3-Foot by 6-Foot Reconfigurable Array

The unwanted component of a signal can lower array gain and raise sidelobe levels. The magnitude of unwanted power is not only dependent upon the filter characteristic, but also on the relative sizes of the functional and blacked-out areas of the aperture.

The computed result shown in figure 2-7 uses an array 3 feet by 6 feet with elements spaced 0.5 inch apart. The array is to operate at S-band (2 GHz). All elements not within the S-band array are set for maximum attenuation. The S-band array is 3 feet by 3 feet.

In this example, the blacked-out elements are assumed to be excited in phase by an incident wave. This is a worst-case assumption because it is likely that the other areas of the array will be operational at other frequency bands and their beams will be directed to different regions of space. Therefore, the phase of the signals collected by these areas at S-band will not be in phase. The attenuation of the filter was adjusted to be 20 dB in the blacked-out area of the antenna. In order to show the spurious signal introduced by finite rejection of the filter, the S-band array was scanned 45 degrees from broadside. The spurious signal is at 0 degree in figure 2-9.

2.3 ARRAY ELEMENT DESIGN

In order to avoid grating lobes, a phased array should have a spacing between radiating elements no greater than about a half-wavelength at the highest frequency. Of course, as the frequency bandwidth of the array is increased, substantially more elements are used than are required at the low end of the frequency bandwidth. The general approach for the reconfigurable array element lattice is shown in figure 2-10. Note the elements are unusually small at the lower end of a decade frequency band.

The type of element appropriate for a reconfigurable array depends upon the operational bandwidth. Many element types have design features that make them inherently incapable of wideband (decade-band) operation. One such narrowband feature is the use of a reflecting plane a quarter-wavelength behind a bidirectional radiator to convert it to a unidirectional radiator. Dipole, slot, and patch radiators need reflecting planes. Substantial departure from the optimum ground plane spacing introduces an unwanted reactance component in the impedance.

Although an element such as a resonant (quarter-wavelength) notch radiates from the edge of a metal sheet, similar undesirable effects on impedance are observed if the bandwidth is sufficiently widened. Arrays consisting of short-notch elements have been operated over maximum bandwidths of 4:1, although a 3:1 bandwidth is more typical.

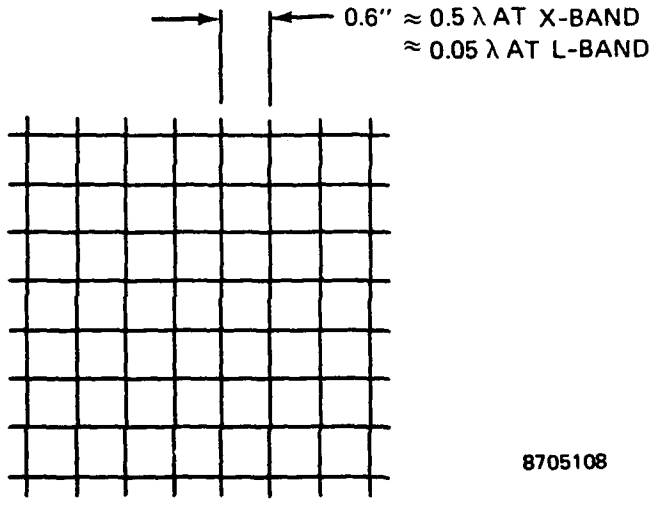

Figure 2-10. Element Lattice for a Reconfigurable Array

For a decade bandwidth, a traveling-wave radiator is the appropriate element choice. This type of radiator is inherently unidirectional and does not need a reflecting plane. If the traveling-wave radiator is at least a half-wavelength long at the lowest operating frequency, and is gradually tapered to provide a good impedance match between the circuit transmission line and free space, then good wideband (perhaps decade-bandwidth) performance can be achieved. Examples of traveling-wave radiators include a horn or a long tapered-notch element.

Historically, either waveguide simulators or small arrays have been used to design radiating elements. These techniques have been more successful than computational methods, since the latter have not been able to model many of the practical aspects of element construction because of computer run-time limitations.

Often, the neglected aspects of the element construction affect the element tuning, requiring a simulator to optimize the design. Therefore, a computational technique is a good first-order method for evaluating radiator performance. A computational capability is essential for evaluating the variety of elements that may be used in the different reconfigurable array approaches. It is the only technique that is practical for evaluating a decade bandwidth element.

For a decade bandwidth array, a serious problem exists with conventional design procedures. Since the wideband elements are electrically quite small at the low-

frequency end of the decade frequency band, an array of, for example, 25 elements may be only about a half-wavelength wide at the low frequency. This is not large enough to guarantee performance close to that of a much larger array.

Of course, a much larger array could be built and tested. However, this would be prohibitively expensive and time consuming, since each modification to the design would require the construction of a large number of elements.

A simulator can be economical and expeditious for narrow or moderate frequency bands. However, for a decade frequency band, many simulators would be needed. A combined small array/simulator, comprising two metal sheets parallel to the H-plane, avoids the need for many simulators and uses fewer elements than a two-dimensional array, but still would necessitate the construction and reconstruction of many elements during the design. Furthermore, scan in the E-plane could not be simulated.

The elements suitable for the reconfigurable array are periodic in two dimensions and may or may not have depth in the third dimension. Thus, a general computer code is needed to model the variety of element types. Georgia Technical Research Institute (GTRI) has performed a mathematical analysis and written a computer program to model an element of arbitrary geometry. The structures that can be modeled are periodic in two dimensions and can have depth in the third dimension.

The radiating elements are composed of imperfect surface conductors in an air medium. The currents on the radiating elements are described with a triangular patch basis that allows the element geometry to be arbitrary. The key feature of this code is that the elements may have depth in the direction perpendicular to the array surface. The electromagnetic scattering properties of this general type of structure are then analyzed in terms of Floquet modes. The array can be either passive, in which case its reflection and transmission coefficients can be determined, or it can be driven with a current ribbon source, in which case the radiated power and input impedance can be computed.

The code has been validated against published impedance data on dipole arrays, as well as against impedance data available on a resonant-notch element located in an infinite array waveguide simulator. This latter case verified the code could accurately model elements with depth. During the validation process, it became apparent that the codes' run time would be excessive for designing a decade bandwidth radiator, since it requires many triangular patch elements to adequately model the radiator.

At this point in time, the code is partially validated and is useful as a tool for evaluating, not designing, a wideband element; the distinction being that a design tool requires a quick turnaround enabling iterations. As a result of the codes' run-time limitations, the element selected for the laboratory model of the array is an existing 3:1 bandwidth notch element developed on a previous RADC program. This element has sufficient bandwidth to show the effect filters have on array performance - a key aspect of the reconfigurable array approach.

SECTION III

DEMONSTRATION ARRAY

3.1 DEMONSTRATION ARRAY OBJECTIVES

The reconfiguration features of the proposed approach are achieved by using filters in the array aperture. Ideally, the filters are transparent within a selected aperture and provide infinite rejection of unwanted power from adjoining apertures. In practice, the amplitude and delay characteristics of a filter can affect the in-band antenna pattern performance. Finite filter rejection can allow unwanted power from neighboring apertures to corrupt the antenna's characteristics by decreasing gain or increasing sidelobes.

The objectives of the demonstration array are, therefore, two-fold: (1) Measure antenna patterns within the passband of the filter. The array excitation amplitude should be tapered showing the filter's effect on low sidelobe illuminations; (2) by using two sets of filters, measure the interaction between adjoining apertures.

3.2 DESCRIPTION OF DEMONSTRATION ARRAY

The laboratory model of the reconfiguration array consists of 32 columns of 3:1 bandwidth notch elements. Each column has 10 elements fed by a 10-way microstrip power divider designed under this program. At the input to each column, and attached to the microstrip board, is a MMIC variable attenuator that will be used to change the array excitation. The columns are connected to a 32-way power divider through a set of cables that permit attachment of different arrangements of filters. Figure 3-1 shows a front view of the reconfigurable array, control box and associated block diagram.

3.3 ELEMENT DESIGN

The element selected for the laboratory model of the reconfigurable array is a folded notch element designed under a previous RADC program (figure 3-2). The array spacing is 0.984 in. in the H-plane and 1.36 in. in the E-plane. The element matching was designed using a parallel plate waveguide simulator with seven elements arrayed in the H-plane (figure 3-3a). The angle of incidence was varied within the guide by using sets of cables that provide the required phase shift between elements. The resulting impedance match for 0-degree incidence is shown in figure 3-3b.

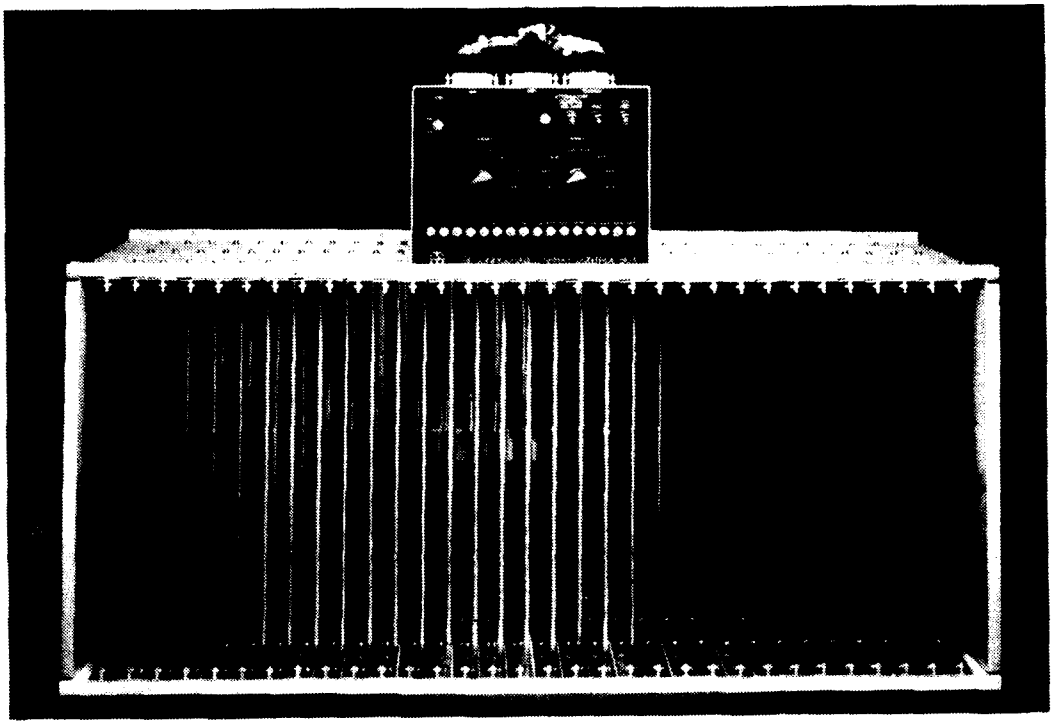

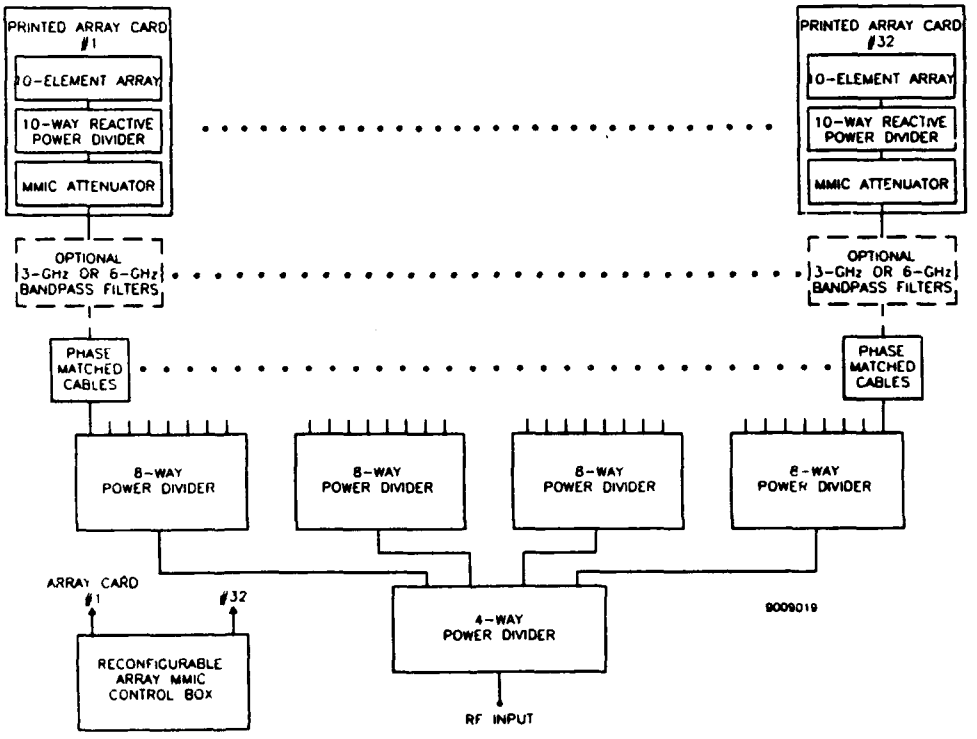

Figure 3-1. Front View of Reconfigurable Array, Control Box and Associated Block Diagram

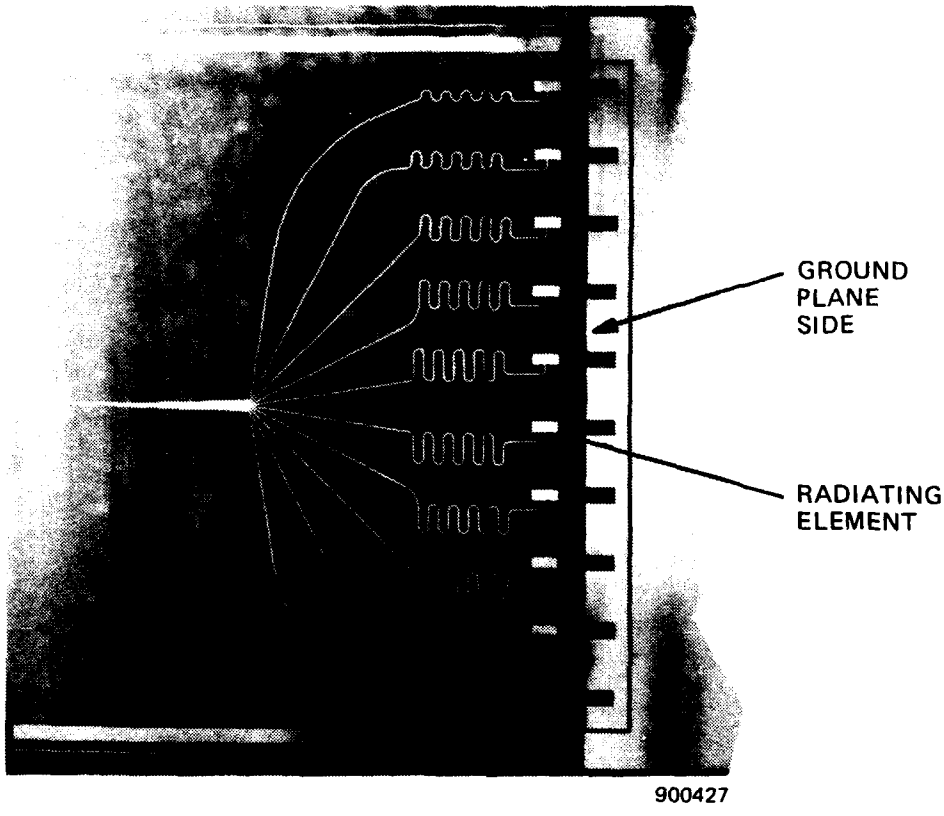

Figure 3-2. Folded Notch Element

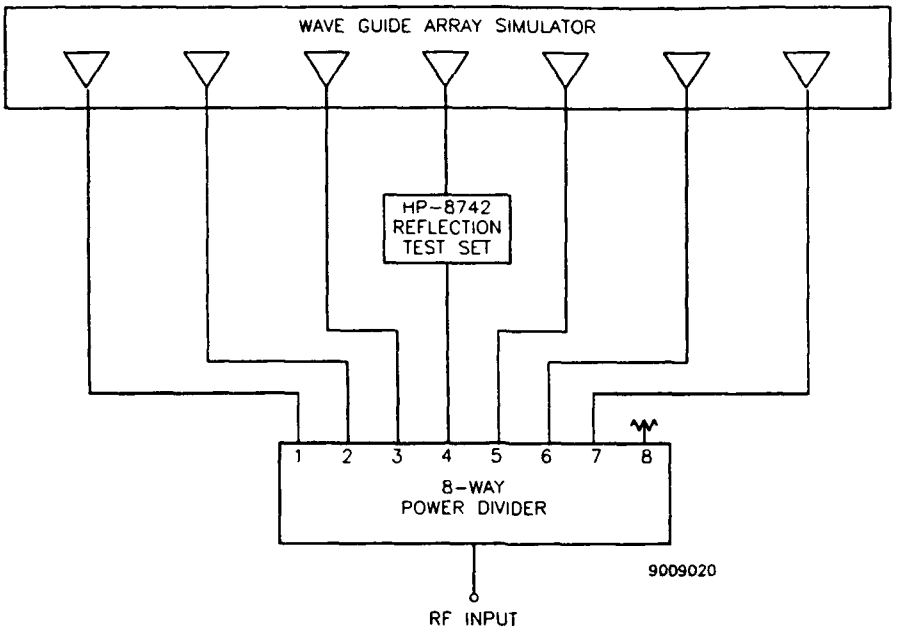

a. Parallel Plate Waveguide Array Simulator

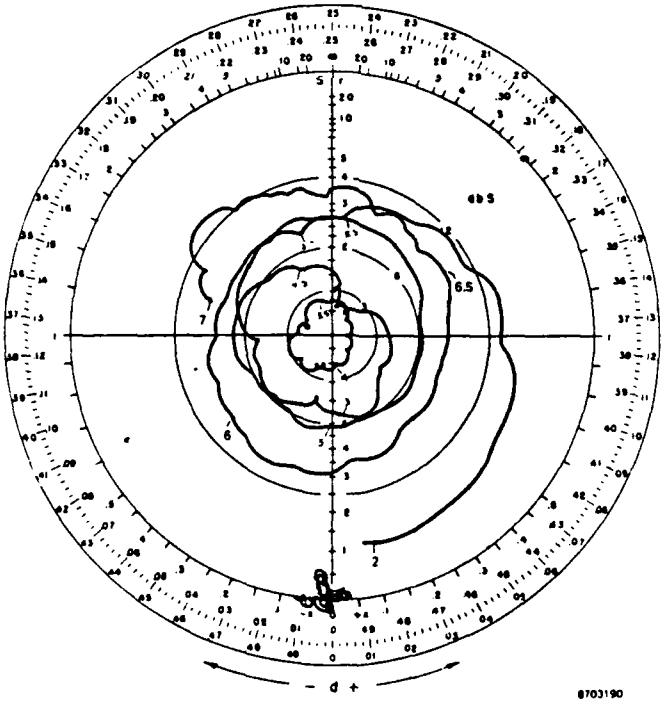

b. Active Reflection Coefficient of Folded Notch Element Measured in Parallel Plate Simulator for 0-Degree Incidence

Figure 3-3. Element Matching and Resulting Impedance

3.4 POWER DIVIDERS

The experimental array of 32 antenna cards is fed by four eight-way Wilkinson type power dividers which, in turn, are fed by a four-way power divider. These purchased parts were chosen for their good isolation between ports, typically 17 dB minimum over a 2- to 8-GHz bandwidth. The use of the purchased components simplifies the antenna layout permitting easy access to the filters, as shown in figure 3-4.

A decade bandwidth 10-way reactive divider was fabricated on 0.010-in. Duroid, as shown in figure 3-5. It is used to feed the 10-notch antenna elements on each antenna card, as shown in figure 3-6.

The power divider branch impedances vary from 122 to 82 ohms. This corresponds to line widths of 0.0046 in. to 0.0124 in., respectively. These branch impedance levels provide an equal 10-way power split across the decade bandwidth while maintaining good impedance match. Figure 3-7 shows the measured amplitude split of the 10-way divider. The output branch lines exponentially taper to 50 ohms (0.030 in.) from the 10-way junction. Serpentine lines provide equal electrical phase lengths to the radiating elements.

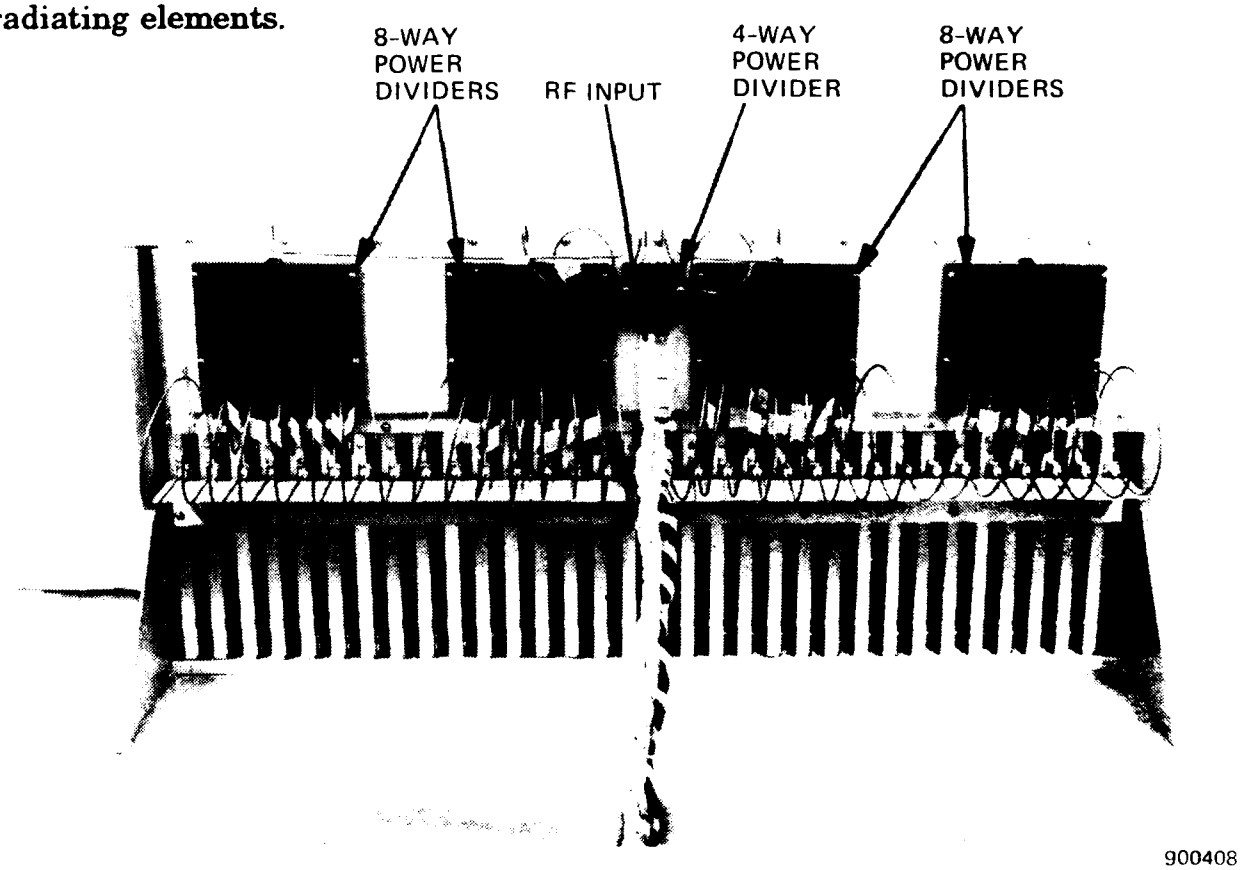

Figure 3-4. Eight-Way and Four-Way Power Dividers

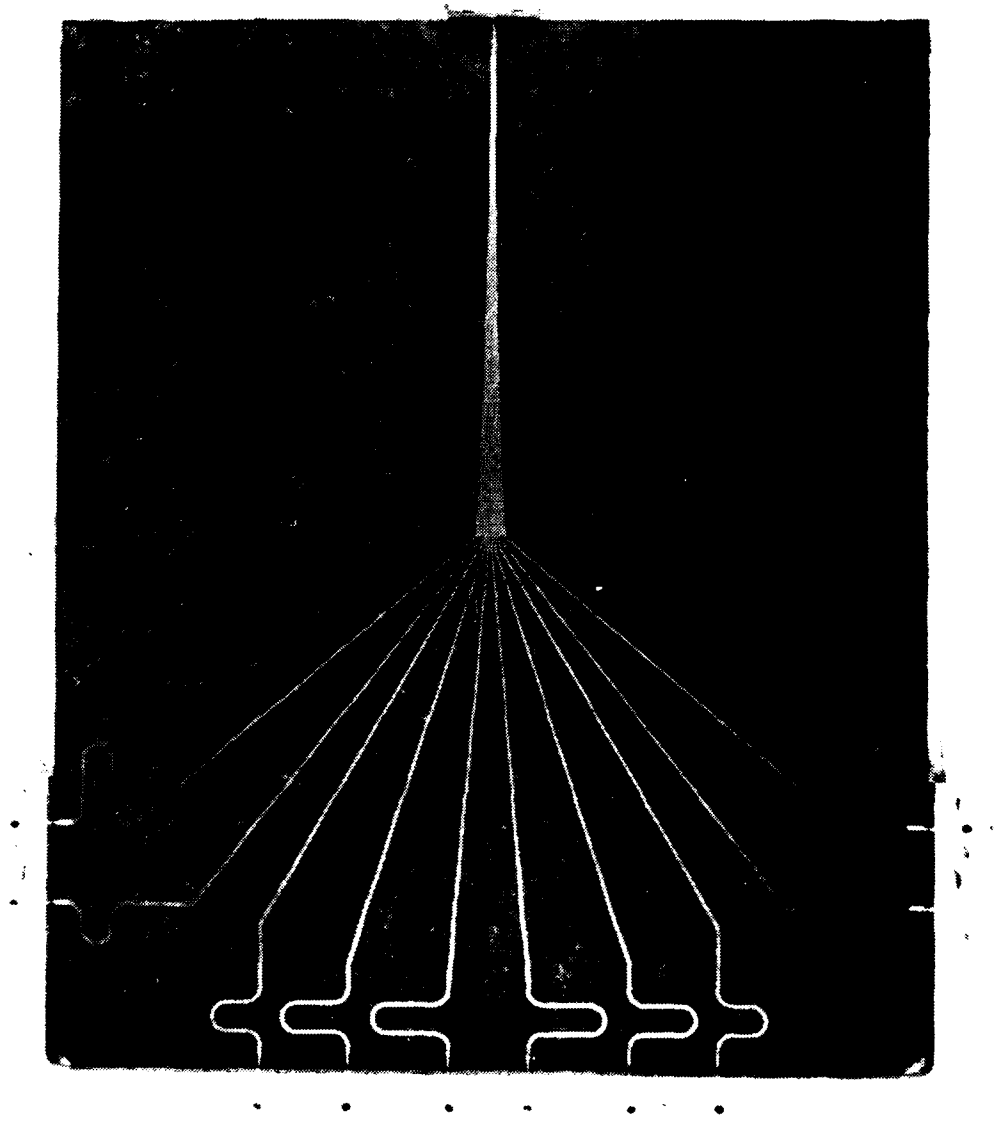

880152

Figure 3-5. Photograph of Decade-Bandwidth 10-Way Reactive Power Divider with Impedance Taper Across Output Branches

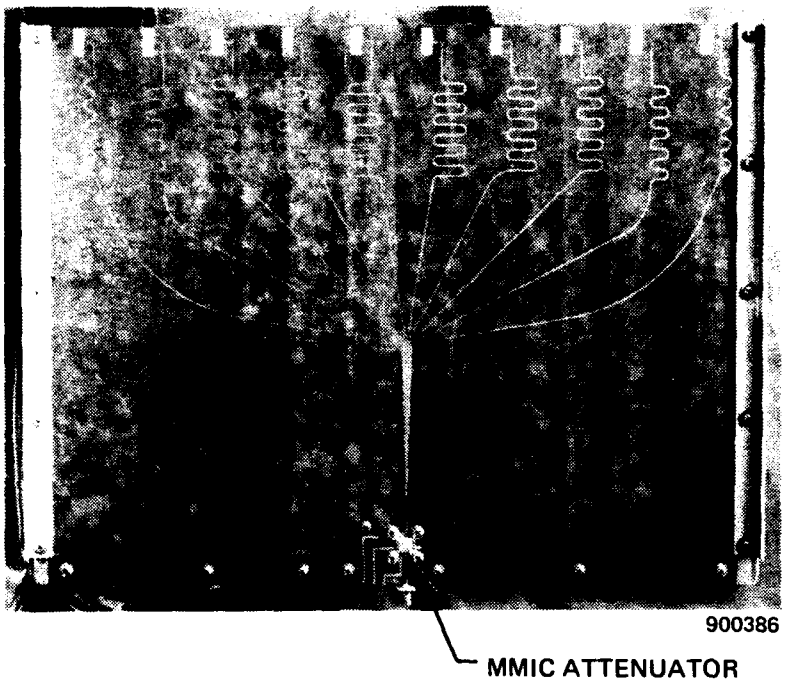

Figure 3-6. Antenna Card

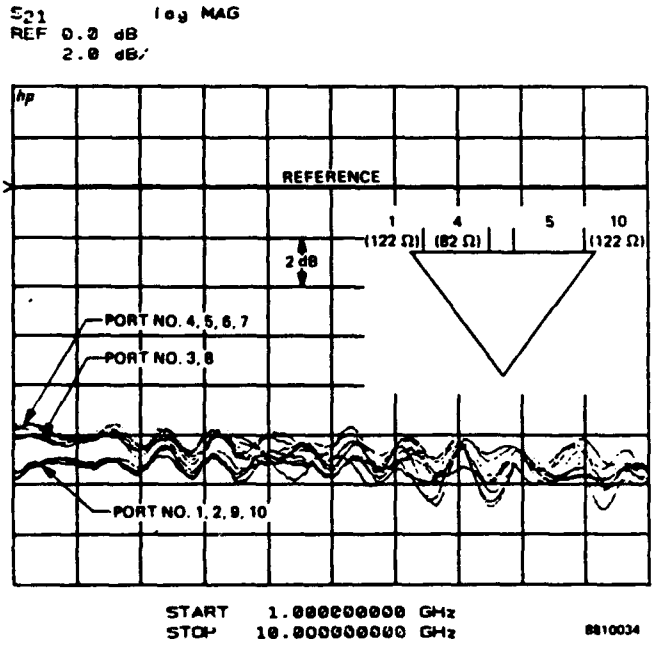

Figure 3-7. Measured Amplitude Split for a 10:1 Bandwidth 10-Way Reactive Power Divider with Impedance Taper Across Output Branches

3.5 MMIC ATTENUATOR

A 1- to 10-GHz Microwave Monolithic Integrated Circuit (MMIC) variable attenuator was installed, as shown in figure 3-6, in each of the 10-element antenna array cards. The attenuator is used to control the aperture illumination.

The MMIC specifications are shown in figure 3-8. Figure 3-9 plots the amplitude and phase of a typical MMIC attenuator versus applied control voltage over a 1- to 10-GHz frequency range. The unit-to-unit phase tracking was measured and is very good. The maximum insertion phase deviation between the 32 units at a given insertion loss was measured to be less than 5 degrees. The voltage deviation among units for the lowest value of attenuation was less than 1.0 volt. Table 3-1 lists the control voltage and phase of each MMIC used for various insertion loss states.

Table 3-1. Phase and Voltage Data

MMIC S/N	Insertion Loss 2 dB		Insertion Loss 5 dB		Insertion Loss 9 dB		Insertion Loss 12 dB		Insertion Loss 14 dB		Voltage = 0.0 V	
	Phase (deg)	Voltage	Phase (deg)	Voltage	Phase (deg)	Voltage	Phase (deg)	Voltage	Phase (deg)	Voltage	Phase (deg)	Insertion Loss (dB)
1	-1.0	3.12	3.4	2.28	12.5	2.00	24.1	1.86	36.3	1.74	41.1	15.66
3	0.96	3.73	5.6	2.50	14.4	2.17	25.3	2.03	37.4	1.93	50.3	16.02
4	-0.36	3.24	4.0	2.29	13.2	2.01	24.8	1.87	37.4	1.76	46.8	15.99
5	-0.7	3.39	3.9	2.5	12.8	2.2	24.3	2.06	36.4	1.95	45.3	16.02
6	0.7	3.22	5.2	2.38	14.5	2.12	25.7	1.99	38.2	1.88	45.8	15.97
7	2.0	3.41	6.4	2.41	15.3	2.12	26.4	1.98	38.5	1.88	48.0	16.1
8	-0.7	3.15	3.7	2.41	13.0	2.12	25.0	1.96	37.0	1.74	34.8	14.72
9	0.1	3.27	4.3	2.40	13.3	2.11	24.7	1.98	36.8	1.87	44.2	15.98
10	0.4	2.97	4.8	2.21	13.9	1.93	25.2	1.79	-	-	-	-
11	0.2	3.01	4.7	2.36	14.1	2.09	26.6	1.94	-	-	-	-
12	2.1	3.00	6.3	2.38	15.9	2.09	28.0	1.94	39.6	1.76	38.4	14.85
13	0.4	2.97	4.8	2.41	14.5	2.14	26.2	1.99	38.6	1.78	36.5	14.72
14	1.0	3.18	5.4	2.43	14.7	2.15	26.3	2.01	39.0	1.87	41.2	15.43
15	0.2	3.35	4.7	2.46	14.0	2.16	25.2	2.03	37.4	1.92	45.7	16.11
16	1.22	2.91	5.7	2.33	15.4	2.05	27.9	1.9	40.7	1.7	39.6	14.9
17	0.8	3.36	4.8	2.5	13.8	2.2	25.5	2.06	37.8	1.94	45.5	16.11
18	-0.1	3.25	4.2	2.35	13.3	2.05	25.3	1.9	37.8	1.75	40.8	15.5
19	-1.4	3.02	3.1	2.31	12.5	2.03	24.8	1.89	37.1	1.74	38.9	15.2
20	0.2	3.19	4.9	2.33	14.2	2.05	26.3	1.92	38.4	1.82	46.7	16.04
21	1.0	3.42	5.5	2.47	14.4	2.17	25.6	2.04	37.5	1.94	48.7	16.39
22	0.5	2.95	4.8	2.37	14.0	2.08	26.2	1.93	38.5	1.73	37.6	14.97
23	-0.1	3.02	4.4	2.41	13.8	2.12	25.7	1.97	38.0	1.79	37.3	14.97
24	0.2	3.13	4.6	2.41	13.8	2.15	25.5	2.01	38.0	1.88	41.7	15.6
25	-0.6	3.06	3.9	2.38	13.4	2.12	25.6	1.99	38.5	1.83	39.3	15.26
26	1.3	3.12	5.8	2.36	14.7	2.09	26.3	1.95	39.6	1.83	45.9	15.95
27	-0.2	3.2	4.3	2.46	12.9	2.13	25.0	1.98	37.4	1.85	41.7	15.65
28	-0.2	3.17	4.3	2.43	13.2	2.14	24.8	2.00	36.7	1.88	42.2	15.77
29	0.1	2.86	4.4	2.24	13.5	1.97	25.6	1.82	38.2	1.66	39.1	15.1
30	-0.1	3.36	4.4	2.47	13.6	2.19	25.6	2.05	38.5	1.92	42.5	15.65
31	0.7	3.39	5.2	2.47	14.0	2.18	25.4	2.04	37.0	1.93	47.5	16.21
32	1.3	2.96	5.5	2.38	14.8	2.10	26.9	1.95	37.9	1.85	35.5	14.5
33	1.3	3.41	5.8	2.5	14.5	2.22	26.0	2.08	38.4	1.97	49.4	16.4

ELECTRICAL CHARACTERISTICS

Absolute Maximum Ratings

	MIN	MAX	UNIT
DC Power Supply		16	V
Operating Temp	-55	+85	°C
Storage Temp	-55	+150	°C
Power Dissipation		1.5	W

DC Characteristics at 25°C (T_C)

	MIN	TYP	MAX	UNIT
DC Power Supply	+10	+12	+15	V
DC Supply Current		25	40	mA
Power Dissipation		0.3	0.6	W
Control Voltage Range		+1 to 4		V

RF Characteristics at 25°C (T_C)

	MIN	TYP	MAX	UNIT
Frequency of Operation	1		10	GHz
Insertion Loss		2.0	3.0	dB
Input/Output VSWR		1.7:1	2:1	
Attenuation Range @ 1GHz	12	15		dB
@ 10GHz	9	12		dB
Response Time (10%-90%)		<50		ns
Max. RF Power		>+20		dBm

PACKAGE OUTLINE

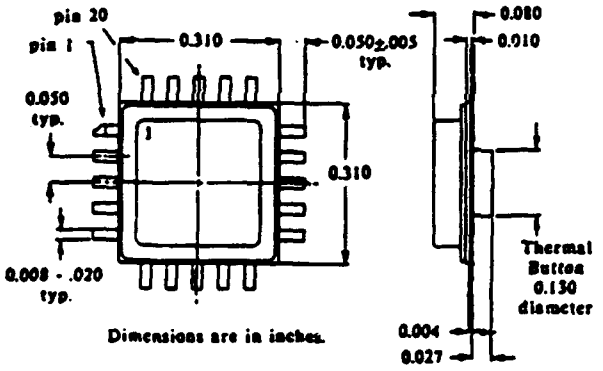

Pin	Function
2	ATTEN CTRL
4	RF I/O
7	Optional RF Bypass
9	-
12	RF I/O
14	-
17	-
19	V_{DD}

Pins 1, 3, 5, 6, 8, 10, 11, 13, 15, 16, 18, 20 are Ground.

TYPICAL TQ9161 PACKAGED PERFORMANCE

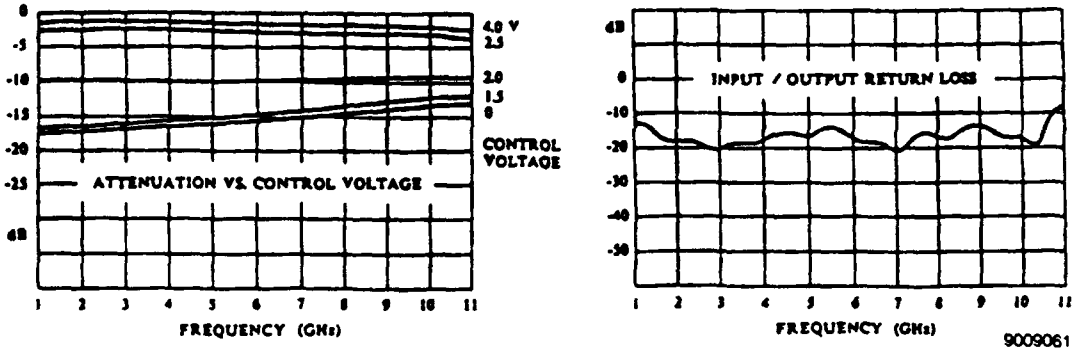

Figure 3-8. MMIC Specification

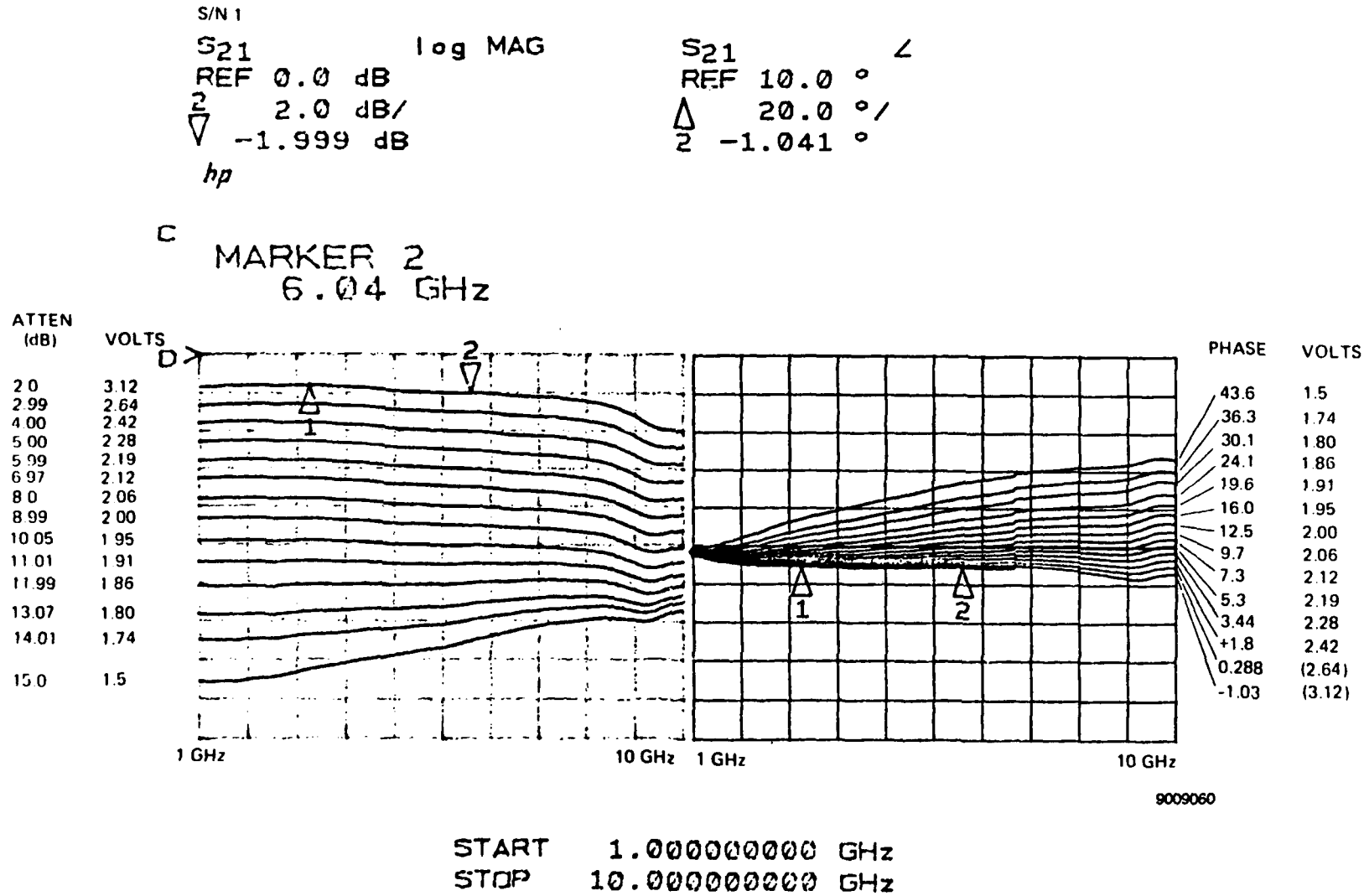

Figure 3-9. Amplitude and Phase versus Control Voltage

3.6 FILTERS

Sixteen 3-GHz bandpass filters and sixteen 6-GHz bandpass filters were purchased from Microphase, Inc. of Norwalk, Connecticut. They are five-pole heavily loaded comb line filters. The filter outline drawing is shown in figure 3-10. The typical insertion loss and return loss for each filter are shown in figure 3-11. The measured insertion loss tracking among filters is shown in figure 3-12. The insertion phase tracking among the 3- and 6-GHz filters is shown in figures 3-13 and 3-14, respectively. Table 3-2 lists the measured insertion phase versus serial number at the 3- and 6-GHz filter band centers.

Table 3-2. Phase versus Serial Number

Unit S/N	R6611 Phase - 3 GHz (Degrees)	R6612 Phase - 6 GHz (Degrees)
1	4.3	-12.7
2	-7.8	4.1
3	-3.1	-4.1
4	0.09 (Ref)	-14.4
5	5.1	4.7
6	25.0	-11.5
7	3.4	-17.4
8	-11.1	1.4
9	-16	-
10	-9.5	-13.3
11	6.9	-0.013 (Ref)
12	-9.5	-
13	-12.0	-5.1
14	-11.0	-11.5
15	1.5	-18.2
16	-6.3	-15.4
17	-	0.2
18	-	2.4

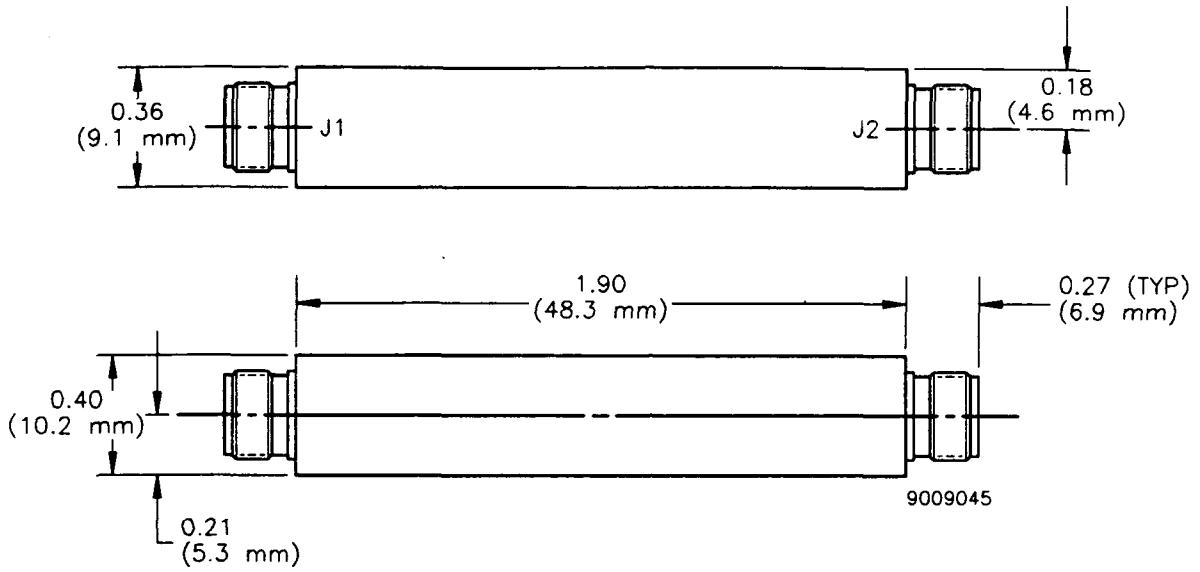

Figure 3-10. Filter Outline

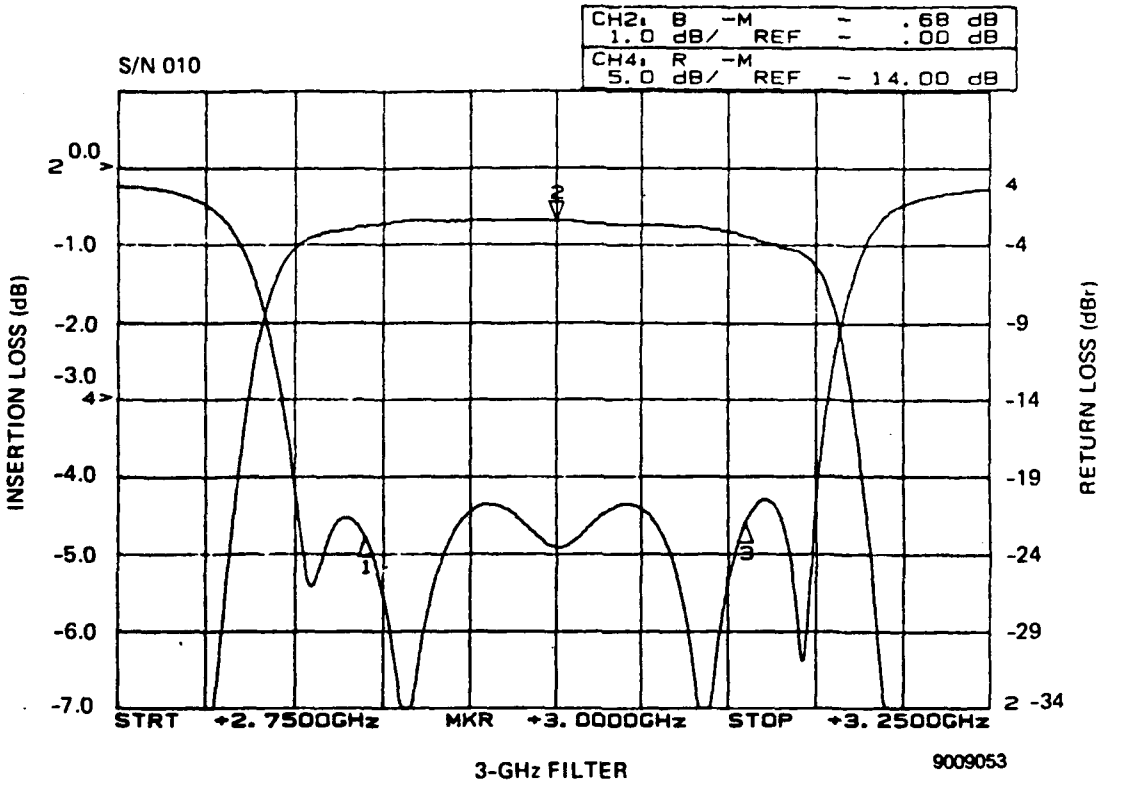

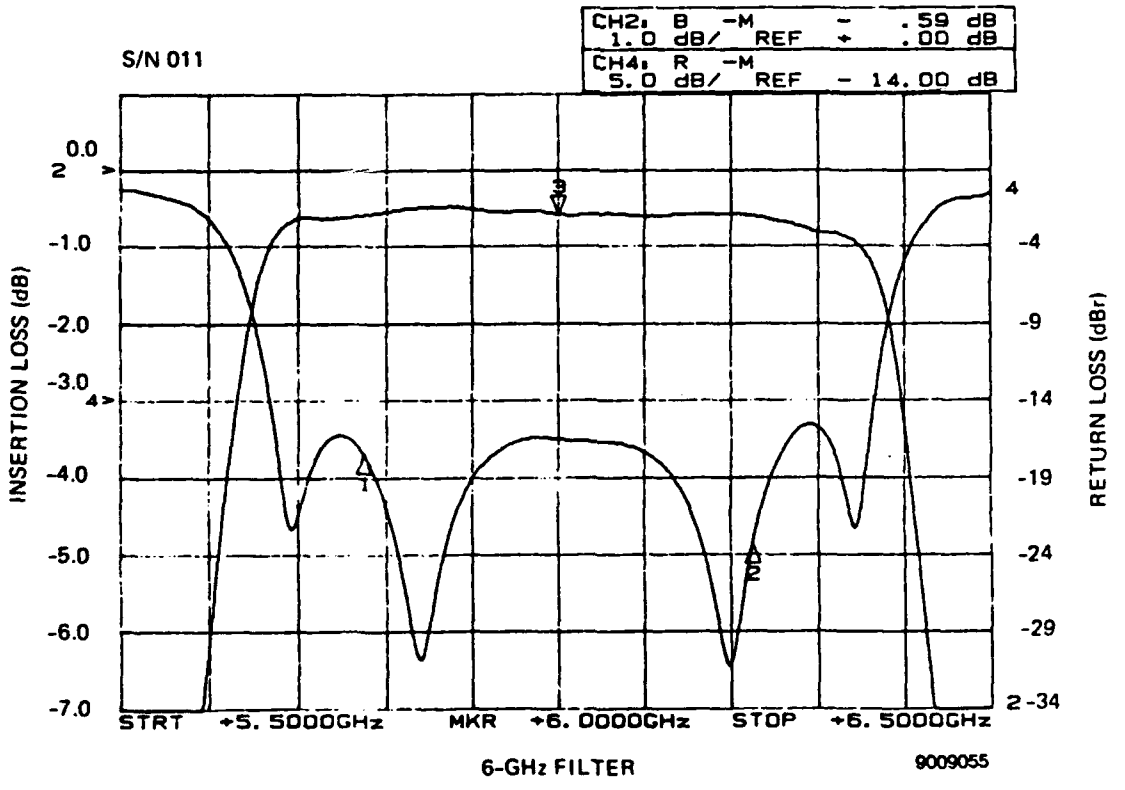

Figure 3-11. Typical Insertion Loss and Return Loss for 3- and 6-GHz Filters

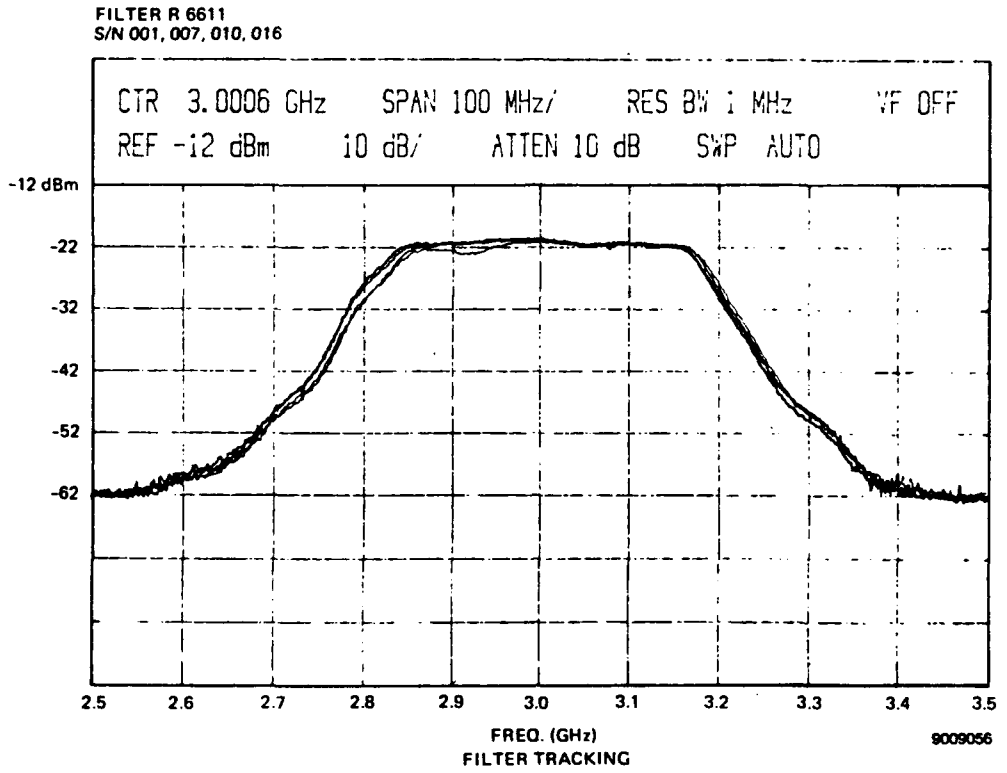

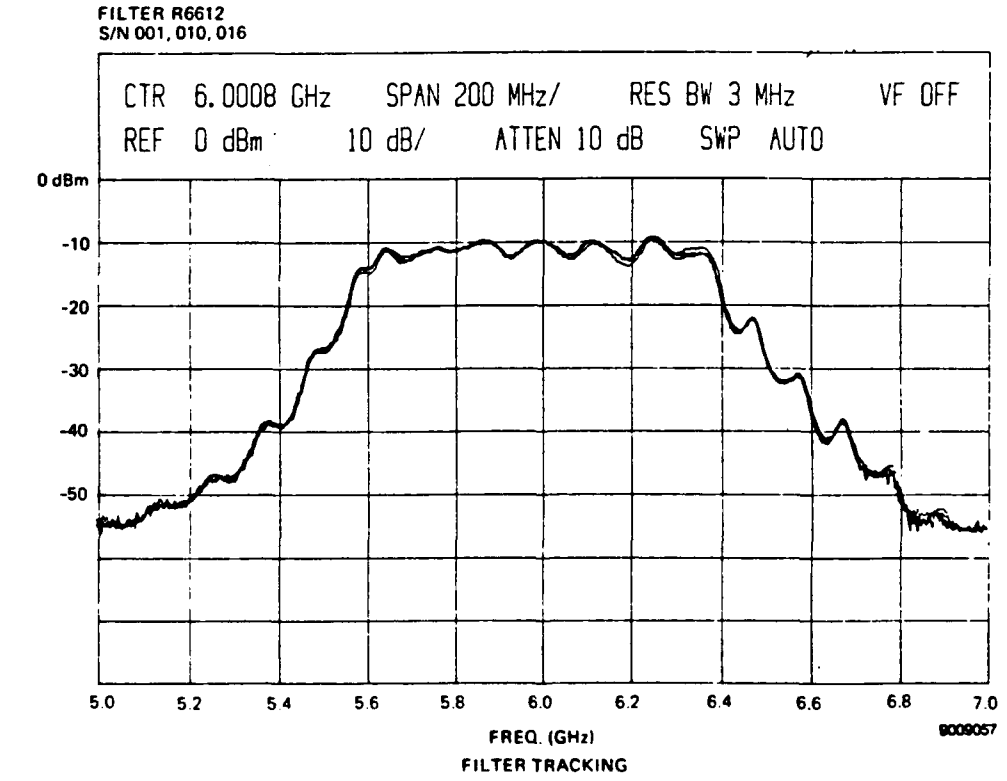

Figure 3-12. Measured Insertion Loss Tracking Between Filters R6611 and R6612

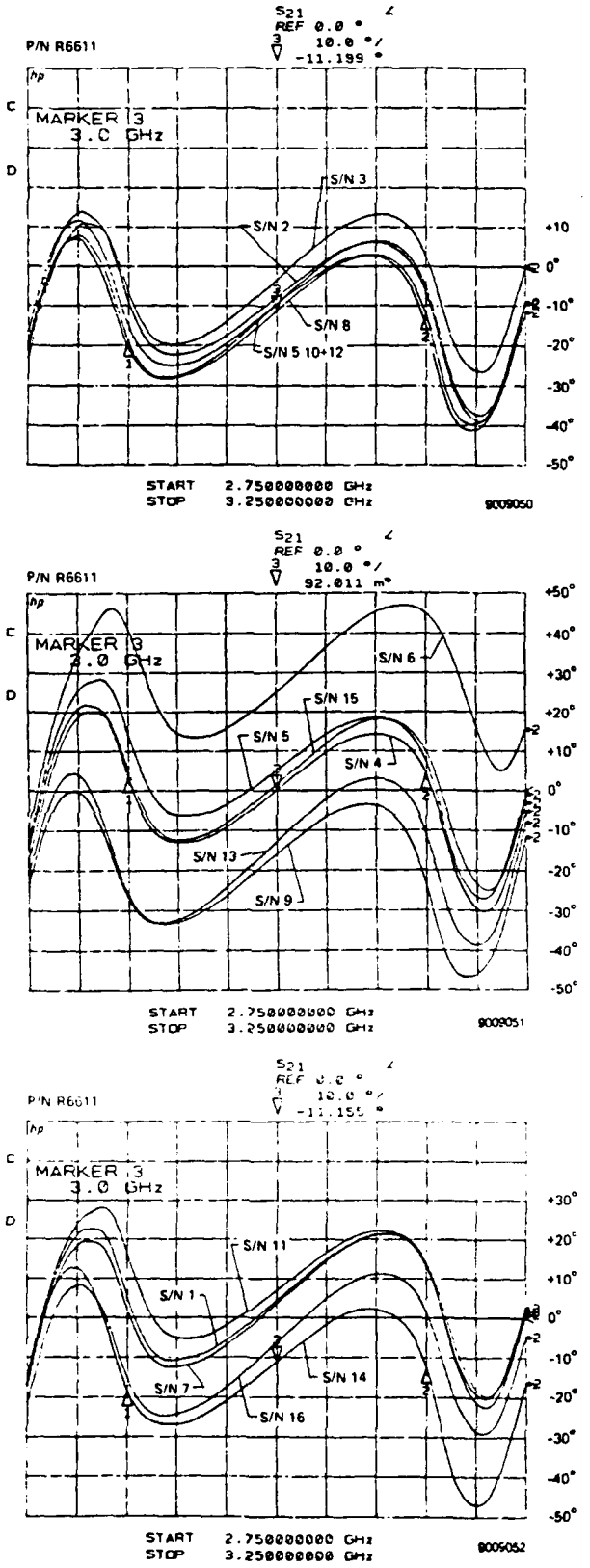

Figure 3-13. Insertion Phase Tracking Among 3-GHz Filters

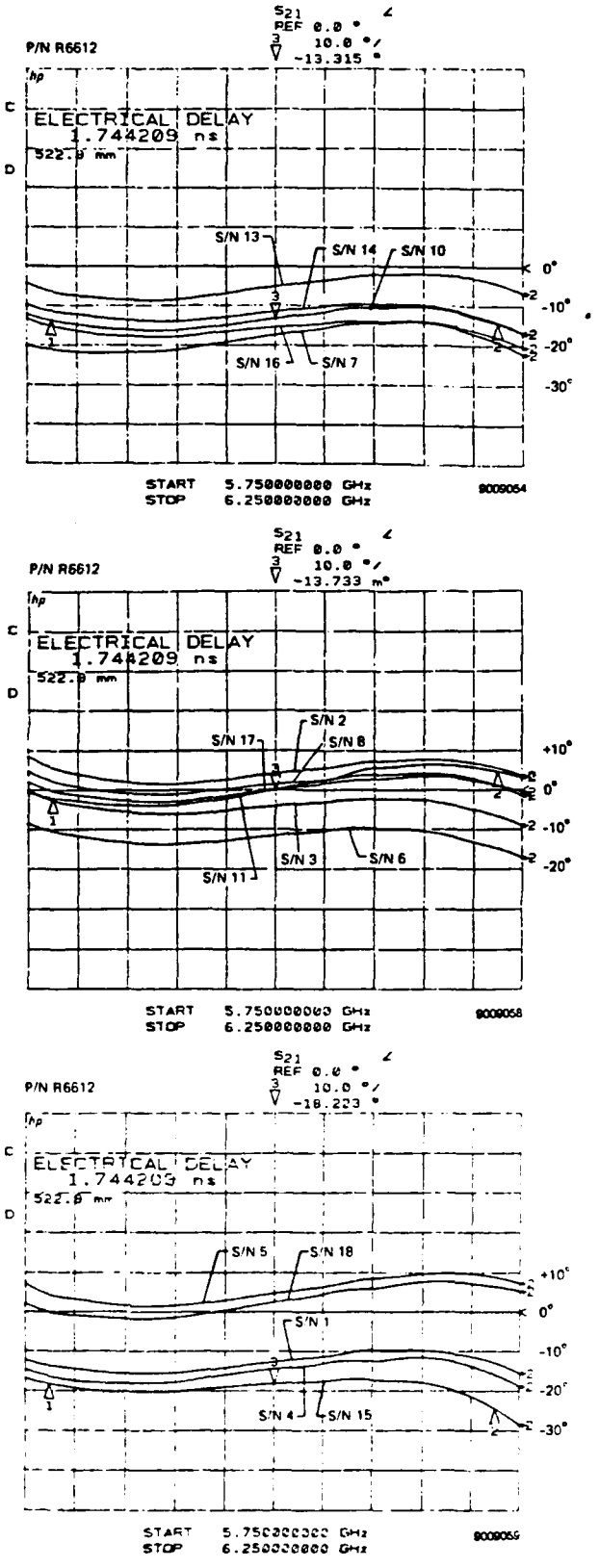

Figure 3-14. Insertion Phase Tracking Among 6-GHz Filters

3.7 ARRAY HOUSING

The experimental array was assembled in an aluminum sheet metal housing approximately 34 in. long by 15 in. high by 11 in. deep, as shown in figures 3-15 and 3-16.

Each 10-element antenna card is attached to its own card frame and is slid into place. The 32 assembled printed antenna cards are spaced about 1 in. apart in the H-plane.

The four 8-way and one 4-way power dividers are attached to the rear of the housing.

Filters, when required for testing, are mounted on the support bracket protruding from the rear of the housing, as shown in figure 3-17.

The control and dc power voltages for the MMIC attenuators (located on each antenna card) are conducted through a wire harness; the harness is routed from a channel behind the power dividers to the Reconfigurable Array Control Box.

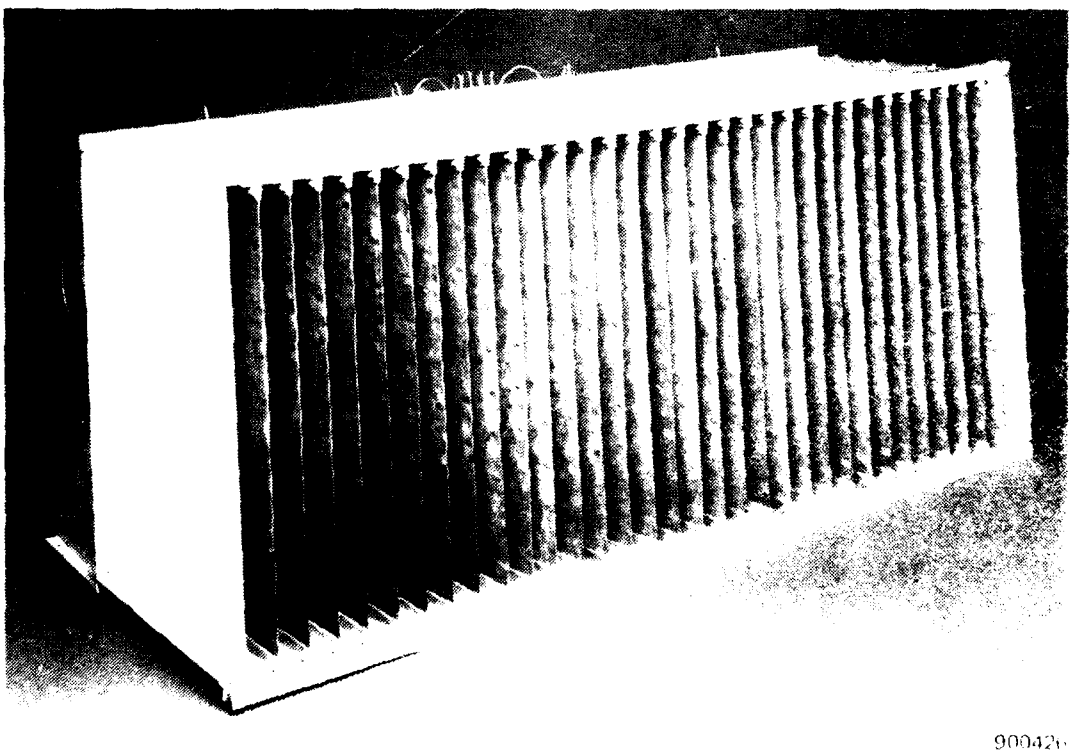

900426

Figure 3-15. Array Housing, Front View

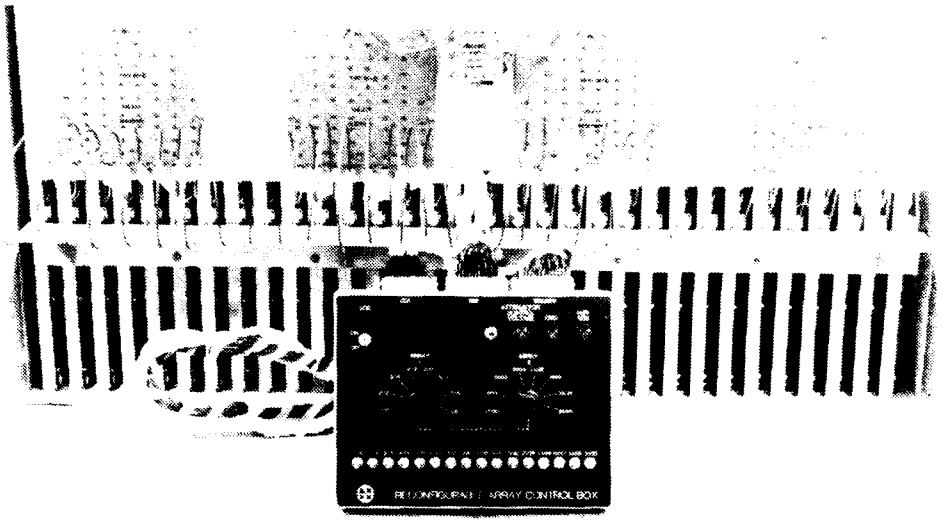

900410

Figure 3-16. Array Housing, Rear View

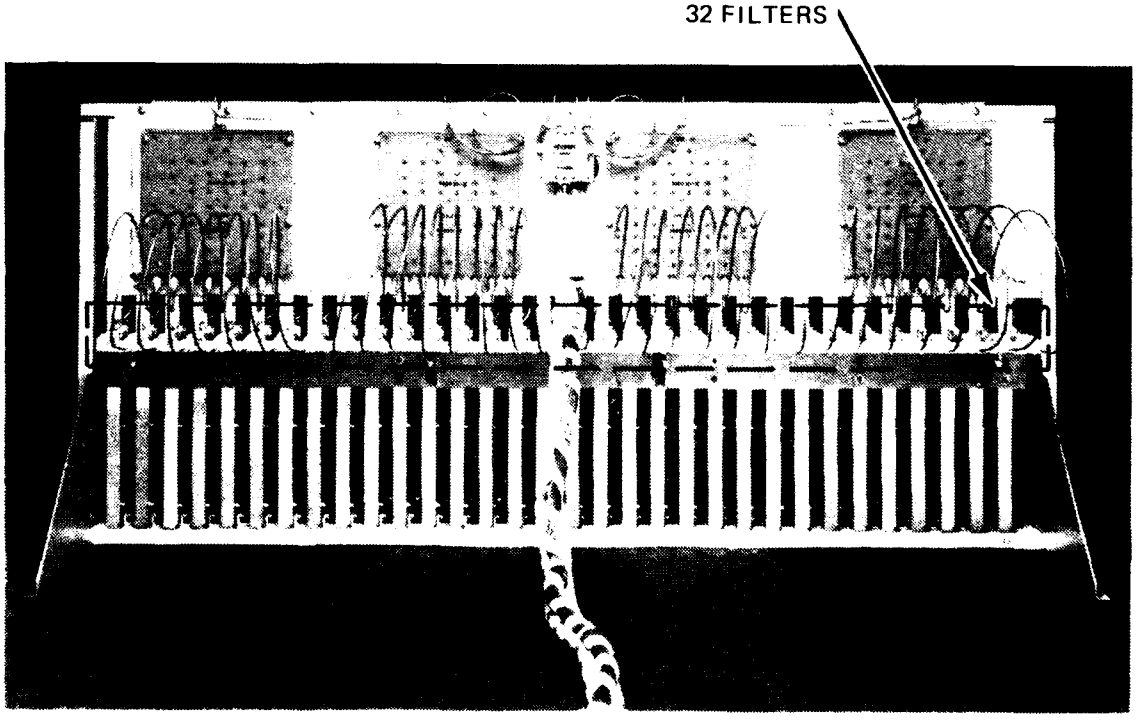

900421

Figure 3-17. Array with Filters

3.8 CONTROL BOX

The 32 columns of the array are partitioned into two arrays of 16 columns each for purposes of testing. The control box is wired to independently adjust the attenuator control voltage to the two arrays. Pairs of attenuators symmetrically located about the centerline of each array are controlled by adjusting potentiometer knobs on the control box. Figure 3-18 is a photograph of the control box, while figure 3-19 shows its schematic. As noted in the schematic, VDD (+12 volts) is the MMIC supply voltage. In the OFF position, the attenuator control voltage switch sets the voltage of all the MMICs to zero and, therefore, sets the attenuation to a maximum level of approximately 15 dB provided the VDD is also on.

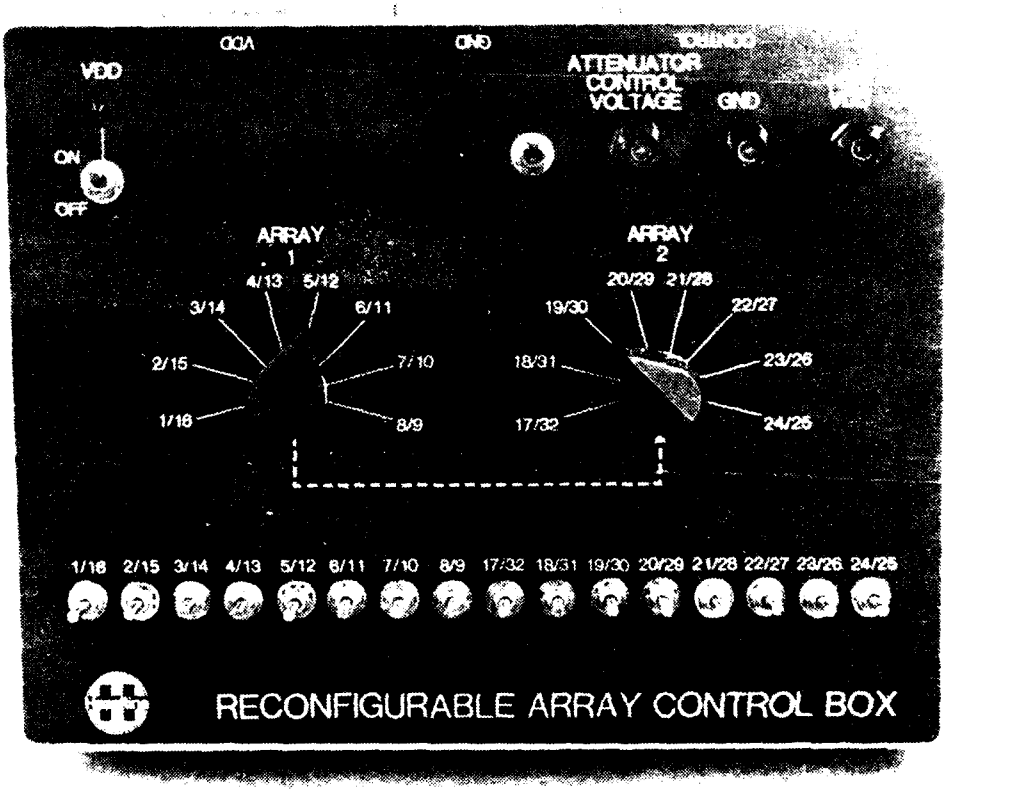

900411

Figure 3-18. Reconfigurable Array Control Box

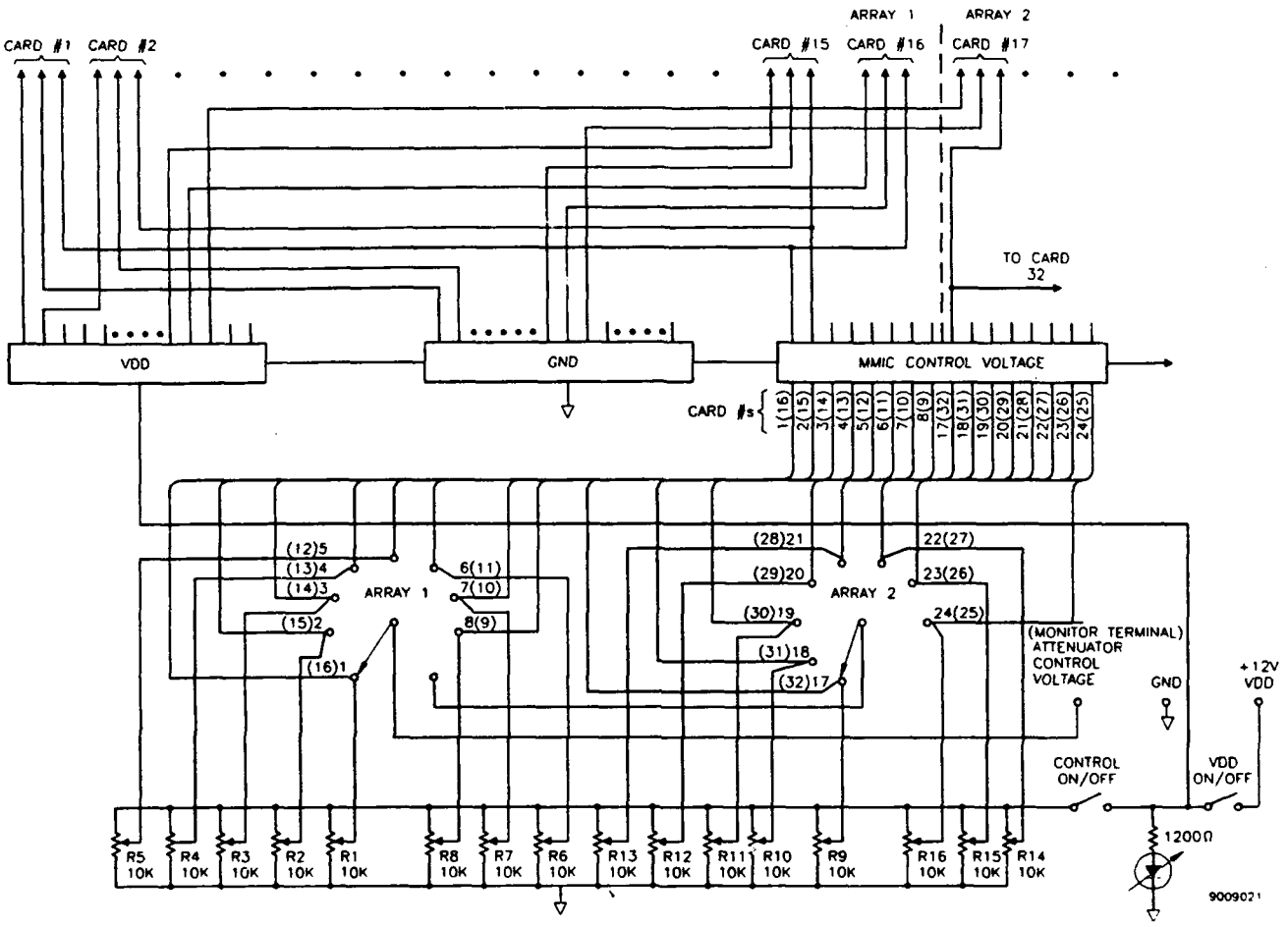

Figure 3-19. Reconfigurable Array Control Box, Schematic

SECTION IV

MEASURED RESULTS ON DEMONSTRATION ARRAY

4.1 OVERVIEW OF TEST PROGRAM

The array has been configured to measure interactions between adjoining apertures over a 3:1 bandwidth and to measure in-band antenna pattern characteristics using low sidelobe array excitations. These test program objectives are achieved by manually changing the aperture filters and by electronically changing the MMIC attenuators.

For the test program, the 32-column array will be divided into two 16-column apertures. Each aperture may be configured with a full complement of filters or no filters. Additionally, each 16-column array may be connected to the main power divider or be terminated. These choices are shown in figure 4-1.

Five arrangements of components are shown in figure 4-1. Configurations a and b are used for reference, enabling changes introduced by the filters to be observed. Configuration c simulates a two-band reconfigurable array. Patterns will be recorded within the passband of each filter. The array amplitude excitation will be adjusted using the variable attenuators.

Configurations d and e measure the filter's reject-band characteristics effect on the patterns of the unfiltered aperture. Patterns will be recorded on either side of the filter's passband over the full 3:1 bandwidth of the array.

4.2 INITIAL MEASUREMENTS ON DEMONSTRATION ARRAY

The array was assembled and tested in several stages. Measurements were made on the individual MMICs and filters as reported in Section III. Also, the cables used to connect the filters to the power divider were phase trimmed to within ±1 degree at 7 GHz. Table 4-1 shows the measured phase distribution at the input to each column.

Prior to assembling the complete array, E-plane patterns of a single column of 10 elements were recorded over the frequency band. Figure 4-2 shows a pattern measured at 5.0 GHz.

The near-in pattern sidelobes are well-focused implying the serpentine lines from the 10-way divider junction to the notch elements provide the desired uniform phase. However, the wide-angle E-plane radiation is substantial, possibly indicating that radiation from the corners of the card is significant. If the corners are the radiation source, then the edges would have to be treated (tapered, resistive loading) to achieve acceptable scanned E-plane patterns.

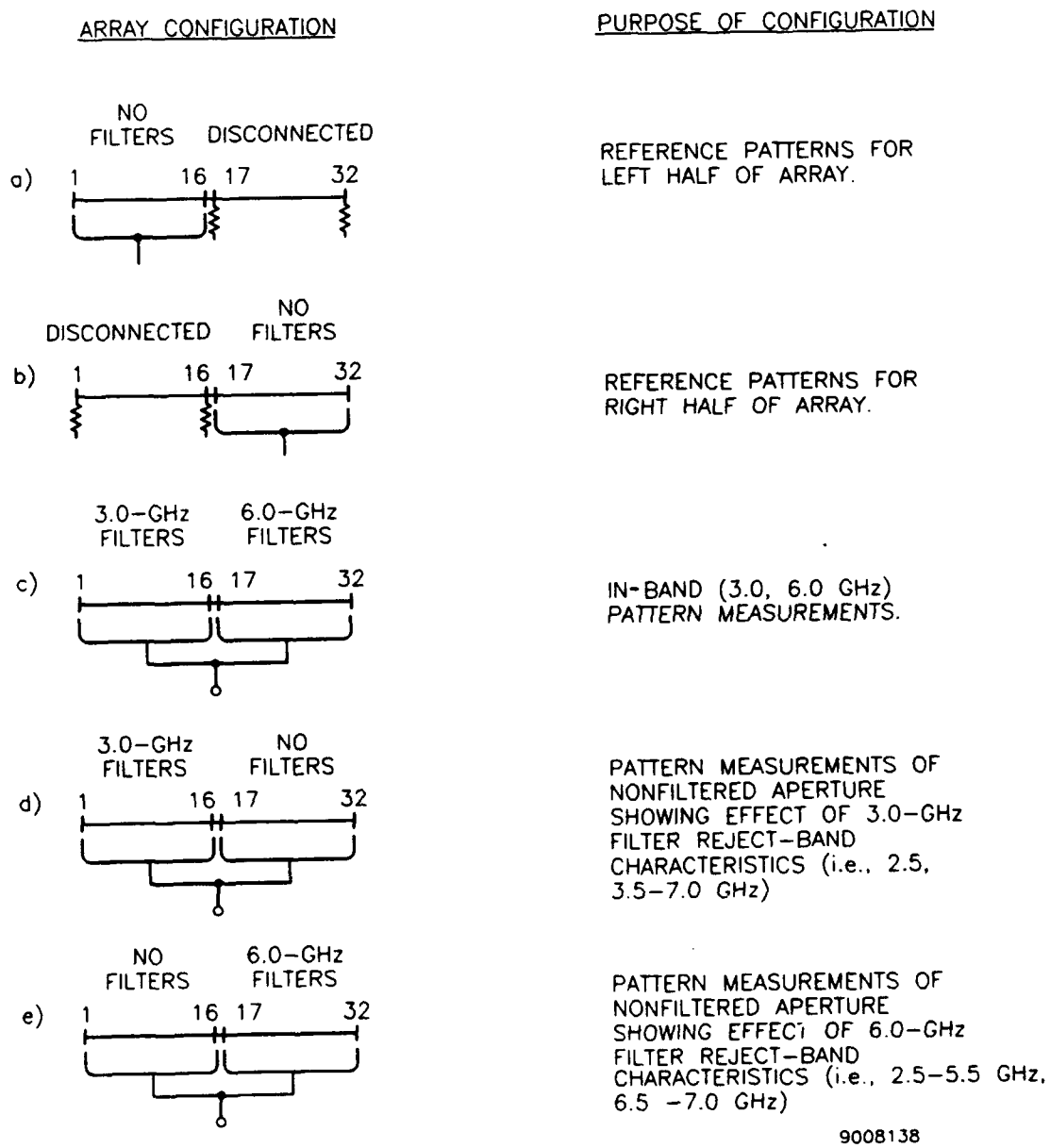

Figure 4-1. Arrangement of Filters for Reconfigurable Array Measurements.

Table 4-1. Thirty-Two Column Aperture Phase Distribution Measured at 7 GHz

Column No.	Phase (deg)	Column No.	Phase (deg)
1	+12.4	17	-0.1
2	+11.1	18	-0.2
3	+7.8	19	0.0
4	+7.9	20	-2.1
5	+6.9	21	+1.5
6	+7.2	22	+0.9
7	+7.1	23	+3.0
8	+9.1	24	+4.0
9	+2.5	25	+6.2
10	+3.1	26	+5.7
11	+2.9	27	+3.3
12	+3.2	28	+2.8
13	+1.5	29	+4.0
14	+1.9	30	+5.0
15	+4.0	31	+4.7
16	+4.9	32	+4.6

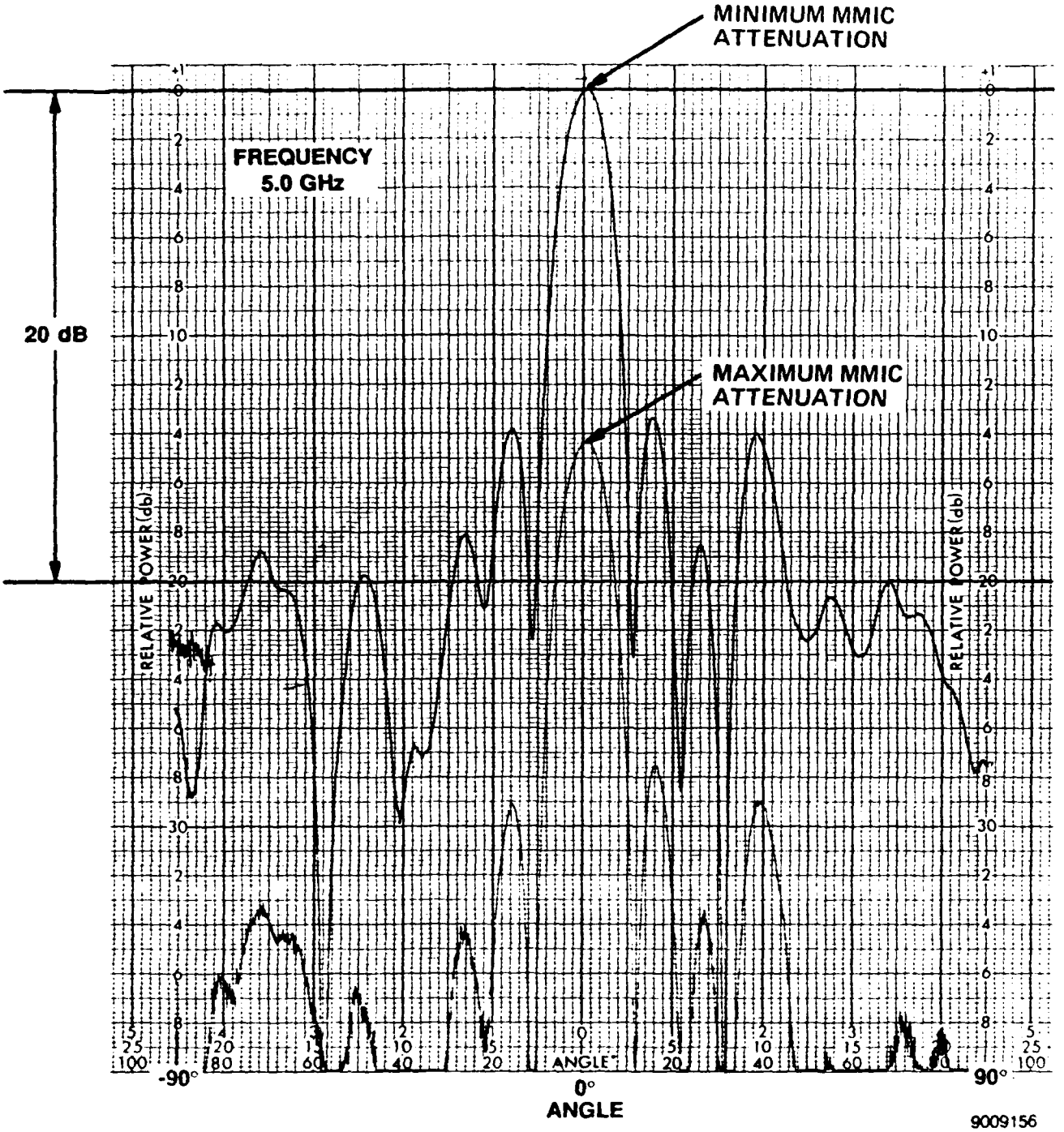

Figure 4-2. Single-Column E-Plane Pattern Measured at 5 GHz

Groups of four and then eight columns were assembled and independently tested. A spectrum analyzer was used to record the signal level received by each group of columns over the 3:1 bandwidth for a fixed (0 degree) beam position. The test setup is shown in figure 4-3. The purpose of the test is to examine the fine frequency gain characteristic of the array. Quite often, discrete gain measurements when made over a wide bandwidth will miss high "Q" resonances that substantially degrade the pattern over a narrow bandwidth. The swept response of the spectrum analyzer (although not calibrated) will show regions where further measurements are warranted.

The swept frequency response of the eight-column array is shown in figure 4-4. There is no evidence of any resonances.

The remainder of the array was assembled and similarly tested using the spectrum analyzer. The results are shown in figure 4-5. Note the dip in signal level at about 7 GHz; this characteristic was not present in the smaller arrays. Even in the larger array, the resonance is only 100 MHz wide and the remainder of the swept response is similar to the smaller arrays. The resonance could be affected by wedging absorber between columns of elements; however, thinner absorber, which didn't touch adjacent columns, had little effect on the resonance. As a result, some of the patterns, measured near 7 GHz, shown in Appendix A, will exhibit sidelobe degradation because of the anomalous resonance. Gain was measured in the vicinity of this frequency and, as expected, was found to be low.

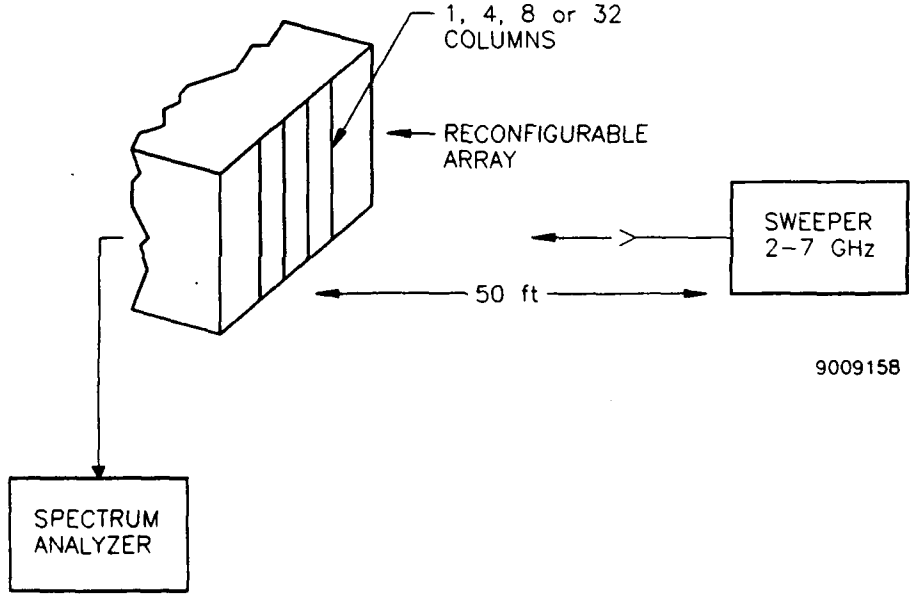

Figure 4-3. Setup to Measure Swept Gain of Array

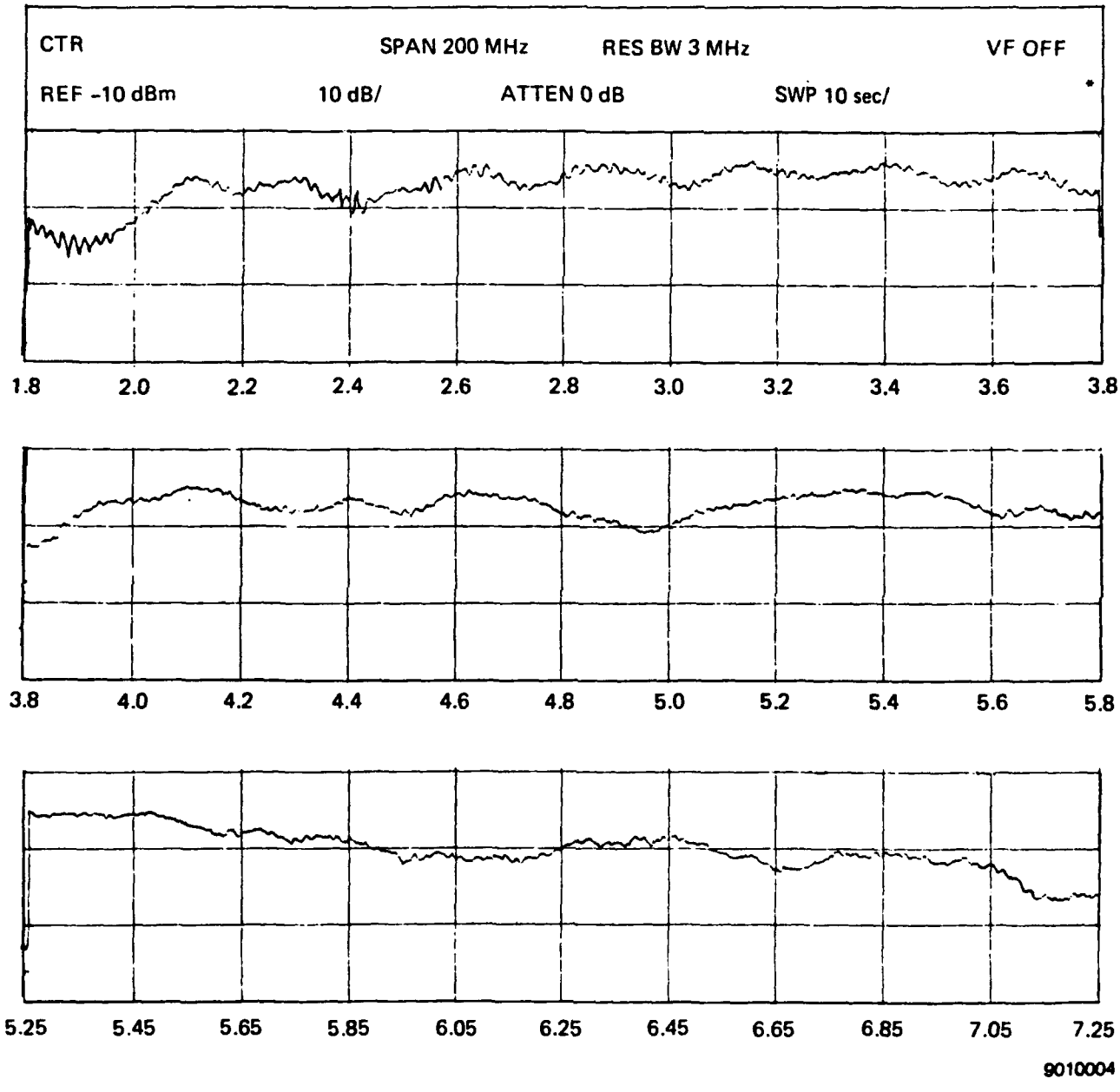

Figure 4-4. Swept Frequency Response of the Eight-Column Array

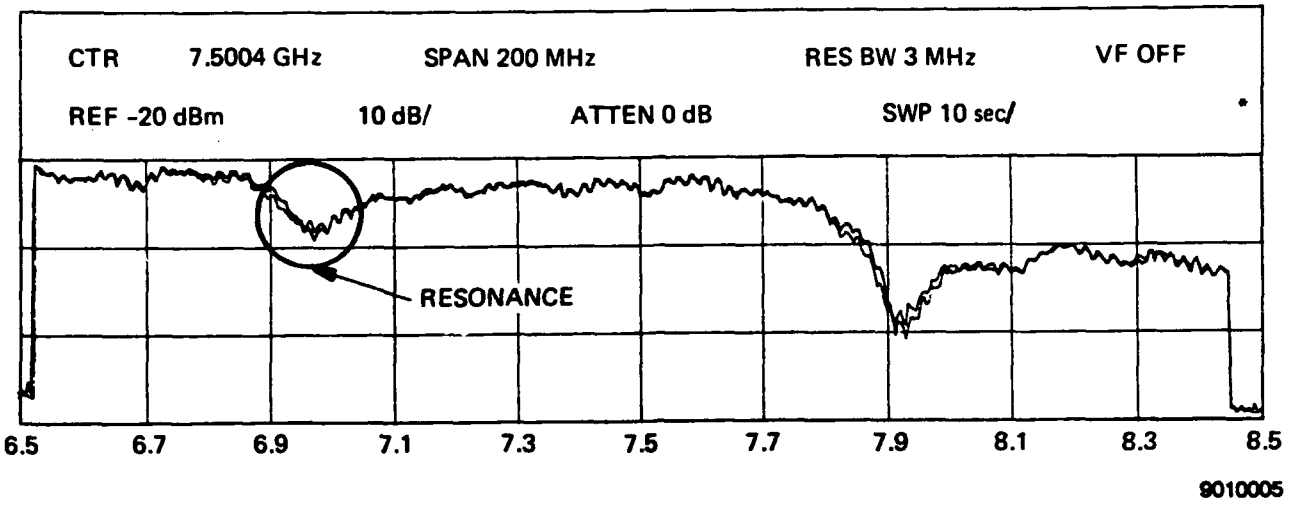

Figure 4-5. Swept Frequency Response of the 32-Column Array

4.3 MEASURED RADIATION PATTERNS SHOWING RECONFIGURABILITY

The bulk of the measured patterns is contained in Appendix A. Each appendix contains a selection of patterns from the cases shown in figure 4-1. Several patterns are shown in this section to illustrate the key features of the array.

A typical pattern of the full 32-column array, with uniform illumination and no filters, is shown in figure 4-6. Two traces are shown on this figure, one for minimum attenuation of the MMIC, the other for maximum attenuation. The remainder of the pattern description in this section will be for pairs of 16-column arrays, as described in figure 4-1.

Reference patterns, using uniform illumination and no filters, are shown in Appendix A1. By referring to Appendix A2, the effect of the filter's reject band characteristic can be observed on the unfiltered aperture. Only when the operating frequency starts to ride up the skirt of the filter characteristic is any change observed in the patterns of the unfiltered aperture. Thus, a single wide-bandwidth power divider can be used in conjunction with filters implemented at each element to provide multiple frequency operation. This is a key aspect of the recommended control circuits discussed in Section II.

The effect of the filter's passband characteristic on a uniform illumination and a 30-dB Chebyschev illumination can be observed by referring to Appendices A3 and A4, and A5 and A6, respectively.

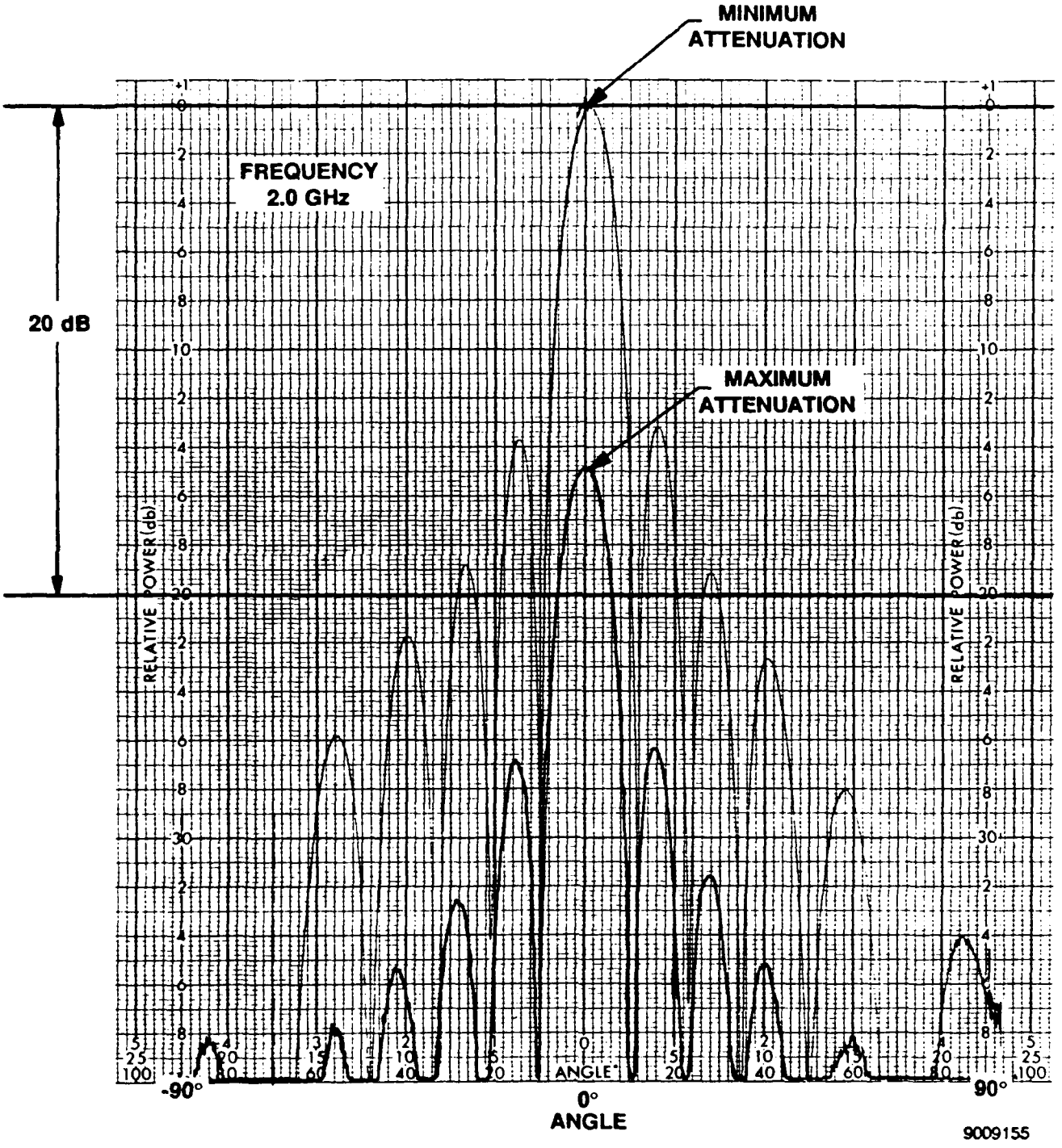

Figure 4-6. Typical Pattern With and Without MMIC Attenuation

In making comparisons for the low-sidelobe illumination, note the reference patterns in Appendix A5 have realized sidelobes of about -25 dB at the higher frequencies. The increase in sidelobe level corresponds to a ±5 degree random phase error through the components that comprise the unfiltered aperture. A calculation that illustrates this effect is shown in figure 4-7. The calculation is for a frequency of 6 GHz, where the columns are about a half-wavelength apart. This same phase error at lower frequencies will have less effect on sidelobes because of the smaller element spacing (measured in wavelengths). This effect, in combination with smaller phase errors and the element pattern, contributes to the slightly better sidelobe levels measured at the lower frequencies.

Adding filters to the array raises the sidelobe levels, but not substantially. The phase and amplitude errors introduced by the filters are shown in subsection 3.6. These phase and amplitude errors do not appreciably affect the more tolerant uniform illumination radiation patterns.

Figure 4-8 summarizes the measured low-sidelobe illumination results contained in Appendix A. In figure 4-8, patterns are shown for a 30-dB Chebyschev illumination, with and without the filters at 3 and 6 GHz.

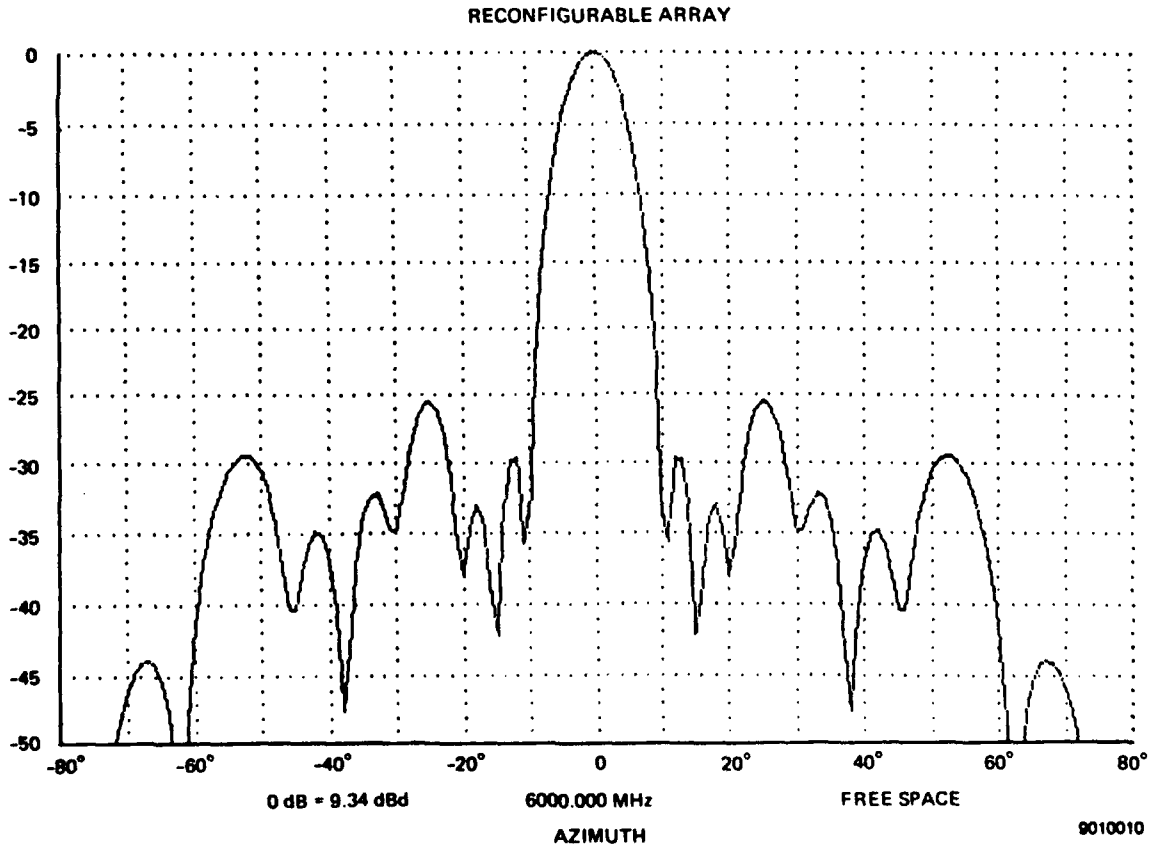

Figure 4-7. Calculated Pattern Showing Increase in Sidelobe Level from a ±5 Degree Random Phase Error

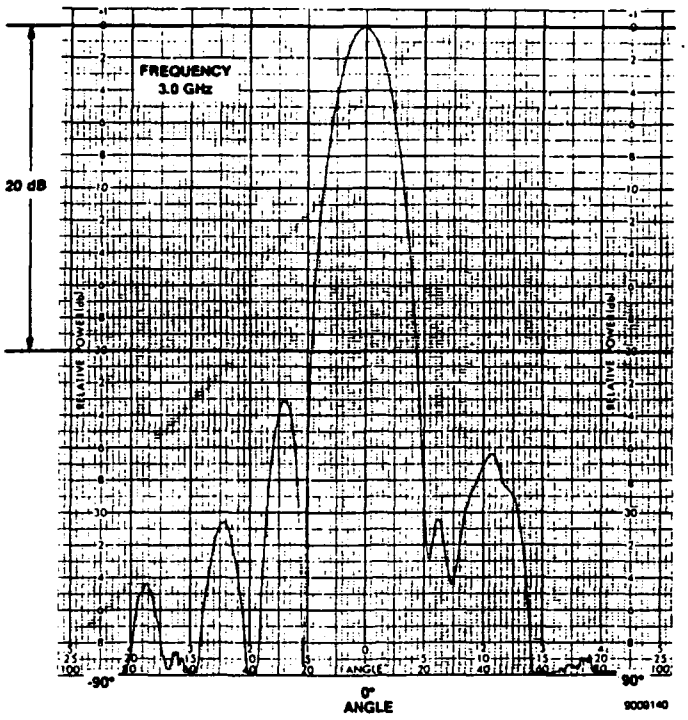

a. No Filters

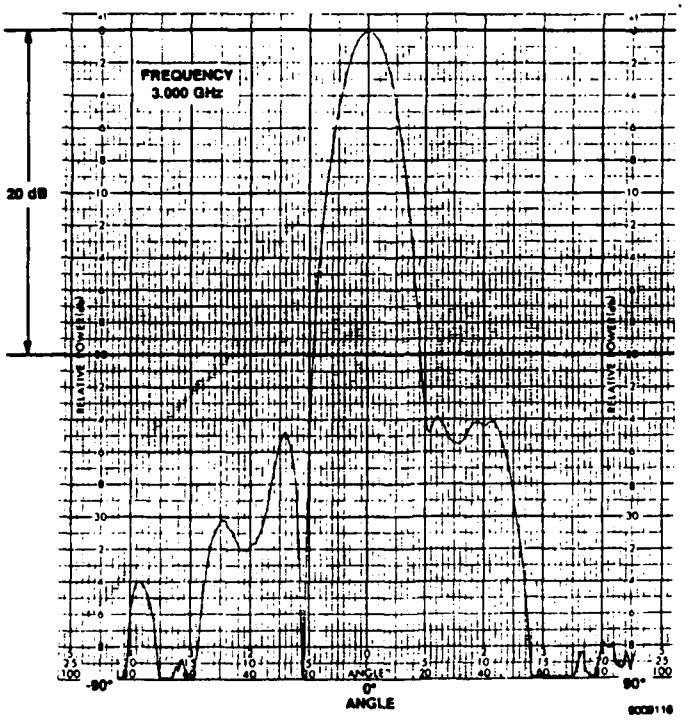

b. With 3-GHz Filters

Figure 4-8. Array Patterns for 30-dB Chebyschev Illumination

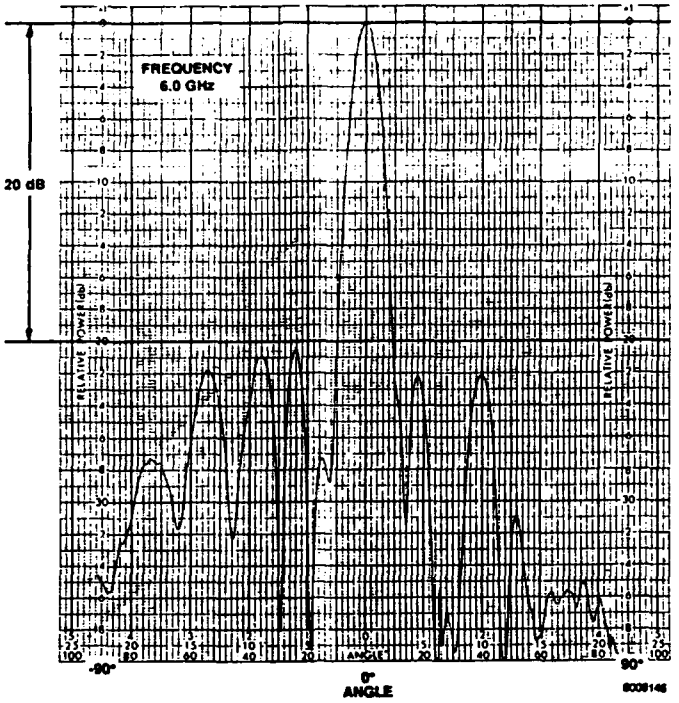

a. No Filters

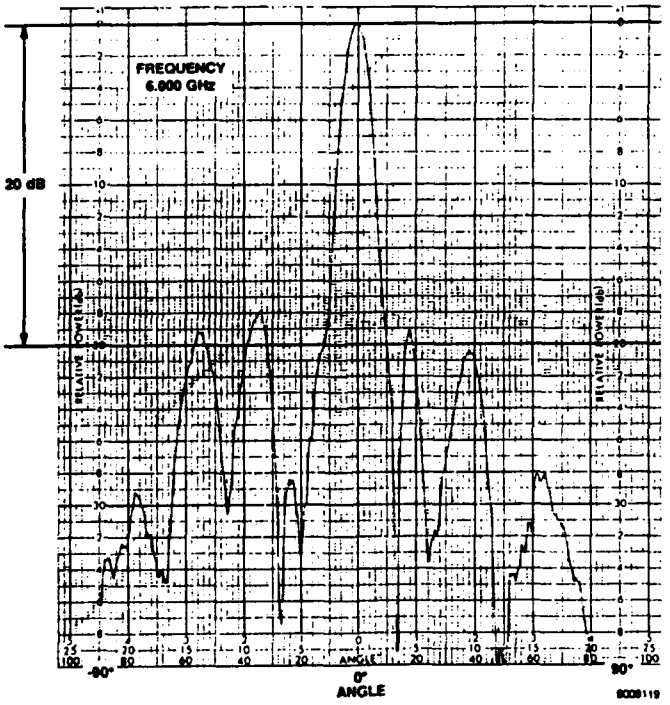

b. With 6-GHz Filters

Figure 4-8. Array Patterns for 30-dB Chebyschev Illumination (Cont)

SECTION V

SUMMARY

The Government's future requirement to operate several systems simultaneously from a common aperture can be achieved by using a control circuit at each element. The control circuit consists of an arrangement of filters, an attenuator and a phase shifter. The filters are used to partition the reconfigurable aperture into several simultaneously operating antennas. The attenuators provide independent illumination control while the phase shifters are used to scan individual antenna beams.

Since the components used in the control circuit can have substantial loss, a pair of amplifiers is used beyond these components to overcome the loss. The amplifier pair consists of low noise and power amplifiers selected by a T/R switch. A cascade of several MMIC circuits is envisioned to implement the control and amplifier circuits.

The radiating element for the reconfigurable array must encompass the full bandwidth of the various systems that share the aperture.

Typically, 3:1 bandwidths are needed to support ESM functions, whereas a decade bandwidth element would be required to include identification functions within the same aperture. In order to evaluate the variety of elements, a general computer code has been written and partially validated during this program.

A laboratory model of a reconfigurable array was designed, fabricated, and tested. The test objective is to measure the effect of using filters at the element level on antenna patterns.

The array consists of 32 columns of notch elements. Each column of 10 elements is fed by a reactive decade bandwidth microstrip power divider. Decade bandwidth MMIC attenuators are attached to the input of the 10-way microstrip power divider. Filters are inserted at the column level. They can be easily removed and rearranged to evaluate different aspects of the array approach.

The measured patterns on the array confirm that a control circuit, used in conjunction with a single multiband power divider provides the desired aspects of reconfigurability. These capabilities are: simultaneous multifrequency operation, altering the array illumination, and reconfiguring around damaged areas.

Measurements of the individual MMIC attenuators show that their characteristics versus control voltage are sufficiently uniform to realize relatively low sidelobe illuminations with common control signals. Calibration of the control voltages versus attenuation would be needed to realize low sidelobe illuminations (>30 dB). The measured patterns of the demonstration array with a 30-dB Chebyschev illumination indicates that the phase error across the aperture introduced by the filters is about ±7 degrees. This level of phase error limits the sidelobe levels that can be achieved, unless a sophisticated calibration technique is implemented. For operating several systems of modest (20 dB to 25 dB) sidelobe requirements, a conventional array architecture similar to the demonstration antenna is adequate.

In general, the approach studied provides the desired reconfigurability. However, without a specific set of functions that have firm specifications, the practical aspects of operating many systems simultaneously cannot be effectively studied. One such aspect is the effect of a transmitting aperture on neighboring receiving antennas. Therefore, the recommendation for the next phase in the development of this approach is to select and evaluate the suitability of those systems that the Government desires to be integrated into a common antenna.

APPENDIX A

RECONFIGURABLE ARRAY PATTERN DATA

APPENDIX A1

This data group contains reference patterns (no filters) for the 16 column arrays, configurations a and b shown below. Because left-half and right-half patterns are similar, only one set (Test 2) is included in this report. The MMIC attenuators have been set to the same voltage, yielding a uniform illumination.

The following frequencies are contained in this appendix.

Frequencies (GHz)			
Test 2	2.0	Test 2	4.5
	2.5		5.0
	3.0		5.5
	3.5		6.0
	4.0		6.5

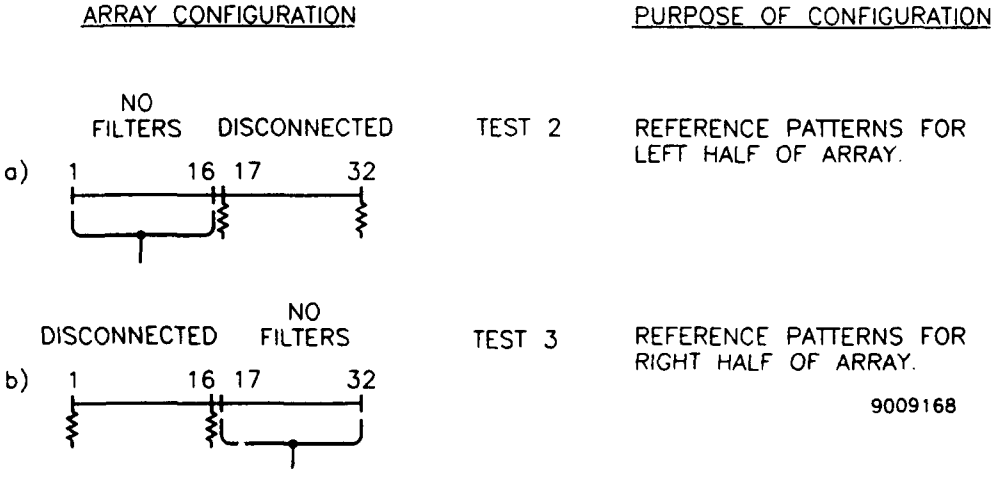

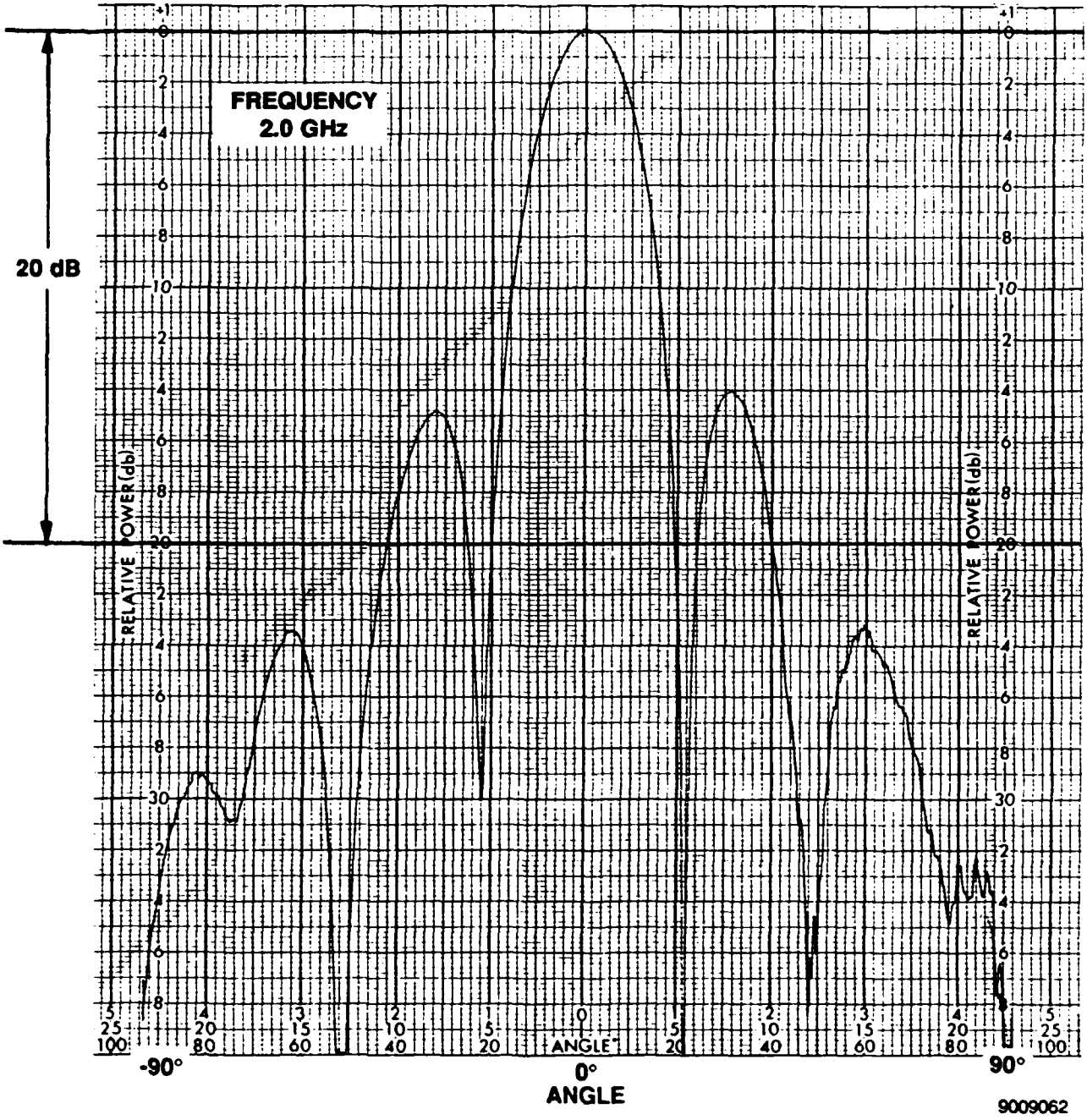
FREQUENCY
2.0 GHz
20 dB
RELATIVE POWER (db)
ANGLE
-90°
0°
90°
ANGLE
9009062

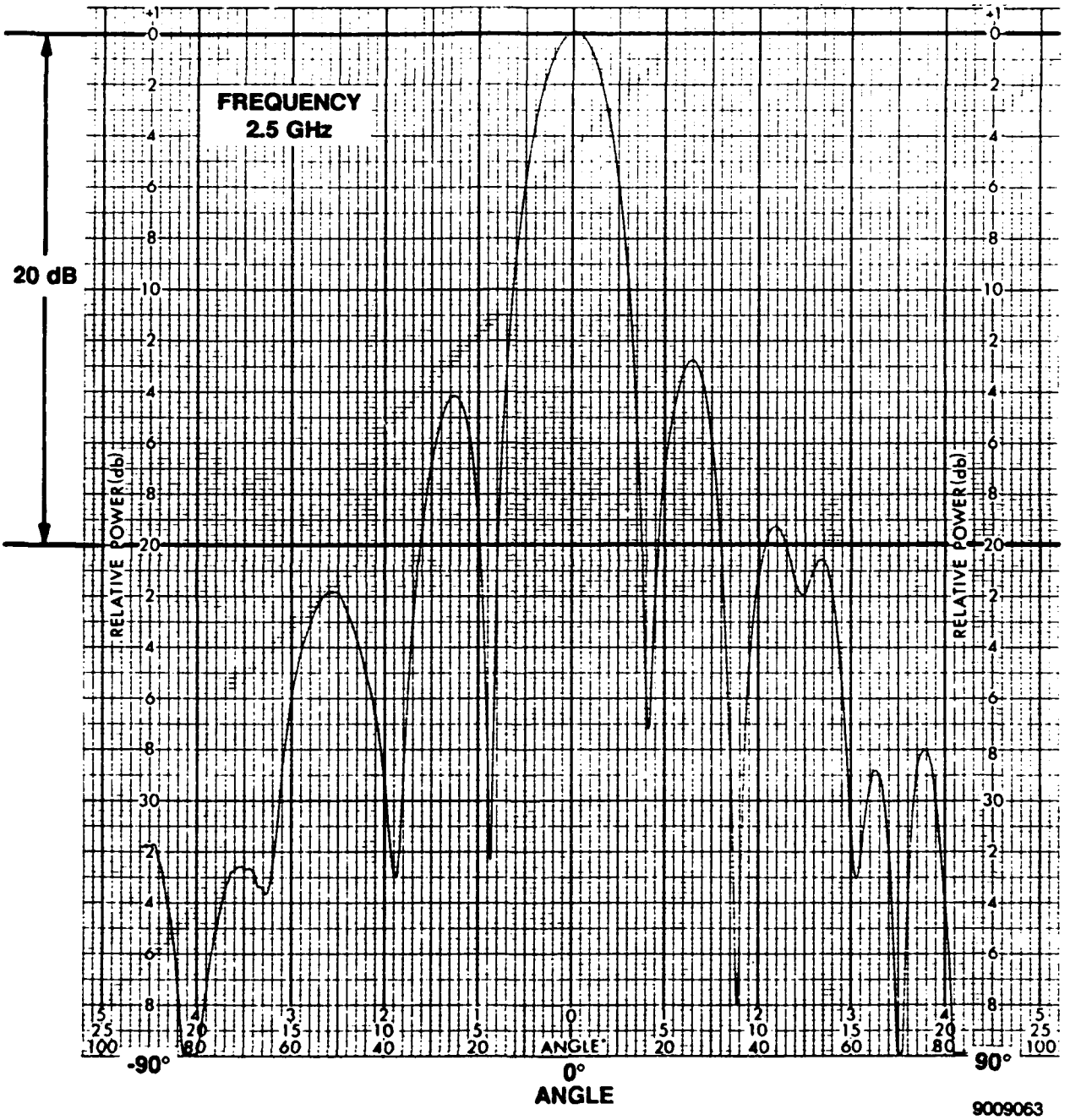
FREQUENCY
2.5 GHz
20 dB
RELATIVE POWER (db)
RELATIVE POWER (db)
ANGLE°
-90°
0°
90°
ANGLE
9009063

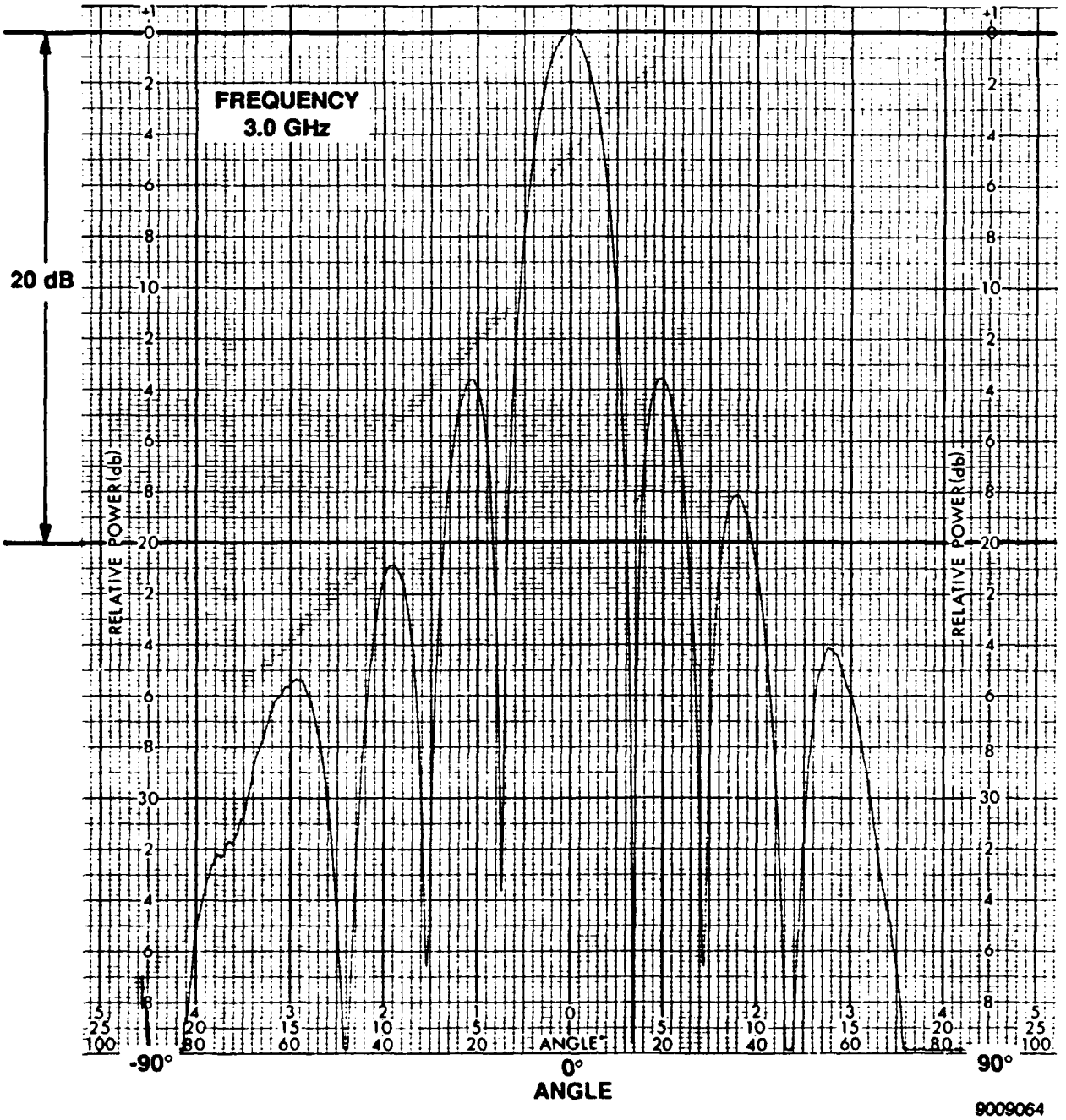
FREQUENCY
3.0 GHz
20 dB
RELATIVE POWER (db)
RELATIVE POWER (db)
ANGLE
-90°
0°
90°
ANGLE
9009064

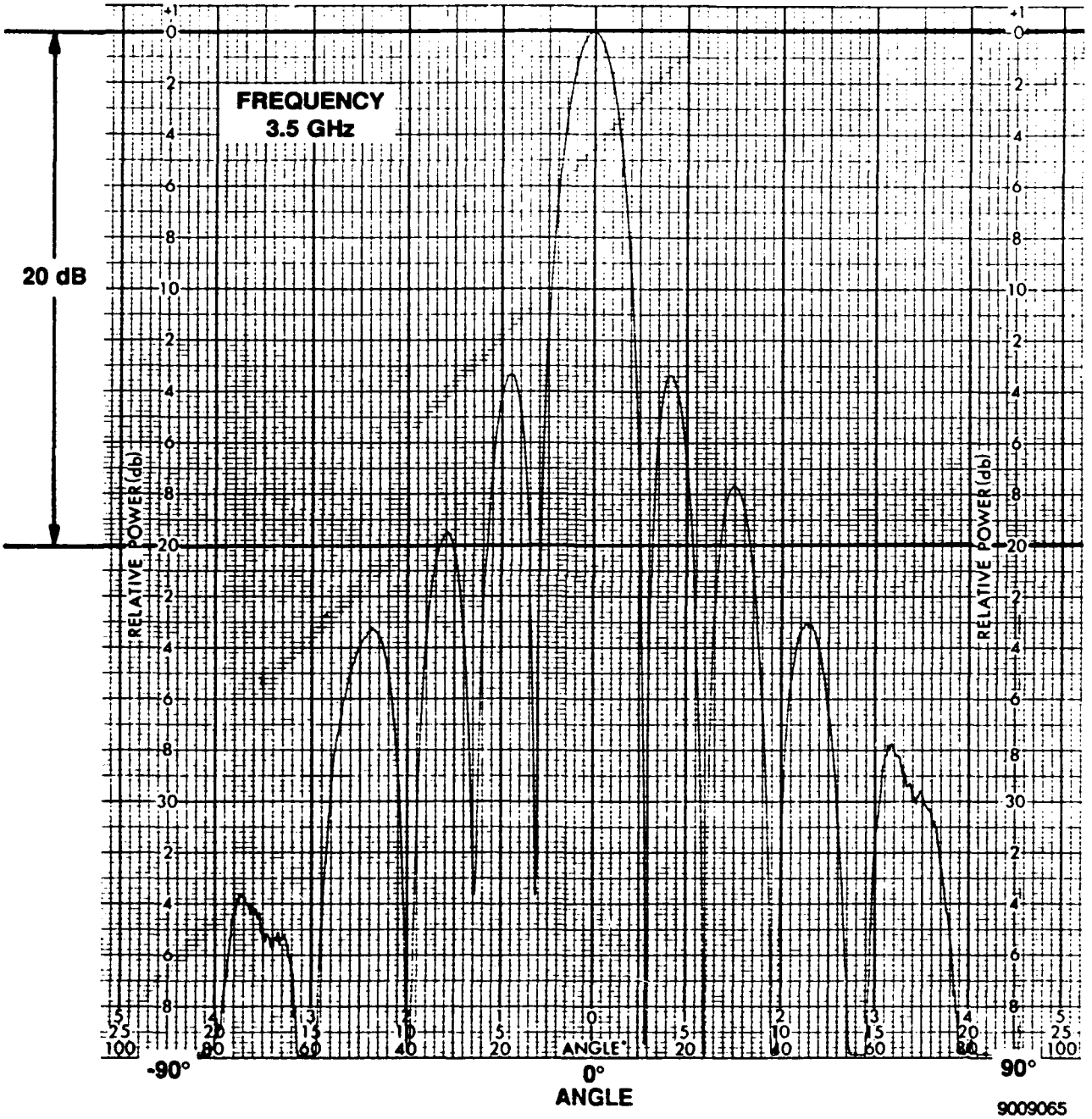
FREQUENCY
3.5 GHz
20 dB
RELATIVE POWER (db)
ANGLE°
-90°
0°
90°
ANGLE
9009065

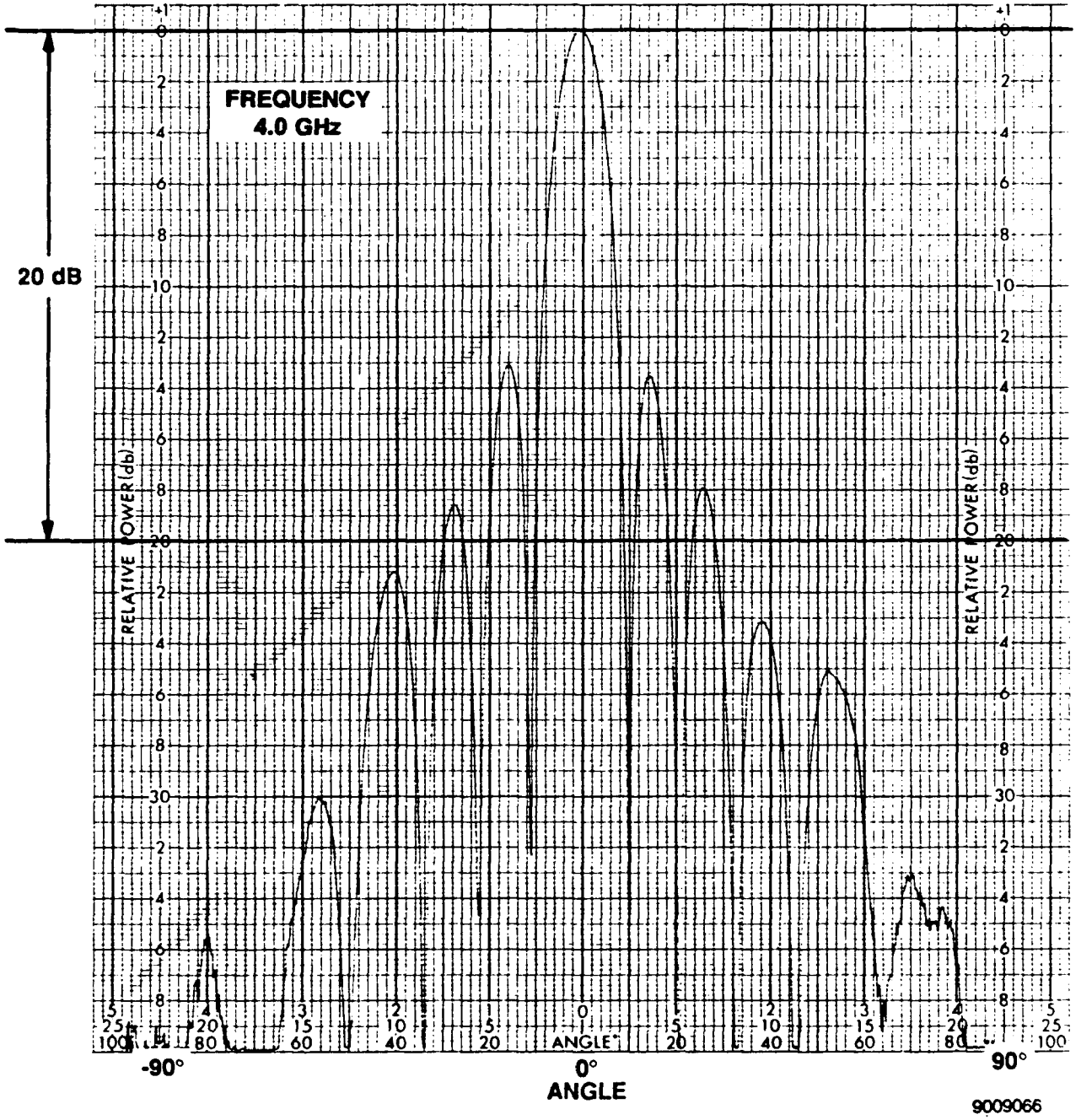
FREQUENCY
4.0 GHz
20 dB
RELATIVE POWER (db)
RELATIVE POWER (db)
ANGLE
-90°
0°
90°
ANGLE
9009066

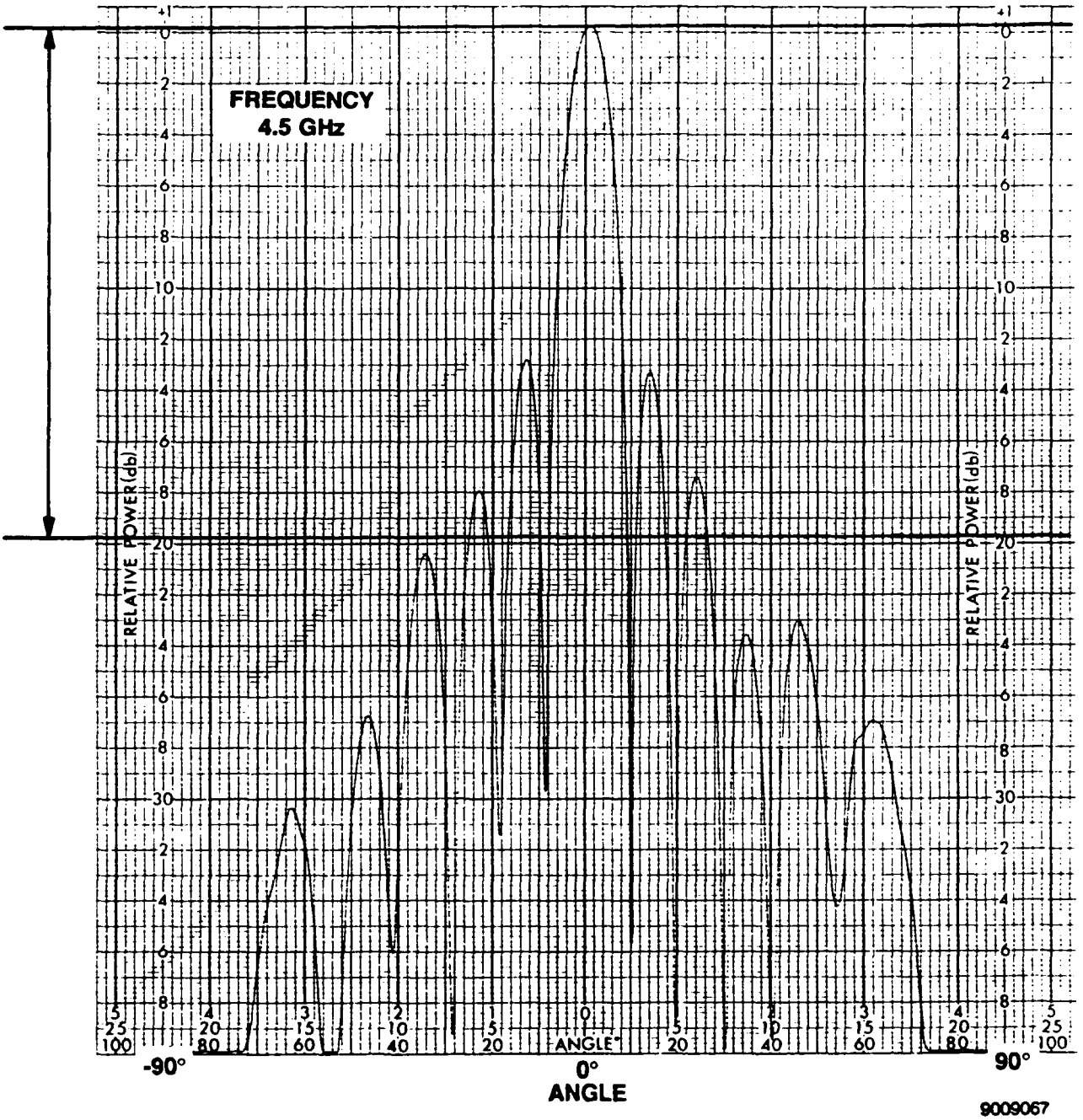
FREQUENCY
4.5 GHz
RELATIVE POWER (db)
RELATIVE POWER (db)
ANGLE°
-90°
0°
90°
ANGLE
9009067

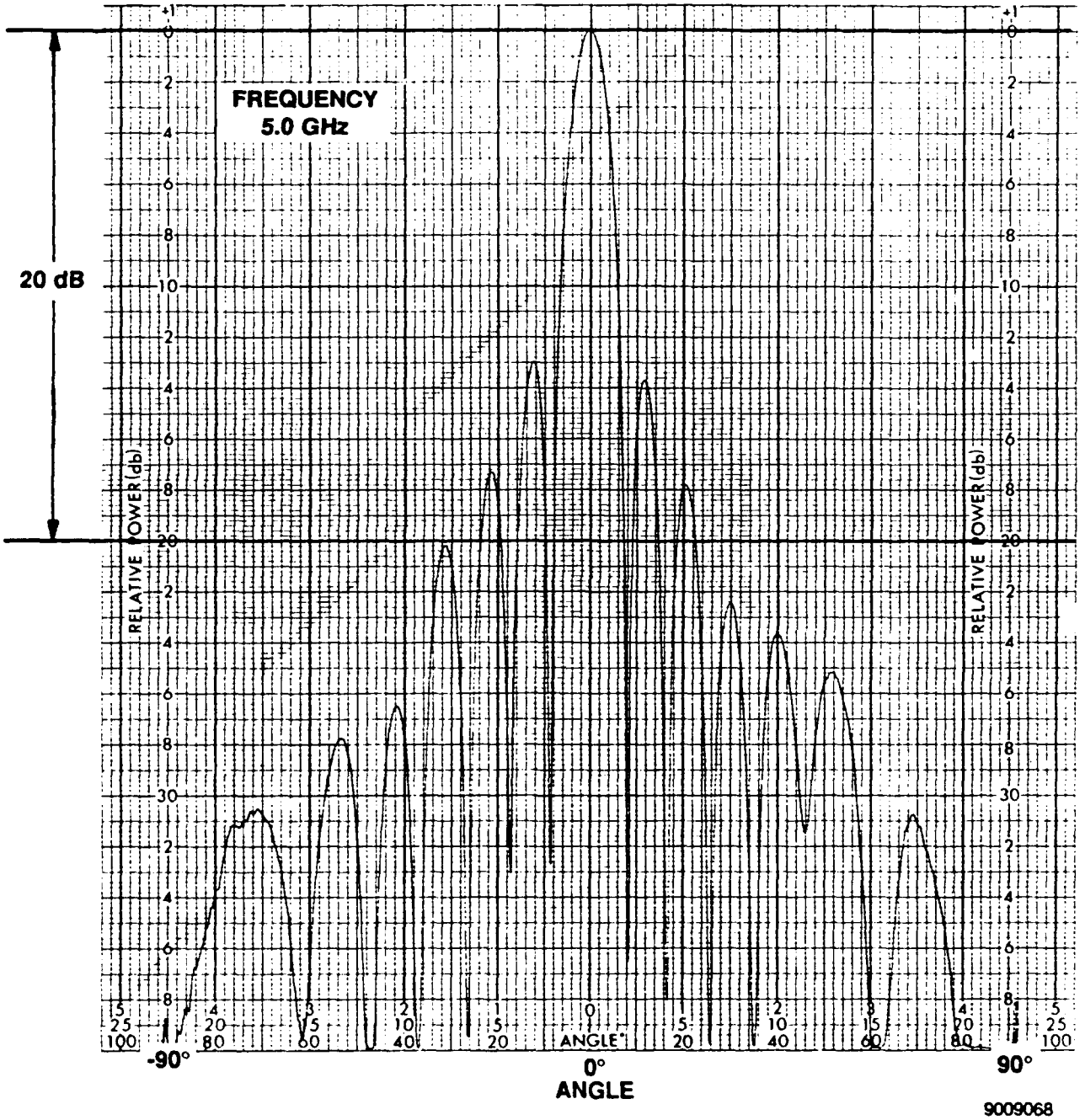
FREQUENCY
5.0 GHz
20 dB
RELATIVE POWER (db)
RELATIVE POWER (db)
ANGLE°
-90°
0°
90°
ANGLE
9009068

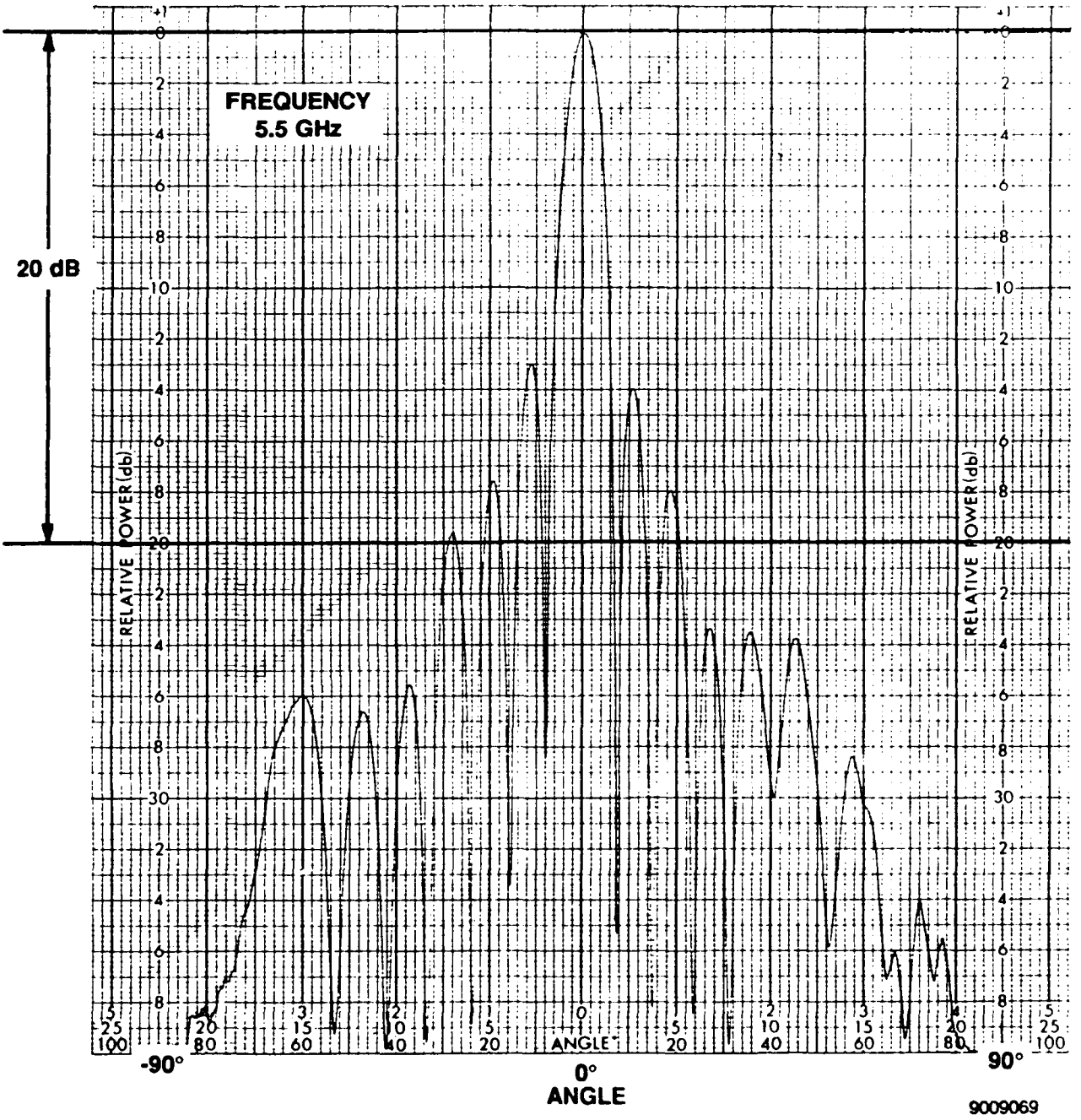
FREQUENCY
5.5 GHz
20 dB
RELATIVE POWER (db)
ANGLE
-90°
0°
90°
ANGLE
9009069

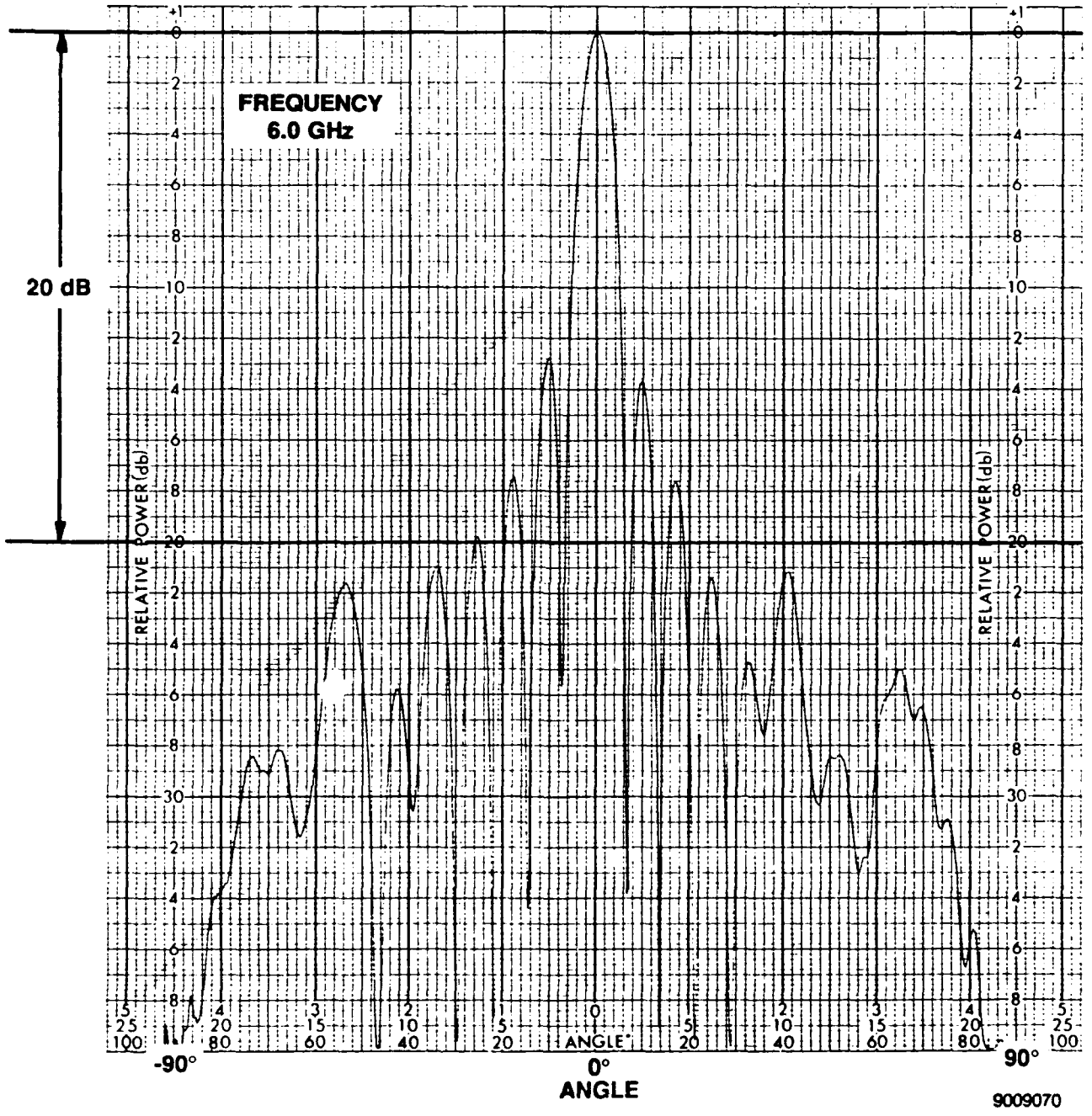
FREQUENCY
6.0 GHz
20 dB
RELATIVE POWER (db)
RELATIVE POWER (db)
ANGLE°
-90°
0°
ANGLE
90°
9009070

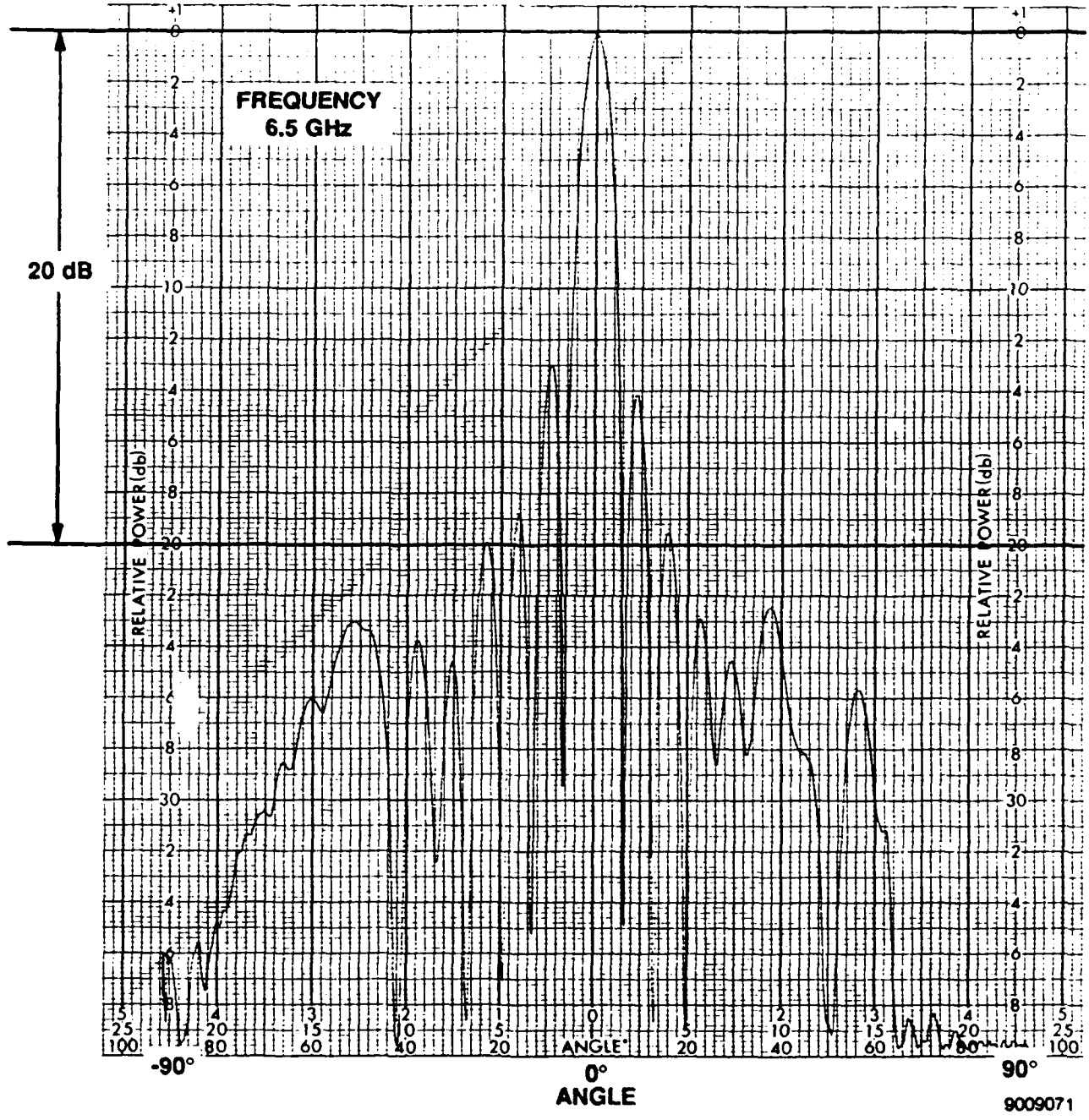
FREQUENCY
6.5 GHz
20 dB
RELATIVE POWER (db)
ANGLE°
-90°
0°
90°
ANGLE
9009071

APPENDIX A2

This data group contains patterns where 16 columns do not contain filters and 16 columns contain either 3- or 6-GHz filters, configurations d and e shown below. This group of patterns shows interaction between adjoining apertures. The aperture has a uniform illumination. The following frequencies, recorded within the passband of each filter, are contained in this appendix.

	Frequency (GHz)	Filter Response (dB)		Frequency (GHz)	Filter Response (dB)
Test 4	2.688	-30	Test 5	5.363	-30
	2.725	-25		5.447	-25
	2.753	-20		5.467	-20
	2.770	-15		5.534	-15
	2.778	-10		5.558	-10
	2.822	-5		5.581	-5
	3.0	0		6.0	0
	3.184	-5		6.387	-5
	3.204	-10		6.404	-10
	3.229	-15		6.486	-15
	3.250	-20		6.506	-20
	3.275	-25		6.593	-25
	3.326	-30		6.610	-30

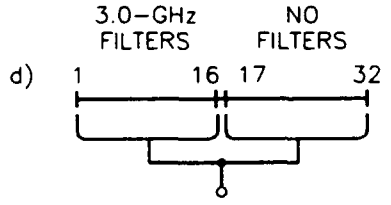

TEST 4

PATTERN MEASUREMENTS OF NONFILTERED APERTURE SHOWING EFFECT OF 3.0–GHz FILTER REJECT–BAND CHARACTERISTICS (i.e., 2.5, 3.5–7.0 GHz)

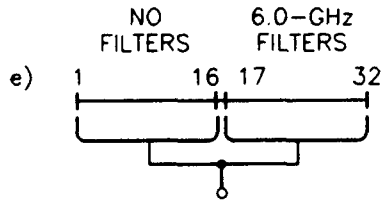

TEST 5

PATTERN MEASUREMENTS OF NONFILTERED APERTURE SHOWING EFFECT OF 6.0–GHz FILTER REJECT–BAND CHARACTERISTICS (i.e., 2.5–5.5 GHz, 6.5–7.0 GHz)

9009169

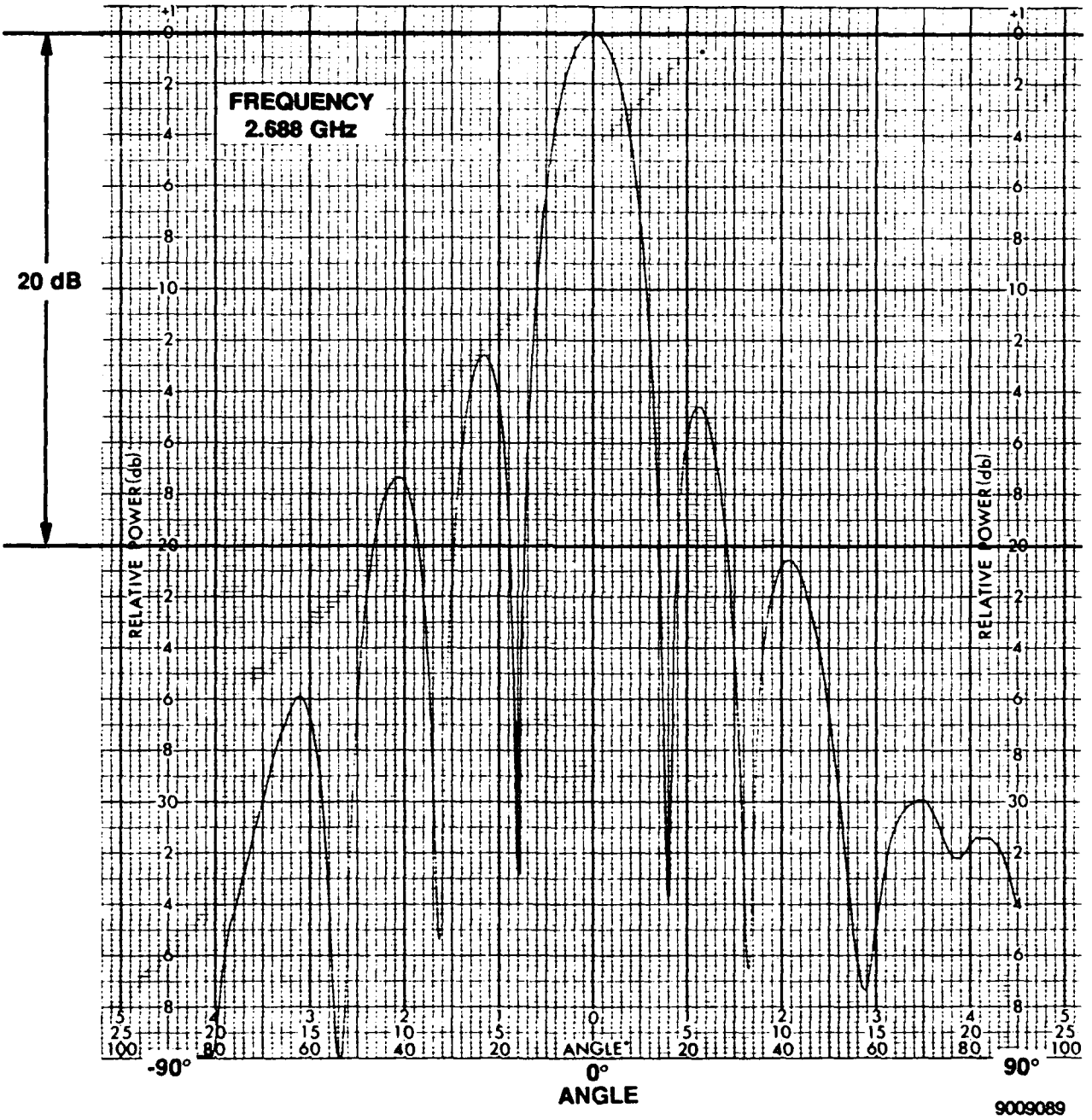
FREQUENCY
2.688 GHz
20 dB
RELATIVE POWER (db)
ANGLE
-90°
0°
90°
ANGLE
9009089

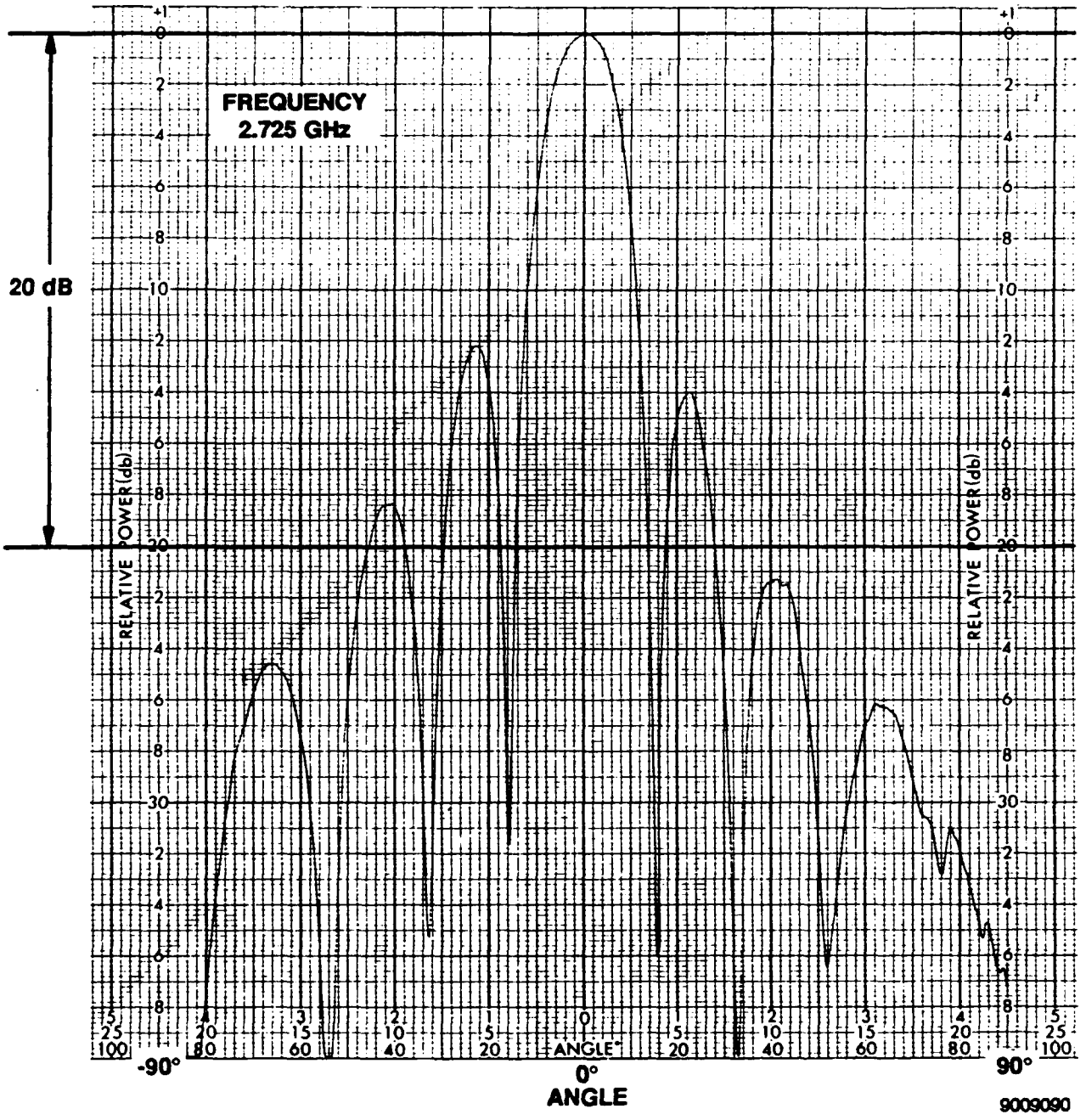
FREQUENCY
2.725 GHz
20 dB
RELATIVE POWER (db)
ANGLE°
-90°
0°
90°
ANGLE
9009090

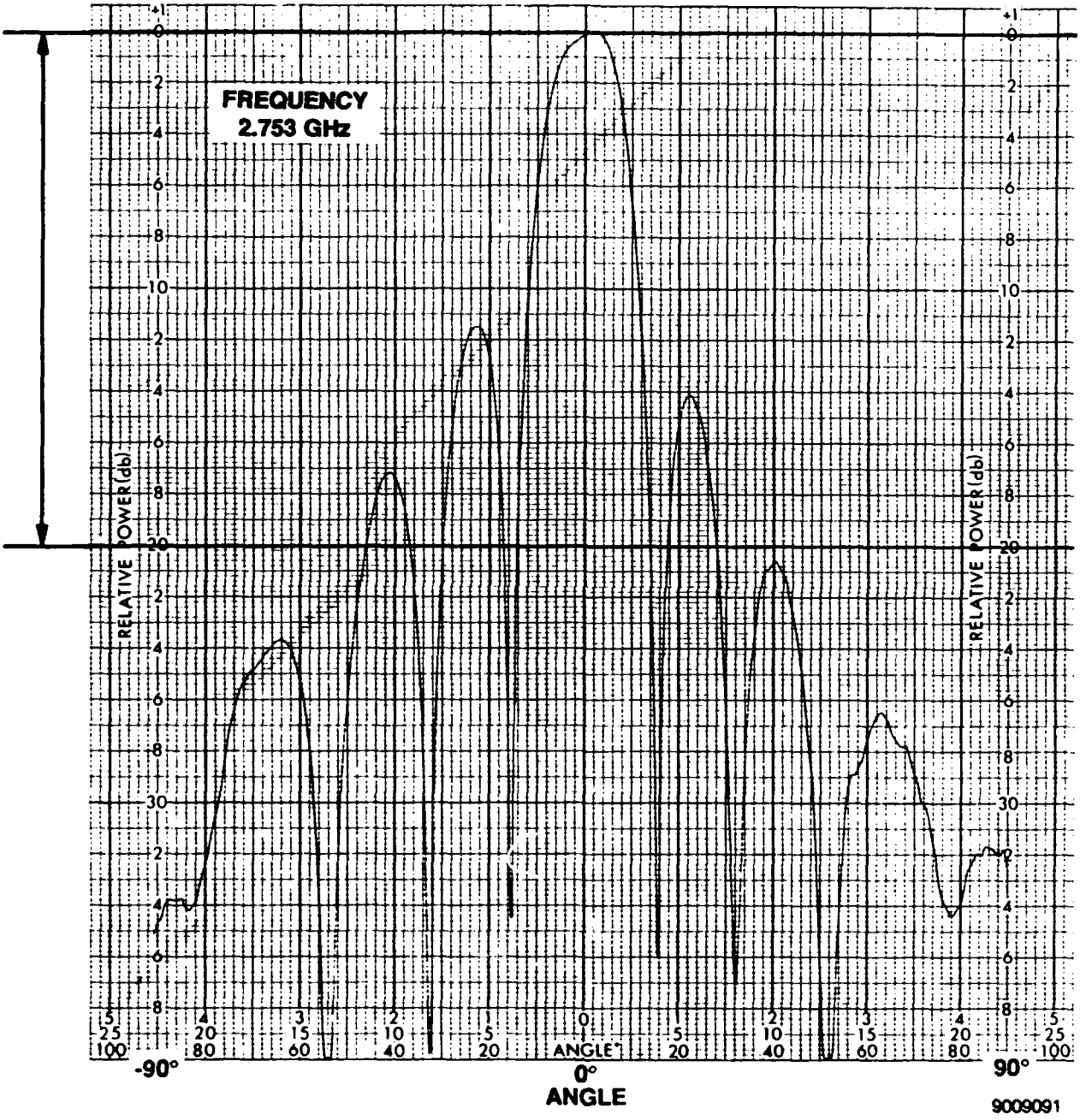
FREQUENCY
2.753 GHz
RELATIVE POWER (db)
RELATIVE POWER (db)
-90°
0°
90°
ANGLE
ANGLE
9009091

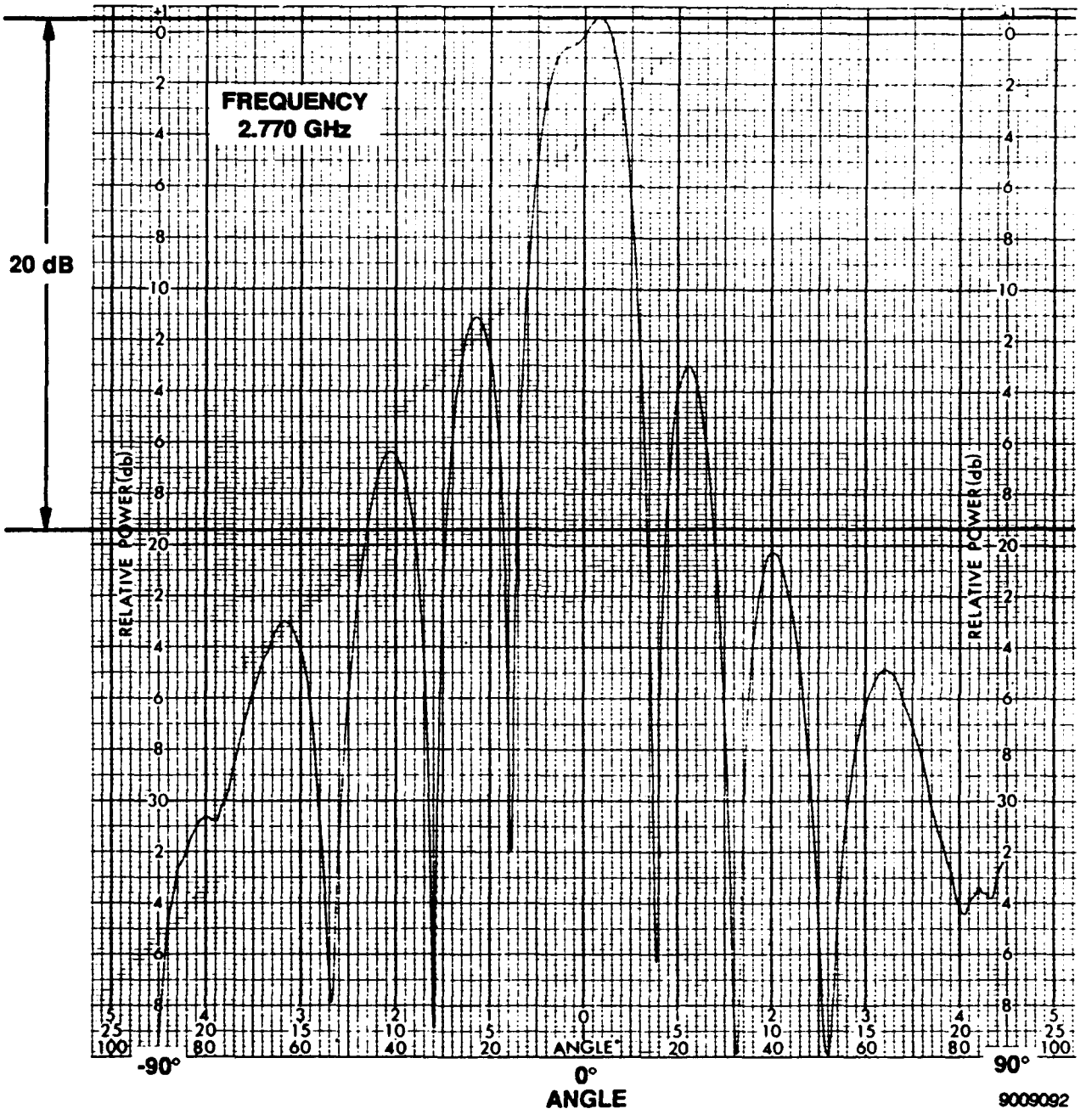
FREQUENCY
2.770 GHz
20 dB
RELATIVE POWER(db)
RELATIVE POWER(db)
ANGLE
-90°
0°
90°
ANGLE
9009092

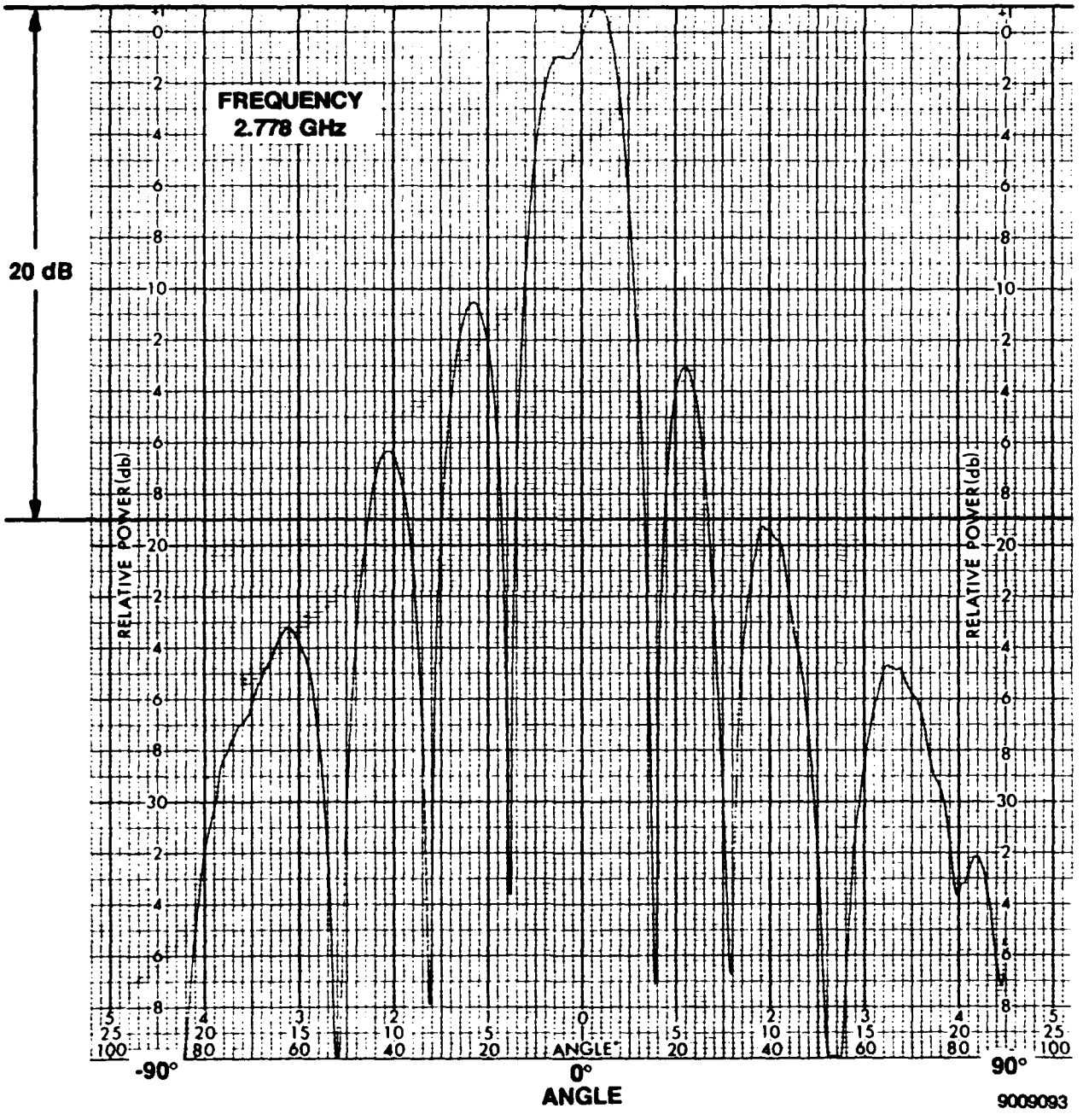
FREQUENCY
2.778 GHz
20 dB
RELATIVE POWER (db)
RELATIVE POWER (db)
ANGLE
-90°
0°
90°
ANGLE
9009093

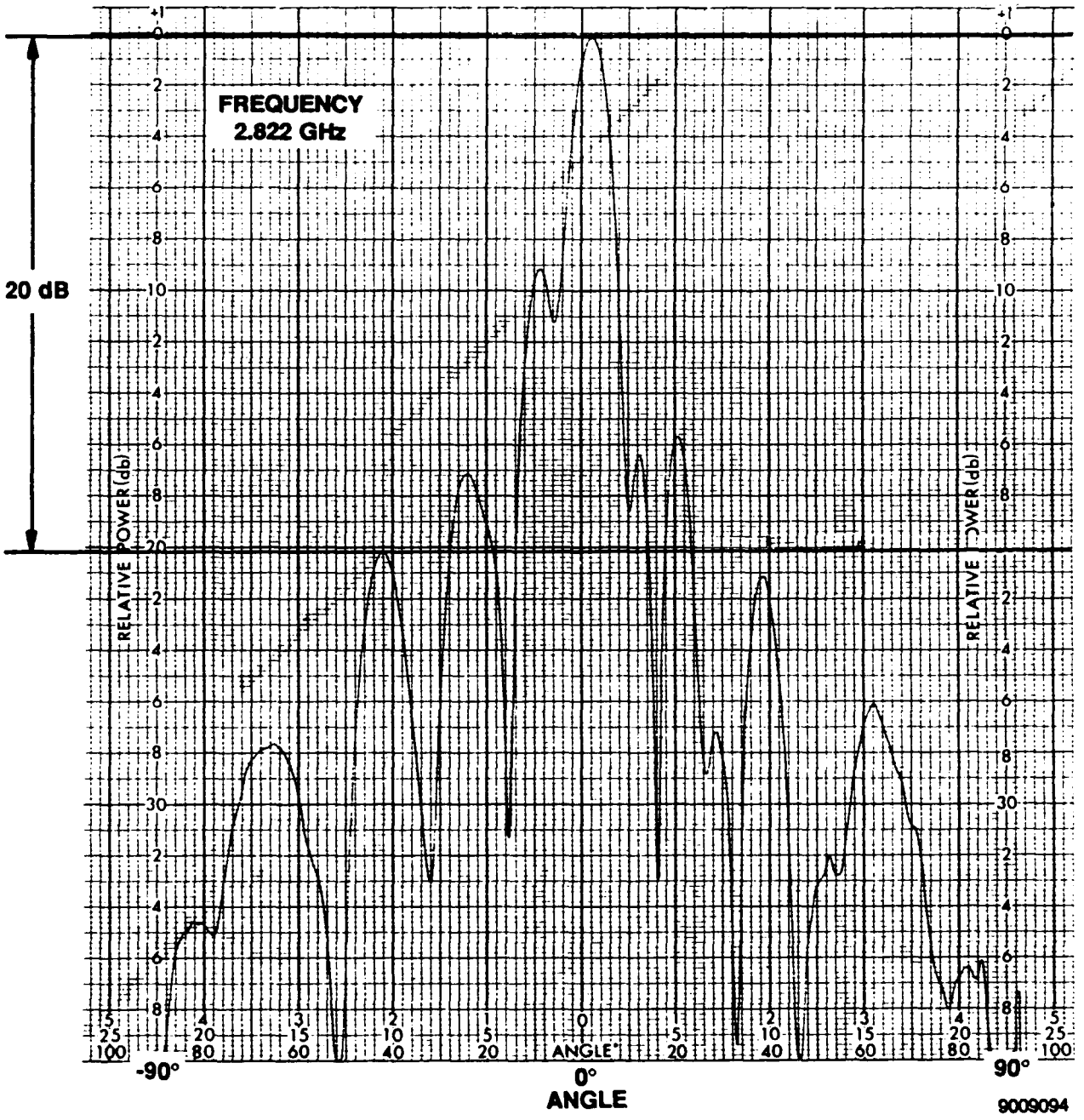
FREQUENCY
2.822 GHz
20 dB
RELATIVE POWER (db)
RELATIVE POWER (db)
ANGLE°
-90°
0°
90°
ANGLE
9009094

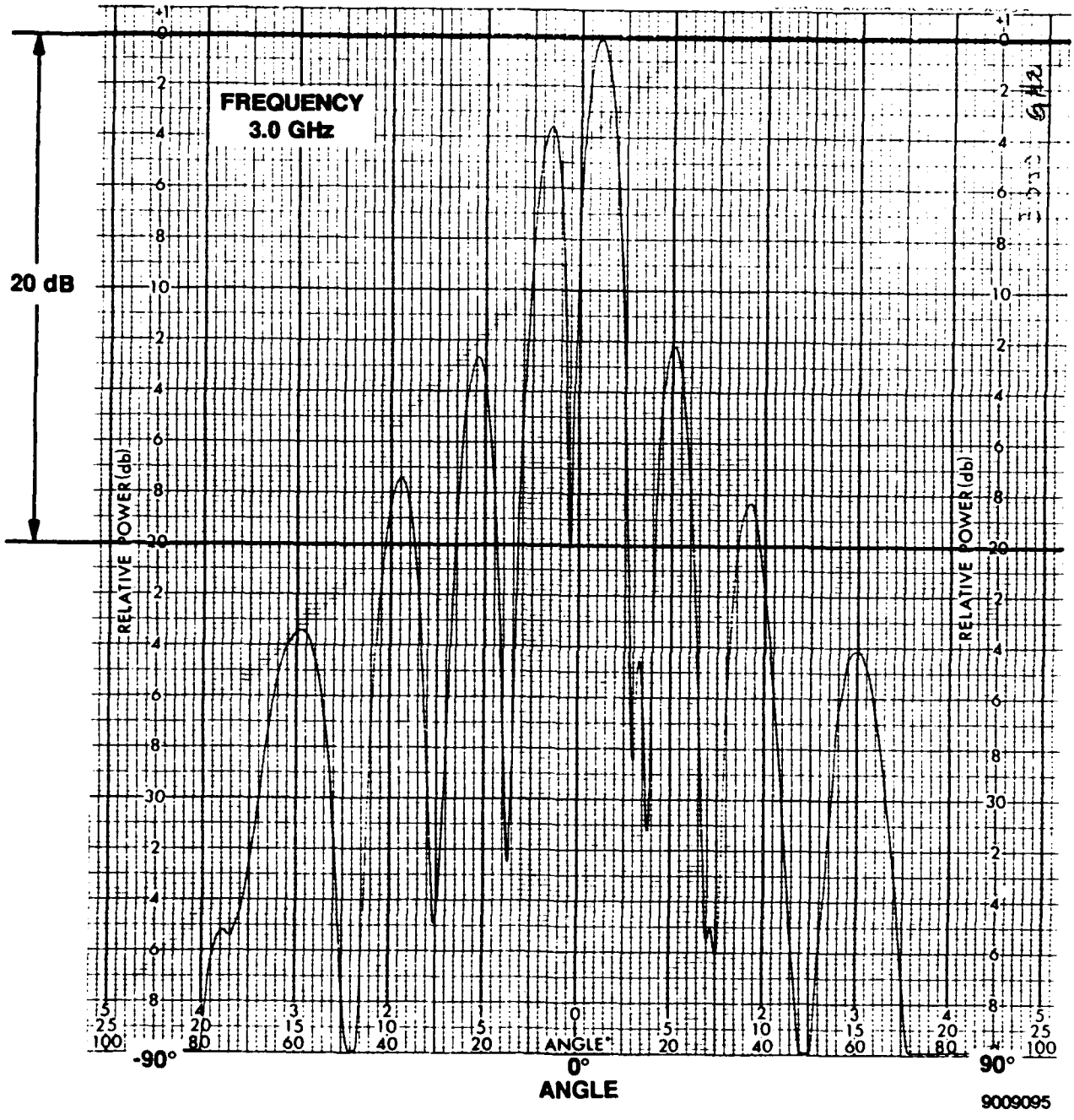
FREQUENCY
3.0 GHz
20 dB
RELATIVE POWER (db)
RELATIVE POWER (db)
ANGLE°
-90°
0°
90°
ANGLE
9009095

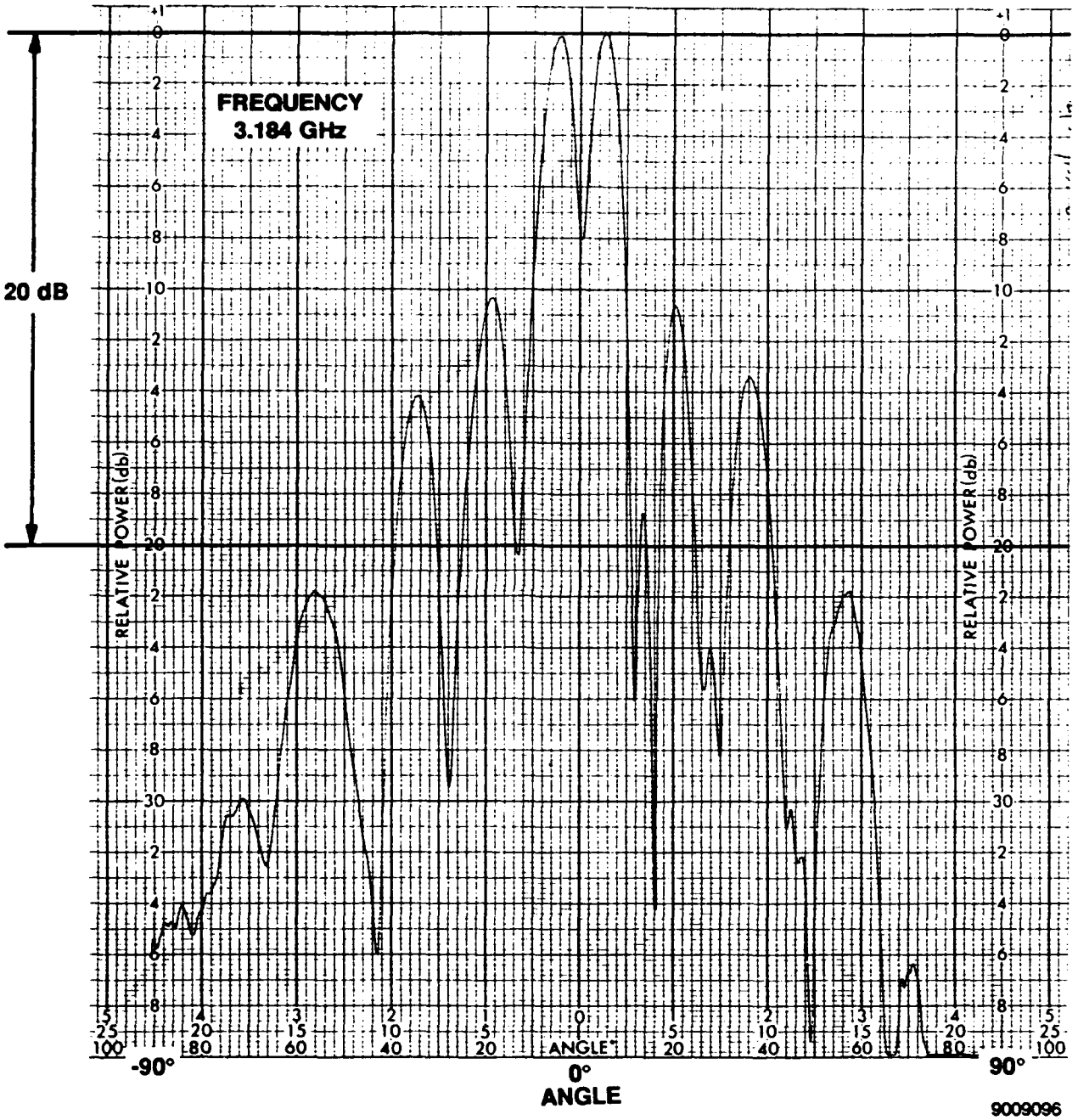
FREQUENCY
3.184 GHz
20 dB
RELATIVE POWER (db)
RELATIVE POWER (db)
-90°
0°
90°
ANGLE
ANGLE
9009096

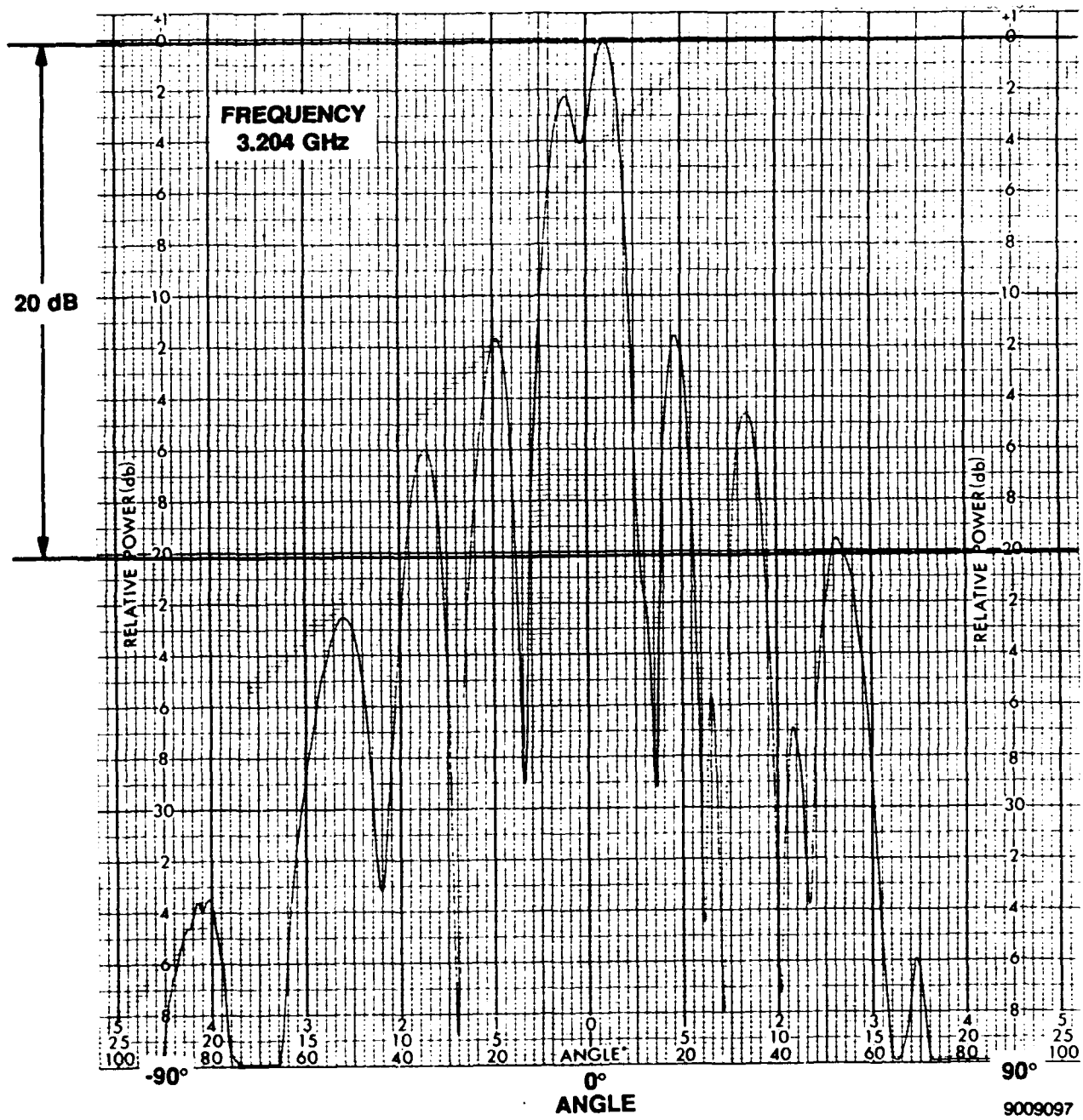
FREQUENCY
3.204 GHz
20 dB
RELATIVE POWER (db)
RELATIVE POWER (db)
ANGLE°
-90°
0°
90°
ANGLE
9009097

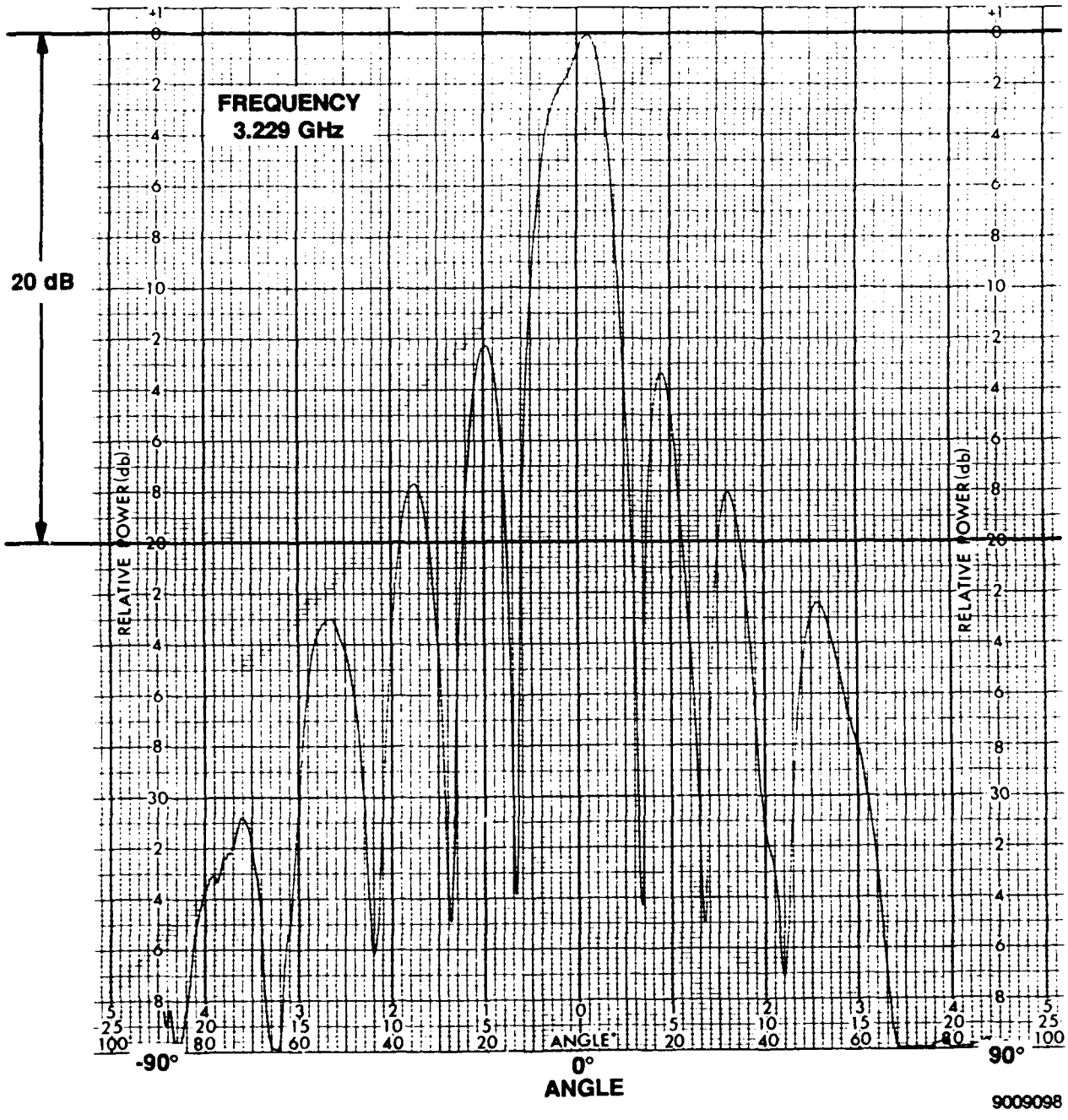
FREQUENCY
3.229 GHz
20 dB
RELATIVE POWER (db)
RELATIVE POWER (db)
ANGLE
-90°
0°
90°
ANGLE
9009098

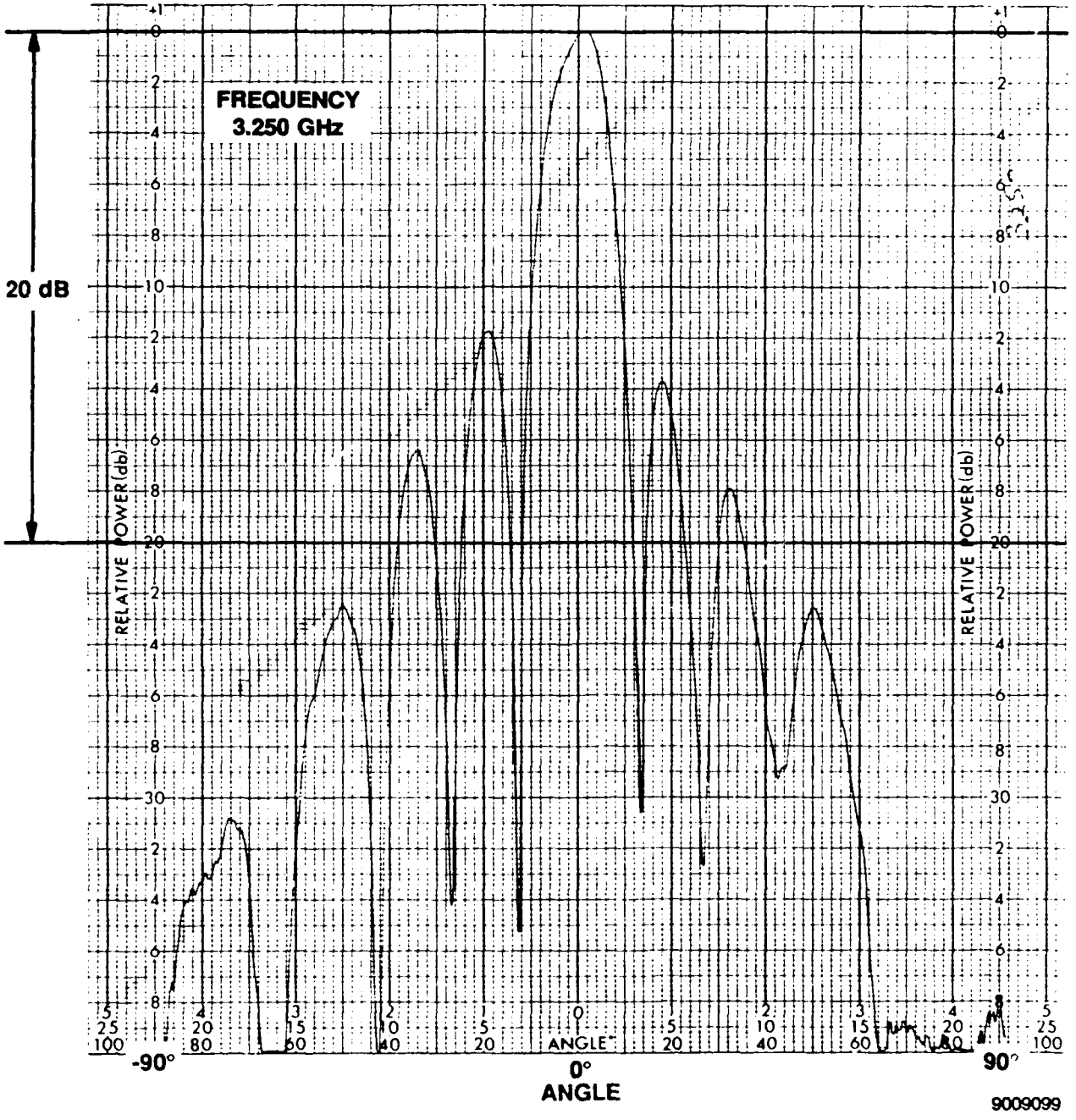
FREQUENCY
3.250 GHz
20 dB
RELATIVE POWER (db)
RELATIVE POWER (db)
ANGLE
-90°
0°
90°
ANGLE
9009099

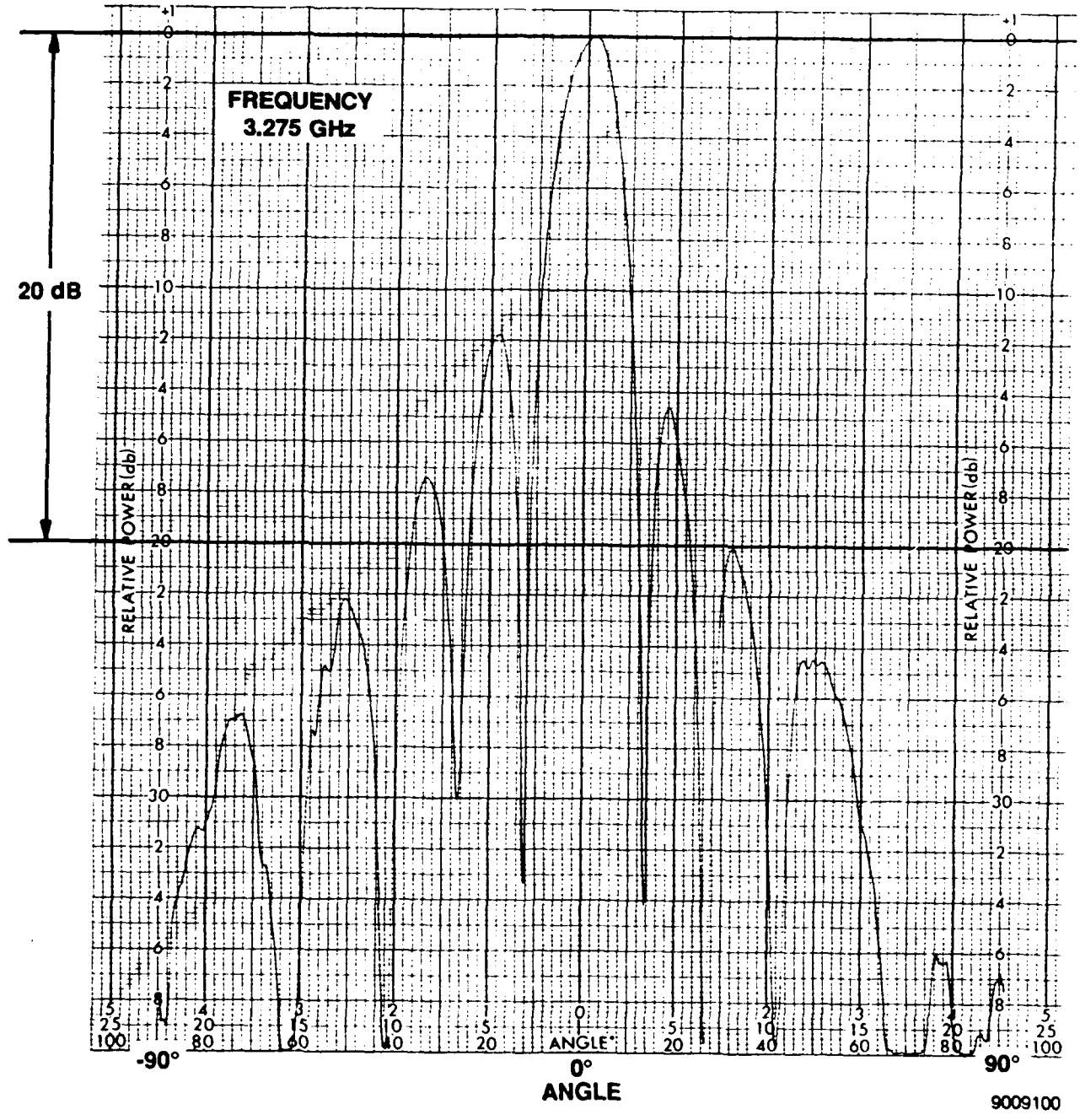
FREQUENCY
3.275 GHz
20 dB
RELATIVE POWER (db)
ANGLE°
-90°
0°
90°
ANGLE
9009100

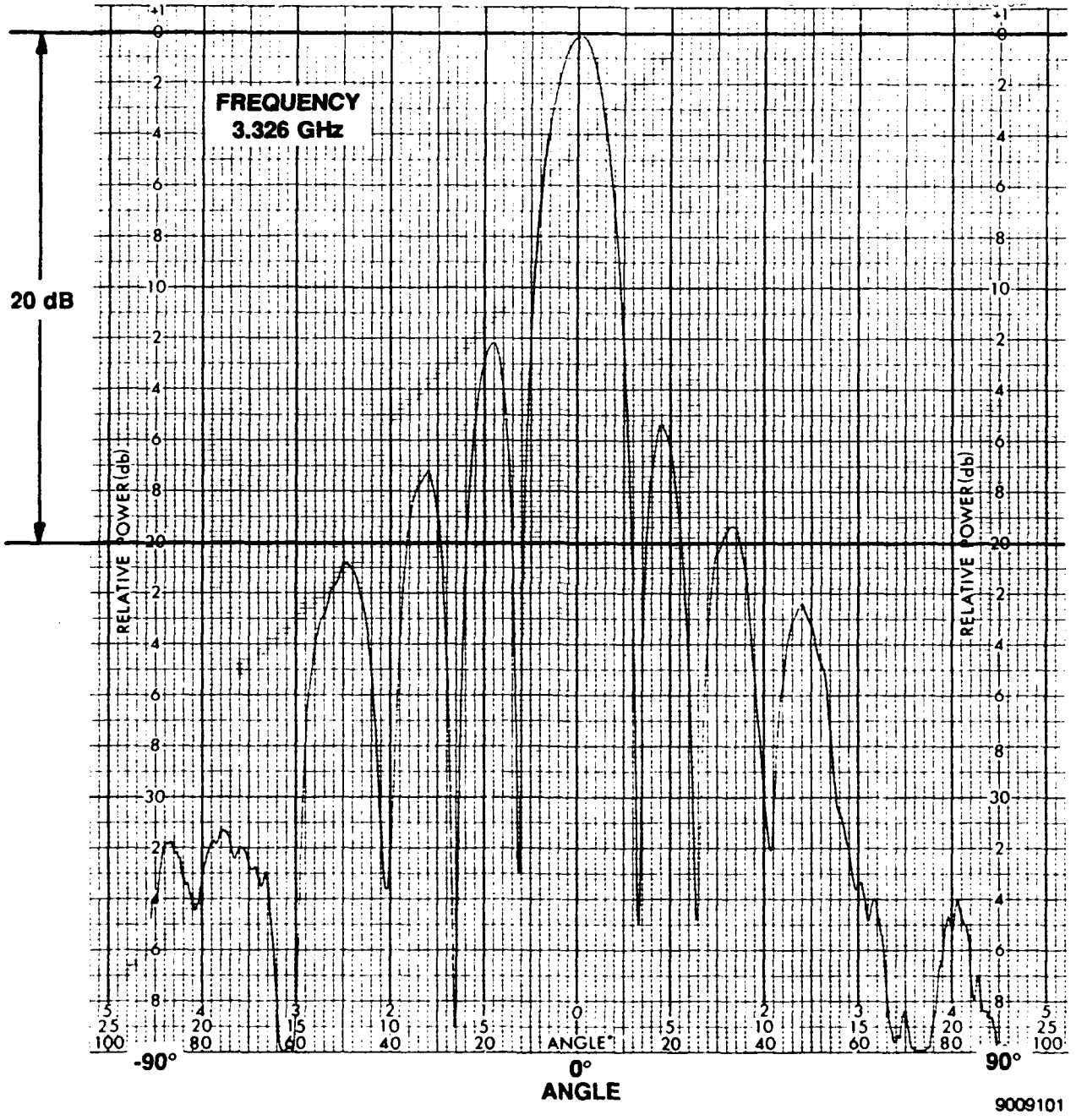
FREQUENCY
3.326 GHz
20 dB
RELATIVE POWER (db)
RELATIVE POWER (db)
ANGLE°
-90°
0°
90°
ANGLE
9009101

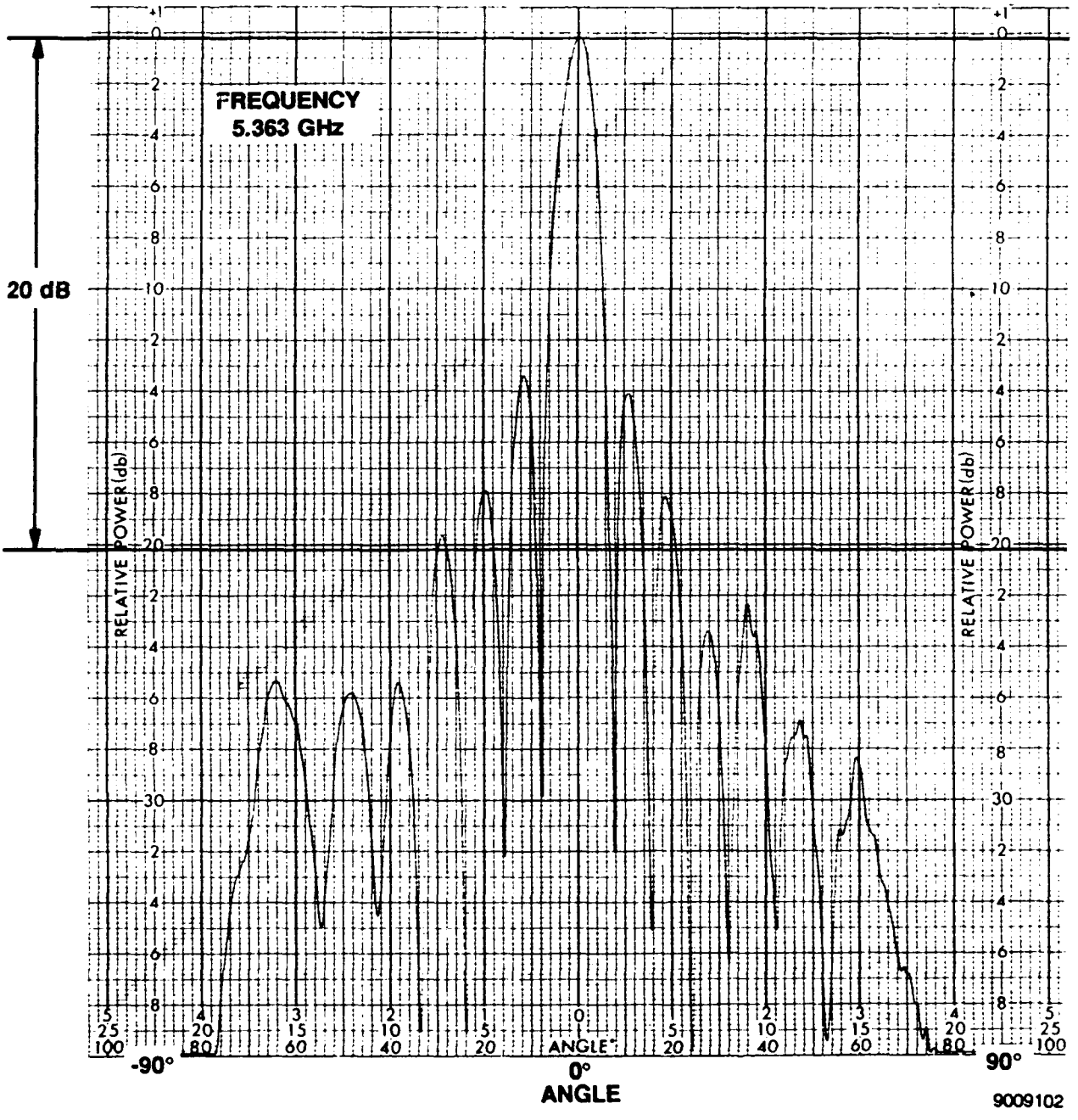
FREQUENCY
5.363 GHz
20 dB
RELATIVE POWER (db)
ANGLE
-90°
0°
90°
ANGLE
9009102

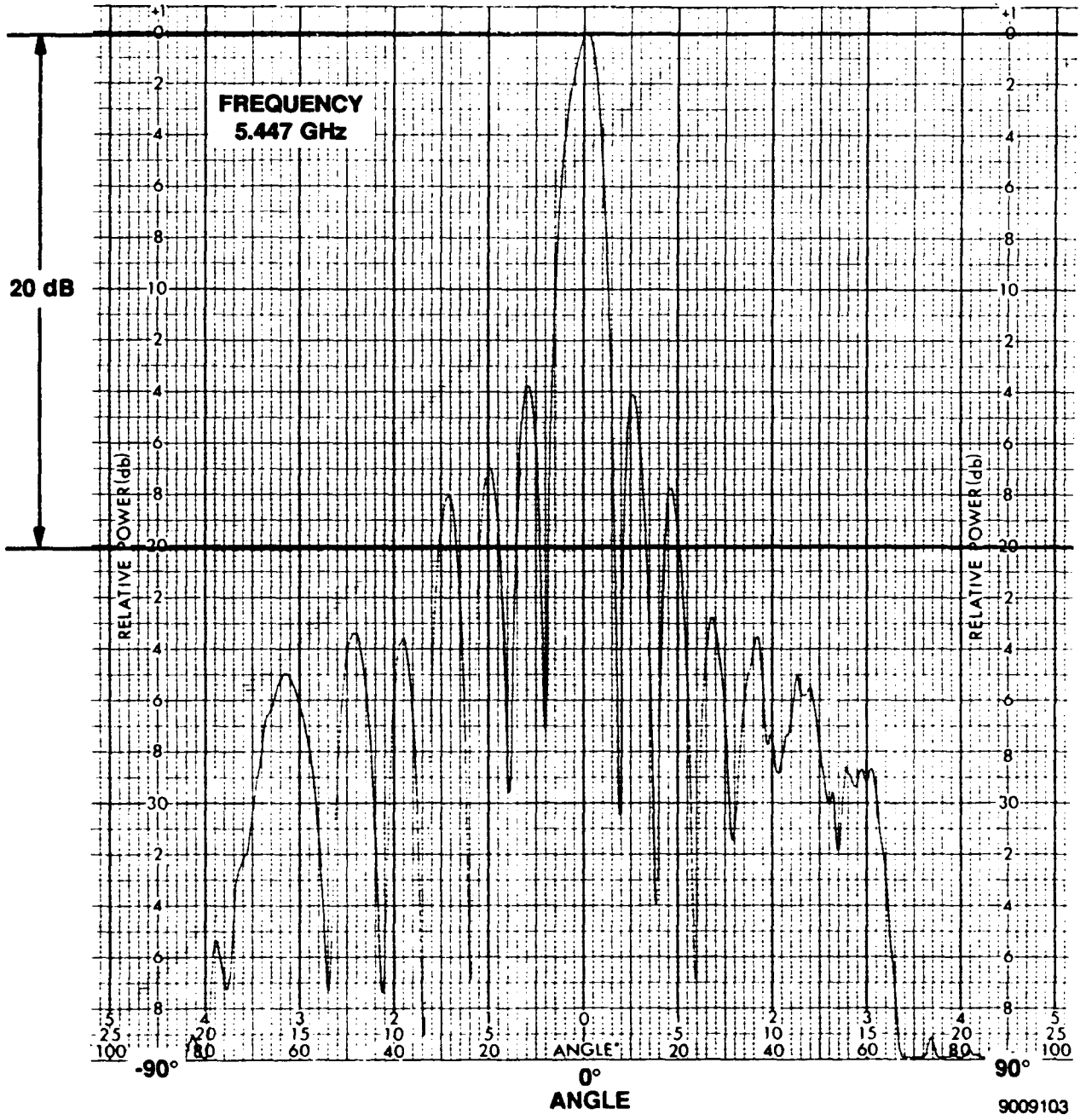
FREQUENCY
5.447 GHz
20 dB
RELATIVE POWER (db)
RELATIVE POWER (db)
ANGLE°
-90°
0°
90°
ANGLE
9009103

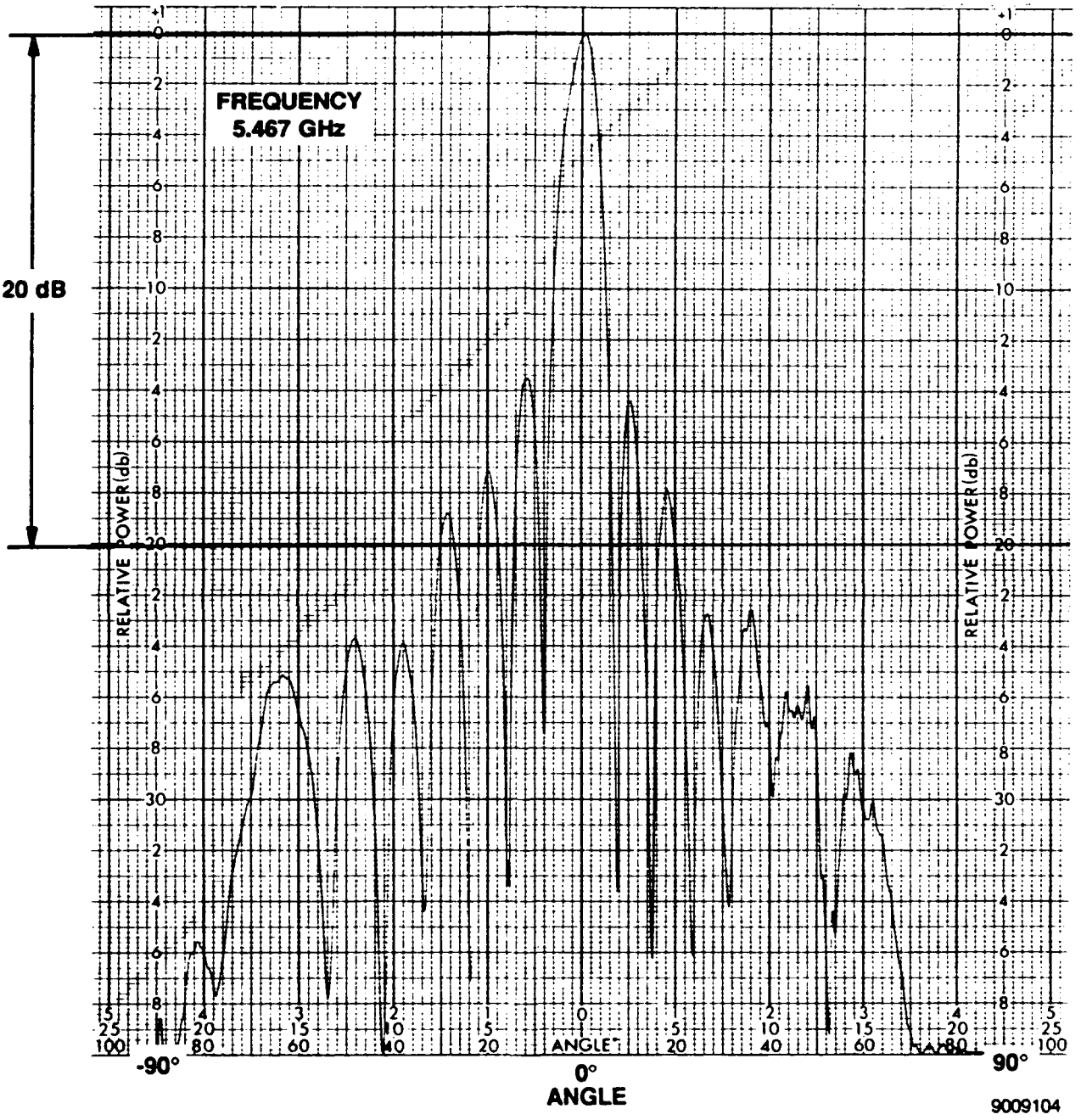
FREQUENCY
5.467 GHz
20 dB
RELATIVE POWER (db)
RELATIVE POWER (db)
ANGLE
-90°
0°
90°
ANGLE
9009104

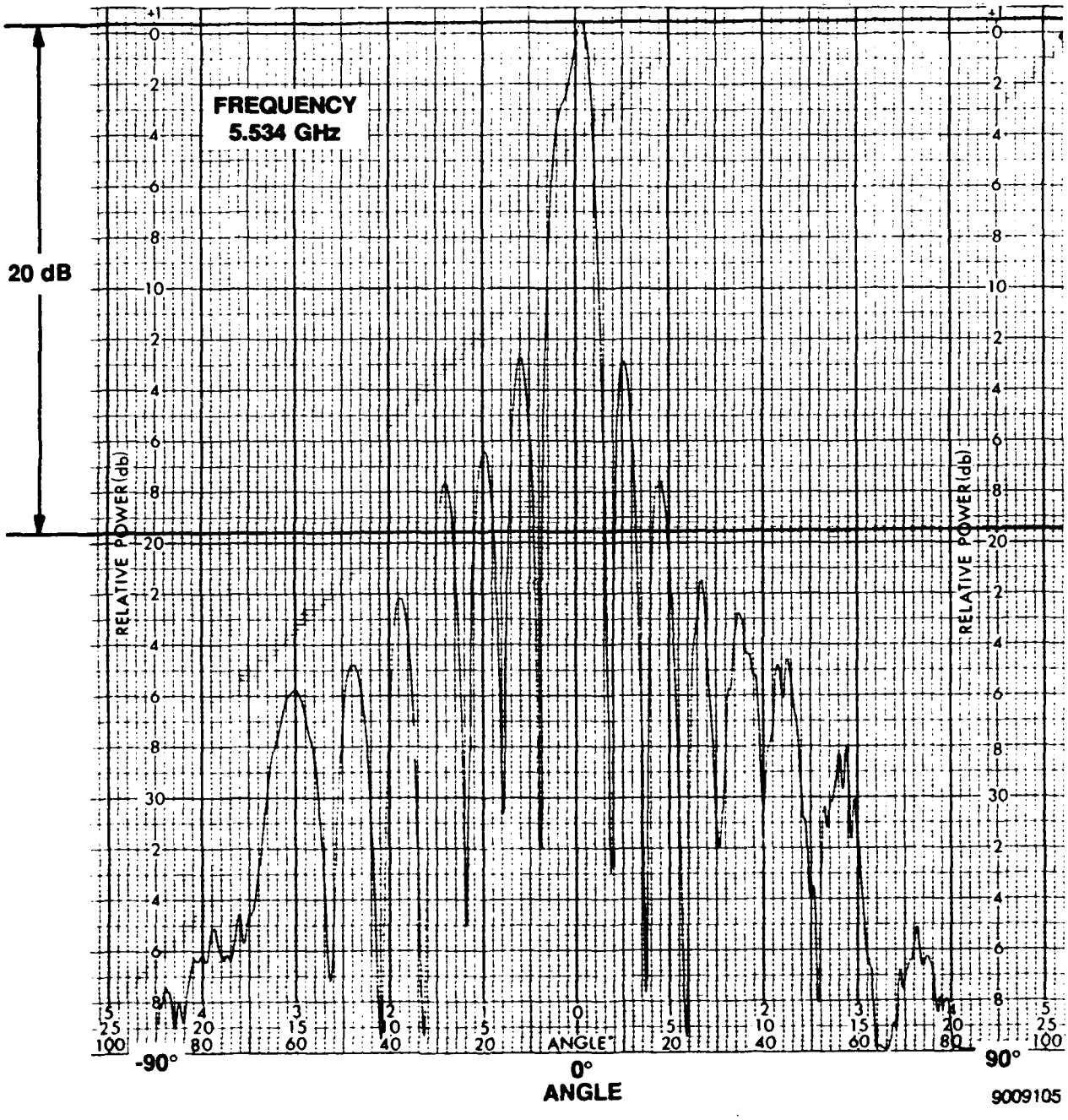
FREQUENCY
5.534 GHz
20 dB
RELATIVE POWER (db)
RELATIVE POWER (db)
ANGLE°
-90°
0°
90°
ANGLE
9009105

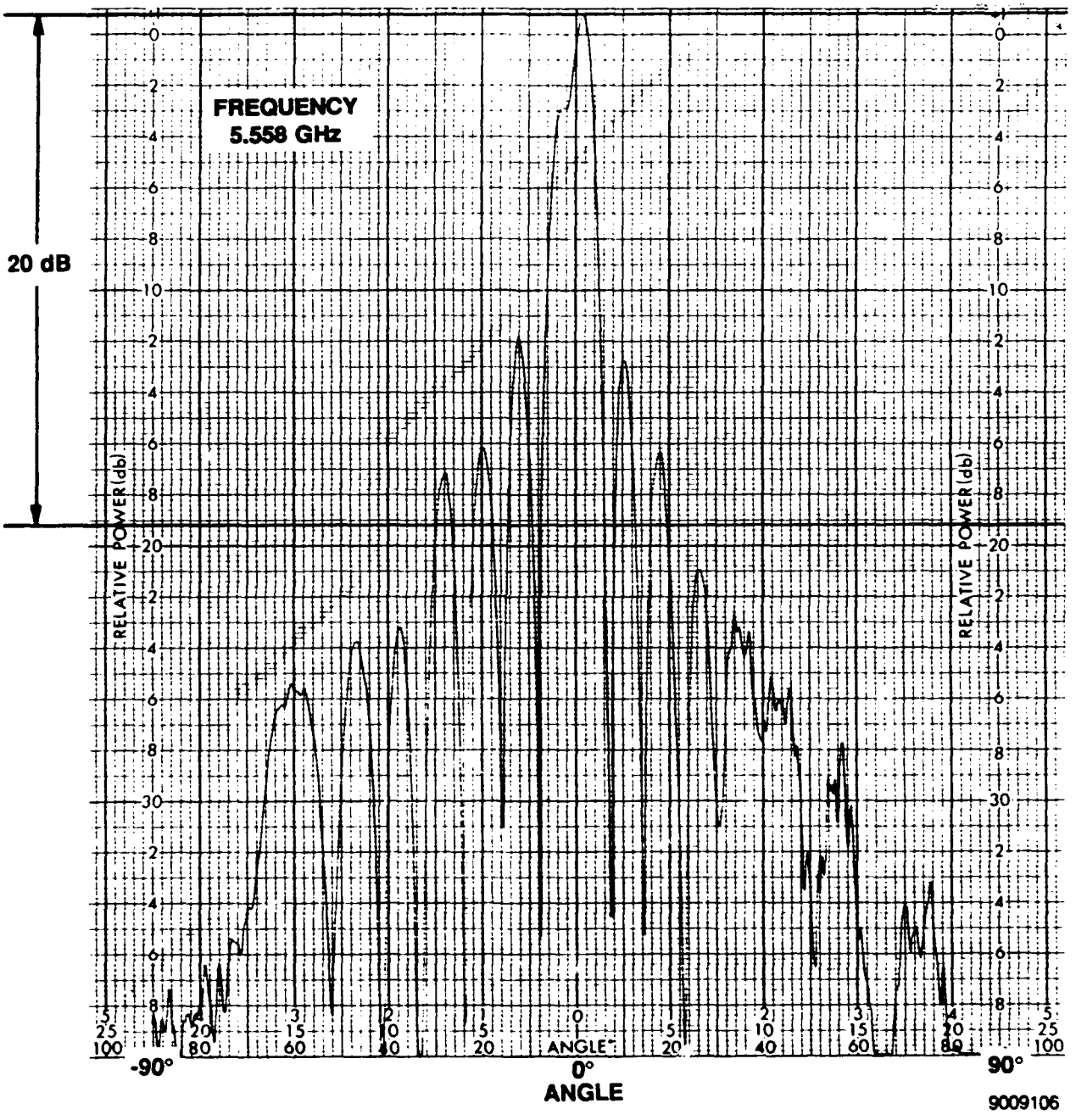
FREQUENCY
5.558 GHz
20 dB
RELATIVE POWER (db)
RELATIVE POWER (db)
ANGLE°
-90°
0°
90°
ANGLE
9009106

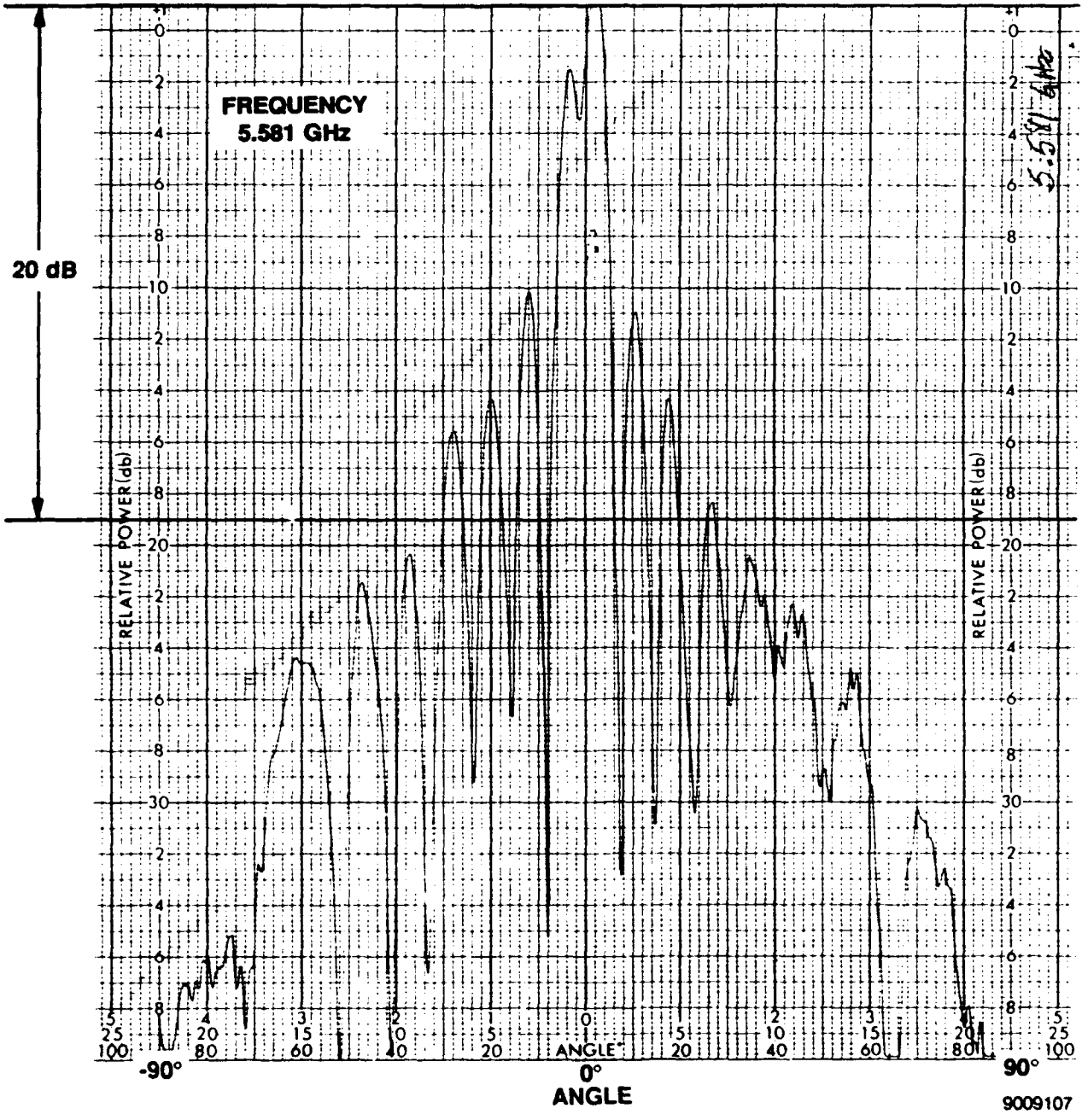
20 dB
FREQUENCY
5.581 GHz
RELATIVE POWER (db)
RELATIVE POWER (db)
-90°
0°
90°
ANGLE
ANGLE
9009107

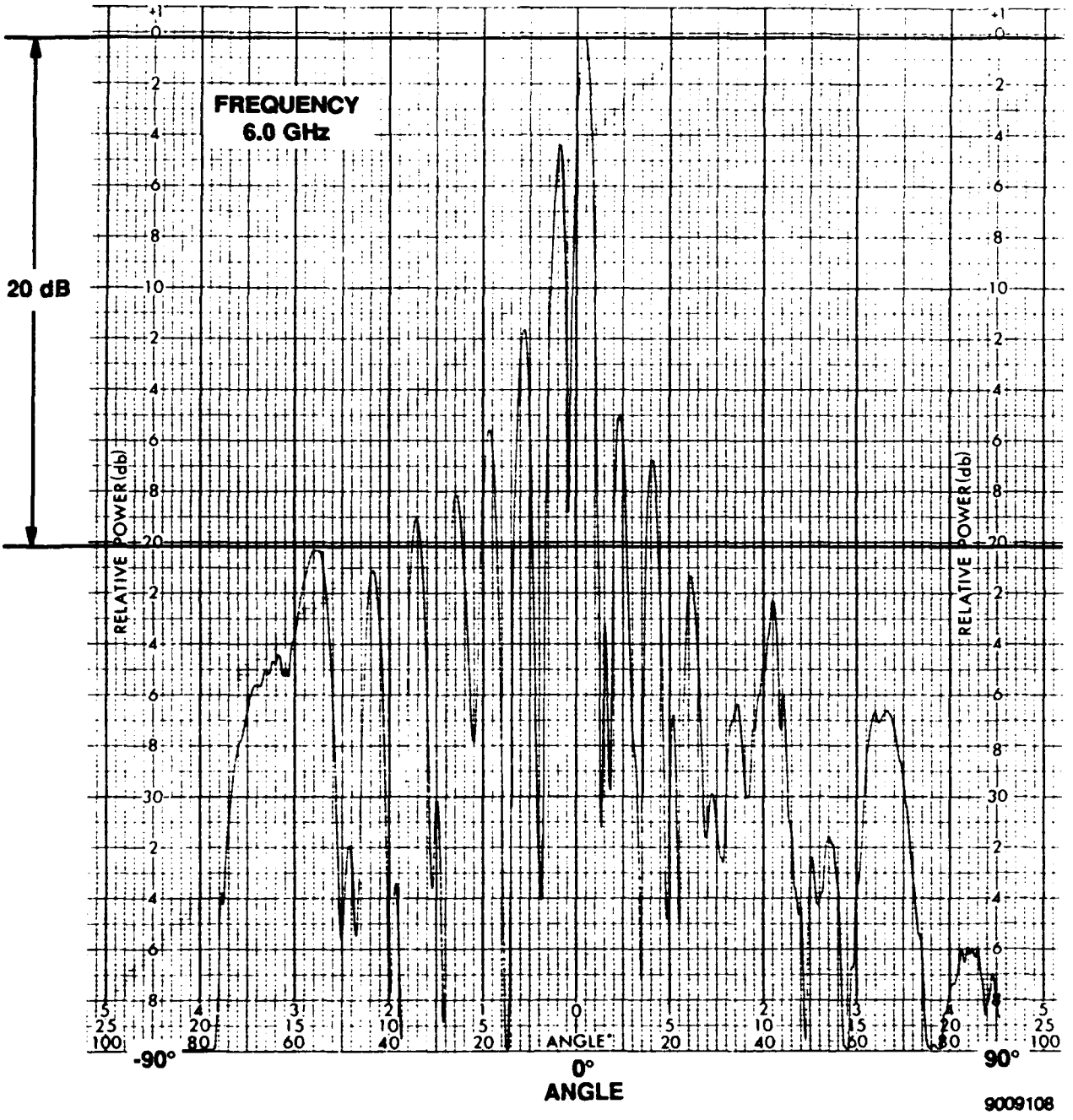
FREQUENCY
6.0 GHz
20 dB
RELATIVE POWER (db)
RELATIVE POWER (db)
ANGLE°
-90°
0°
90°
ANGLE
9009108

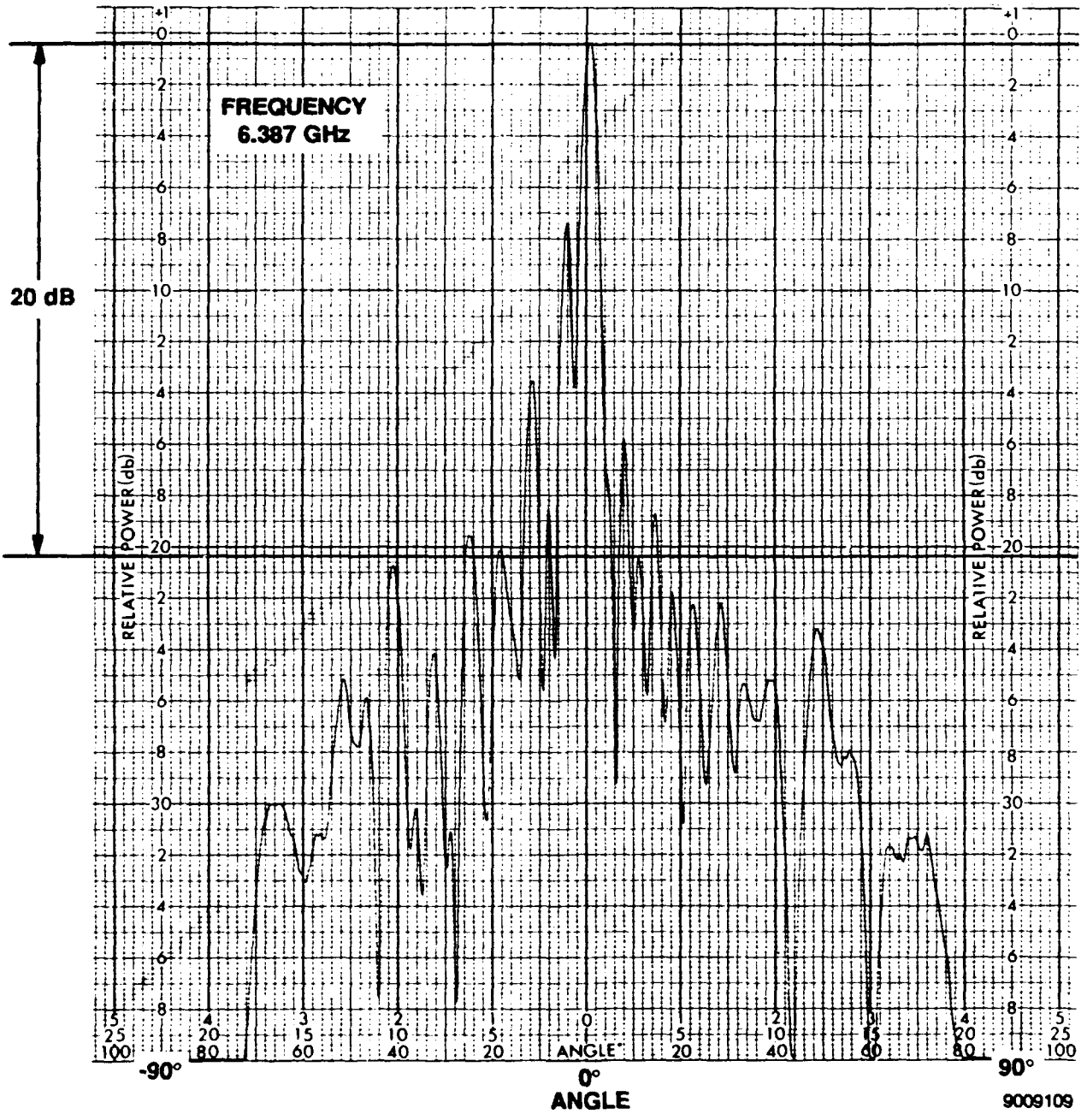
FREQUENCY
6.387 GHz
20 dB
RELATIVE POWER (db)
RELATIVE POWER (db)
ANGLE°
-90°
0°
90°
ANGLE
9009109

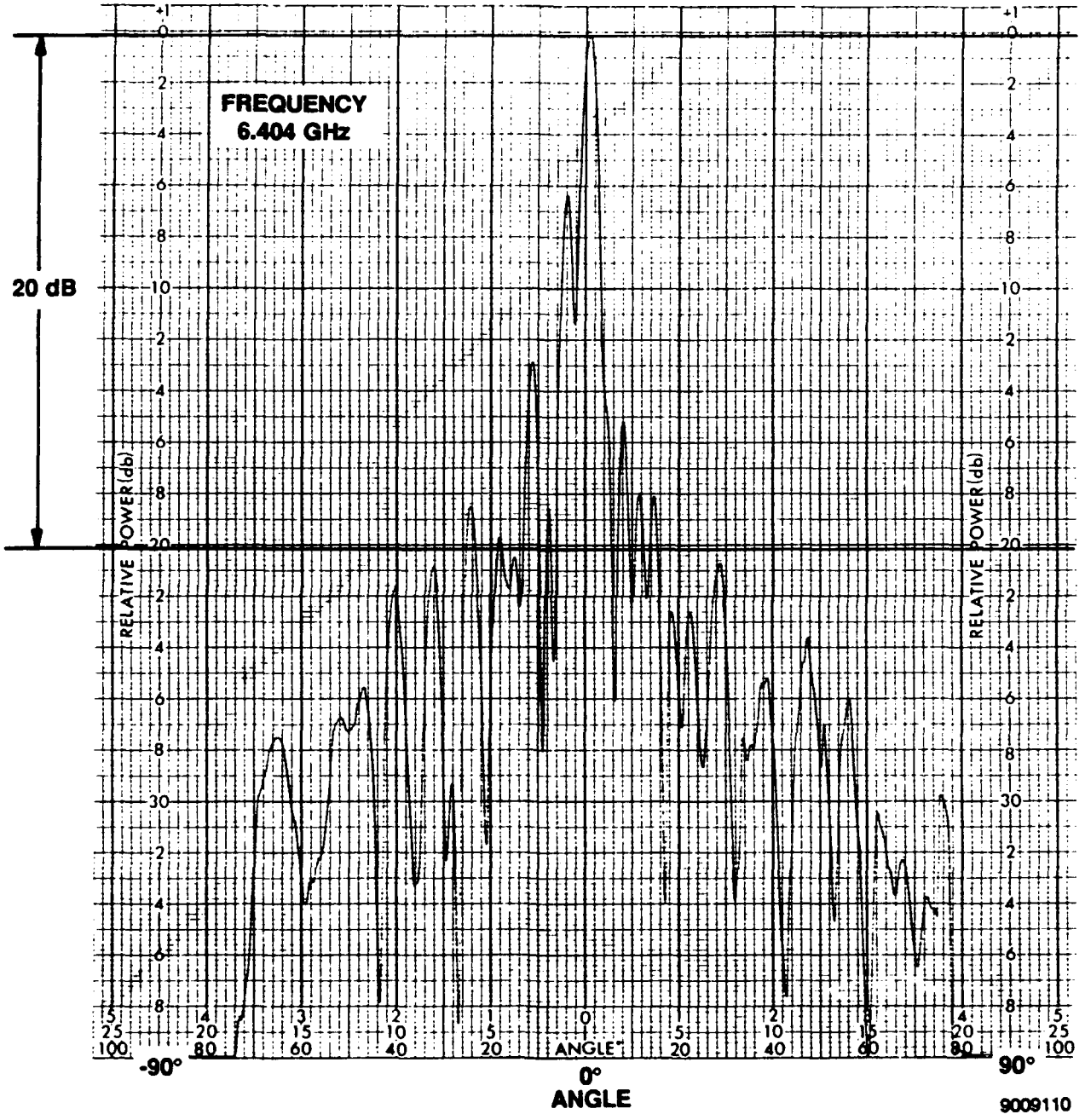
FREQUENCY
6.404 GHz
20 dB
RELATIVE POWER (db)
ANGLE
-90°
0°
90°
ANGLE
9009110

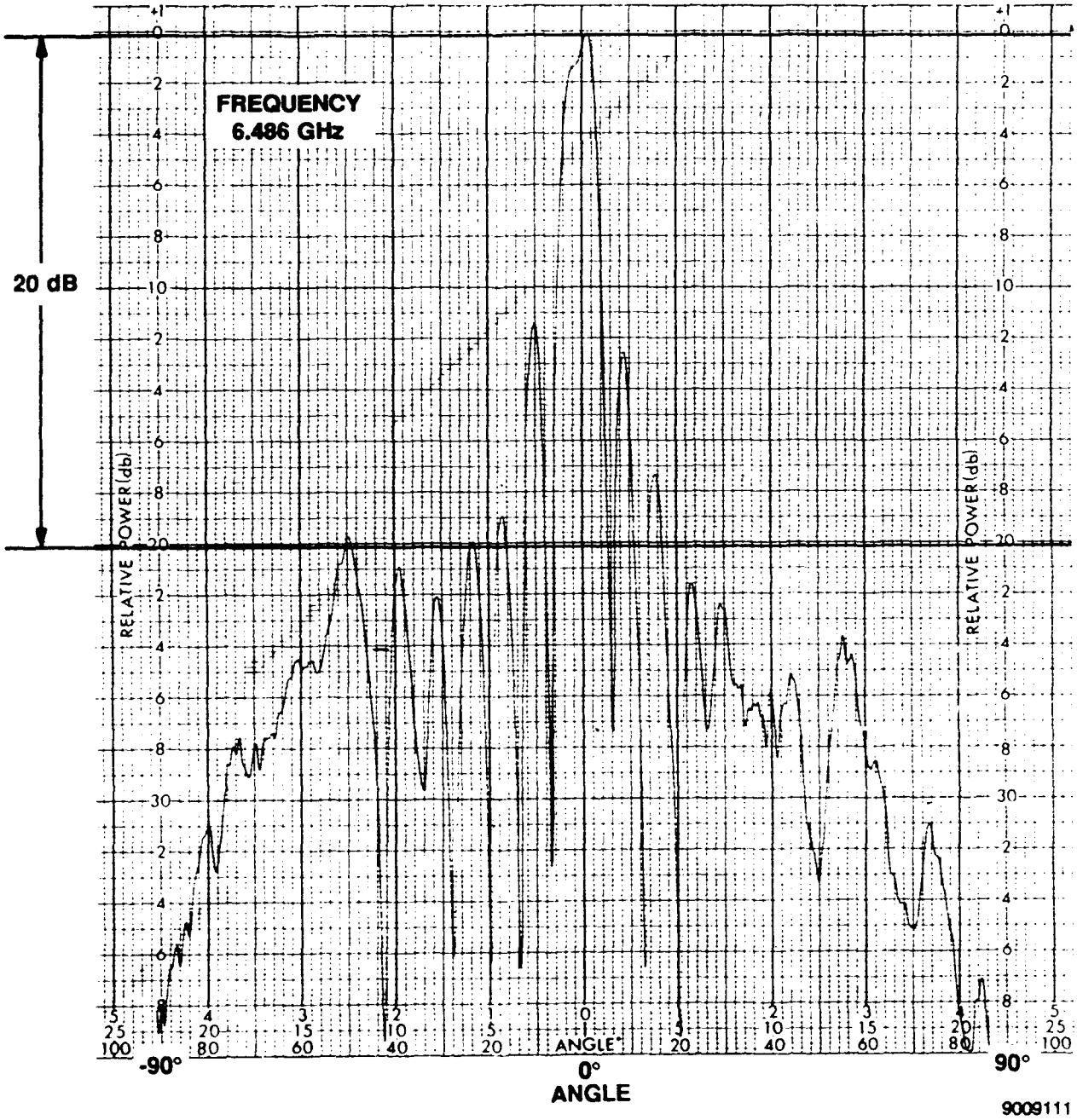
FREQUENCY
6.486 GHz
20 dB
RELATIVE POWER (db)
ANGLE
-90°
0°
90°
9009111

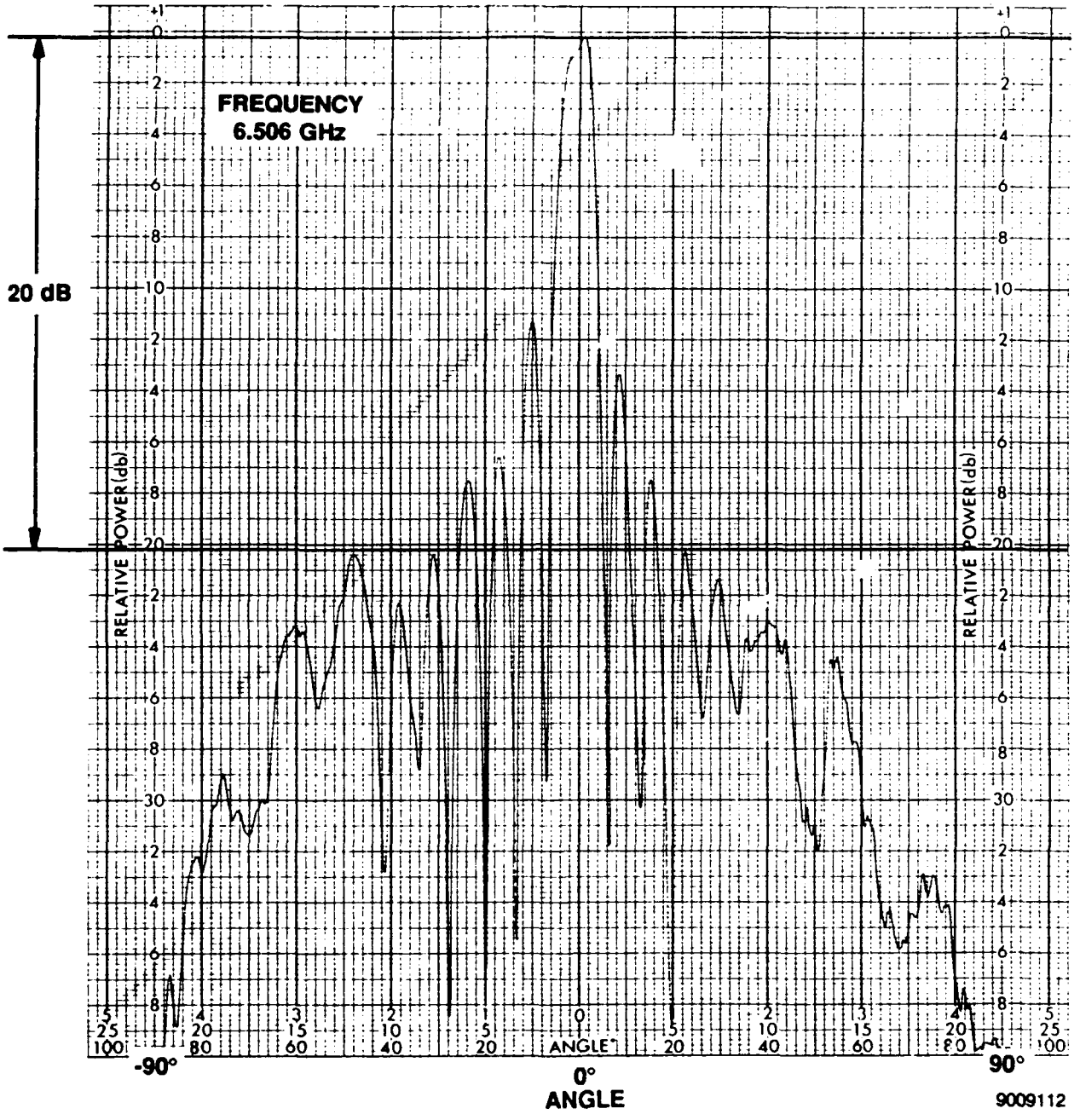
FREQUENCY
6.506 GHz
20 dB
RELATIVE POWER (db)
ANGLE
-90°
0°
90°
ANGLE
9009112

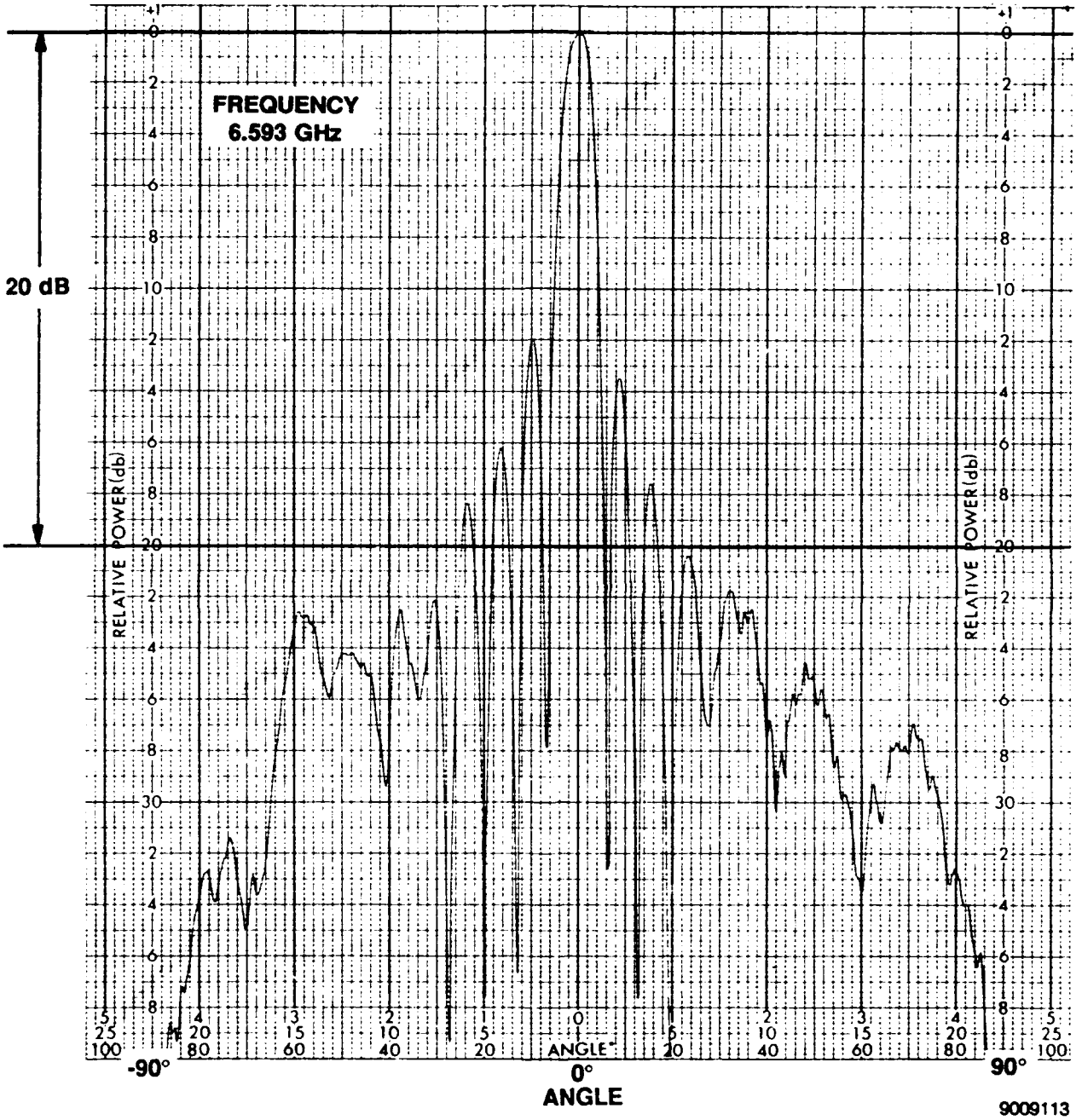
FREQUENCY
6.593 GHz
20 dB
RELATIVE POWER (db)
RELATIVE POWER (db)
ANGLE
-90°
0°
90°
ANGLE
9009113

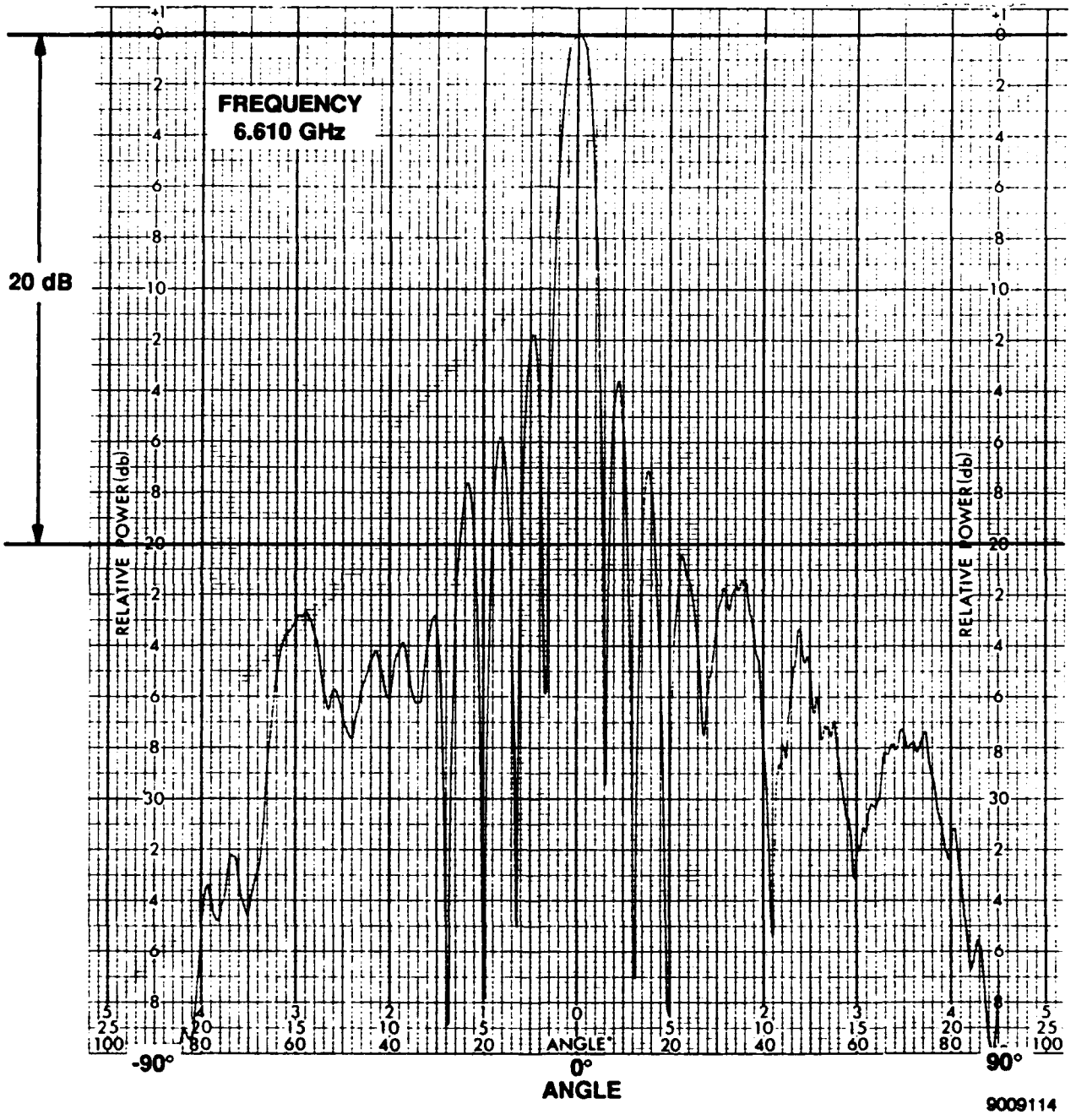
FREQUENCY
6.610 GHz
20 dB
RELATIVE POWER (db)
RELATIVE POWER (db)
ANGLE°
-90°
0°
90°
ANGLE
9009114

APPENDIX A3

This data group contains patterns with 16 columns with either 3- or 6-GHz filters and 16 columns without filters, configurations d and e shown below. This pattern set shows independent operation of the nonfiltered aperture. The apertures have uniform illumination. The following frequencies are contained in this data set.

Frequencies (GHz)			
Test 5	2.0	Test 4	2.0
	2.5		2.5
	3.0		3.5
	3.5		4.0
	4.0		4.5
	4.5		5.0
	5.0		5.5
	6.797		6.0
			6.5

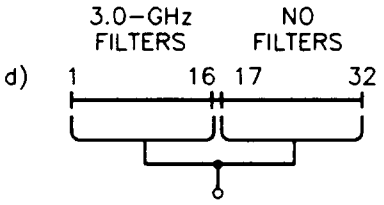

d) TEST 4 PATTERN MEASUREMENTS OF NONFILTERED APERTURE.

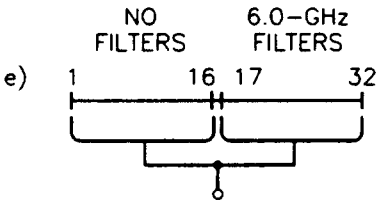

e) TEST 5 PATTERN MEASUREMENTS OF NONFILTERED APERTURE.

9009170

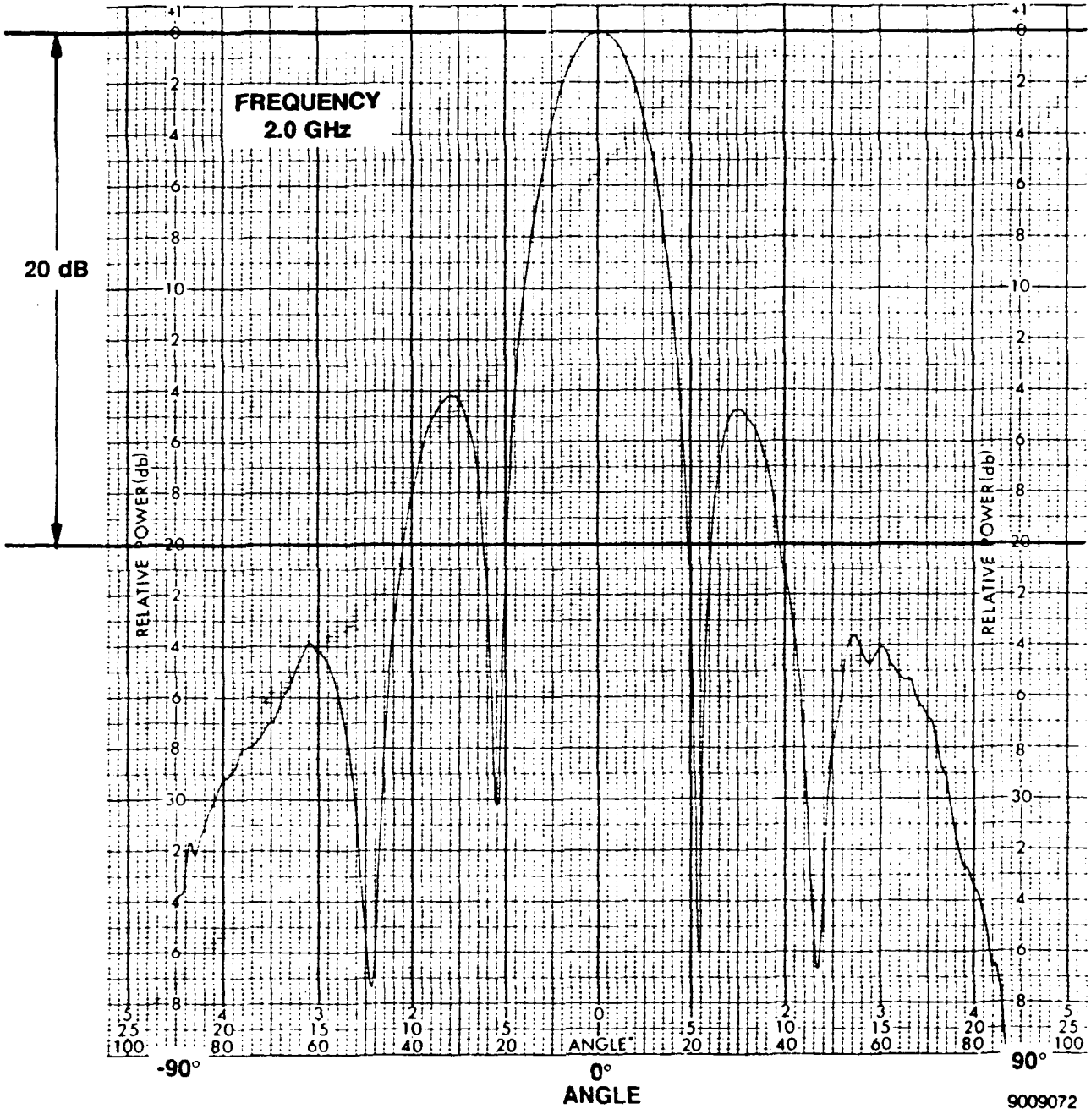
FREQUENCY
2.0 GHz
20 dB
RELATIVE POWER (db)
ANGLE
-90°
0°
90°
ANGLE
9009072

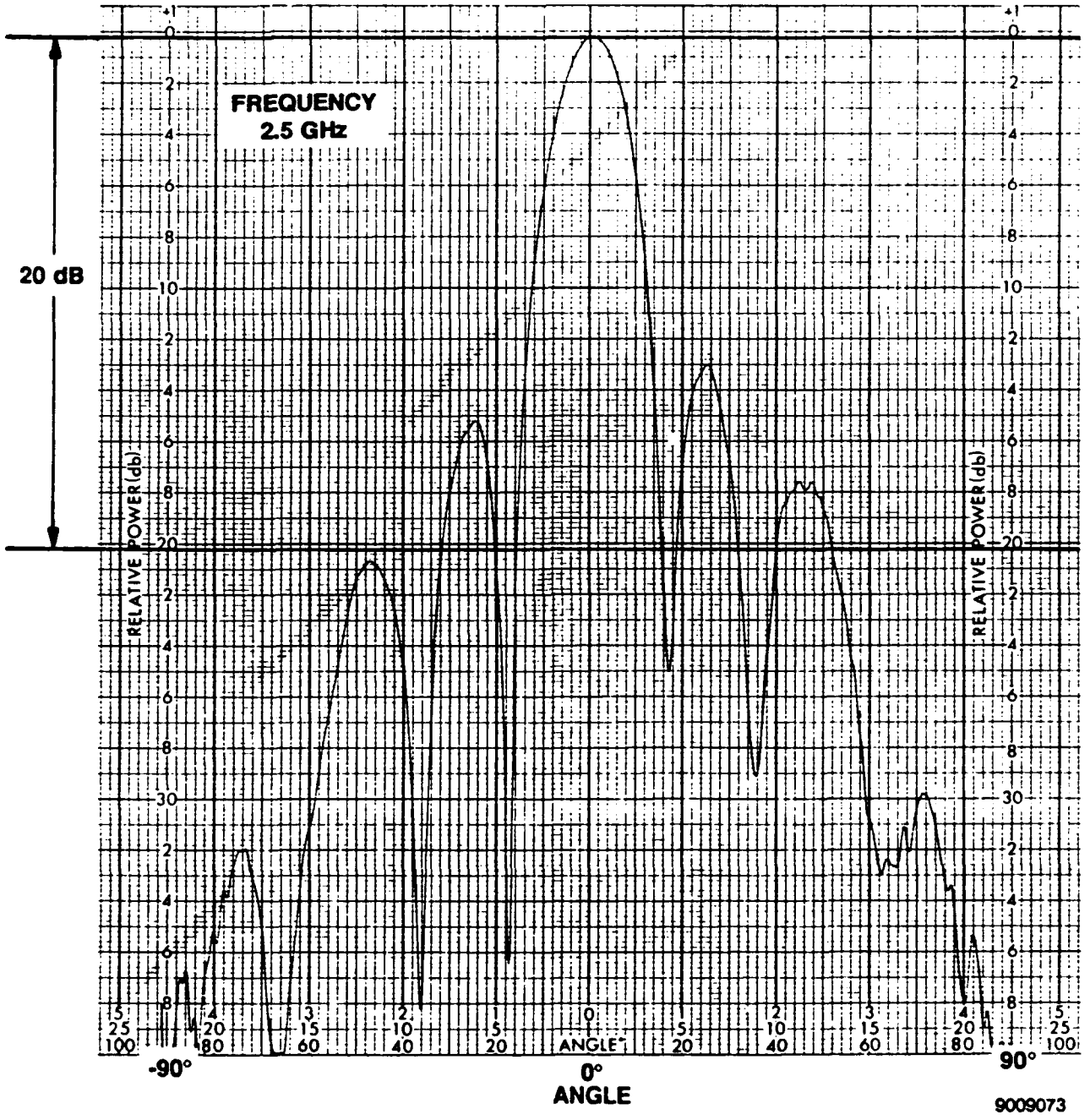
FREQUENCY
2.5 GHz
20 dB
RELATIVE POWER (db)
ANGLE°
-90°
0°
90°
ANGLE
9009073

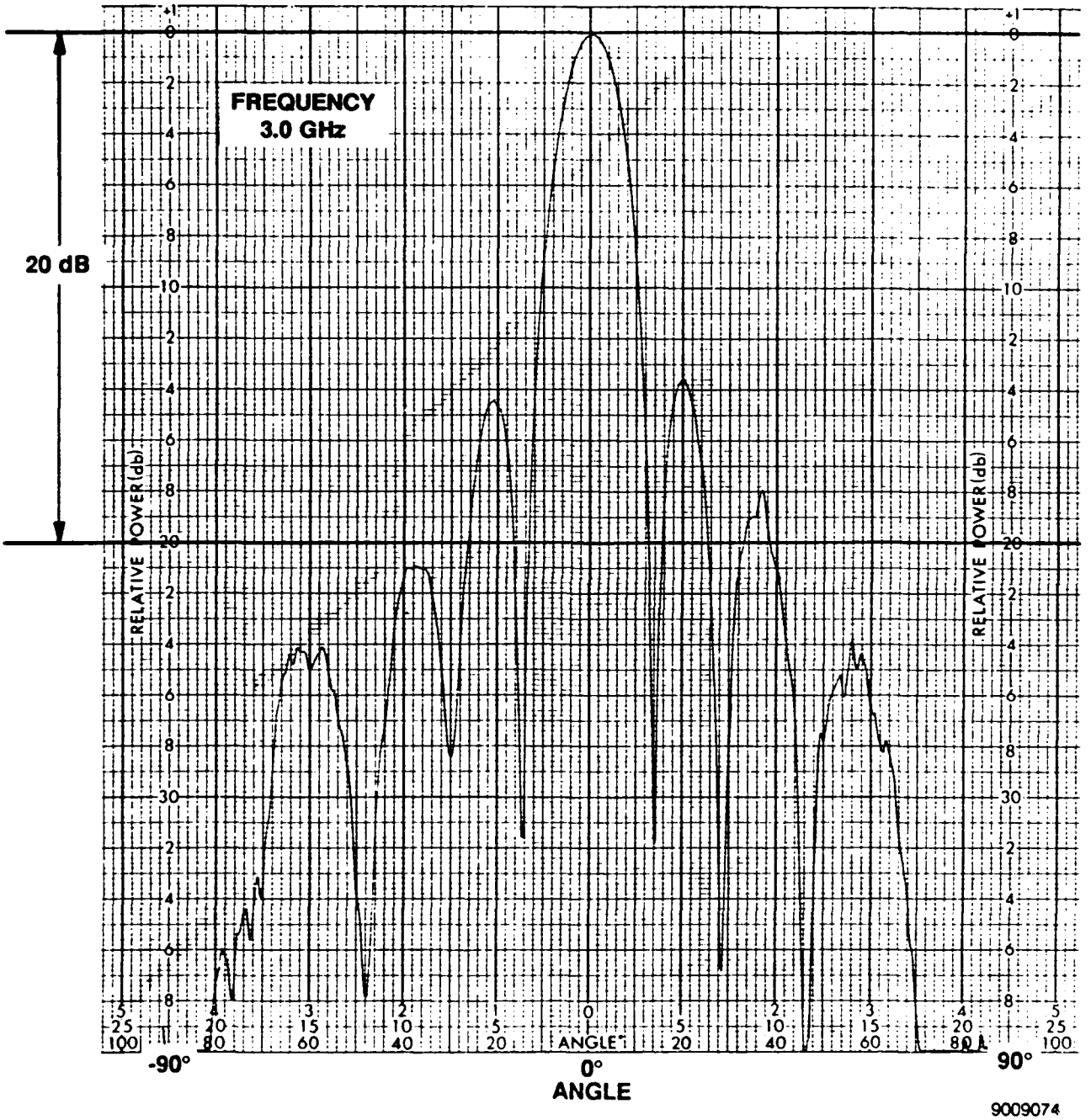
FREQUENCY
3.0 GHz
20 dB
RELATIVE POWER (db)
RELATIVE POWER (db)
-90°
0°
90°
ANGLE
ANGLE
9009074

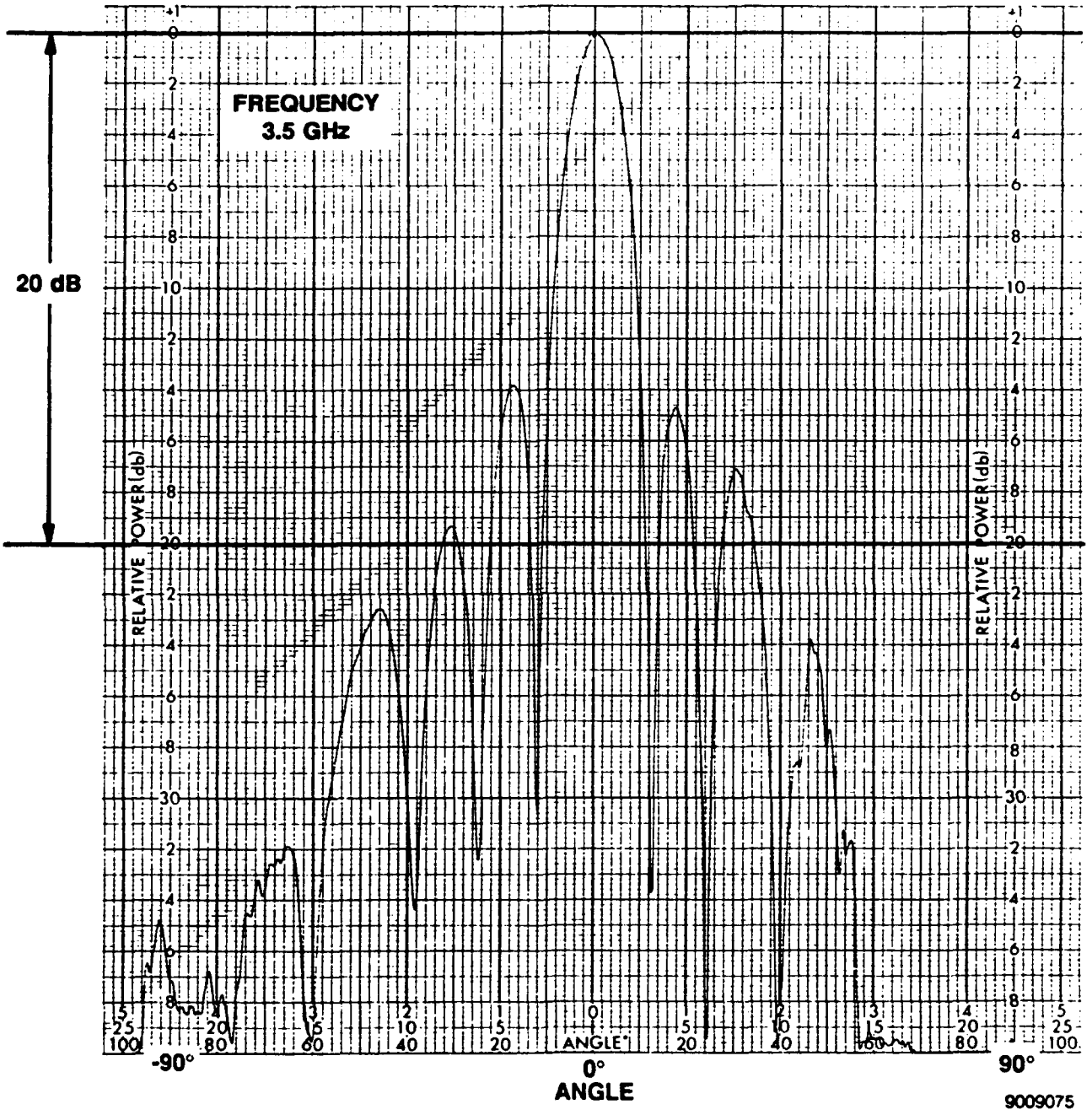
FREQUENCY
3.5 GHz
20 dB
RELATIVE POWER (db)
ANGLE°
-90°
0°
90°
ANGLE
9009075

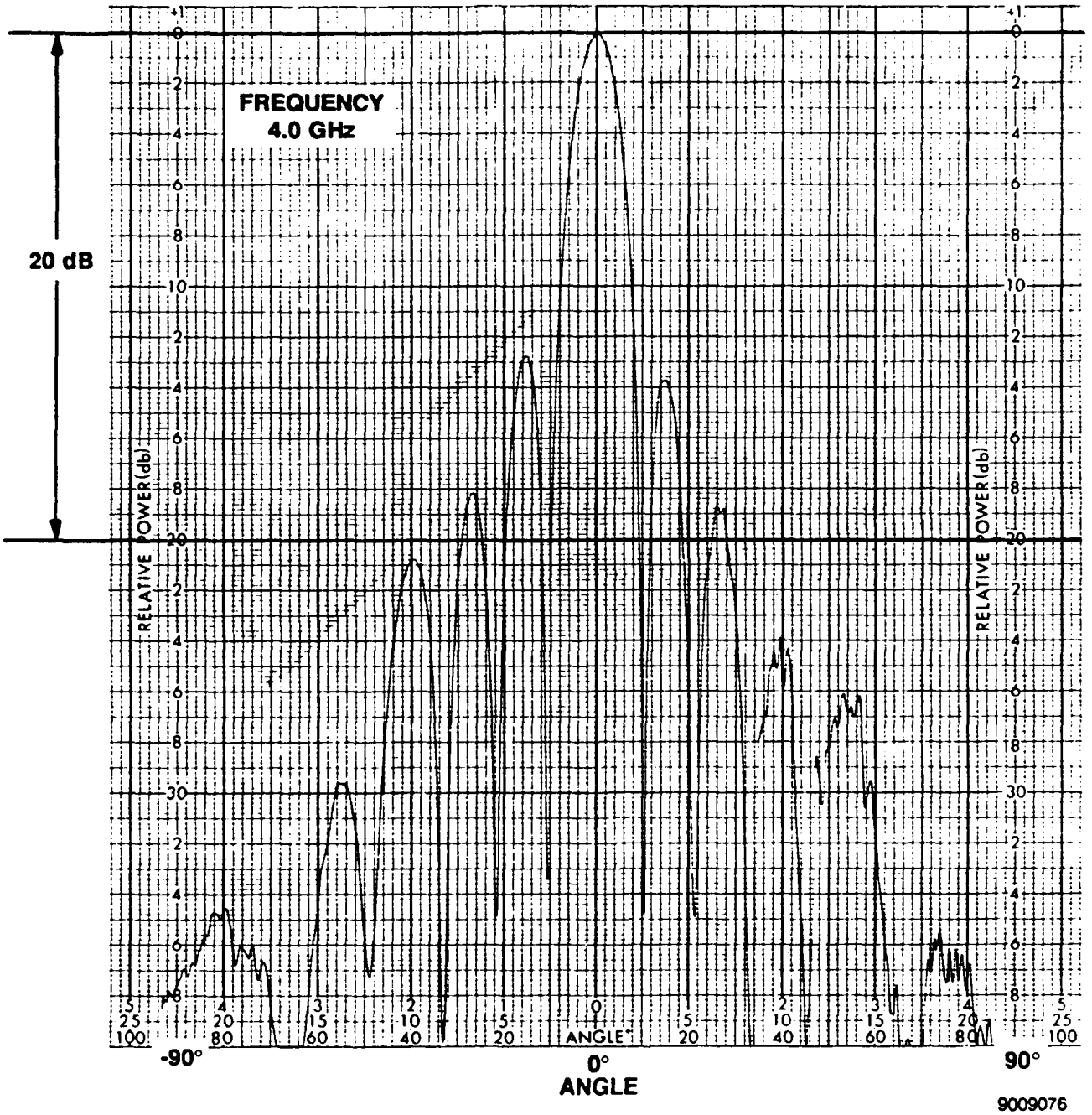
FREQUENCY
4.0 GHz
20 dB
RELATIVE POWER (db)
ANGLE
-90°
0°
90°
ANGLE
9009076

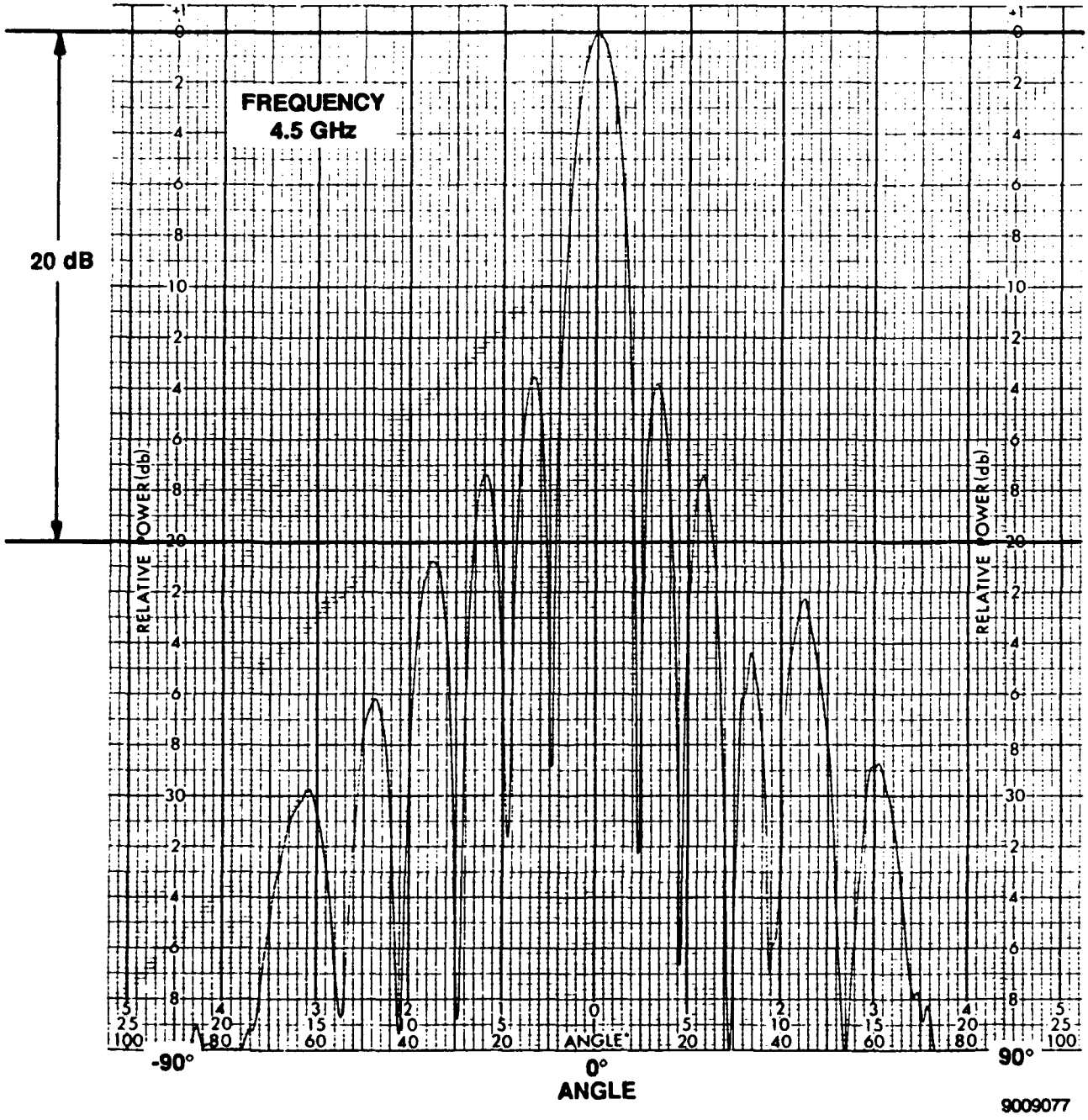
FREQUENCY
4.5 GHz
20 dB
RELATIVE POWER (db)
ANGLE°
-90°
0°
ANGLE
90°
9009077

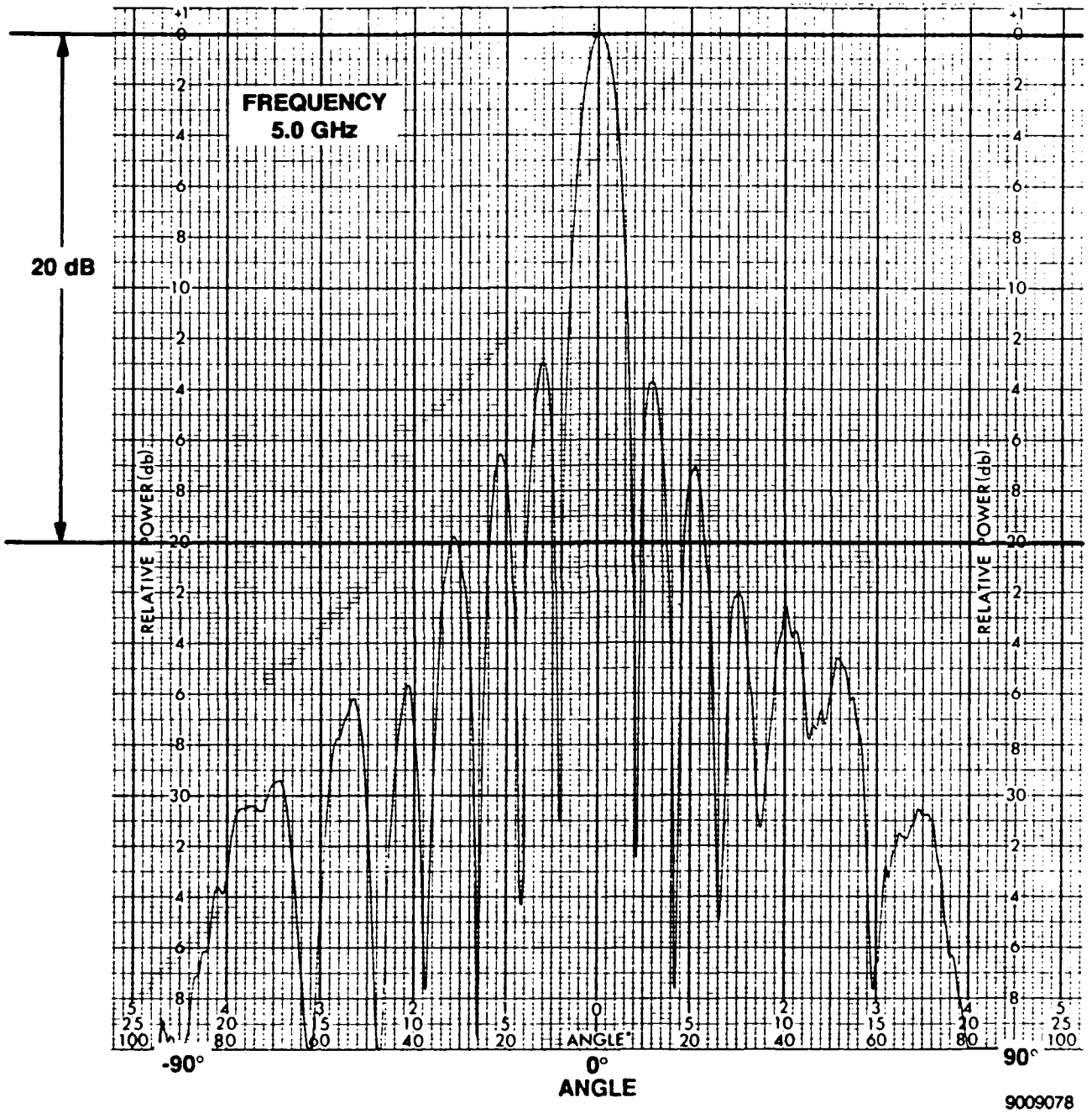
FREQUENCY
5.0 GHz
20 dB
RELATIVE POWER (db)
RELATIVE POWER (db)
ANGLE°
-90°
0°
90°
ANGLE
9009078

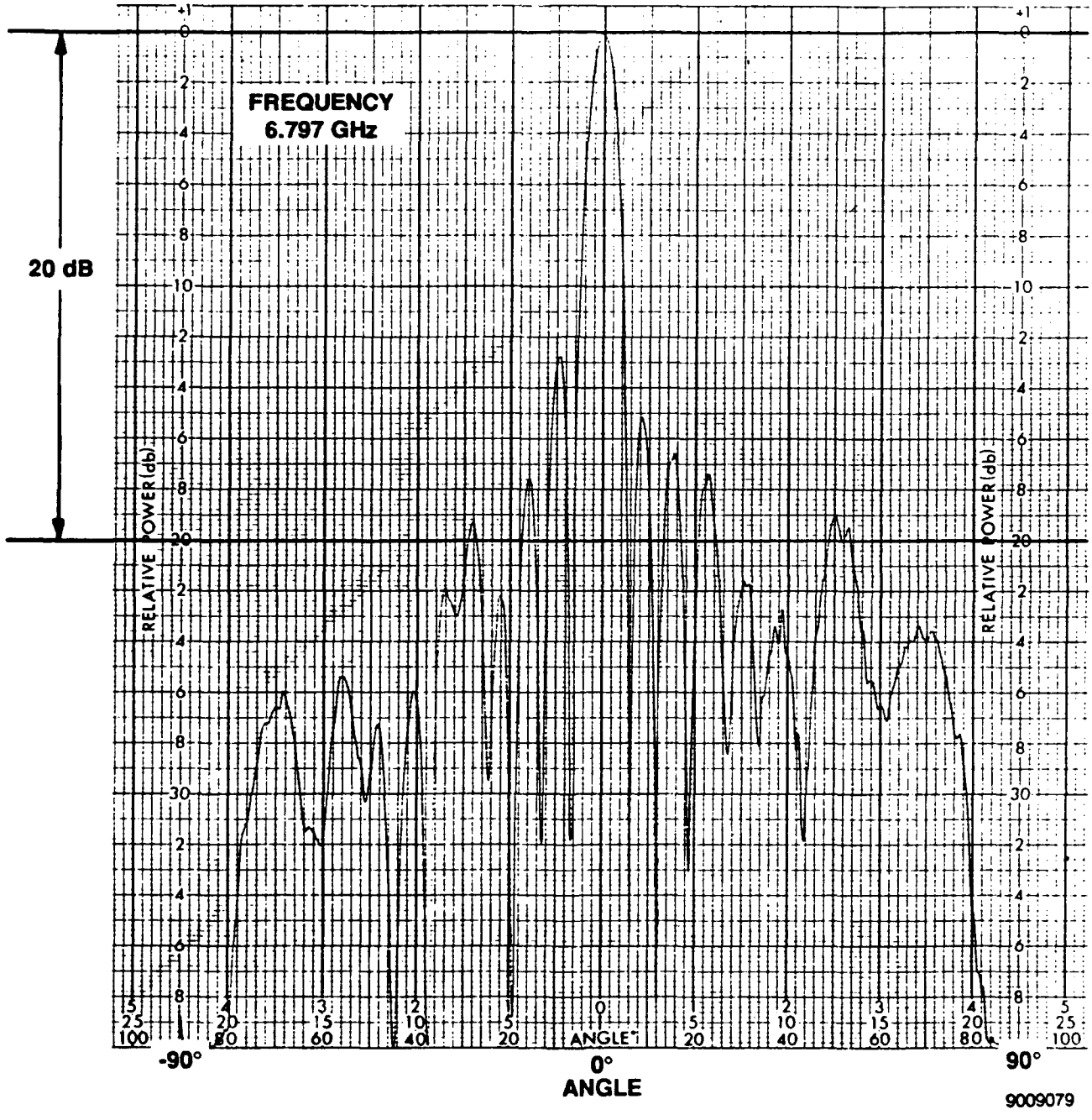
FREQUENCY
6.797 GHz
20 dB
RELATIVE POWER (db)
-90°
0°
90°
ANGLE
9009079

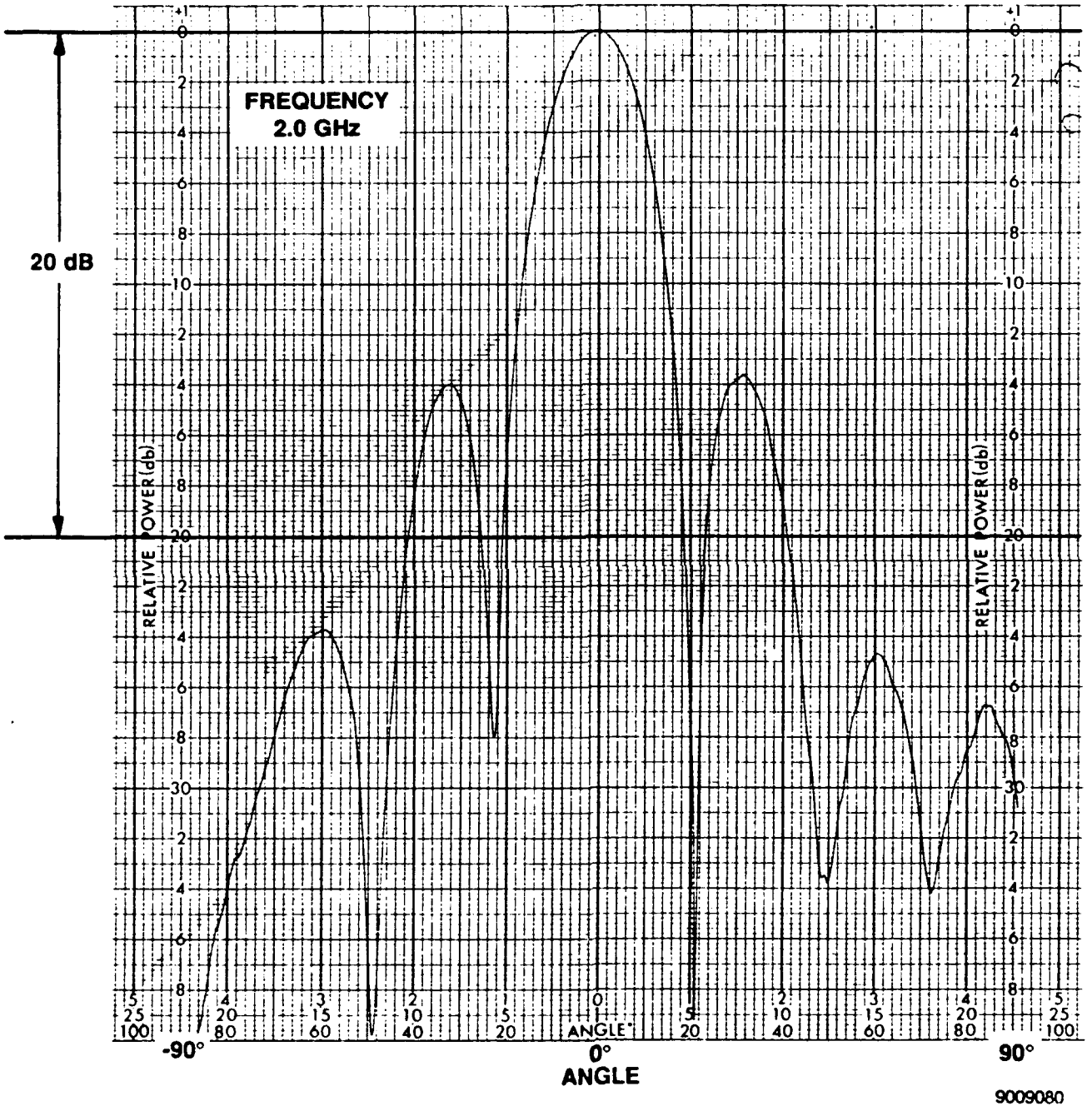
FREQUENCY
2.0 GHz
20 dB
RELATIVE POWER (db)
RELATIVE POWER (db)
ANGLE°
-90°
0°
90°
ANGLE
9009080

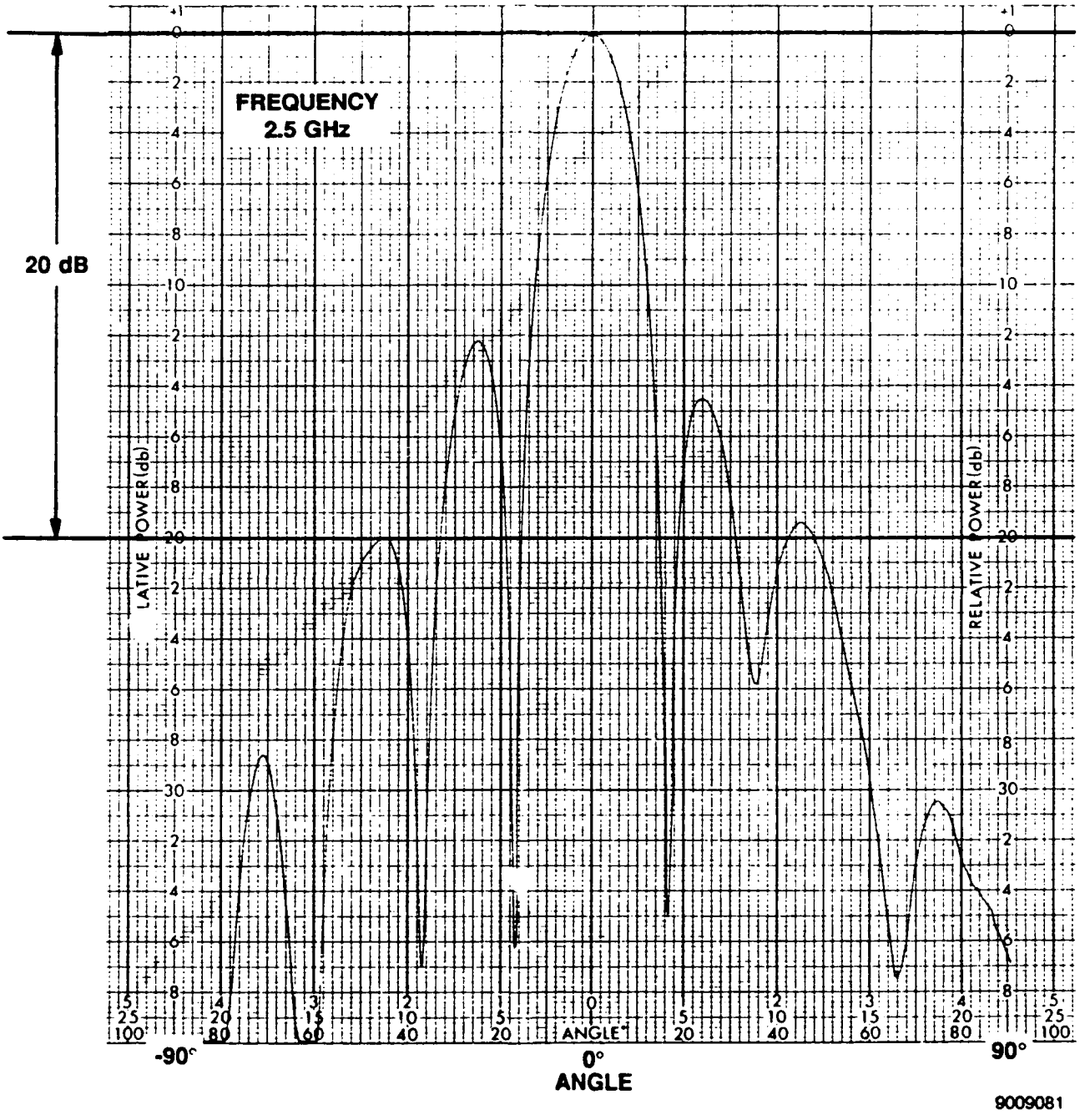
FREQUENCY
2.5 GHz
20 dB
RELATIVE POWER (db)
RELATIVE POWER (db)
ANGLE°
-90°
0°
90°
ANGLE
9009081

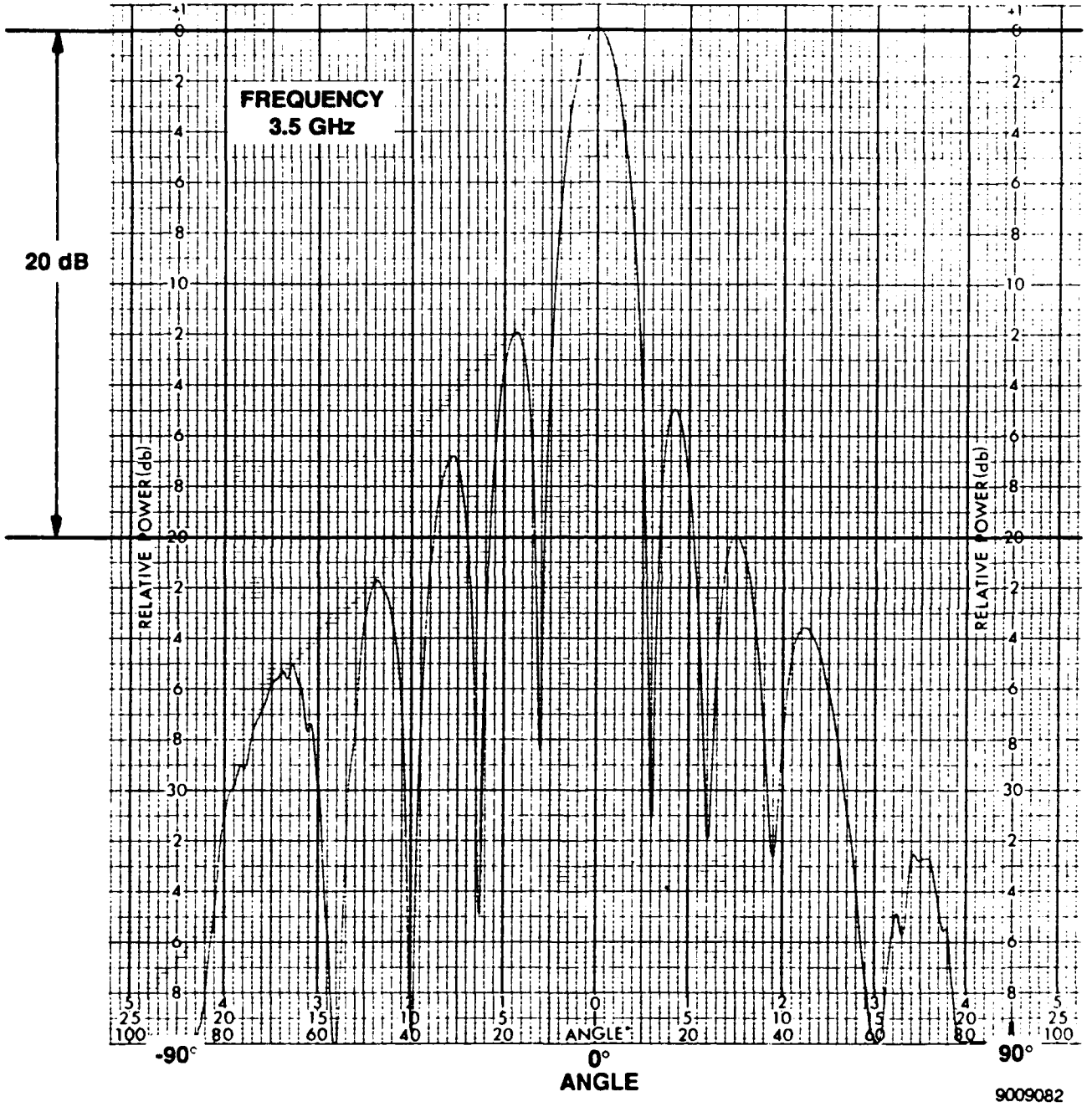
20 dB
FREQUENCY
3.5 GHz
RELATIVE POWER (db)
RELATIVE POWER (db)
ANGLE°
-90°
0°
90°
ANGLE
9009082

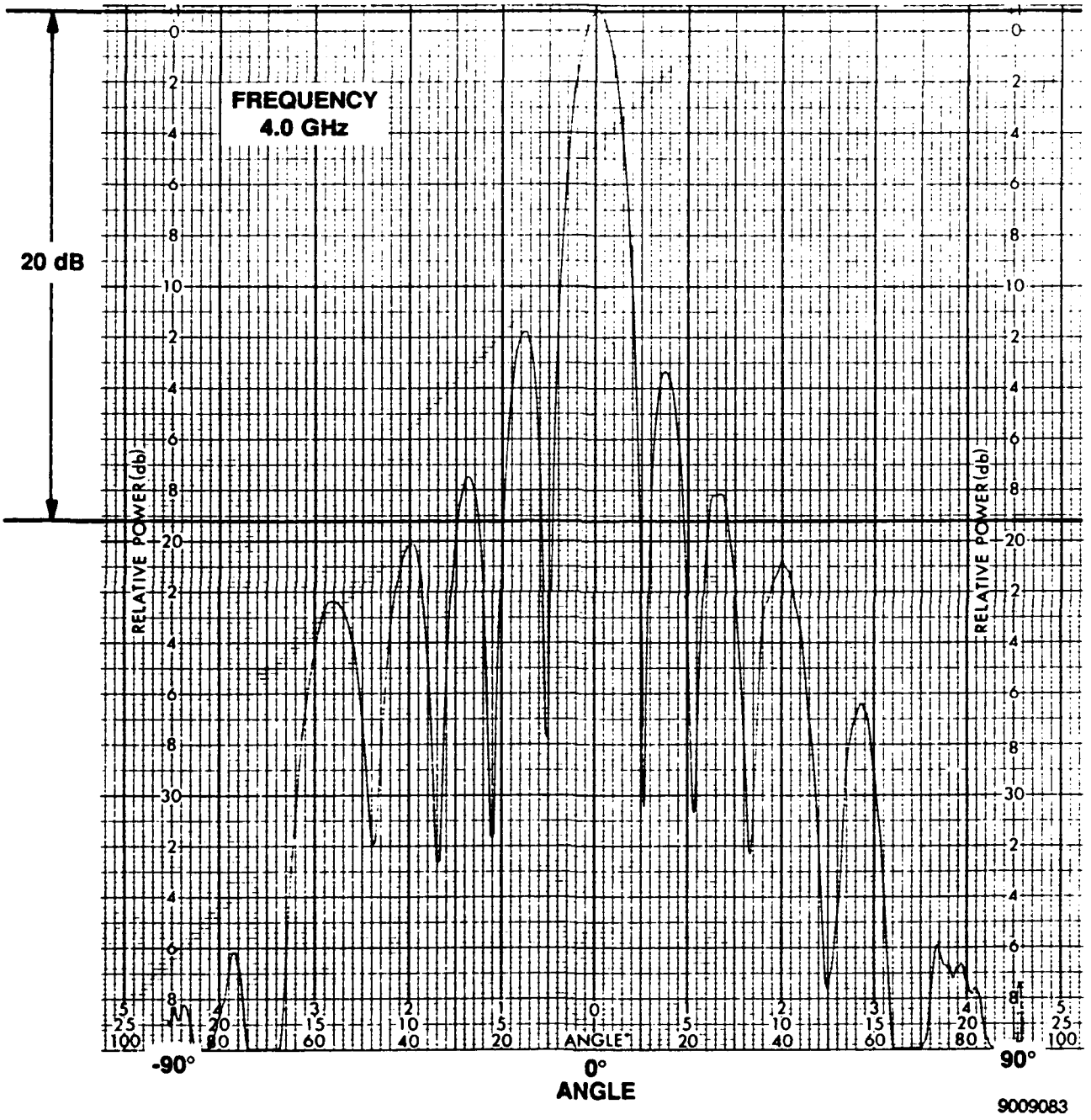
20 dB
FREQUENCY
4.0 GHz
RELATIVE POWER (db)
RELATIVE POWER (db)
ANGLE°
-90°
0°
90°
ANGLE
9009083

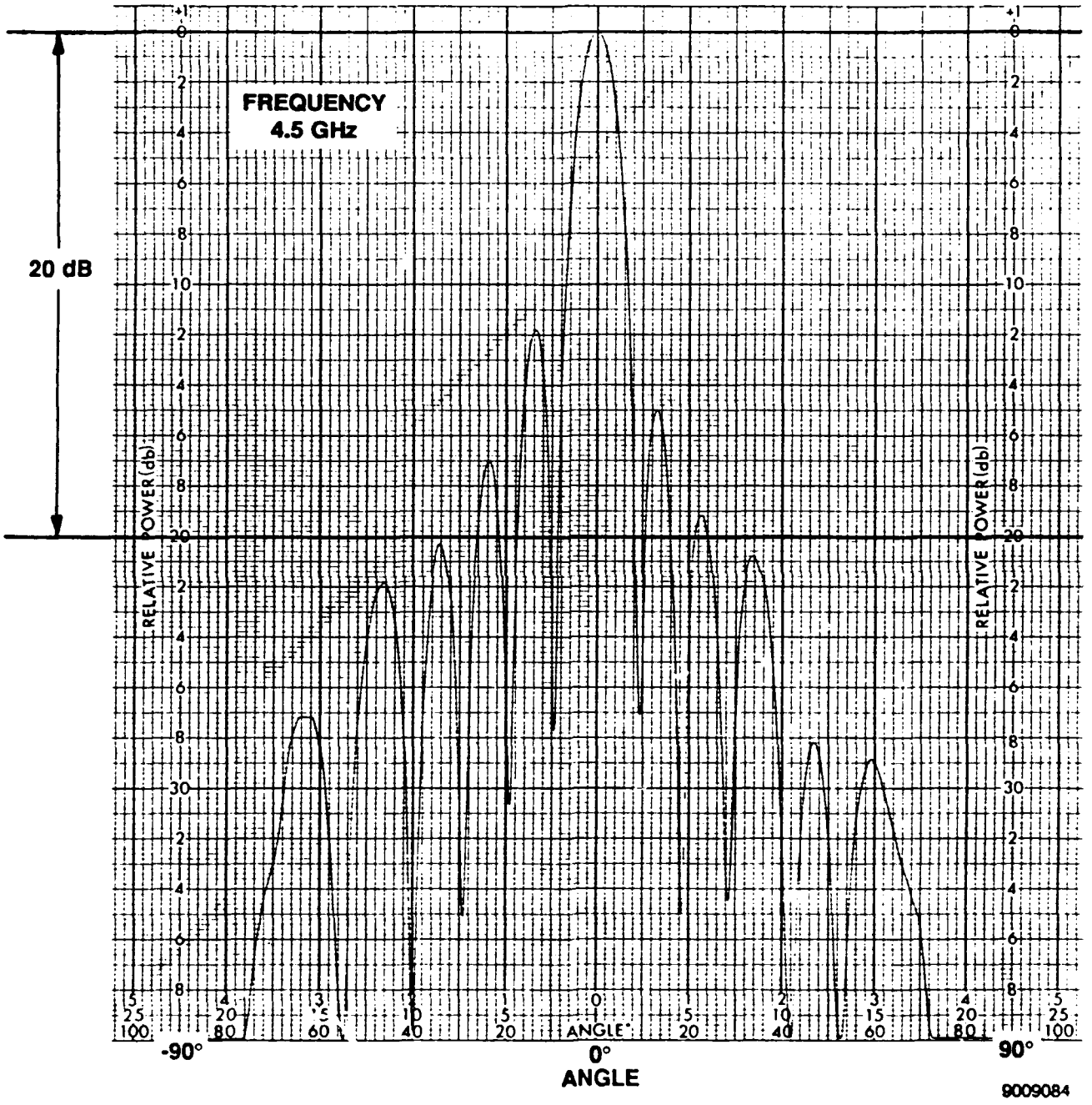
FREQUENCY
4.5 GHz
20 dB
RELATIVE POWER (db)
RELATIVE POWER (db)
ANGLE°
-90°
0°
90°
ANGLE
9009084

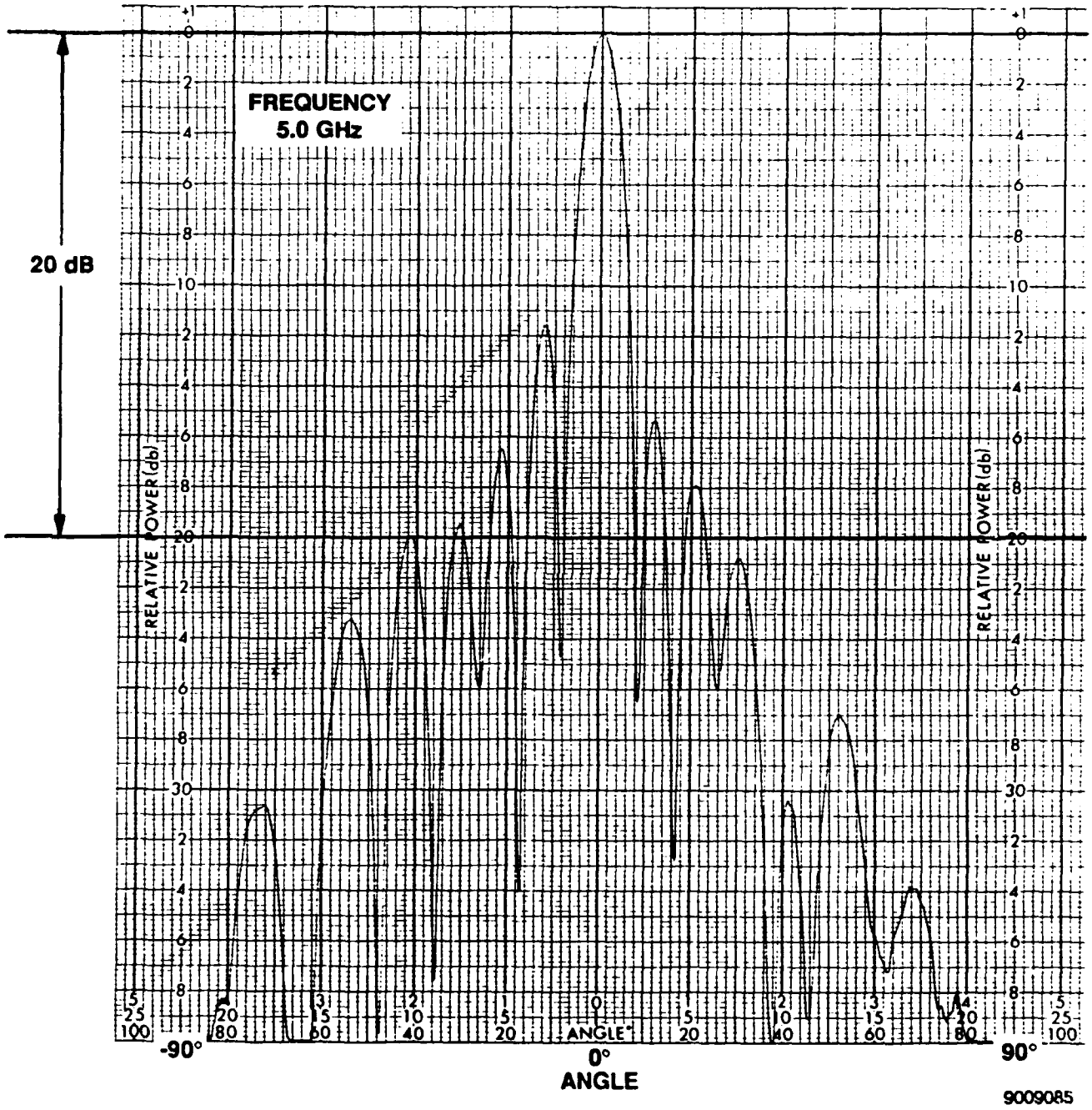
FREQUENCY
5.0 GHz
20 dB
RELATIVE POWER (db)
ANGLE°
-90°
0°
90°
ANGLE
9009085

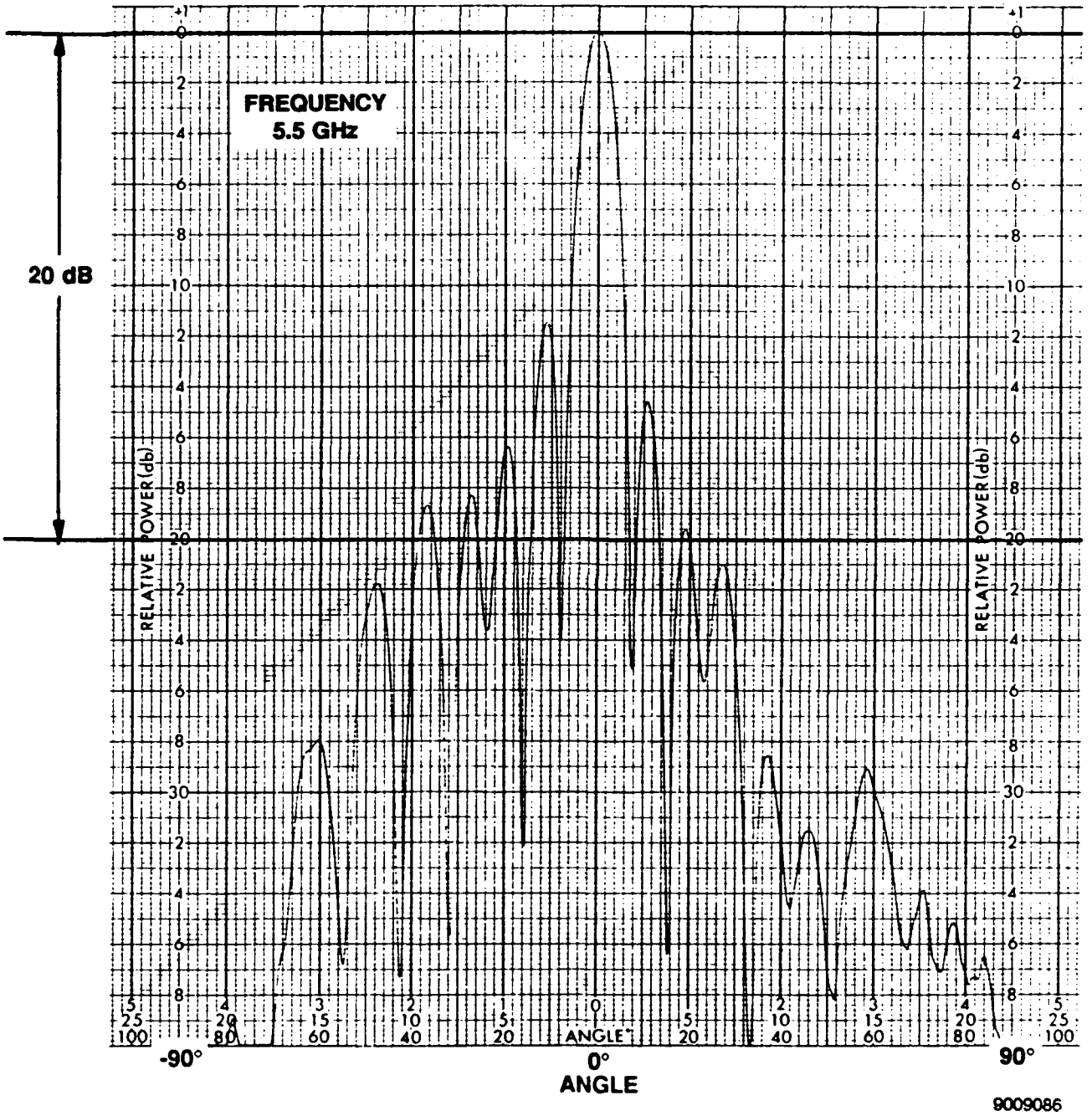
FREQUENCY
5.5 GHz
20 dB
RELATIVE POWER (db)
RELATIVE POWER (db)
ANGLE
-90°
0°
90°
ANGLE
9009086

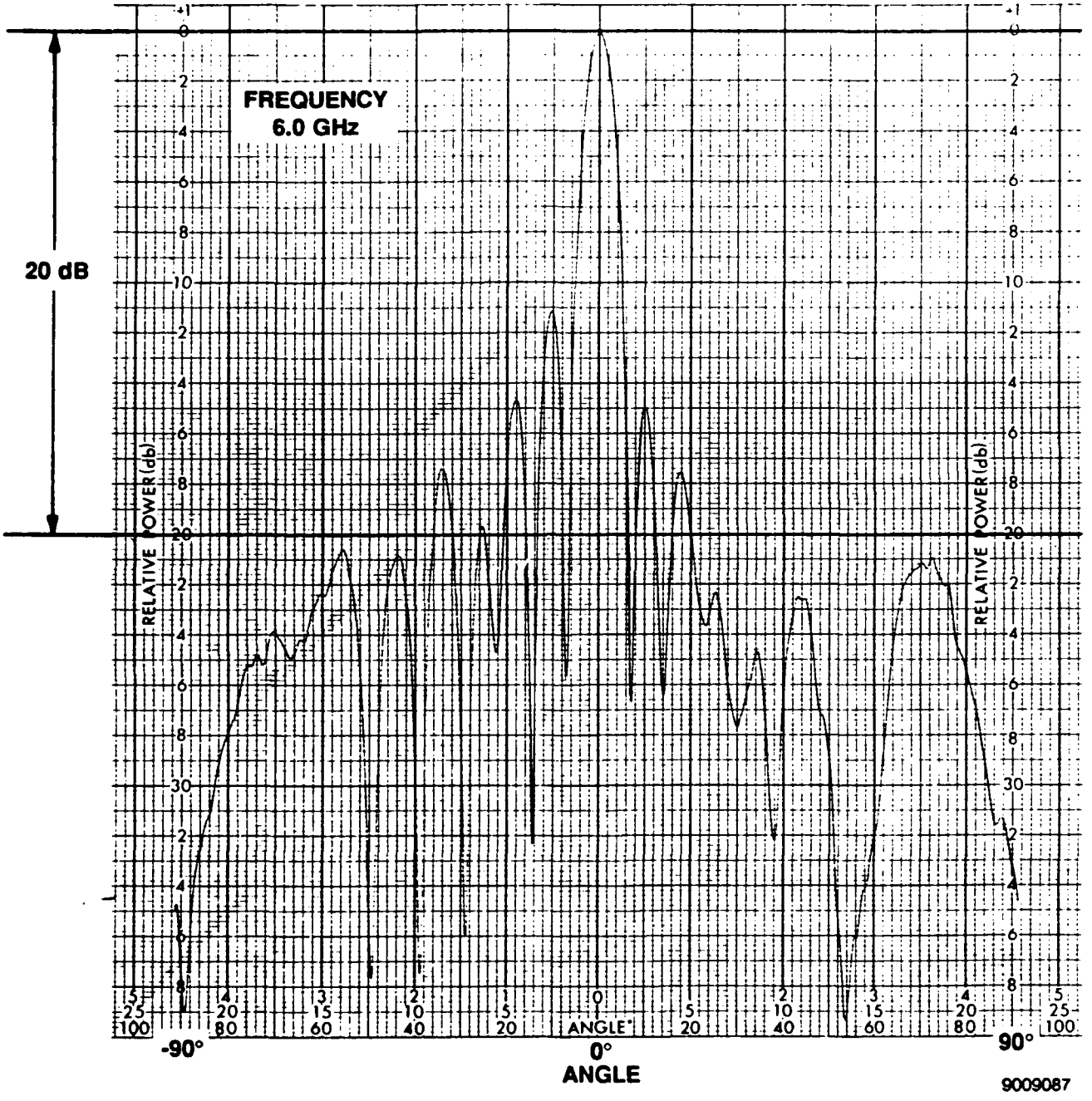
FREQUENCY
6.0 GHz
20 dB
RELATIVE POWER (db)
RELATIVE POWER (db)
ANGLE°
-90°
0°
90°
ANGLE
9009087

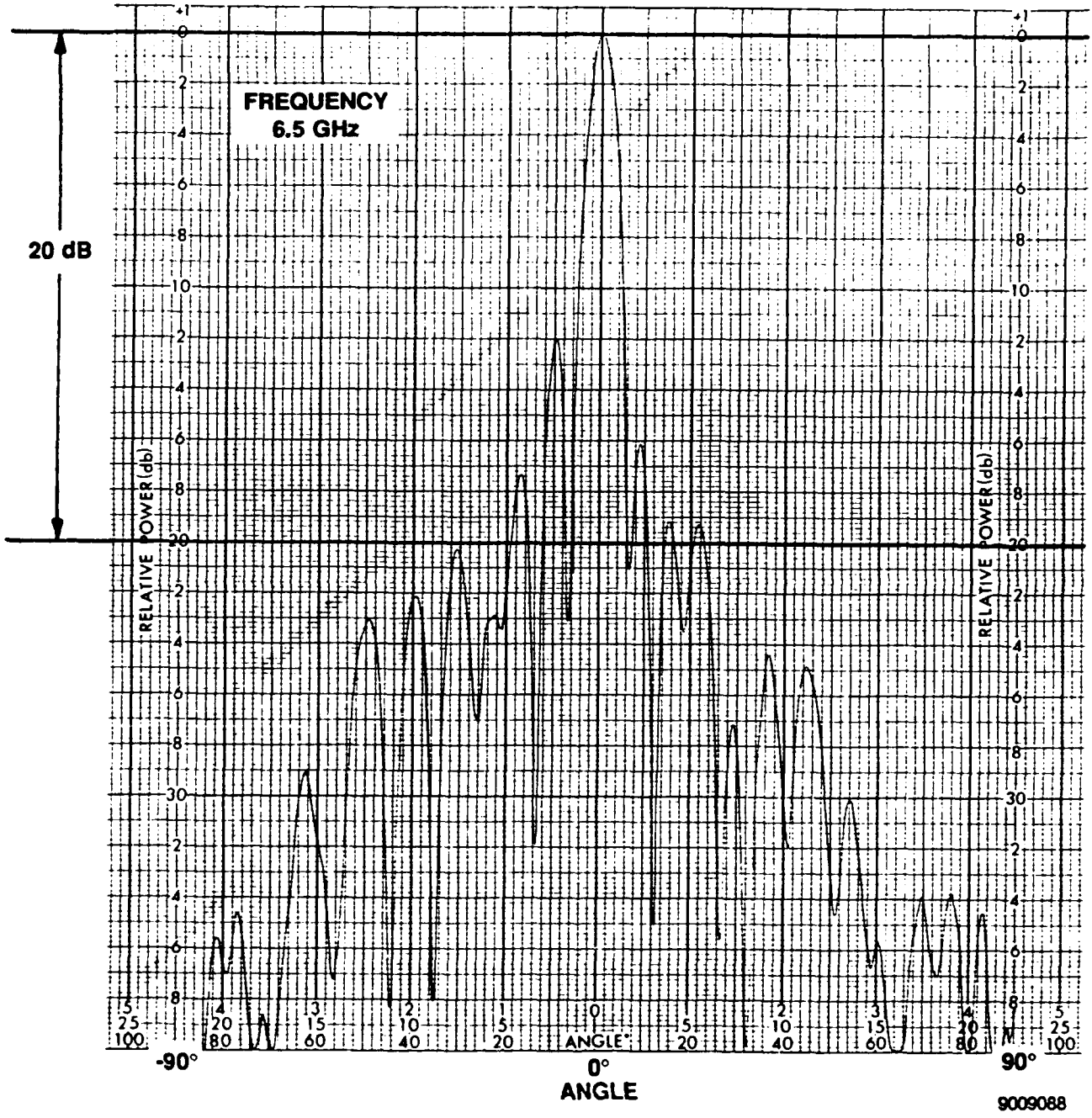
FREQUENCY
6.5 GHz
20 dB
RELATIVE POWER (db)
ANGLE°
-90°
0°
90°
ANGLE
9009088

APPENDIX A4

This data group contains patterns with 16 columns terminated and 16 columns with a 30-dB Chebyshev sidelobe illumination, configuration a shown below. The MMIC ability to provide a low sidelobe illumination is shown in this pattern set, which contains the following frequencies.

Frequencies (GHz)			
Test 13c, No. 2	2.882	Test 13c, No. 1	2.0
	3.0		2.5
	3.184		3.0
	5.581		3.5
	6.0		4.0
	6.387		4.5
			5.0
			5.5
			6.0
			7.5

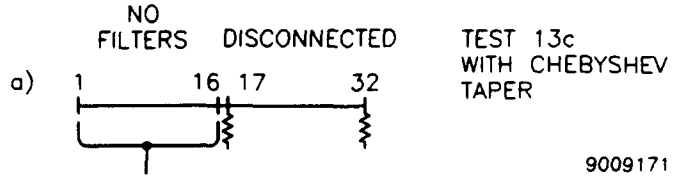

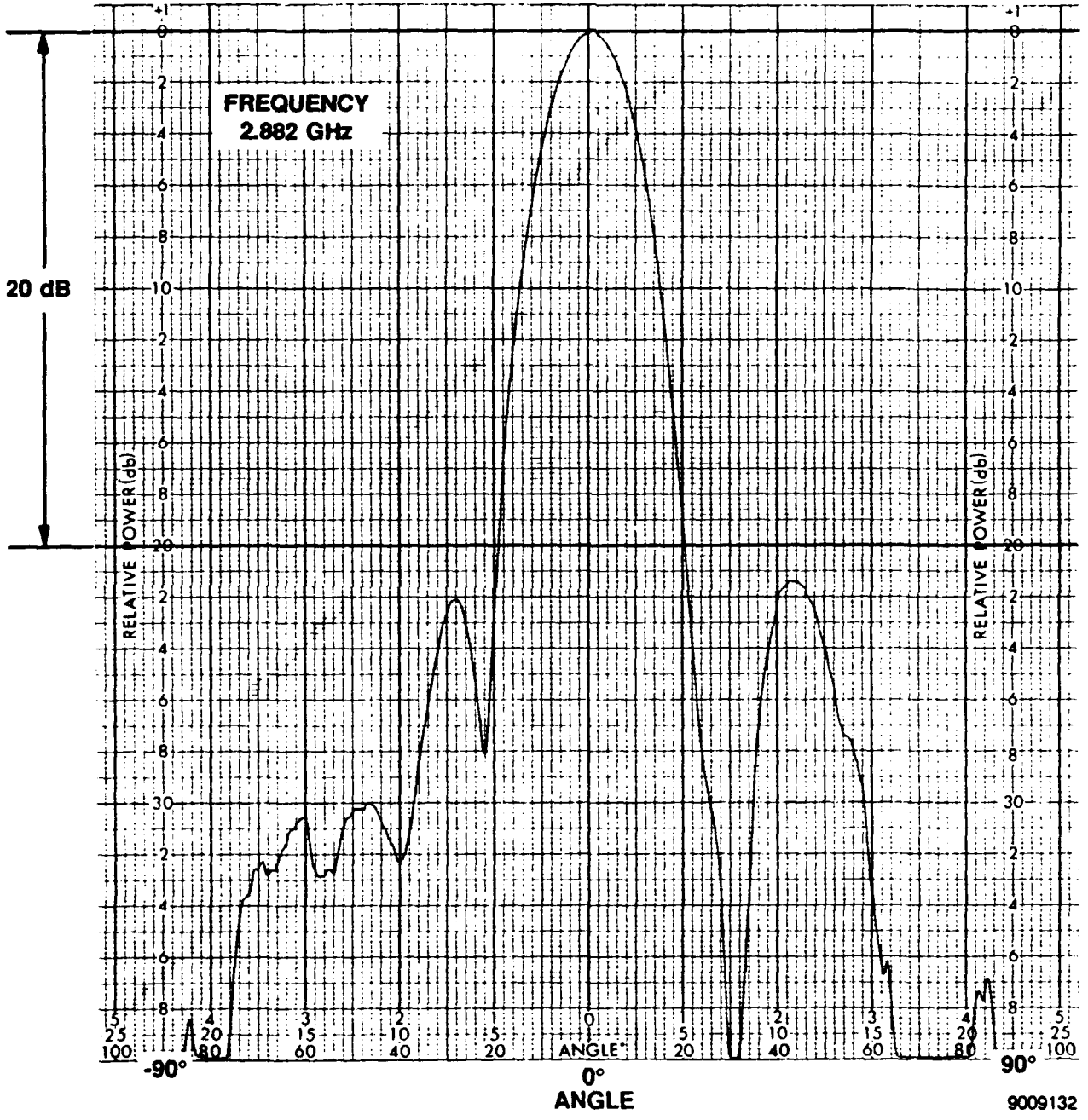
FREQUENCY
2.882 GHz
20 dB
RELATIVE POWER (db)
RELATIVE POWER (db)
ANGLE°
-90°
0°
90°
ANGLE
9009132

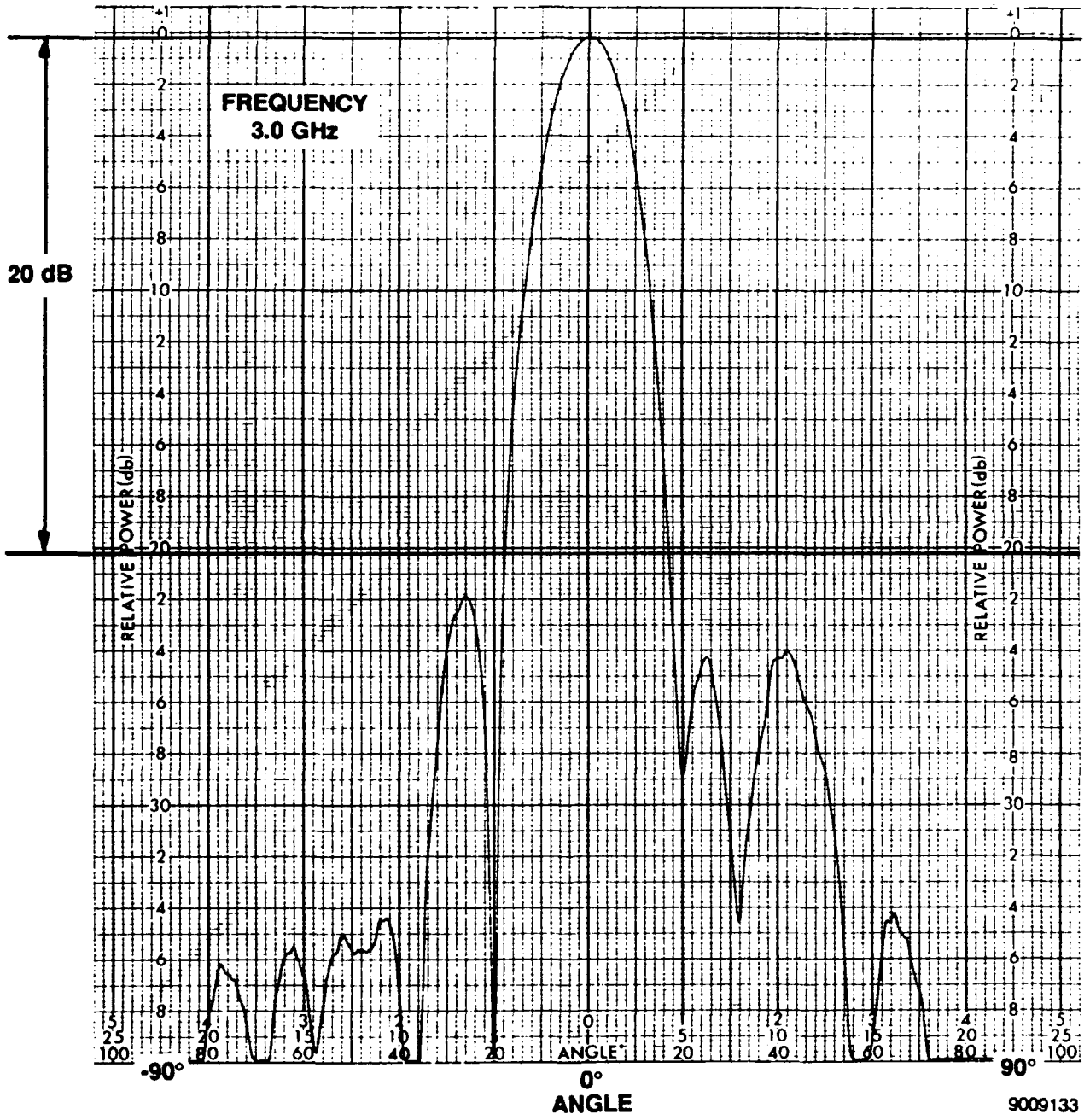
FREQUENCY
3.0 GHz
20 dB
RELATIVE POWER (db)
ANGLE°
-90°
0°
90°
ANGLE
9009133

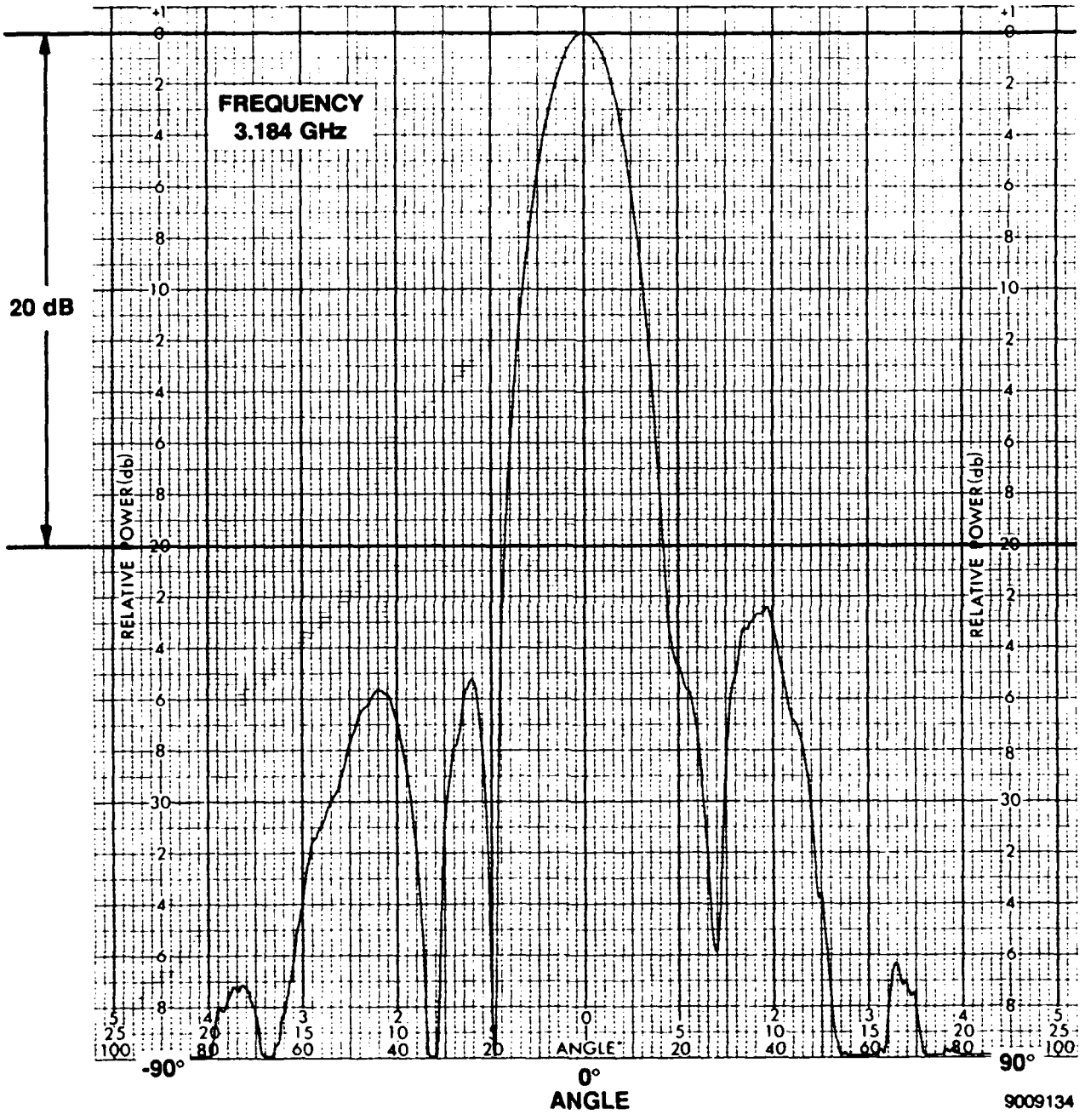
FREQUENCY
3.184 GHz
20 dB
RELATIVE POWER (db)
ANGLE°
-90°
0°
90°
ANGLE
9009134

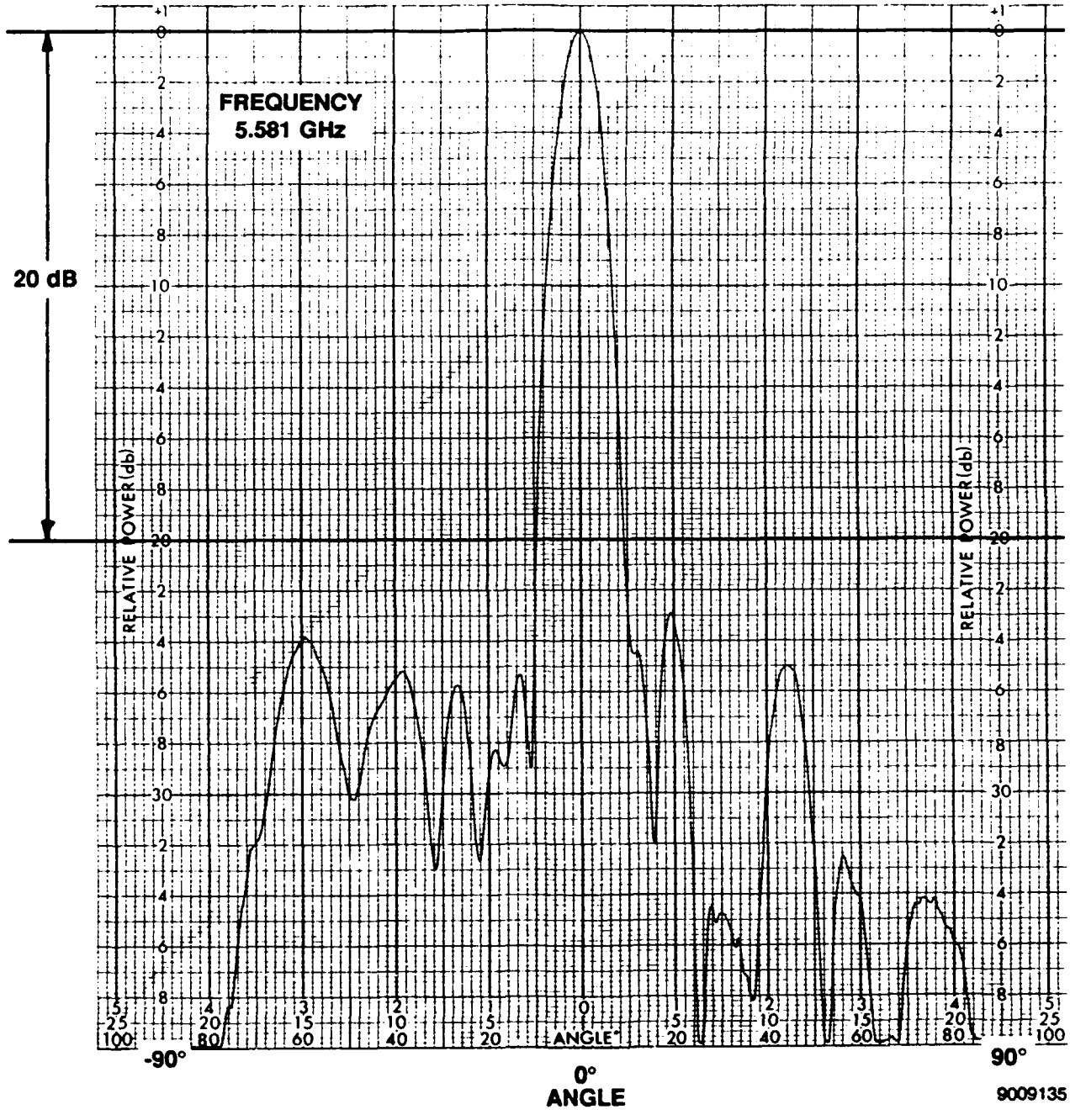
FREQUENCY
5.581 GHz
20 dB
RELATIVE POWER (db)
RELATIVE POWER (db)
-90°
0°
90°
ANGLE
ANGLE
9009135

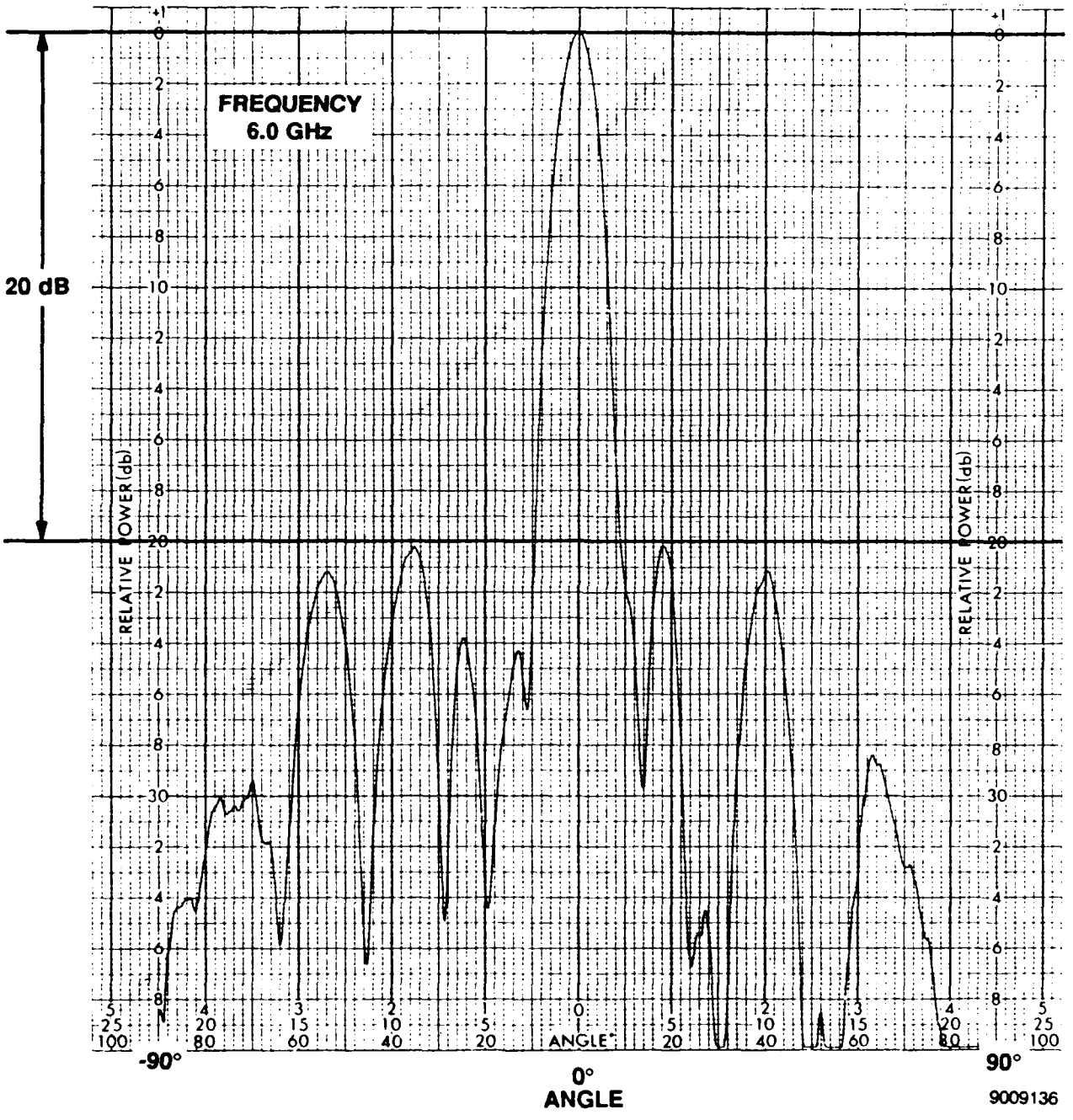
FREQUENCY
6.0 GHz
20 dB
RELATIVE POWER (db)
ANGLE
-90°
0°
90°
ANGLE
9009136

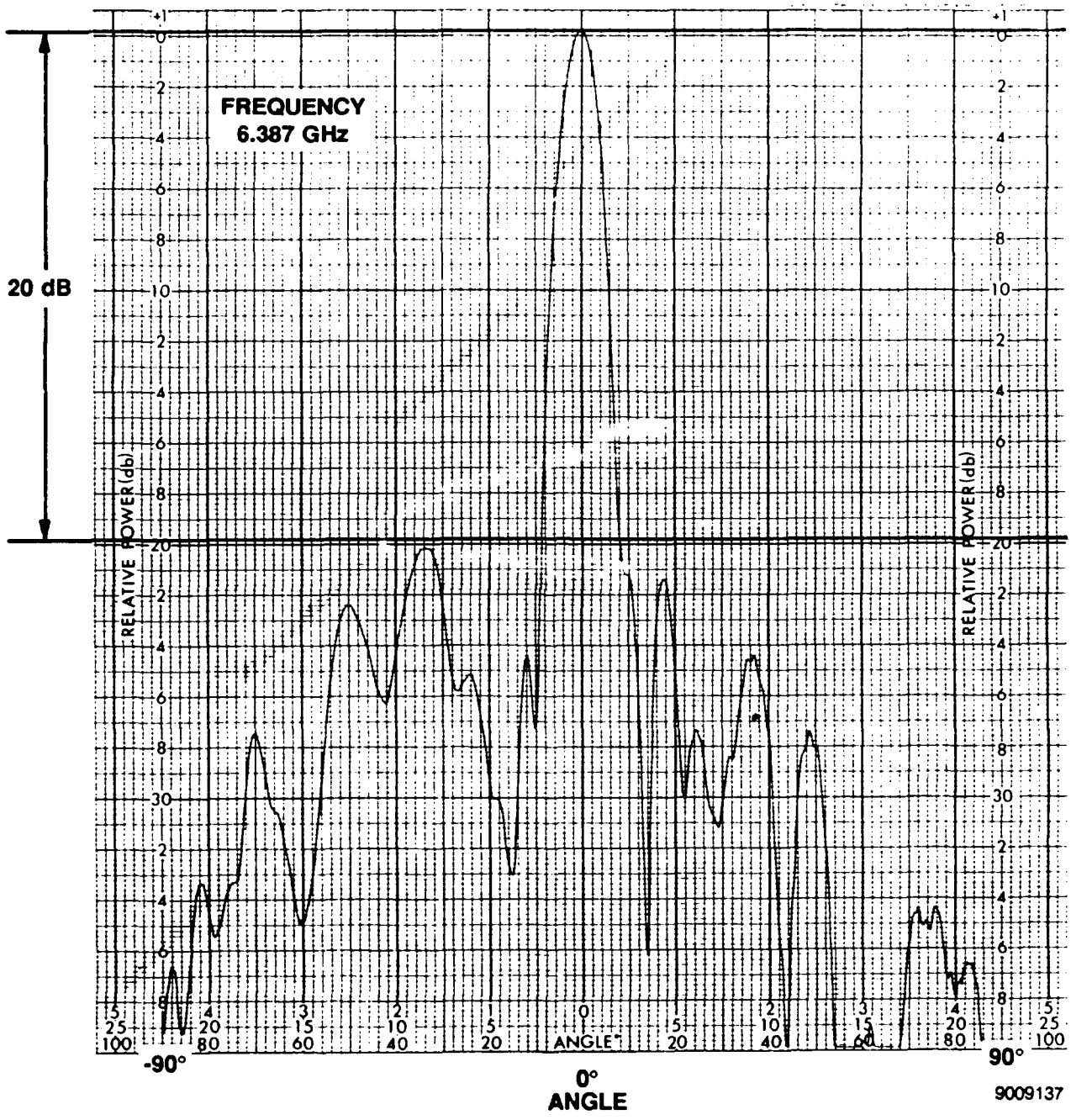
FREQUENCY
6.387 GHz
20 dB
RELATIVE POWER (db)
ANGLE
-90°
0°
90°
9009137

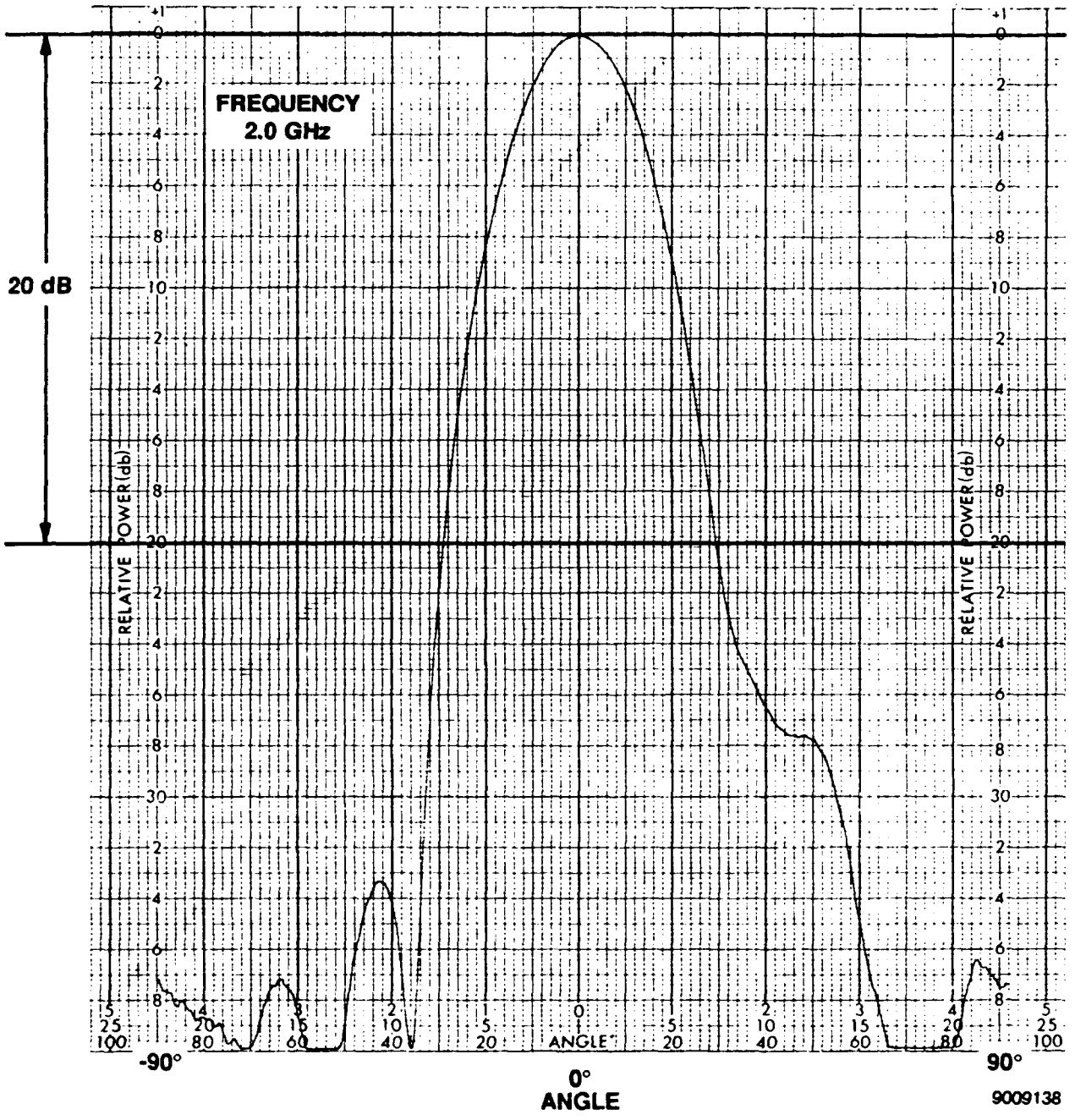
FREQUENCY
2.0 GHz
20 dB
RELATIVE POWER (db)
ANGLE
-90°
0°
90°
ANGLE
9009138

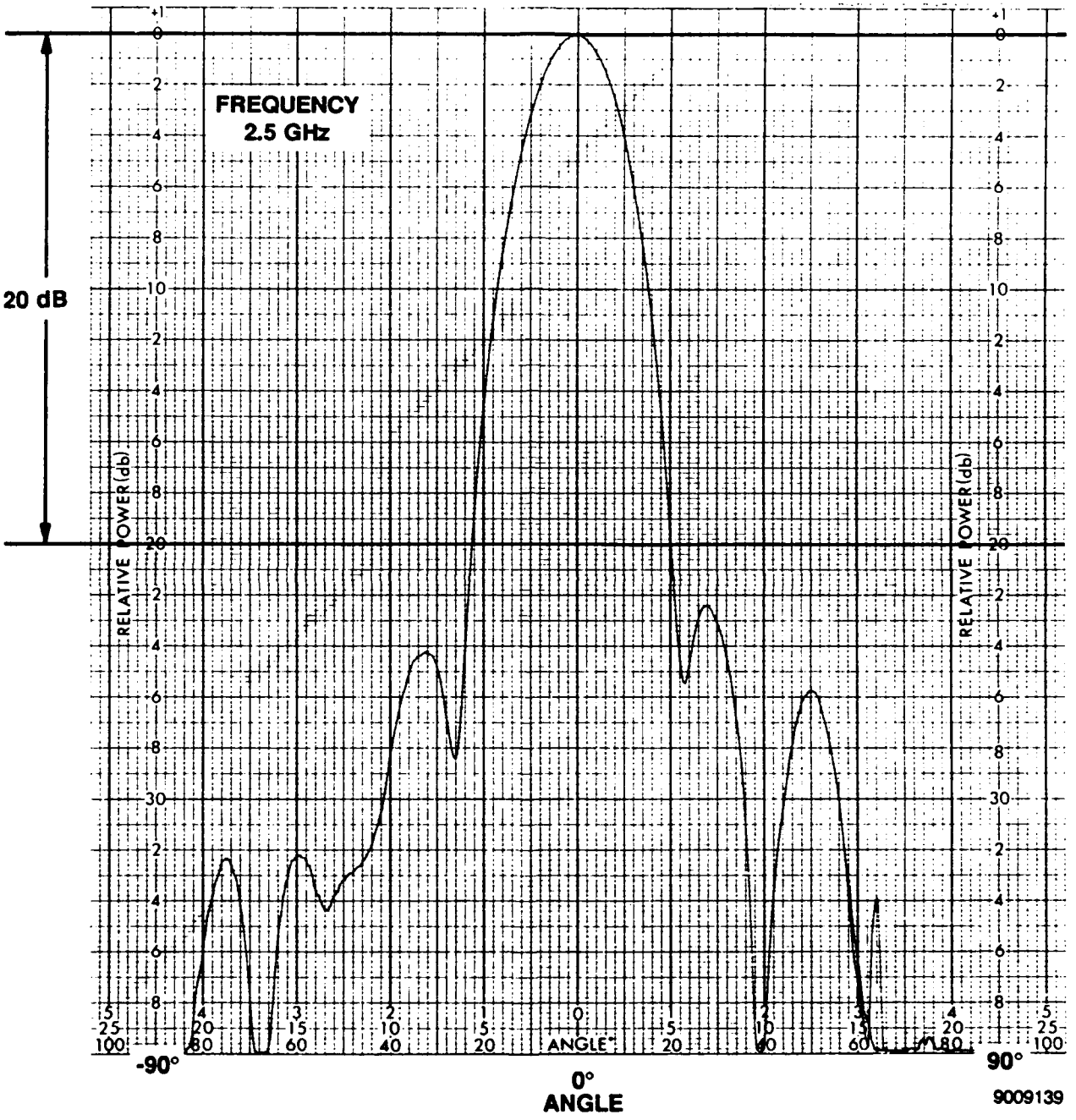
FREQUENCY
2.5 GHz
20 dB
RELATIVE POWER (db)
RELATIVE POWER (db)
ANGLE°
-90°
0°
90°
ANGLE
9009139

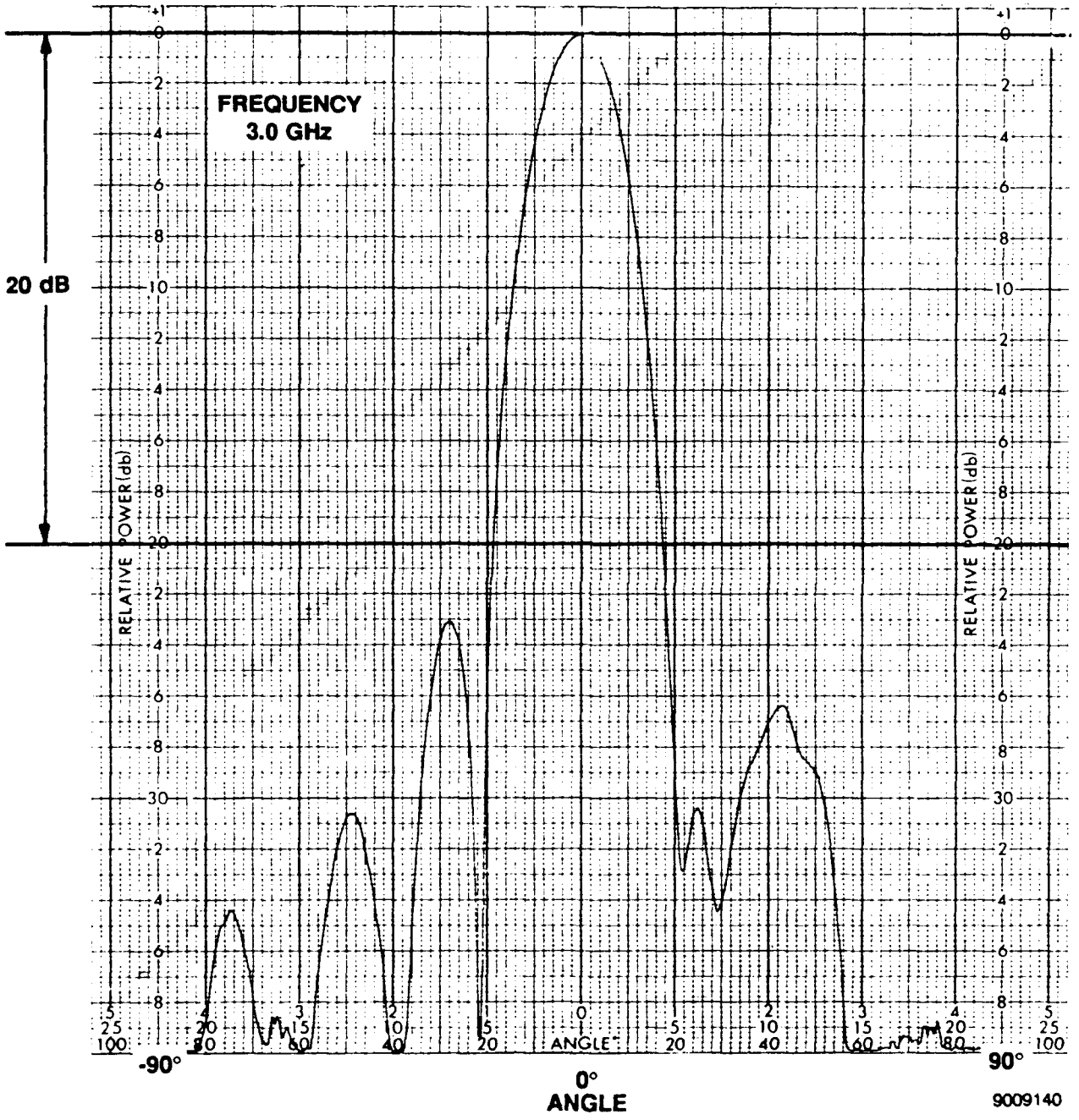
FREQUENCY
3.0 GHz
20 dB
RELATIVE POWER (db)
ANGLE°
-90°
0°
90°
ANGLE
9009140

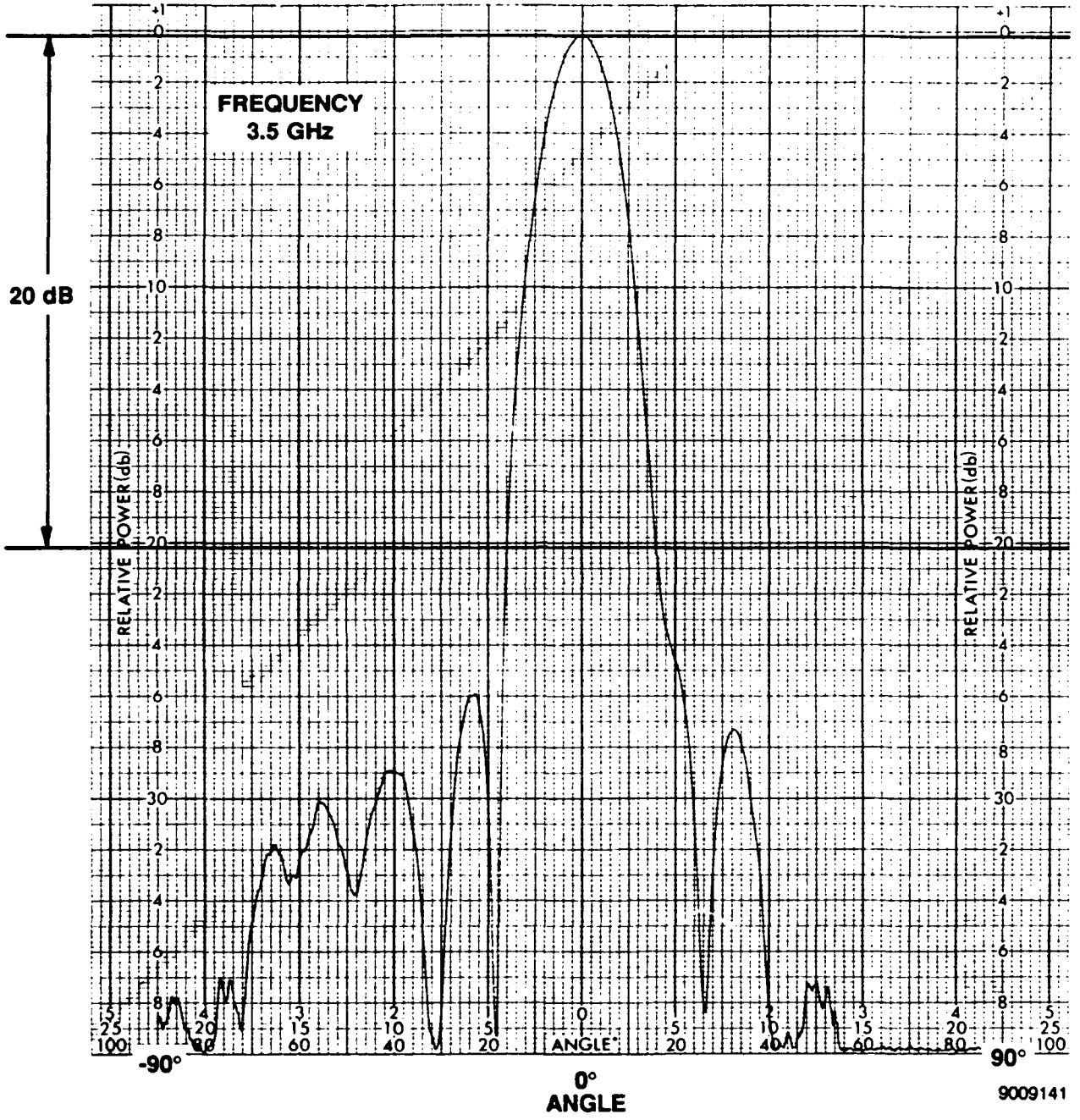
FREQUENCY
3.5 GHz
20 dB
RELATIVE POWER (db)
RELATIVE POWER (db)
ANGLE°
-90°
0°
90°
0°
ANGLE
9009141

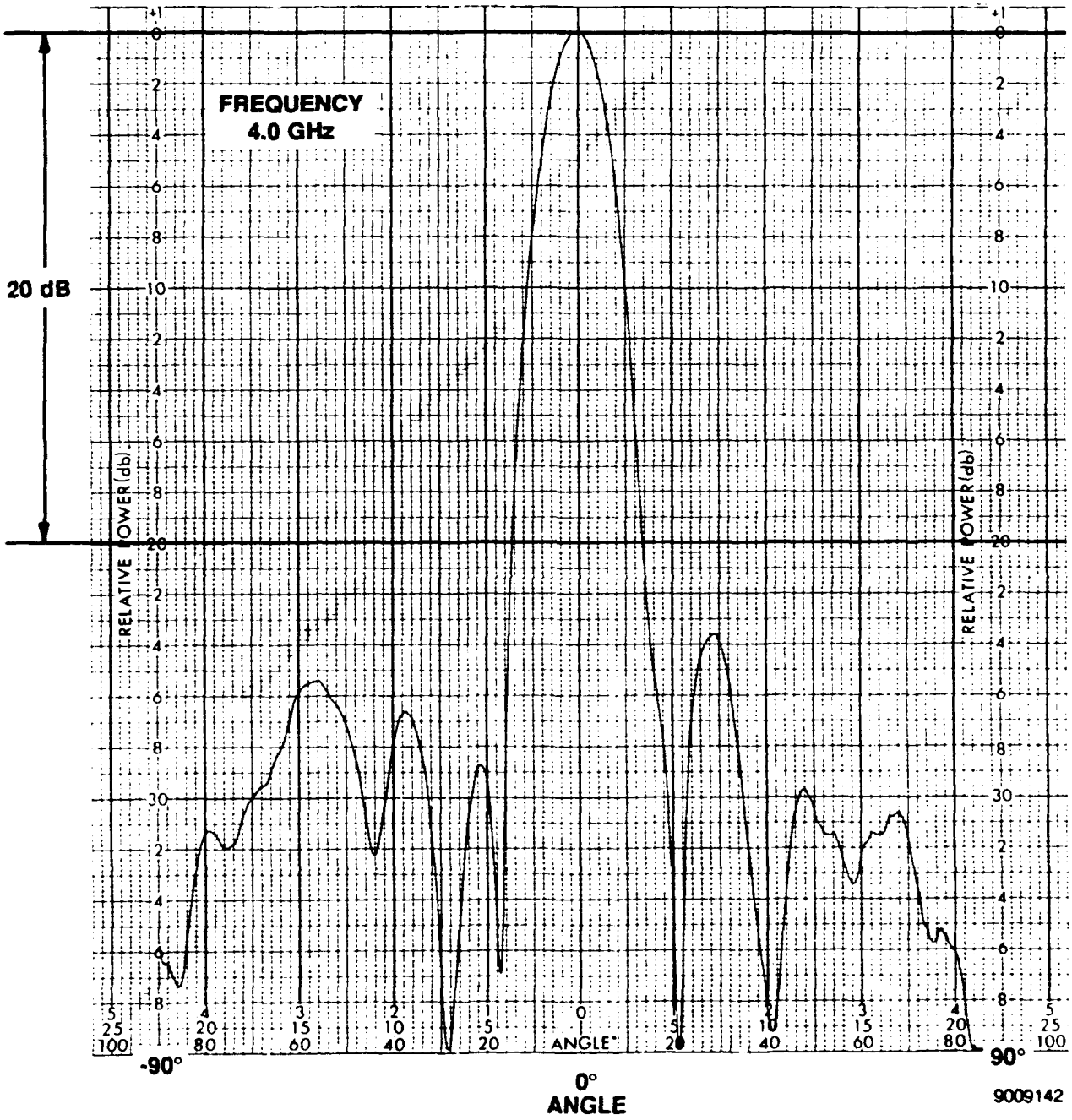
FREQUENCY
4.0 GHz
20 dB
RELATIVE POWER (db)
RELATIVE POWER (db)
ANGLE°
-90°
0°
90°
ANGLE
9009142

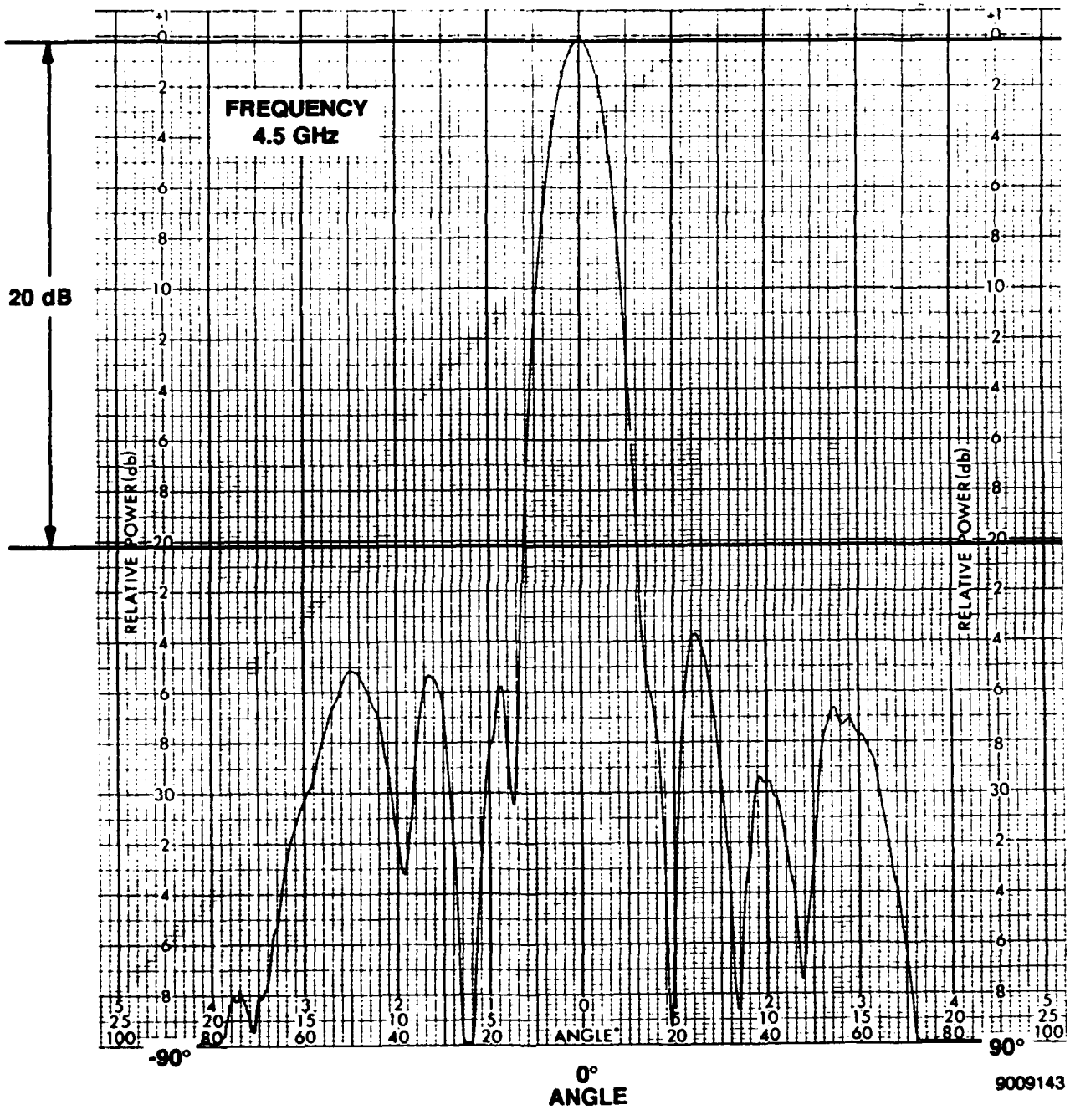
FREQUENCY
4.5 GHz
20 dB
RELATIVE POWER (db)
RELATIVE POWER (db)
ANGLE
-90°
0°
90°
0°
ANGLE
9009143

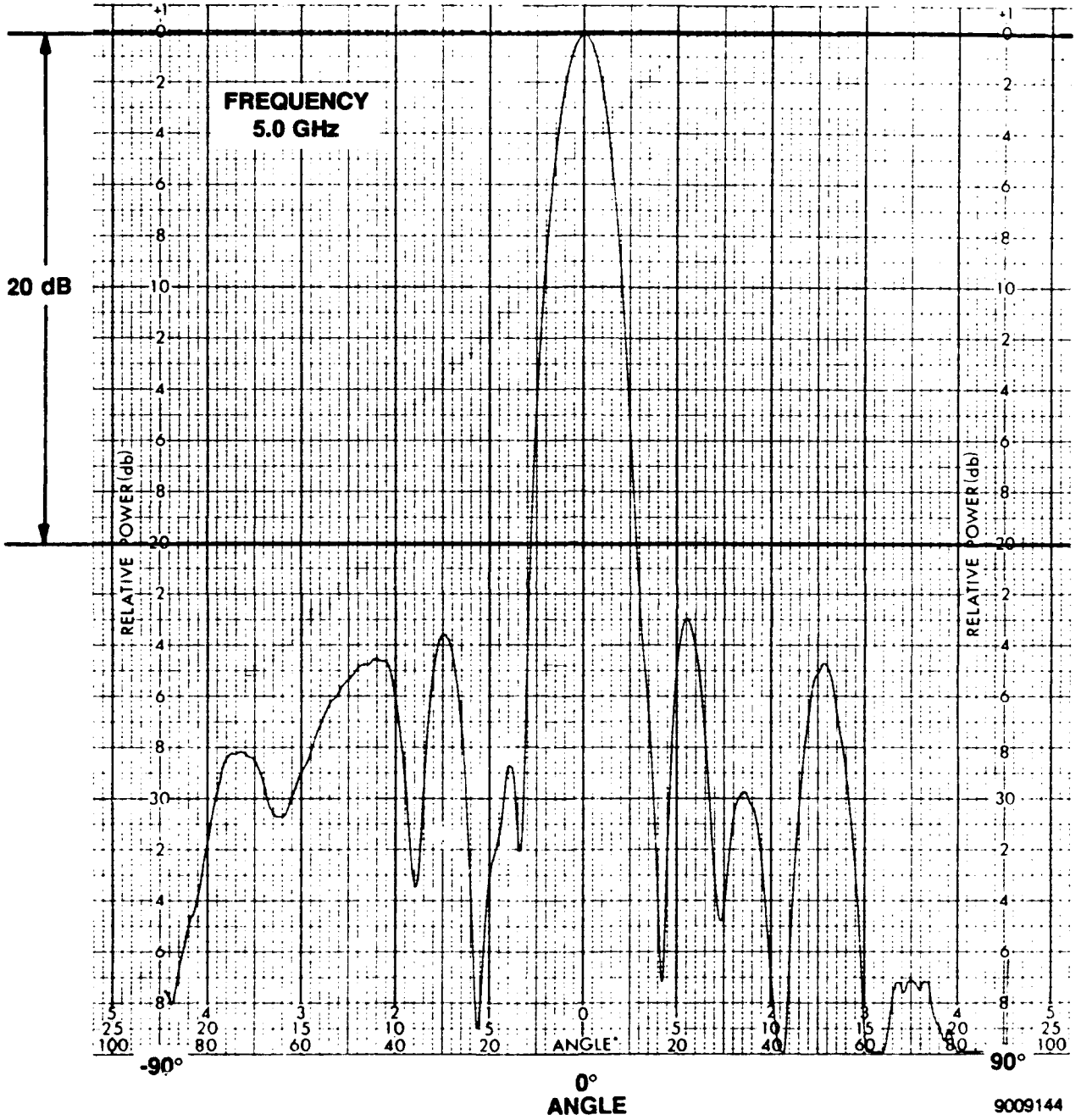
FREQUENCY
5.0 GHz
20 dB
RELATIVE POWER (db)
ANGLE°
-90°
0°
90°
ANGLE
9009144

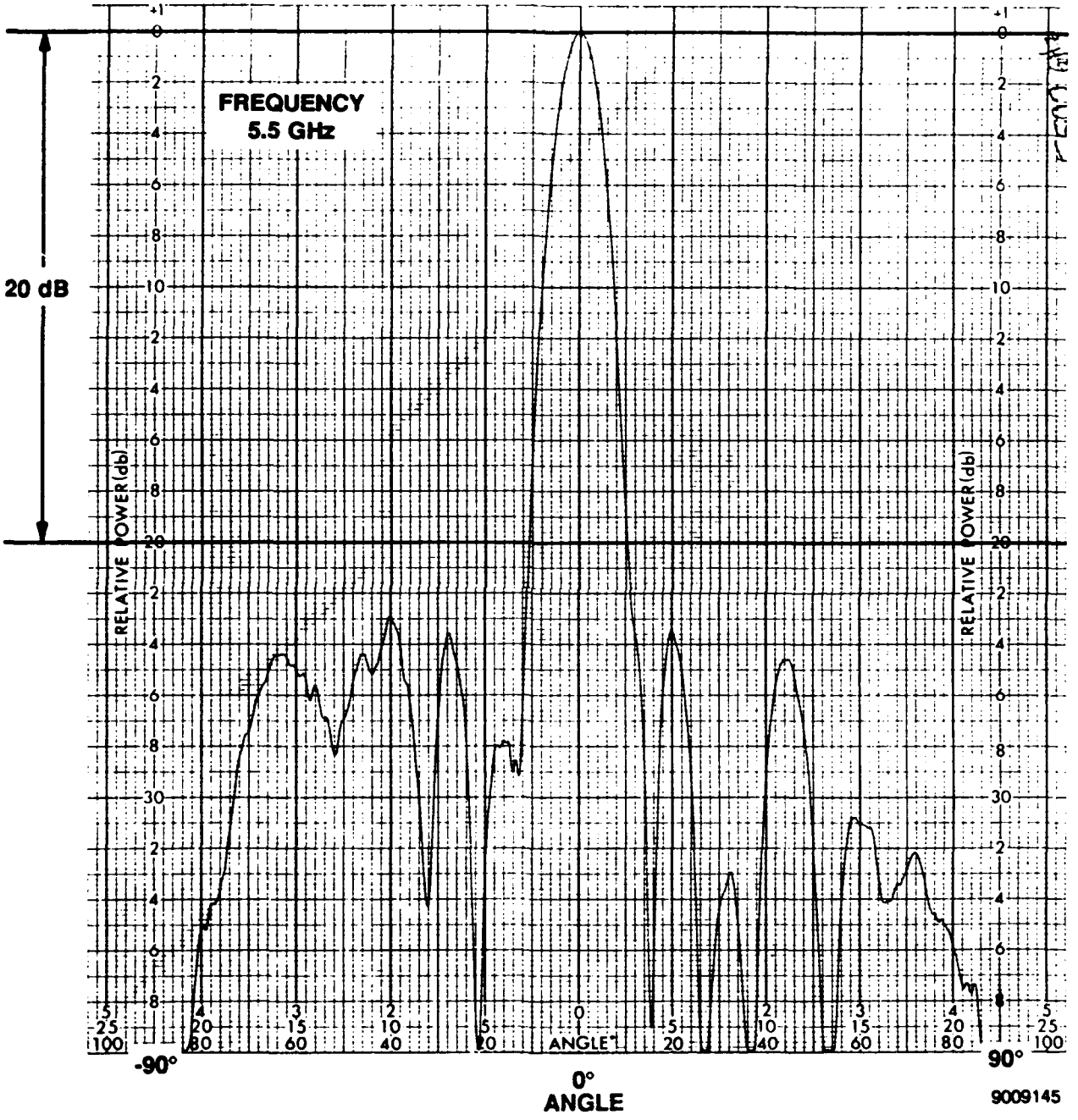
FREQUENCY
5.5 GHz
20 dB
RELATIVE POWER (db)
RELATIVE POWER (db)
ANGLE
-90°
0°
ANGLE
90°
9009145

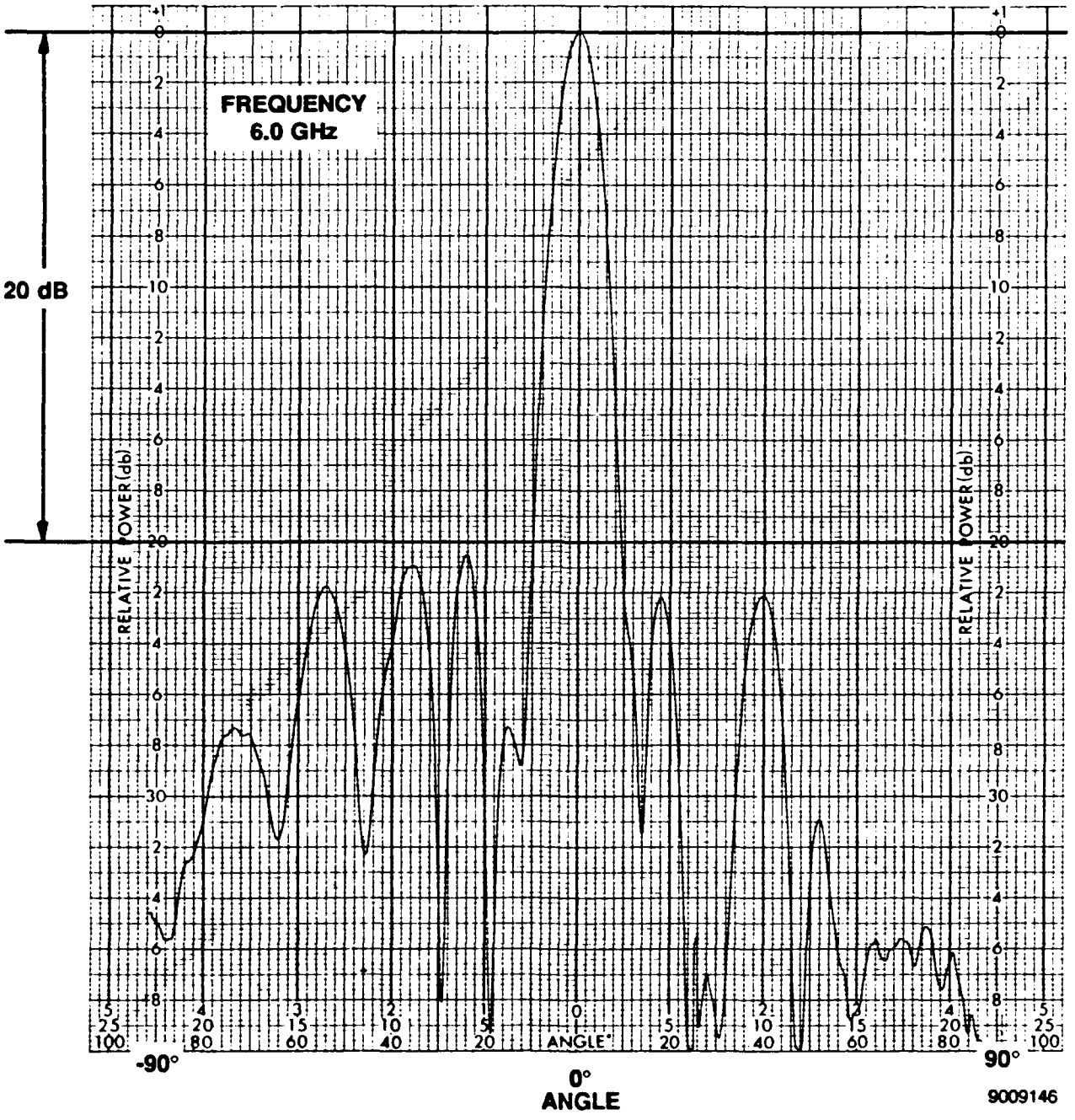
FREQUENCY
6.0 GHz
20 dB
RELATIVE POWER (db)
RELATIVE POWER (db)
ANGLE°
-90°
0°
ANGLE
90°
9009146

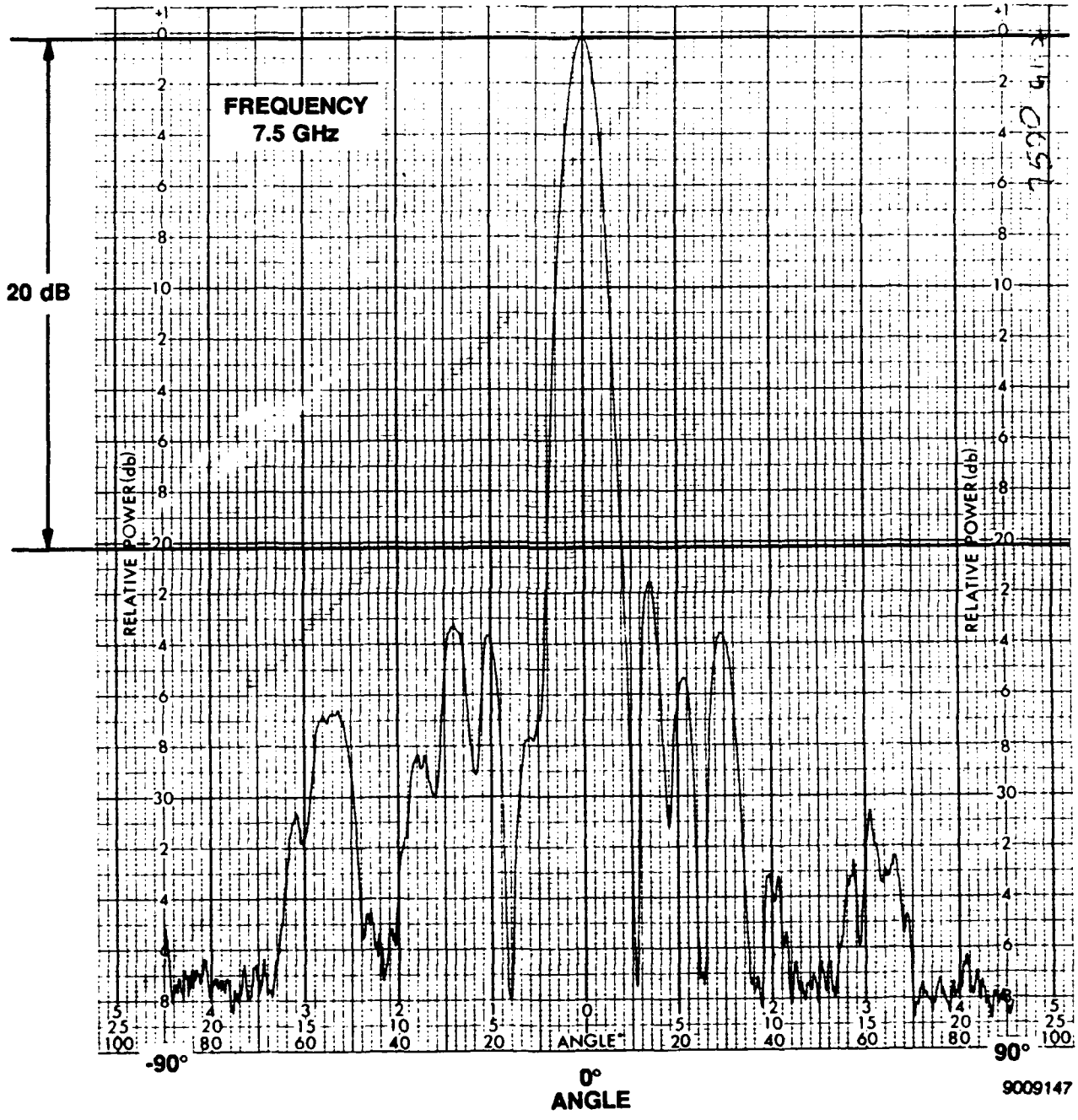
FREQUENCY
7.5 GHz
20 dB
RELATIVE POWER (db)
RELATIVE POWER (db)
ANGLE°
-90°
0°
90°
0°
ANGLE
9009147

APPENDIX A5

This data group contains patterns with 16 columns terminated and 16 columns with either 3- or 6-GHz filters as shown below. The array illumination is a 30-dB Chebyshev. This pattern set shows the degradation in sidelobe performance by adding filters to the aperture. The following frequencies are contained in this data set.

	Frequency (GHz)	Filter Response (dB)		Frequency (GHz)	Filter Response (dB)
Test 15	5.581	-5	Test 14	2.822	-5
	6.000	0		3.000	0
	6.387	-5		3.184	-5

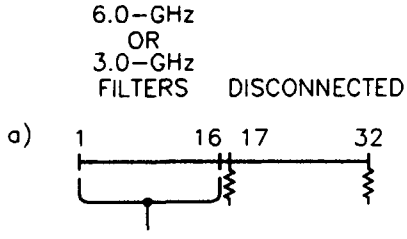

IN-BAND (3.0, 6.0 GHz) PATTERN MEASUREMENTS WITH CHEBYSHEV TAPER.

9009172

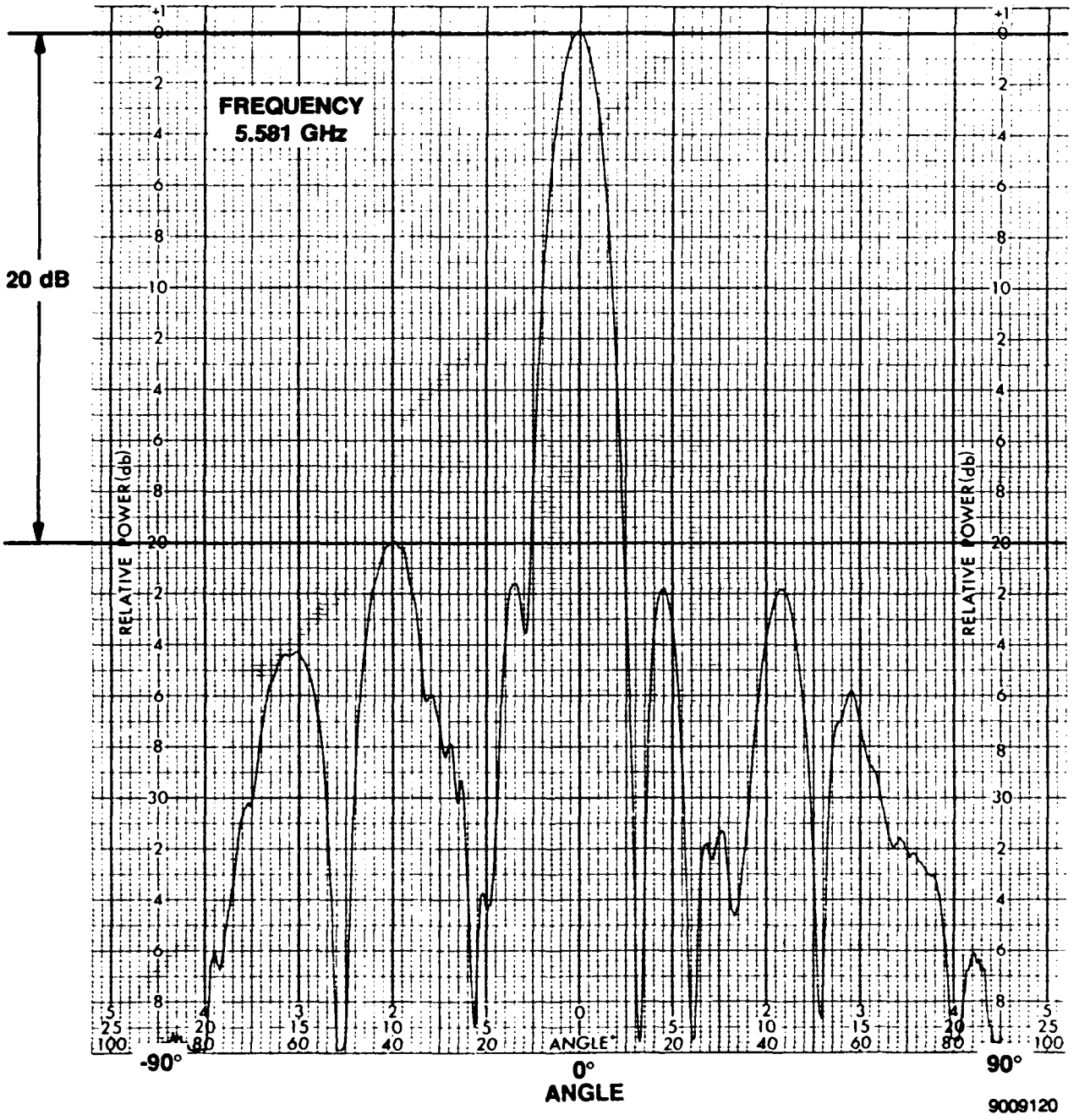
FREQUENCY
5.581 GHz
20 dB
RELATIVE POWER (db)
RELATIVE POWER (db)
ANGLE°
-90°
0°
90°
ANGLE
9009120

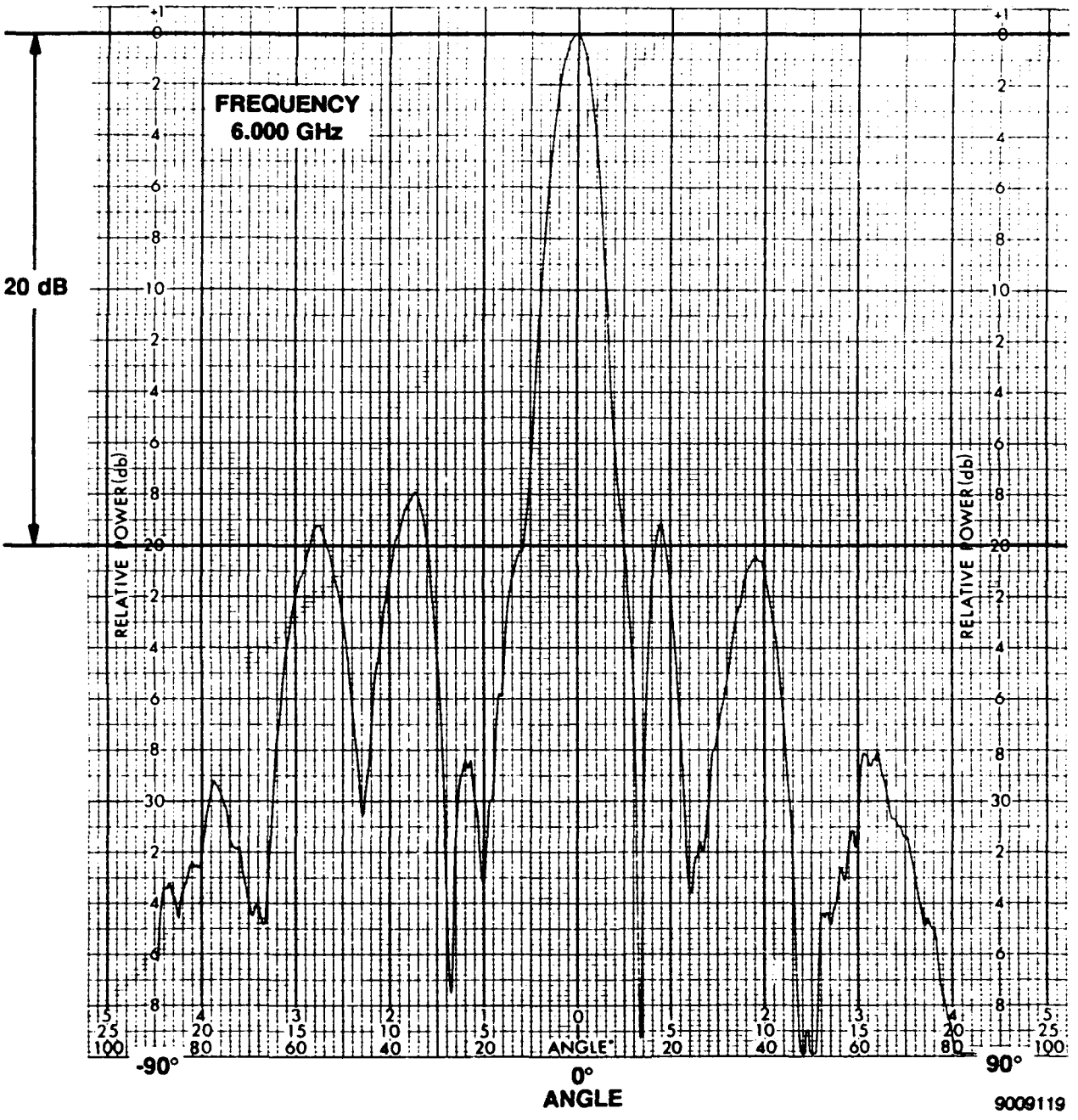
FREQUENCY
6.000 GHz
20 dB
RELATIVE POWER (db)
RELATIVE POWER (db)
ANGLE°
-90°
0°
90°
ANGLE
9009119

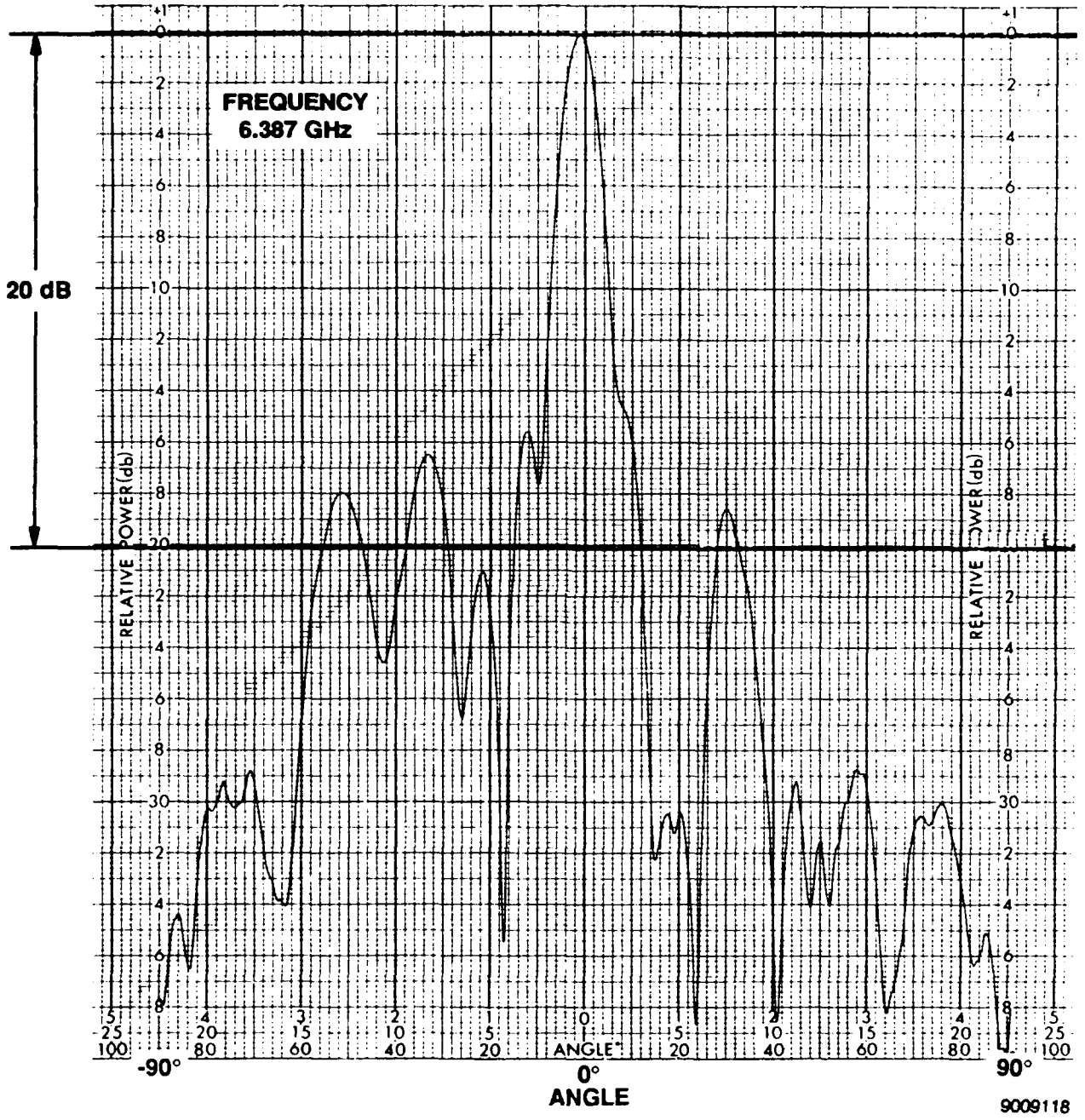
FREQUENCY
6.387 GHz
20 dB
RELATIVE POWER (db)
RELATIVE POWER (db)
ANGLE
-90°
0°
90°
ANGLE
9009118

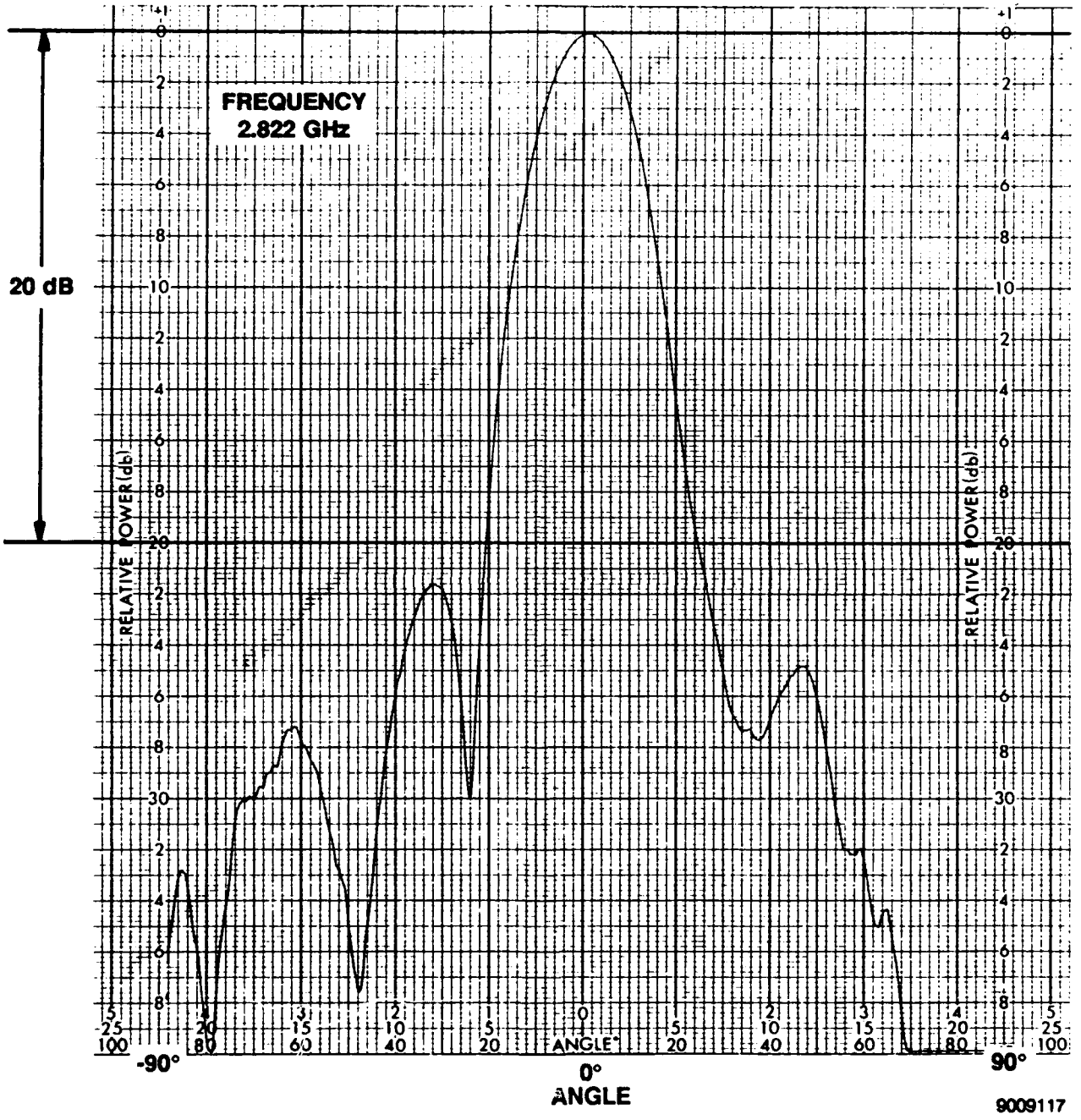
FREQUENCY
2.822 GHz
20 dB
RELATIVE POWER (db)
RELATIVE POWER (db)
ANGLE°
-90°
0°
90°
ANGLE
9009117

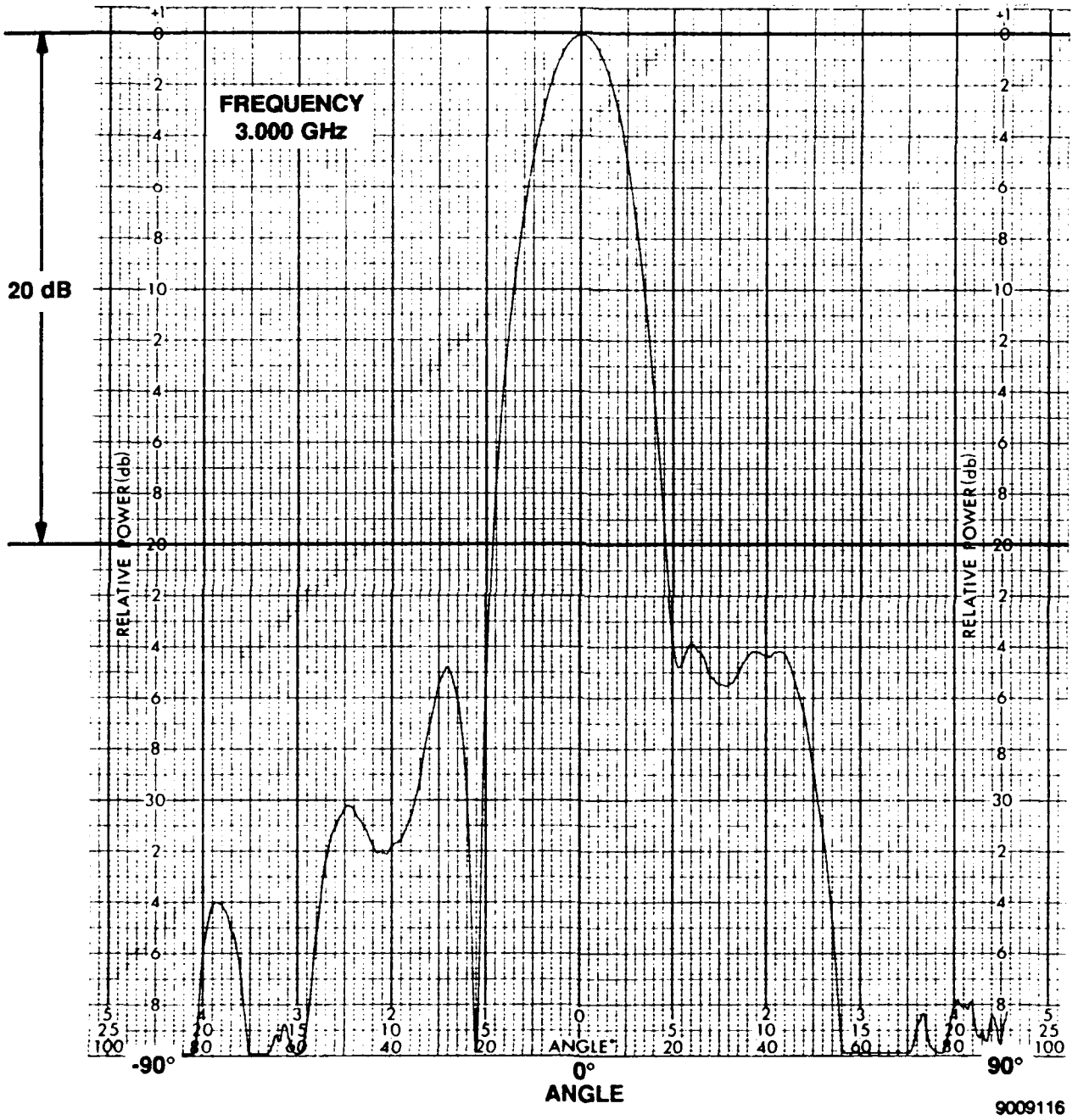
FREQUENCY
3.000 GHz
20 dB
RELATIVE POWER (db)
RELATIVE POWER (db)
ANGLE
-90°
0°
90°
ANGLE
9009116

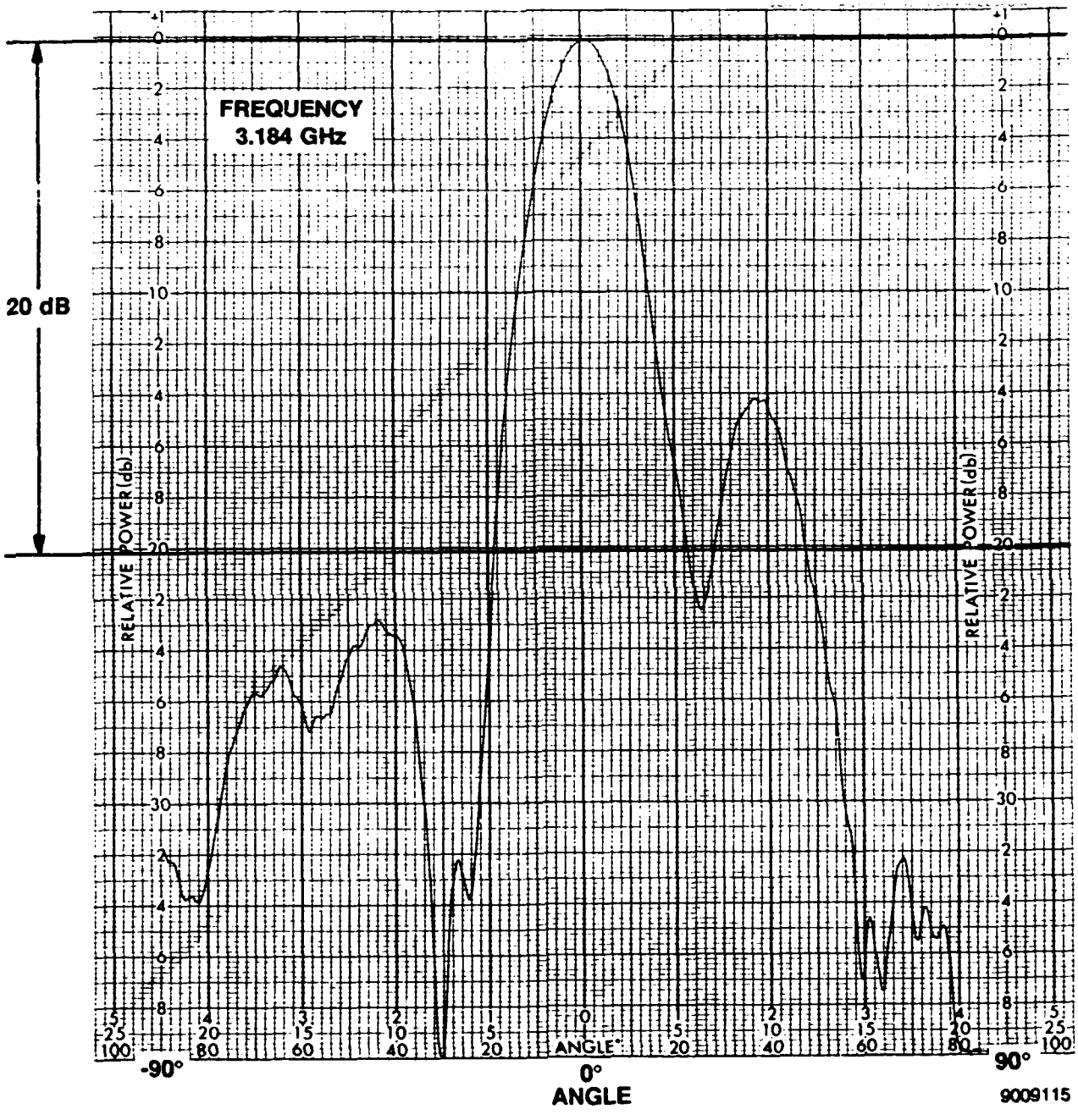
FREQUENCY
3.184 GHz
20 dB
RELATIVE POWER (db)
ANGLE°
-90°
0°
90°
ANGLE
9009115

APPENDIX A6

This data group contains patterns with 16 columns with 3.0-GHz filters and 16 columns with 6.0-GHz filters, configuration c shown below. This pattern set shows simultaneous two-band operation of the array and includes the following frequencies.

	Frequencies (GHz)		Filter Response (dB)
Test 6	2.770	5.534	-15
	2.778	5.558	-10
	2.822	5.581	-5
	3.000	6.000	0
	3.184	6.387	-5
	3.204	6.407	-10
	3.229	6.486	-15

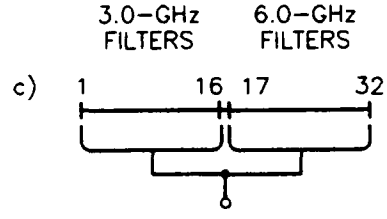

TEST 6 IN–BAND (3.0, 6.0 GHz) PATTERN MEASUREMENTS.

9009173

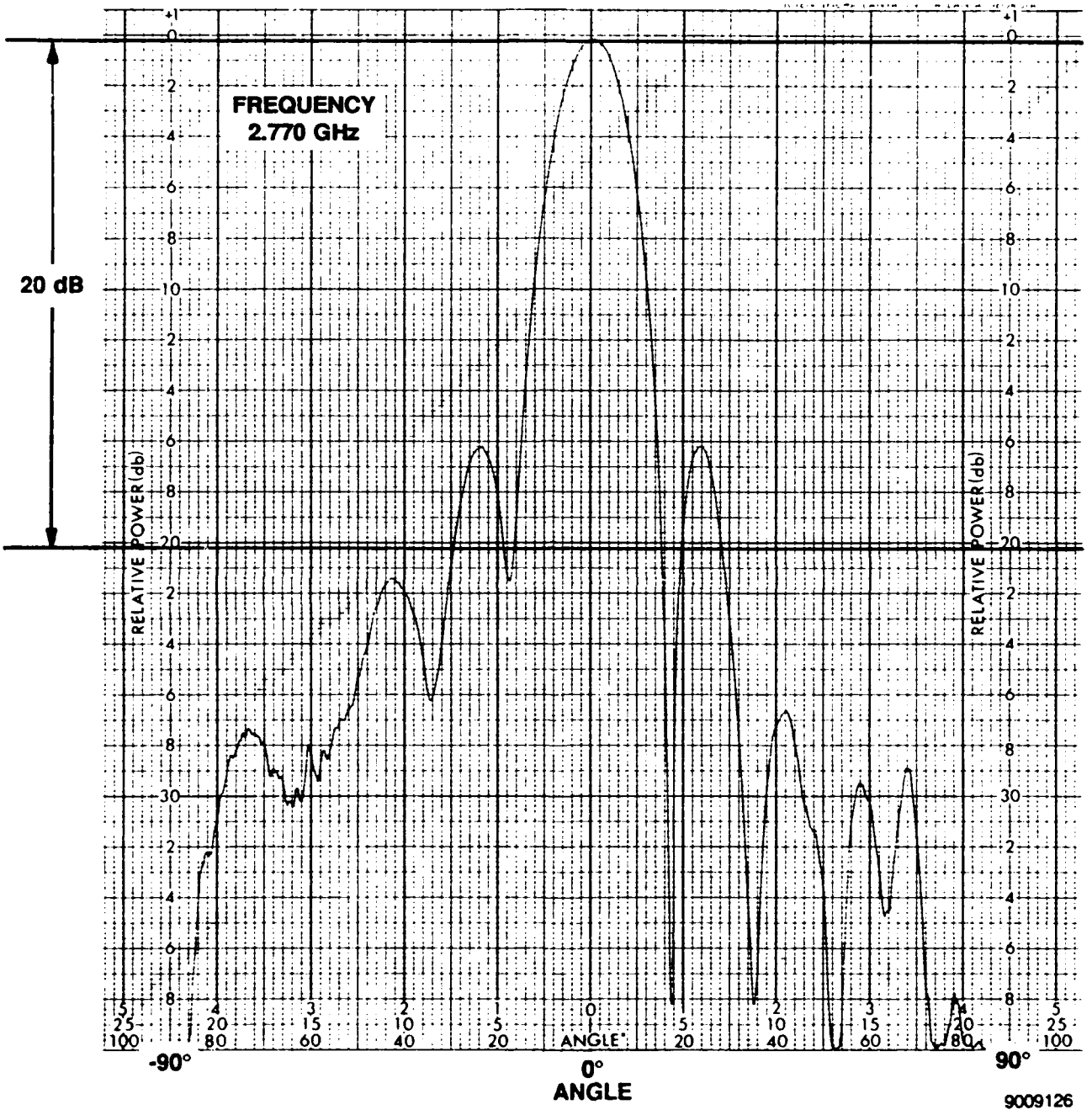
FREQUENCY
2.770 GHz
20 dB
RELATIVE POWER (db)
ANGLE°
-90°
0°
90°
ANGLE
9009126

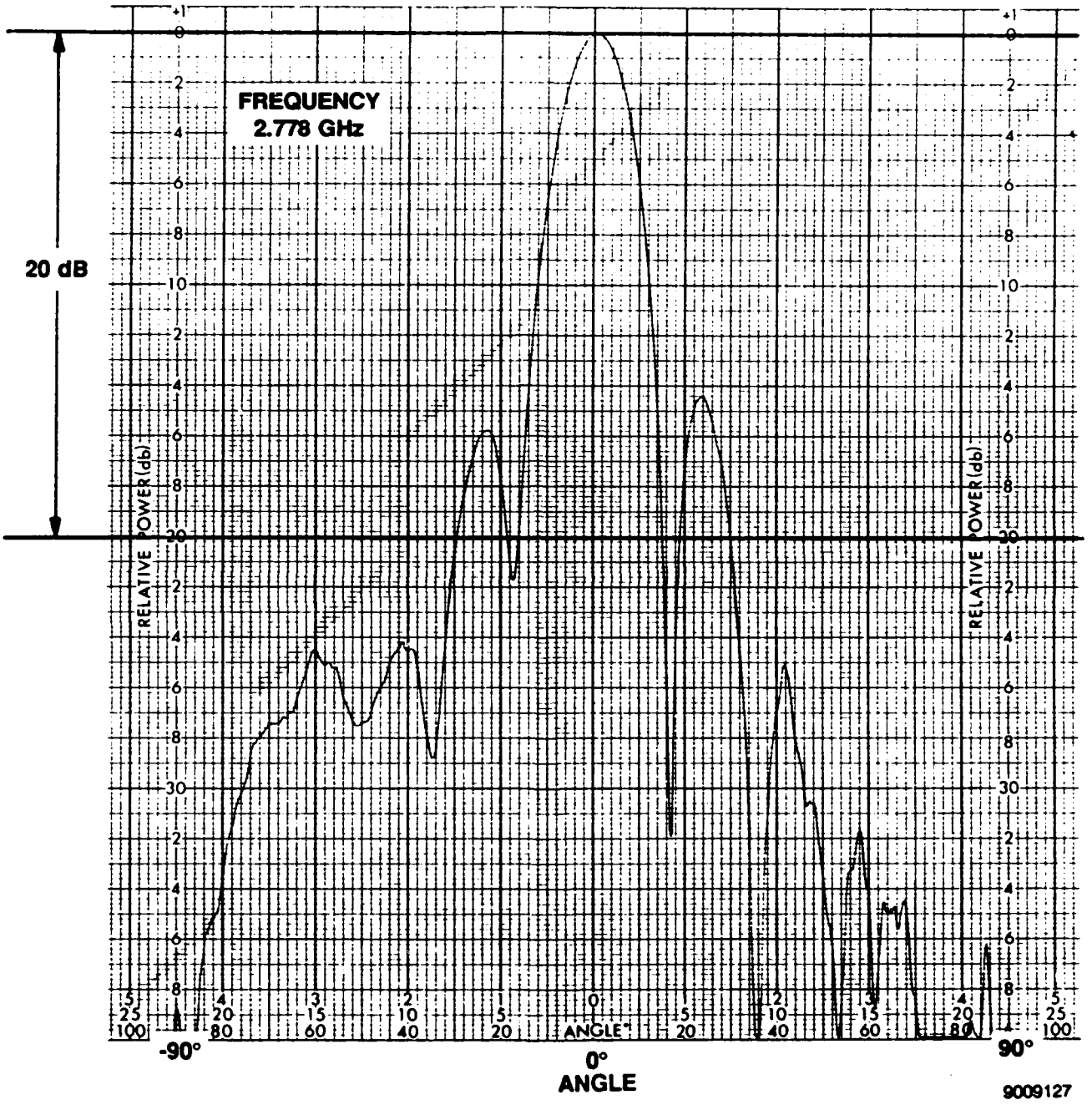
FREQUENCY
2.778 GHz
20 dB
RELATIVE POWER (db)
ANGLE°
-90°
0°
90°
ANGLE
9009127

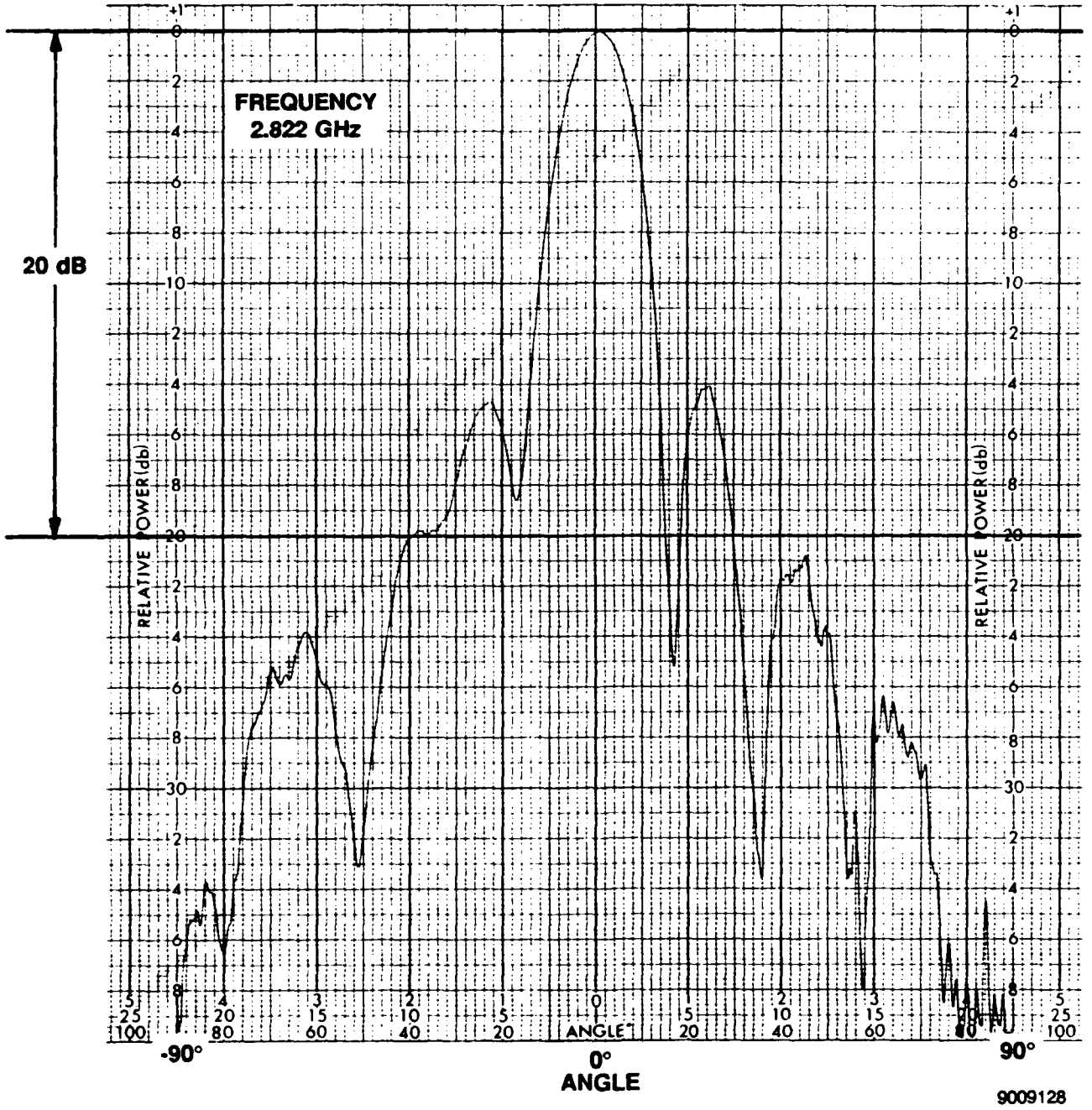
FREQUENCY
2.822 GHz
20 dB
RELATIVE POWER (db)
RELATIVE POWER (db)
-90°
0°
90°
ANGLE
ANGLE
9009128

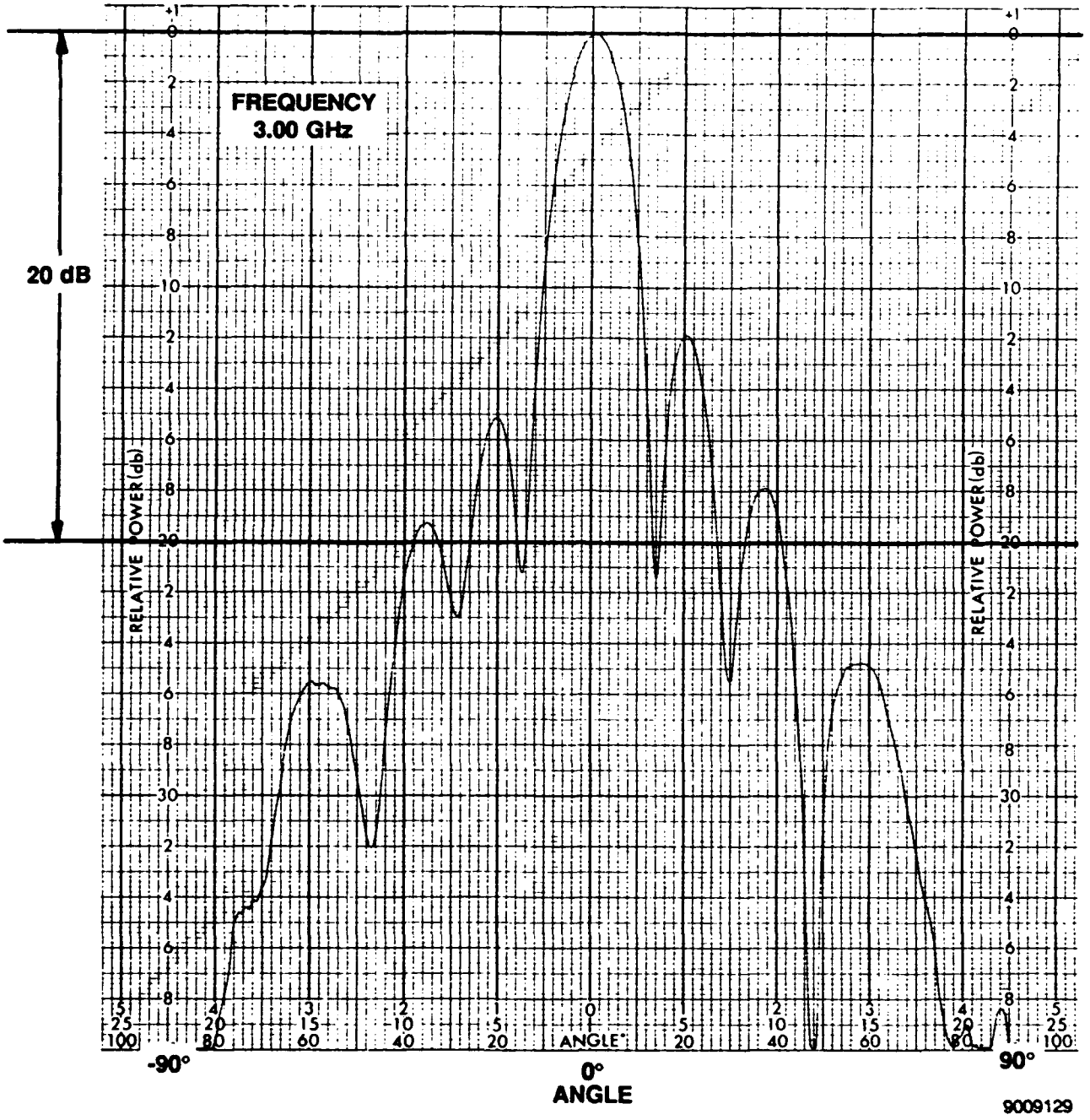
FREQUENCY
3.00 GHz
20 dB
RELATIVE POWER (db)
ANGLE°
-90°
0°
90°
ANGLE
9009129

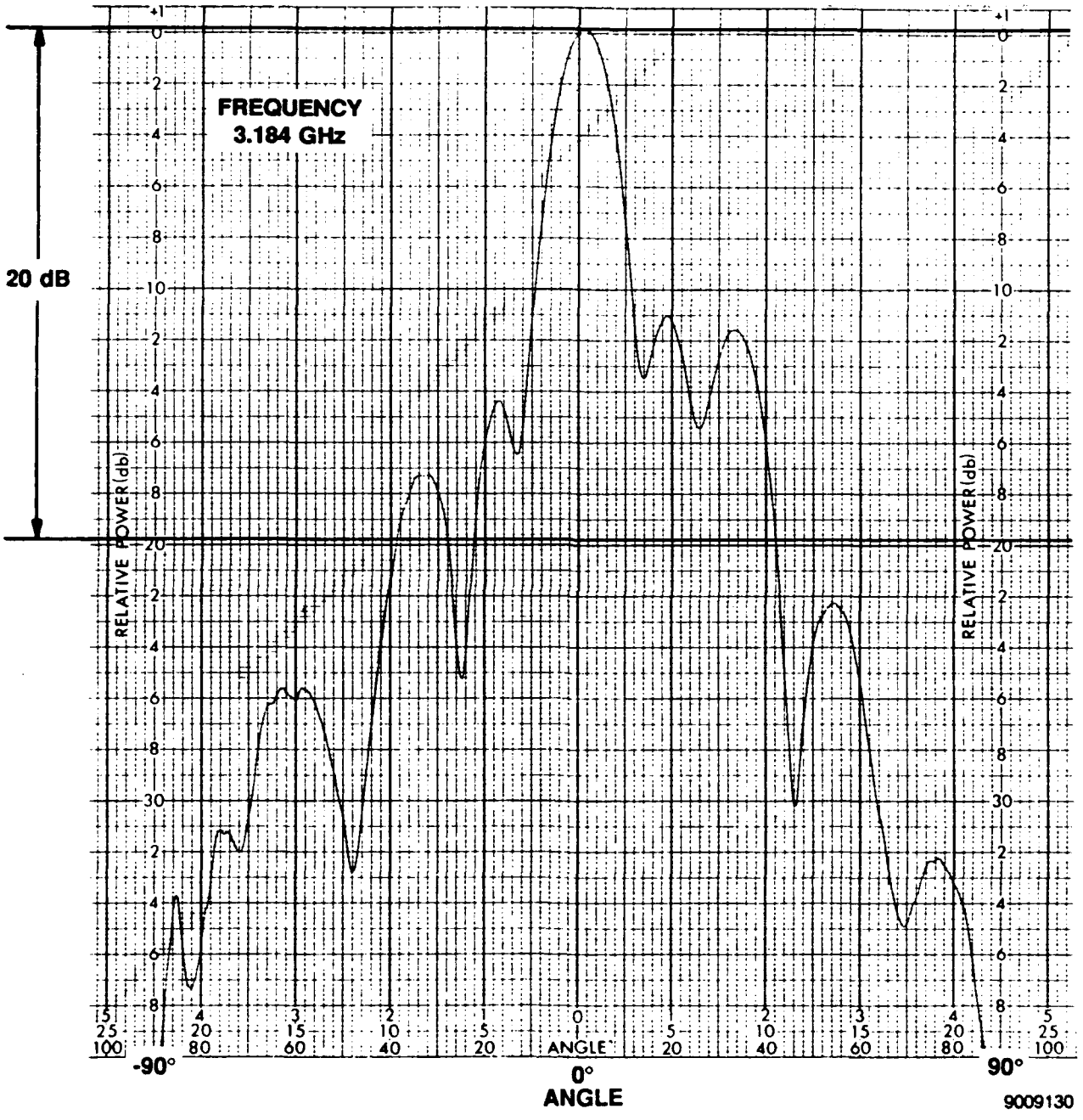
FREQUENCY
3.184 GHz
20 dB
RELATIVE POWER (db)
RELATIVE POWER (db)
ANGLE
-90°
0°
90°
ANGLE
9009130

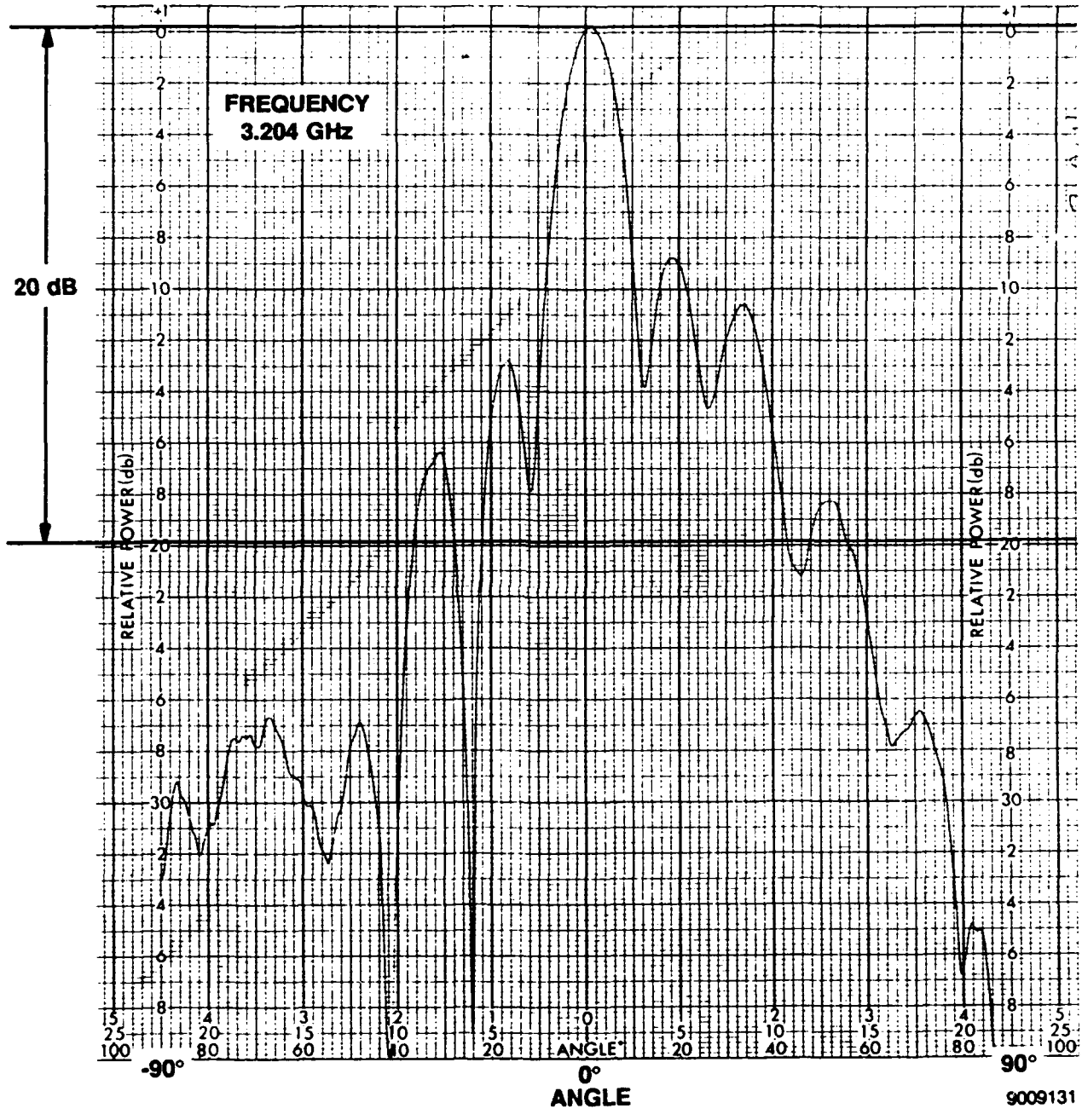
FREQUENCY
3.204 GHz
20 dB
RELATIVE POWER (db)
ANGLE
-90°
0°
90°
ANGLE
9009131

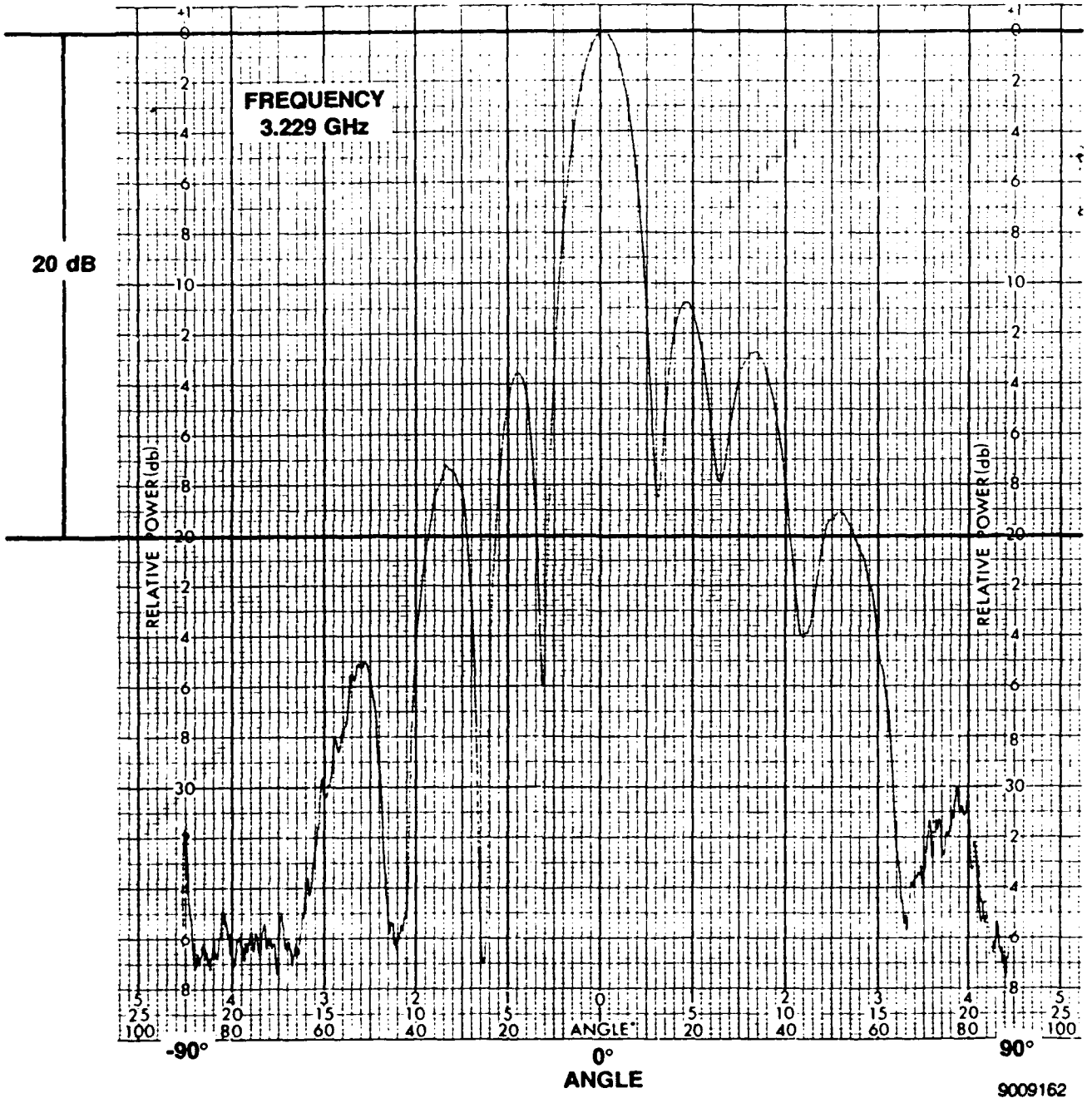
FREQUENCY
3.229 GHz
20 dB
RELATIVE POWER (db)
ANGLE°
-90°
0°
90°
ANGLE
9009162

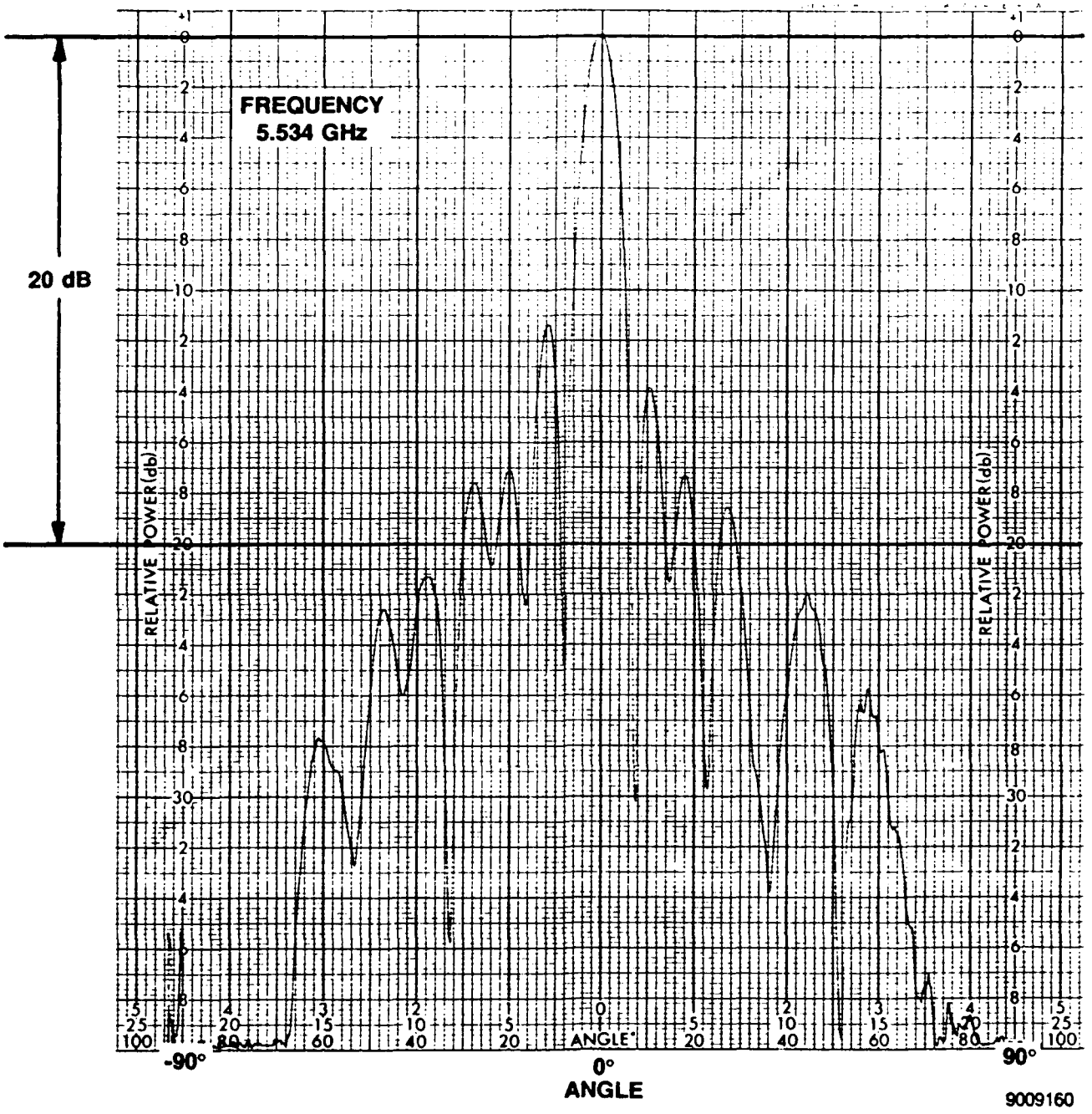
FREQUENCY
5.534 GHz
20 dB
RELATIVE POWER (db)
ANGLE°
-90°
0°
90°
ANGLE
9009160

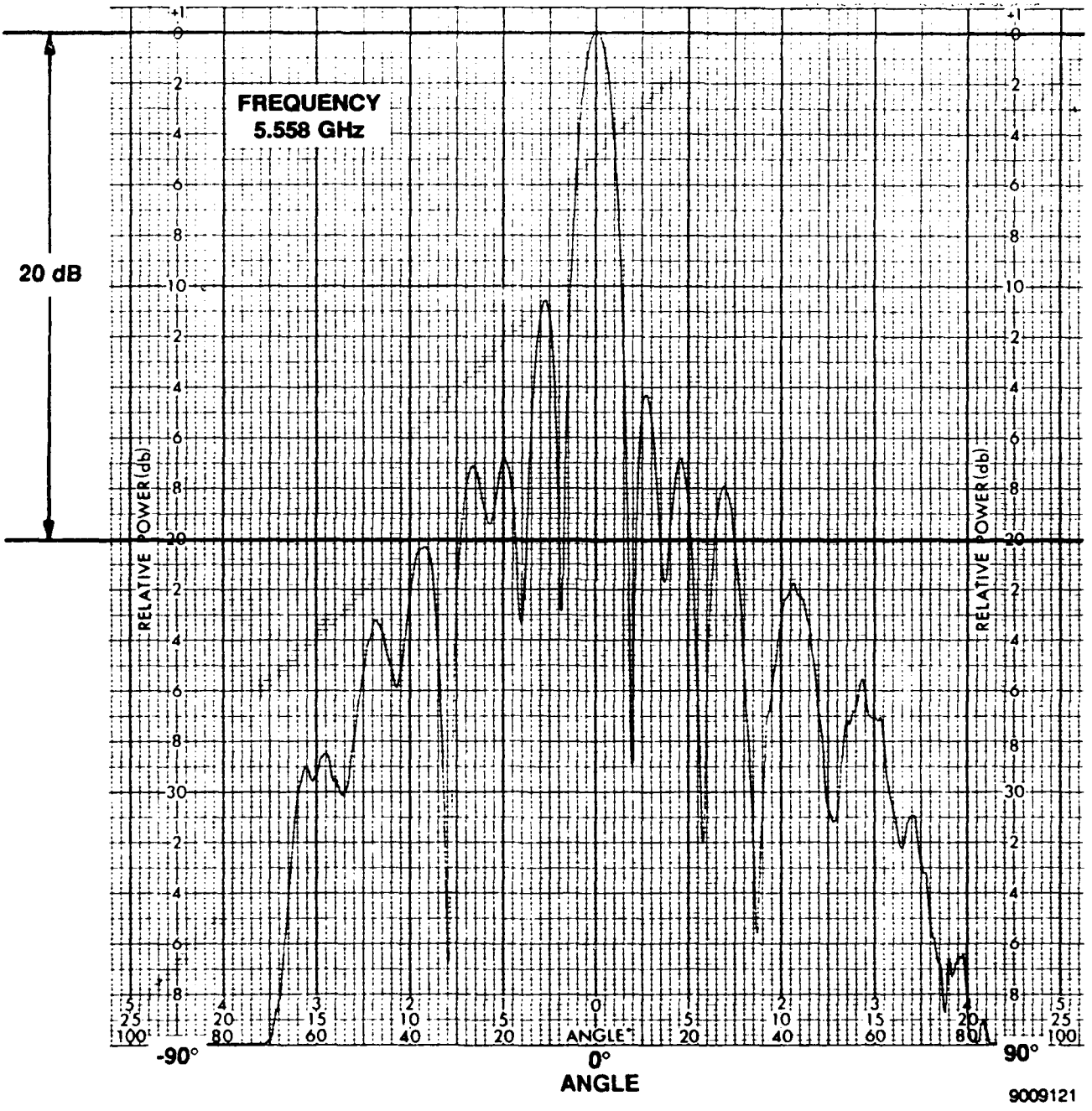
FREQUENCY
5.558 GHz
20 dB
RELATIVE POWER (db)
RELATIVE POWER (db)
ANGLE
-90°
0°
90°
ANGLE
9009121

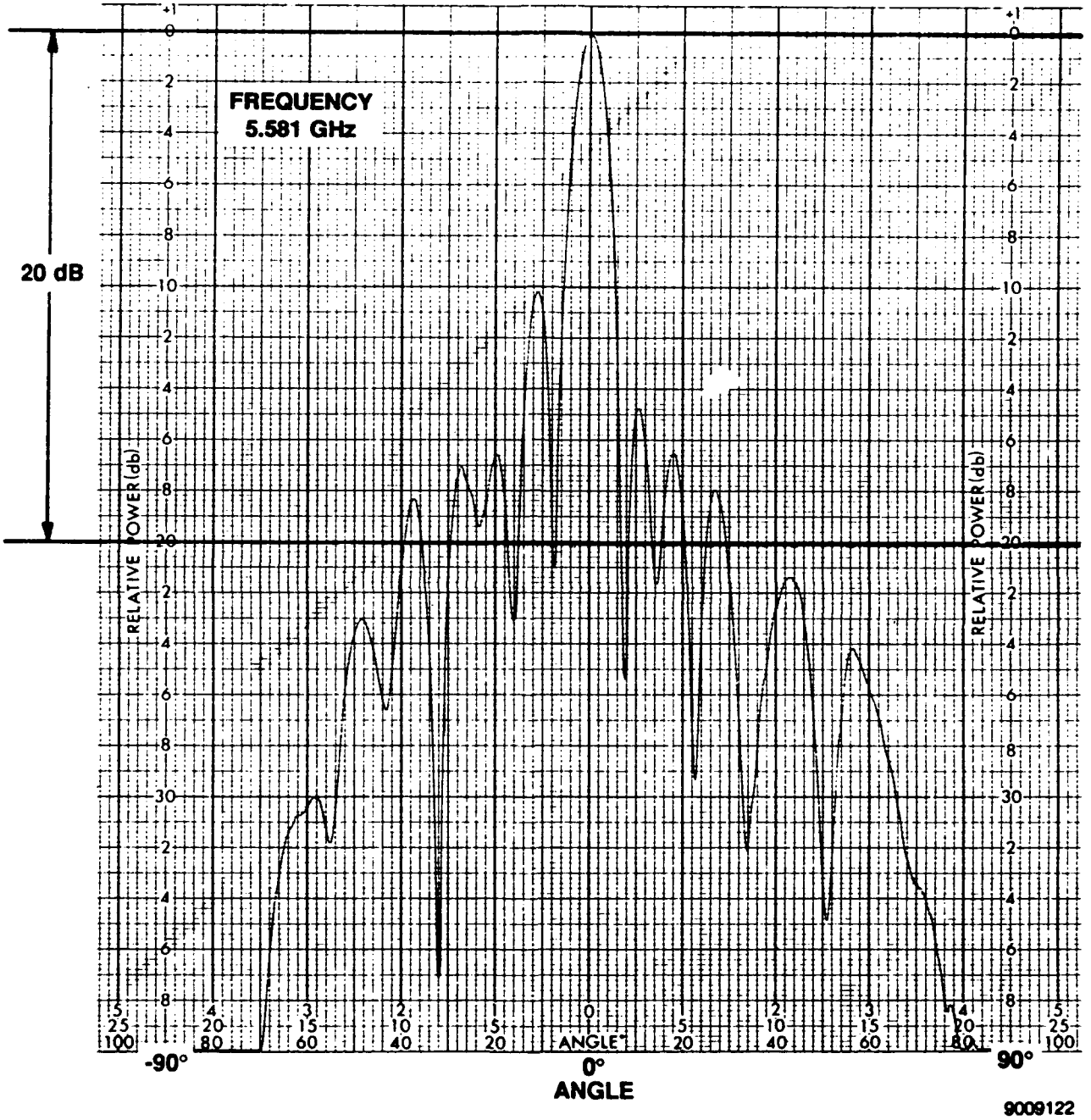
FREQUENCY
5.581 GHz
20 dB
RELATIVE POWER (db)
RELATIVE POWER (db)
ANGLE
-90°
0°
90°
ANGLE
9009122

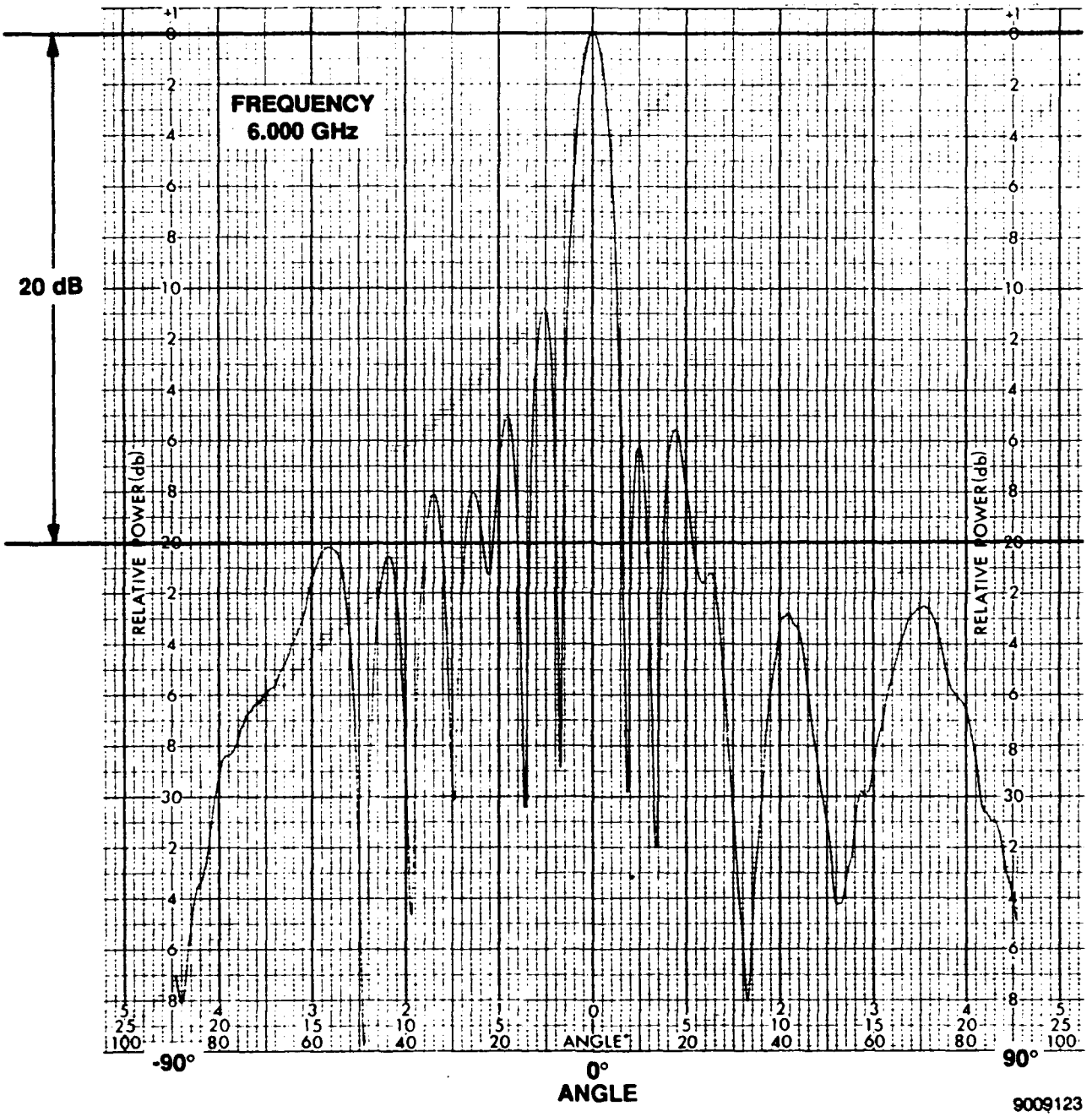
FREQUENCY
6.000 GHz
20 dB
RELATIVE POWER (db)
RELATIVE POWER (db)
ANGLE°
-90°
0°
90°
ANGLE
9009123

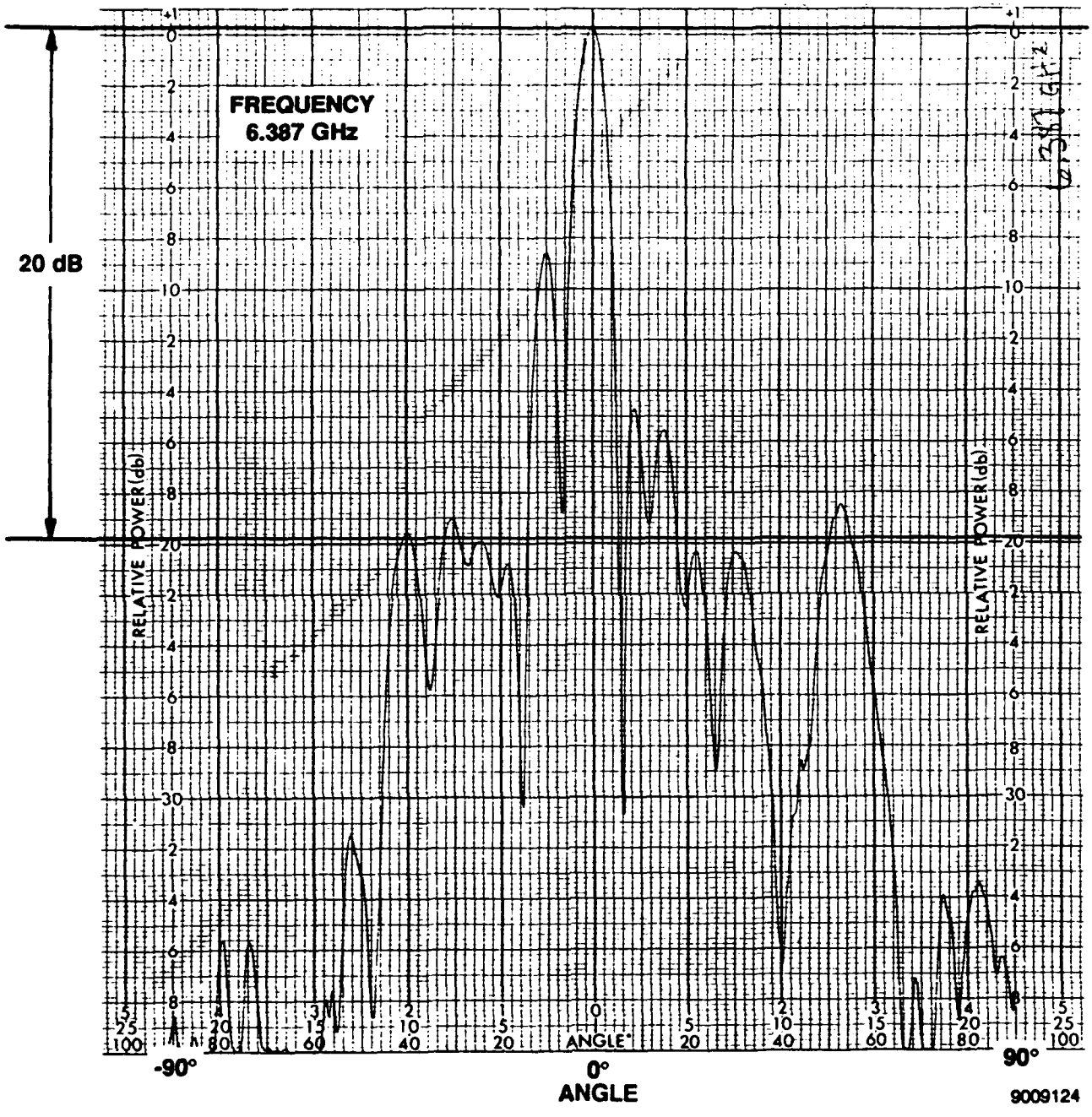
FREQUENCY
6.387 GHz
20 dB
RELATIVE POWER (db)
RELATIVE POWER (db)
ANGLE
-90°
0°
90°
ANGLE
9009124

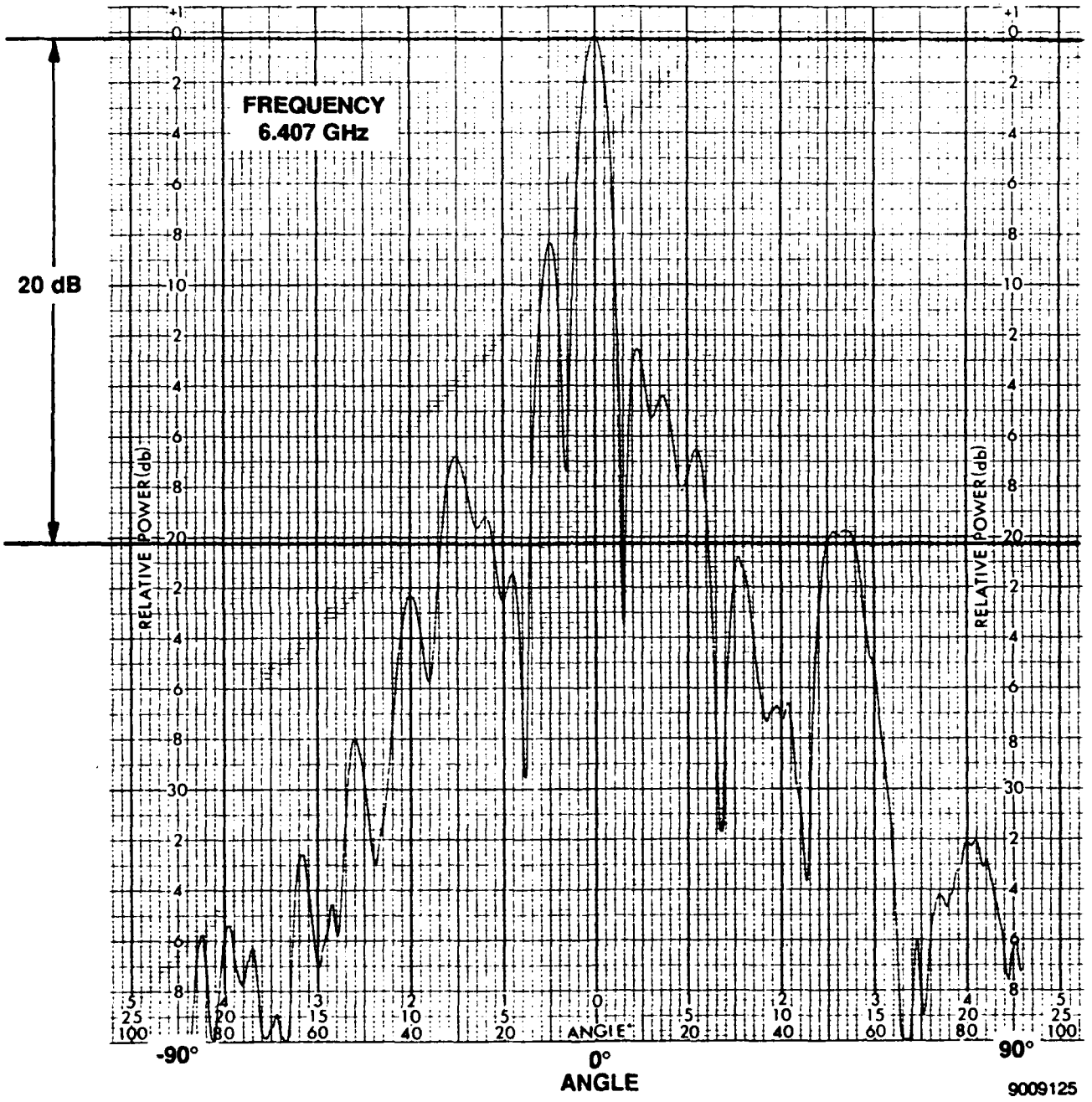
FREQUENCY
6.407 GHz
20 dB
RELATIVE POWER (db)
RELATIVE POWER (db)
ANGLE°
-90°
0°
90°
ANGLE
9009125

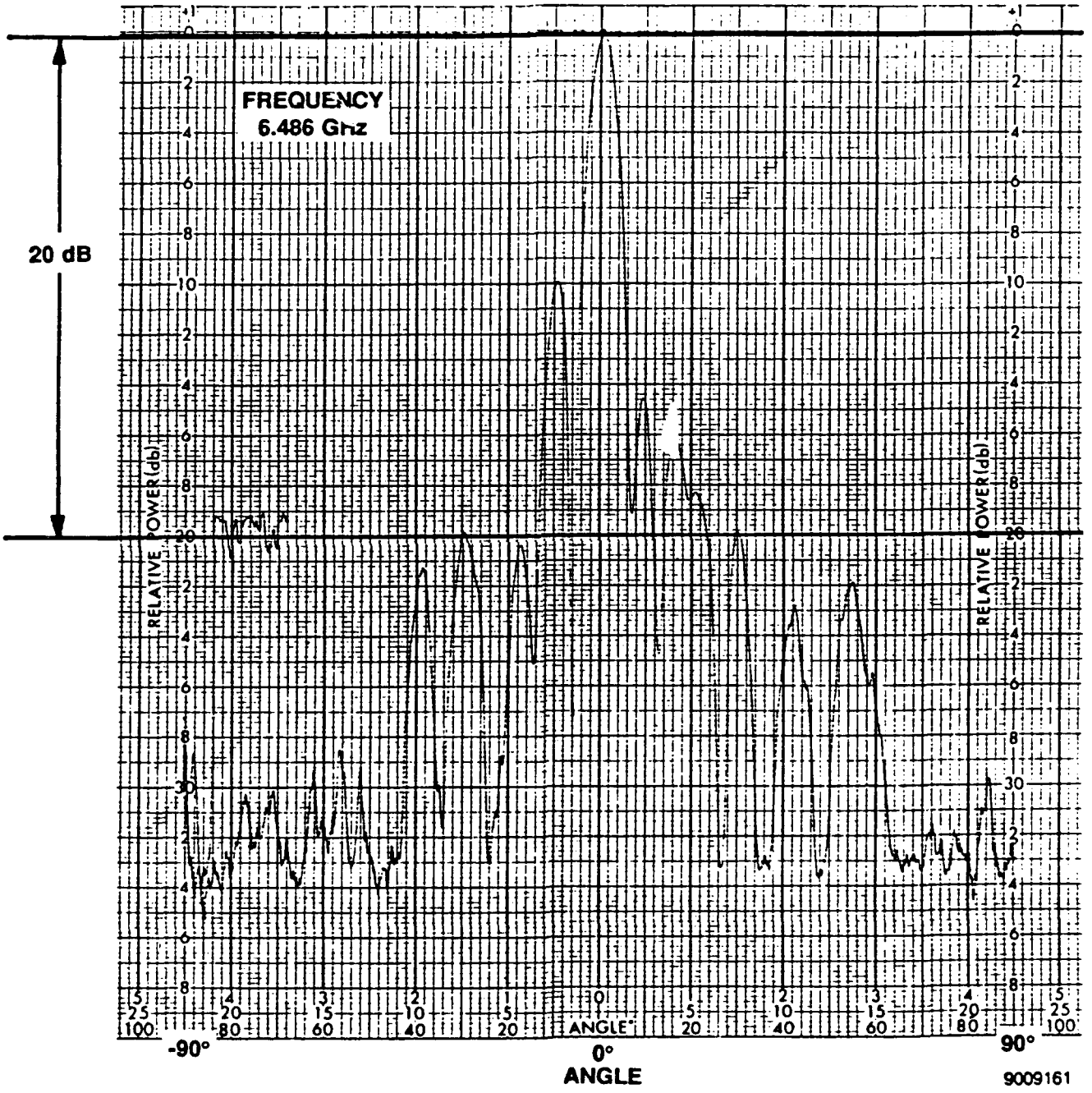
20 dB
FREQUENCY
6.486 GHz
RELATIVE POWER (db)
RELATIVE POWER (db)
ANGLE°
-90°
0°
90°
ANGLE
9009161

MISSION

OF

ROME LABORATORY

Rome Laboratory plans and executes an interdisciplinary program in research, development, test, and technology transition in support of Air Force Command, Control, Communications and Intelligence (C^3I) activities for all Air Force platforms. It also executes selected acquisition programs in several areas of expertise. Technical and engineering support within areas of competence is provided to ESD Program Offices (POs) and other ESD elements to perform effective acquisition of C^3I systems. In addition, Rome Laboratory's technology supports other AFSC Product Divisions, the Air Force user community, and other DOD and non-DOD agencies. Rome Laboratory maintains technical competence and research programs in areas including, but not limited to, communications, command and control, battle management, intelligence information processing, computational sciences and software producibility, wide area surveillance/sensors, signal processing, solid state sciences, photonics, electromagnetic technology, superconductivity, and electronic reliability/maintainability and testability.